AD NUMBER
ADA800053
CLASSIFICATION CHANGES
TO: **unclassified**
FROM: **confidential**
LIMITATION CHANGES
TO: **Approved for public release; distribution is unlimited.**
FROM: **Distribution authorized to DoD only; Administrative/Operational Use; 18 JUL 1952. Other requests shall be referred to Naval Research Laboratory, Washington, DC. Pre-dates formal DoD distribution statements. Treat as DoD only.**
AUTHORITY
NRL ltr dtd 22 Feb 1982; NRL ltr dtd 22 Feb 1982

CONFIDENTIAL

AD 205 443

Reproduced by the

ARMED SERVICES TECHNICAL INFORMATION AGENCY
ARLINGTON HALL STATION
ARLINGTON 12, VIRGINIA

U.S.N.L.–36 June 61

EXCLUDED FROM AUTOMATIC
REGRADING; ~~DOD DIR 5200.10~~
DOES NOT APPLY

CONFIDENTIAL

205443

NAVAL RESEARCH LABORATORY

WASHINGTON, D.C.

CONFIDENTIAL

NRL-14127

confidential
security information

Proceedings

FOURTH SYMPOSIUM ON SCANNING ANTENNAS

under the auspices of the

Antenna Research Branch
Radio Division 1

21 - 22 April 1952

Naval Research Laboratory
Washington, D. C.

confidential
security information

FOREWORD

This symposium is the fourth in a series which was begun in 1943. Each was held in an effort to acquaint workers in the scanning field and other interested parties with the latest developments in antenna scanning systems. It is felt that these symposia have proven useful not only in disseminating existing information but also in stimulating new ideas. It is hoped that they will continue to be held whenever enough significant work is available for presentation.

One objection to a meeting of this type is that the size of the audience limits the interchange of ideas. Fortunately, this has not been altogether true. Each symposium has included interesting discussion periods initiated by the audience. However, there has been a time limitation on the discussion; so it appeared worthwhile to introduce smaller group meetings for the purpose of discussing specialized subjects. This idea was suggested by Dr. R. C. Spencer of Air Force Cambridge Research Center, and two such sessions were held in conjunction with this symposium.

Considerable space could be used in discussing the techniques of these symposia, but it might be better to consider here some of the impressions which have grown out of them. One of the most striking of these is the increased interest in this field. Evidence of this is seen in the large number of participants in the last two symposia. Further evidence of this is provided by the fact that twenty-four papers were presented at this symposium, held only eighteen months after the third symposium. A number of other papers had to be refused in order to avoid crowding the program.

This increase in interest has resulted in the development of new solutions to scanning problems and the improvement of the other methods. Scanning requirements are no longer looked upon as a combination of impossibilities, but for some problems many different solutions have been offered. The problem now becomes one of choosing the most convenient method for the particular application.

Another significant impression was obtained from the discussion during the third session of this symposium. At this time, it was pointed out that the rapidity of scan is not limited by the scanner. The antenna system must energize the target with a number of pulses during the time that the beam scans past the target. Since there is a finite number of pulses available there is a limit to the rate at which the beam can scan. This rate can almost invariably be obtained by a mechanical rotation in the feed assembly. It would be well then for everyone in the field to speak of a "scanning problem" rather than a "rapid-scanning problem." The rapidity of scan is no longer a problem in existing systems.

One further impression: Since solutions exist for most scanning problems, future efforts will generally be concentrated on simplifying existing solutions or developing new solutions which can be demonstrated to be superior to existing solutions. This superiority must be evidenced not only by improved electrical performance but also by an inherent simplicity of design. Simplicity should be the keynote in future scanners. It will not be sufficient to demonstrate perfect optics with a system of inherent complexity. The concept of complexity versus improved performance should not be the concern of the project engineer alone. The scanner designer must be aware of this concept and must govern his day-to-day thinking accordingly.

The useful information obtained from these meetings was not these impressions, but rather the data presented and interpreted in the various papers and in the discussion periods. The present publication contains summaries of most of the talks and the discussion periods. The discussion material has not been edited by the individual participants, so that any inaccuracies or misstatements are due to the shortcoming of the transcription processes.

The success of this program required the efforts of many people. We are grateful to the speakers for their interesting papers. We wish to thank Dr. M. B. Sledd and Dr. W. F. Gabriel for supplying us with information on the two round table discussions. The work of Miss Rosemary B. Kelly in handling the details of the arrangements and in doing the very large amount of necessary typing is particularly appreciated. The cooperation and assistance of LCDR C. C. Rust was very effective in producing a smooth-running program. Finally, the efforts of Mr. R. Hudgins have enabled us to publish this material in a very brief time. For this, we are grateful.

Kenneth S. Kelleher

Kenneth S. Kelleher
Antenna Research Branch
Radio Division I
Naval Research Laboratory

VISITING PARTICIPANTS

NAME	ORGANIZATION
Abbey, E. K.	NEL
Aitken, R. K.	Hazeltine
Allen, C. C.	GE
Anderson, D. B.	Hazeltine
Anderson, R. S.	SRI
Arelt, Charles	Am. Mach. & Foundry
Badenoch, D. C. (Capt.)	Directorate of Armament Dev. (Canada)
Barrett, R. M.	AFCRC
Bartelt, A. D.	BuOrd
Bawer, Robert	Melpar
Bayer, P. J.	BuShips
Beam, R. E.	Northwestern Univ.
Berkowitz, B.	Sperry
Bernstein, B.	JHU Applied Physics Lab.
[illegible]sschop, H. P.	BuOrd
[illegible], J. E.	Georgia Tech
Bris[illegible]	British JSM
Brown, [illegible]	Natl. Research Council (Canada)
Brunelle, [illegible]	GE
Budenbom, H. T.	BTL
Burlingham, M.	Reeves
Byrnes, E. M., Lt. (L)RCN	Canadian Joint Staff
Cacheris, J. C.	Natl. Bureau of Standards
Carnine, R. L.	Melpar
Carter, P. S.	RCA
Chu, L. J.	M.I.T.
Cogan, H. F.	BuShips
Corbin, J. E.	BTL
Counter, V. A.	North Amer. Aviation
Crain, C. M.	EERL Univ. of Texas
Dailey, W. P.	Sponge Rubber Products
Dantzig, H. P.	Bendix Radio
Deschamps, G. A.	Fed. Tel. Labs.
Diab, M. A.	RDAC
Dix, W. E.	BuShips
Ducore, Harold	Sig. Corps Eng. Labs.
DuHamel, R. H.	RCA
Dunbar, A. S.	SRI
Emerson, J.	Sperry
Felker, G. E.	GE
Ferrara, R. F.	Am. Mach. & Foundry
Fine, Ellen C.	Raytheon
Flood, J. D.	Stavid Engineering
Foster, J. S.	McGill
Galane, Irma	BuAer
Greenough, R. K.	GE
Gruenberg, Harry	Natl. Research Council (Canada)
Gruss, R. F.	BuOrd
Guarrera, J. J.	Reeves
Gunter, R. C., Jr.	Clark University
Haisler, W. D. (Maj.) USMC	BuOrd
Harbaugh, A. W.	Univ. of Texas
H[illegible], C. M.	Bendix Radio
Hritch[illegible], R. D.	Natl. Bureau of Standards
Hatkin, Leonard	SCEL
Hershfield, Sanford	Gl. Martin
Hiatt, R. E.	AFCRC
Hohl, J. S.	GE
Hollabaugh, M. G.	Avion Instrument Corp.
Hollis, J. S.	Georgia Tech
Holt, F. S.	AFCRC
Honer, R. E.	Georgia Tech
Horton, M. C.	Goodyear Aircraft
House, H. J.	NADC
Howard, R. R.	JHU Applied Physics Lab.
Jasik, Henry	Airborne Instruments Lab.
Jones, C. C.	Westinghouse
Jones, S. S. D.	RRDE
Jordan, E. C.	Univ. of Illinois

NAME	ORGANIZATION
Keary, T. J.	NEL
Kilgallen, A.	BuOrd
Kuhn, B. G. (F/L RCAF)	CEPE (Canada)
Kuck, J. H.	JHU Applied Physics Lab.
Lengyel, B. A.	ONR
Lince, A. H.	BTL
Lisicky, A. J.	RCA
Locus, S.	Sandia Corp.
Long, M. W.	Georgia Tech
Lovenstein, A. S.	Evans Sig. Labs.
Maclese, A.	British JSM
Mather, D. L.	RADC
McCabe, A. P.	Spec. Weapons Div. Northrop Air.
McDade, E. J.	Pickard & Burns
Meadows, E. L.	BuShips
Miller, G. A.	Natl. Research Council (Canada)
Moeder, W. D.	Stavid Engineering
Moore, J. R.	BuAer
Mulvey, J. X., Jr.	Consolidated Vultee
Nassetta, F. C.	BuOrd
Norwood, Virginia T.	SCEL
Noji, T. T.	Hazeltine
Pankiewicz, C. L.	RDAC
Parker, R. O.	
Perry, E. V.	BuShips
Portmann, P. A.	JHU Applied Physics Lab
Fortune, W. J.	WADC
Pressell, Paul	Antenna Research Lab.
Raschke, R. R.	GE
Rayment, C. V.	Canadian Defense Research Board
Reynolds, James M.	RADC
Rexroth, J. A.	BuOrd
Riblet, Henry J.	Microwave Dev. Labs.
Ross, D. K. Lt. (jg) USNR	BuOrd
Rotman, Walter	AFCRC
Rowland, H. J.	Pickard & Burns
Rush, Stanley (Capt.)	RADC
Scavullo, J. J.	BuAer
Schlecht, F.	GE
Schn[illegible], S.	Hughes
Serice, D. S.	BuAer
Shapiro, L.	Stavid Engineering
Sheitelman, R. D.	BuShips
Shoemaker, L. E.	BuShips
Sledd, M. B.	Georgia Tech
Sletten, C. J.	AFCRC
Smith, P. H.	BTL
Spencer, R. C.	AFCRC
Springer, P. W.	WADC
Steele, E. R.	NADC
Tait, W. O.	Reeves
Taylor, T. T.	Hughes
Telford, W. M.	McGill
Thomas, C. E., Jr.	Gl. Martin
Turner, W. P. (Lt.)	RADC
Van Akin, H.	BuShips
Van Atta, L. C.	Hughes
Vann, W. L.	JHU Applied Physics Lab.
Varenhorst, V. D.	GE
Wallingford, L. E.	BuOrd
Wentush, E.	Fairchild Guided Missiles
Warren, F. G. R.	RCA (Canada)
Wehner, R. S.	Hughes
Weichardt, H. H.	Fairchild Guided Missiles
Wheeler, G. W.	BTL
Wilk, A. J.	JHU Applied Physics Lab.
Wilkes, Gilbert	JHU Applied Physics Lab.
Wilkinson, W. C.	RCA
Williamson, J. C.	GE
Wolf, B. H.	Stavid Engineering
Wynne, J. J.	BuAer

NOTE

The papers presented at the Side Lobe Conference will be included in a separate publication. Those on the attendance list will receive copies.

CONTENTS

WELCOME

Captain F. R. Furth, USN, Director
Naval Research Laboratory

This is the fourth of a series of symposia on scanning antennas. Approximately 18 months have elapsed since our third symposium. In that period, many advances have been made in the art of scanning antennas. It is hoped that we may be able to fully acquaint all the people here with the developments and advances which have been made during this time. We are at least blessed with good weather, and those members from California are going to have to work hard to brag about their weather for it is being duplicated here. It is a pleasure to welcome you to the Laboratory. We are always happy to have you here and we hope that you will benefit by the papers which are to be delivered during the three days. We want you to make yourself at home here, and if you have the opportunity we hope that you will visit some of our laboratories. We are always anxious to welcome visitors, and our scientists are always eager to talk about those phases of their work about which they may talk. It is indeed a pleasure to have you here and we hope that you will enjoy your time. Dr. J. I. Bohnert, Head of the Antenna Research Branch will open the symposium.

OPENING REMARKS

Dr. J. I. Bohnert, Head
Antenna Research Branch, Radio Division I
Naval Research Laboratory

In arriving at our decision to hold this symposium, we used two criteria. First, we felt that enough significant work had been done since the previous symposium in November 1950; and second, we felt that there was enough general interest by workers in the field to have another such get-together. We think that the last symposium did some good in that ideas were discussed, exchanged, and then put into practical antenna design. Some examples would be the Schmidt lens and the Organ-Pipe feed. The success of this symposium will depend not only upon the quality of the papers to be given, but also on the quality and quantity of the discussion from the floor. We therefore hope that you, the members of the audience, will feel free to comment on the papers. I would like at this time to give recognition to Mr. K. S. Kelleher of the Antenna Research Branch who planned and organized this symposium.

WIDE-ANGLE SCANNERS

Dr. R. C. Spencer, AFCRC
(Chairman)

CONCENTRIC SYSTEM SCANNERS *

A. S. Dunbar
Stanford Research Institute

A spherical mirror operating at about f/1 would make a highly satisfactory reflector for all but extremely high-gain antennas. For a shorter focal length system, however, it is necessary to introduce correction for the spherical aberration of the spherical mirror. The Schmidt System, consisting of a spherical reflector and an aspheric corrector plate, is one of the more successful corrected systems. It operates up to speeds of f/0.7. The adaptation of the Schmidt System to a microwave antenna has been described by Chait.[1] Another highly corrected spherical mirror system is the Bouwers-Maksutov or Concentric System.[2,3,4] A third is the Berti System.[5] These latter two systems have been investigated in the course of the work on this project and will be discussed briefly here.

The Concentric System consists of a spherical reflector and a dielectric corrector which is a portion of a spherical shell concentric with the spherical reflector. The corrector introduces spherical aberration comparable to the spherical aberration of the reflector but opposite in sign. A small residual aberration which is independent of the field angle remains, since the focal surface is also spherical and concentric with the reflector and corrector. The Concentric System is represented in the diagram of Figure 1.

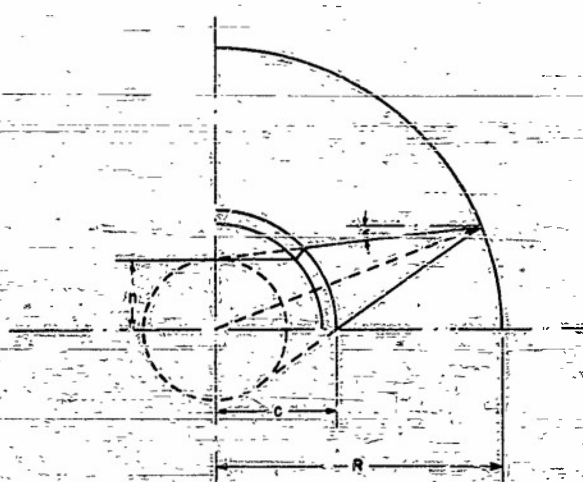

Figure 1 - Concentric System

* This work was supported by the Evans Signal Laboratory Contract No. DA 36-039-sc-5435

1 H. N. Chait, "A Microwave Schmidt System," paper presented at I.R.E. National Convention, 1951

2 D. D. Maksutove, "New Catadioptric Meniscus Systems," J. Opt. Soc. Amer., 34:270, 1944

3 A. Bouwers, "Achievements in Optics," Elsivier Pub. Co., 1946

4 "Wide Field Fast Cameras," OSRD Report No. 4504, Yerkes Observatory, 1945

5 L. Berti, "Un Nuovo Obbiettivo Catadiottrico a Forte Apertura," Nuovo Cimento, 6:131, 1949

It may readily be seen that in this completely centered system the performance at any field angle is precisely that at zero angle, provided the stop is placed at the common center. Thus the only requirement to obtain excellent over-all performance is to reduce the residual aberration to tolerable limits.

The paraxial value of C, the point at which a ray crosses the axis, is given by

$$\frac{1}{C_p} = \frac{1}{F} + \frac{1}{f},$$

where F is the focal length of the reflector (R/2) and f is the focal length of the corrector. The latter is given by the relation

$$\frac{1}{f} = \frac{n-1}{n}\left(\frac{1}{R_1} - \frac{1}{R_2}\right).$$

In order to obtain good corrections it is necessary that C for any given ray should coincide with or differ only slightly from C_p. Consequently, C must be computed as a function of R_1, and R_2, and the ray height h.

From the diagram of Figure 1 and the construction of Figure 2, it may be seen that

$$C = \frac{h}{\sin\left[2 \sin^{-1} (h/R) + \epsilon\right]}$$

and

$$\epsilon = \sin^{-1} (h/R_1) - \sin^{-1}(h/R_2) - \sin^{-1} (h/nR_1) + \sin^{-1} (h/nR_2).$$

Computations have been performed to determine the optimum values of R_1 and R_2, with the reflector radius R taken as unity, for various values of the refractive index.[6] A sample set of parameters is $n = 1.52$, $R_1 = 0.410$, and $R_2 = 0.355$.

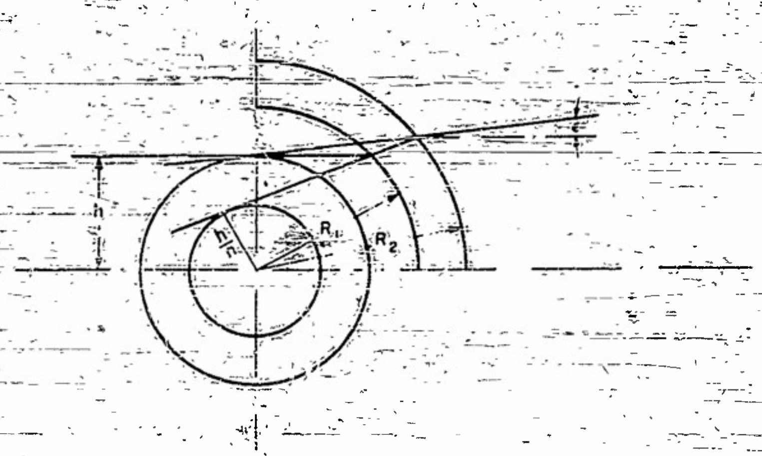

Figure 2 - Construction for ray tracing in Concentric System

6 Second and Third Quarterly Progress Reports, Contract DA 36-039-sc-5435, Stanford Research Institute, pp. 6-9 and 4-5 respectively

An experimental f/0.78 Concentric System has been constructed. A 60-inch hemispherical reflector was procured from the C. W. Torngren Co., Somerville, Massachusetts, and the correcting lens was obtained from Bondwel, Inc., Oakland, California. A novel technique was used in fabricating the polyethylene corrector. Molten polyethylene was sprayed onto an aluminum hemispherical dome, thus building up a shell of the plastic about 2 inches thick. The shell was then machined to the proper thickness and contour.

A photograph of the spherical reflector, feed horn, and lens support is shown in Figure 3; a photograph of the assembled antenna is given in Figure 4.

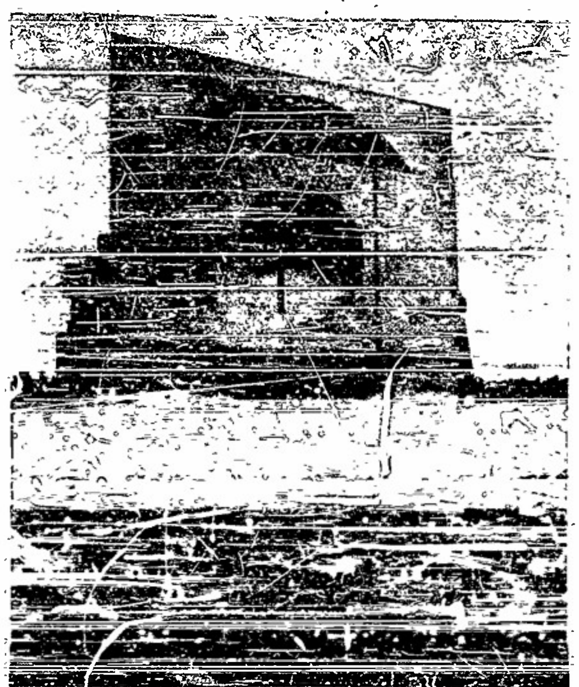

Figure 3 - Spherical reflector, feed horn, and lens support

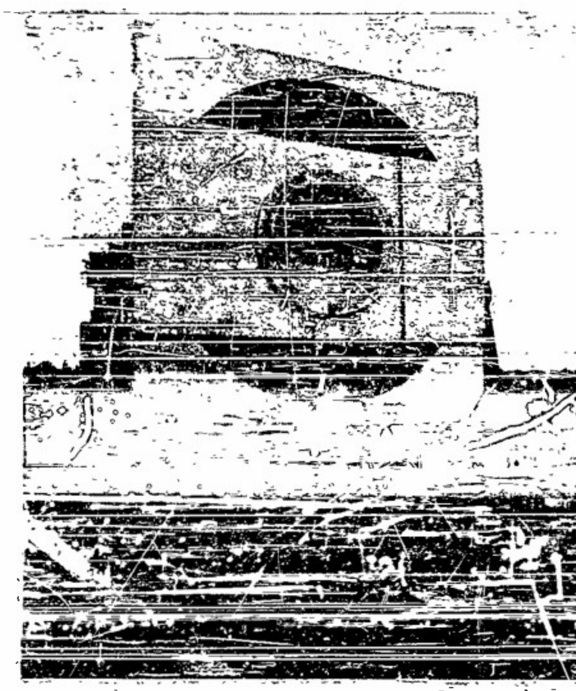

Figure 4 - Assembled antenna

Experimentally measured patterns at $\lambda = 3.2$ cm are shown in Figure 5, for 0° (on axis), 27°, and 41°. These patterns indicate that the field is in excess of $\pm 40^\circ$.

The Berti System is an interesting variation of the Concentric System and consists of spherical reflector and a thick corrector in contact with the reflector. A diagram of the Berti System is shown in Figure 6.

With the aid of the construction of Figure 7, it may be seen that

$$\underline{\epsilon} = \sin^{-1}(\underline{h}/\underline{R}_1) - \sin^{-1}(\underline{h}/\underline{nR}_1),$$

and therefore

$$\underline{C} = \frac{\underline{h}/\underline{n}}{\sin\left[\sin^{-1}(\underline{h}/\underline{nR}) + \sin^{-1}(\underline{h}/\underline{R}_1) - \sin^{-1}(\underline{h}/\underline{nR}_1)\right]}.$$

The paraxial value of C is

$$C_p = \frac{1}{2/R + (n - 1)/R_1}.$$

The focal length of the Berti System is given by

$$\frac{1}{F} = \frac{2(n - 1)}{R_1}\left[1 + \frac{n - 1}{n}\left(\frac{R - R_1}{R_1}\right)\right]\left(1 + \frac{R - R_1}{R}\right).$$

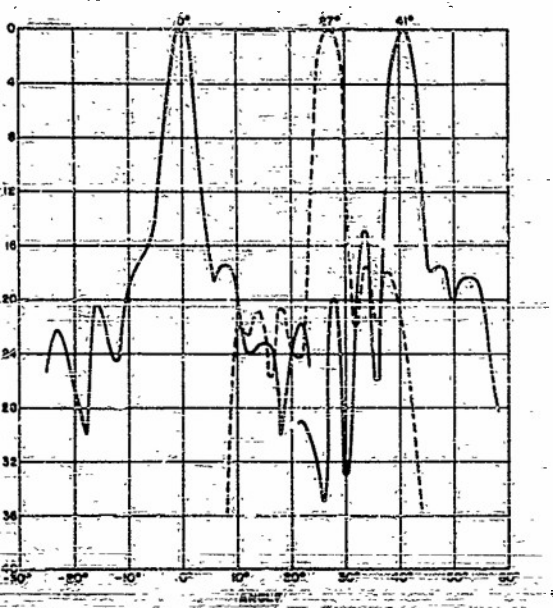

Figure 5 - Concentric System antenna patterns (H-plane)

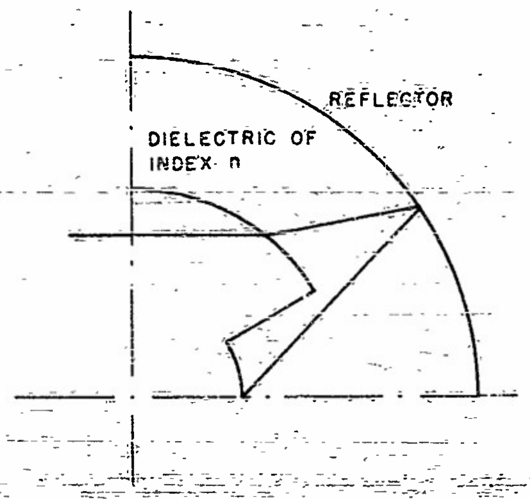

Figure 6 - The Berti System

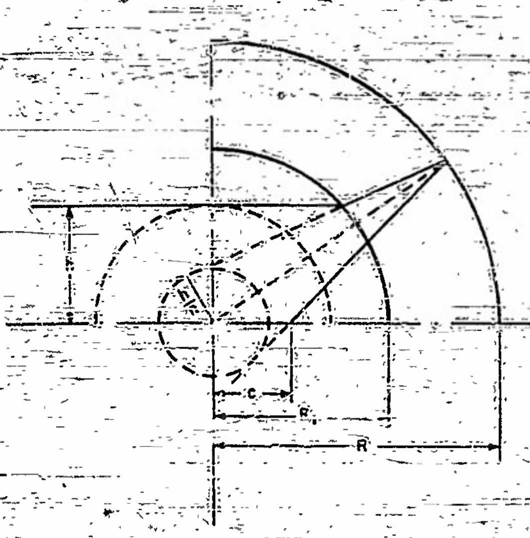

Figure 7 - Construction for ray tracing in Berti System

CONFIDENTIAL
SECURITY INFORMATION

Computations to determine the optimum value of $\underline{R}_1$ for $\underline{n}$ = 1.8 have been made[7] with $\underline{R}$ taken as unity. The result is $\underline{R}_1$ = 0.470. An experimental f/0.47 Berti System has been constructed in a double-layer pillbox. A drawing of the system is shown in Figure 8, and a photograph of the antenna is shown in Figure 9.

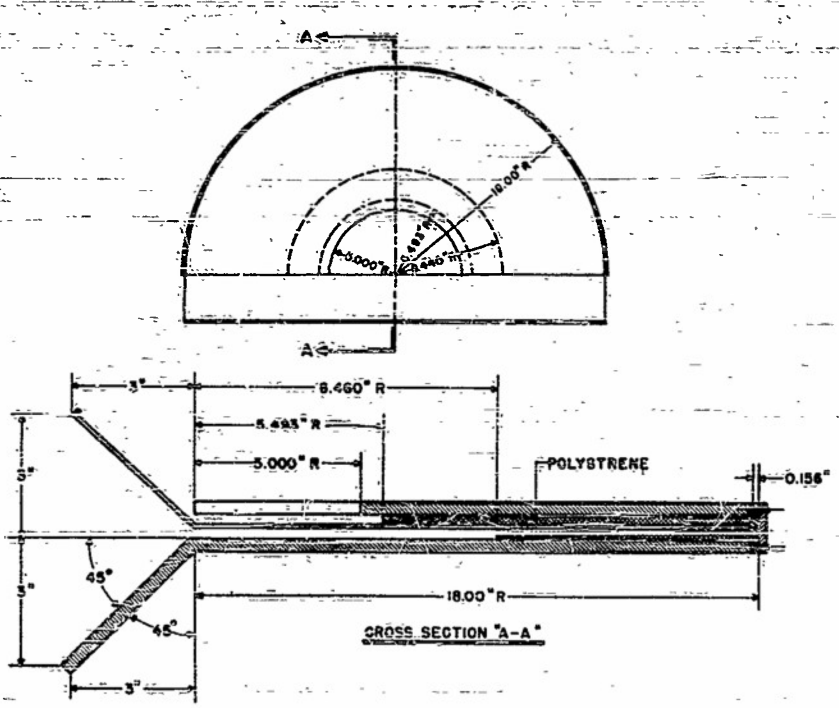

Figure 8 - Cross section of experimental Berti System

Figure 9 - Actual antenna employing the Berti System

[7] Second and Third Quarterly Progress Reports, Contract DA 36-039-sc-5435, pp. 9-10 and 5-7 respectively

Tests of the antenna have been made at $\lambda = 3.2$ cm. Typical patterns are shown in Figure 8. These patterns are seen to be symmetrical neither with respect to their own major lobe nor with respect to the antenna axis. This fact is due principally to the lack of contact between the dielectric sheets and the conducting plates of the double-layer pillbox. Small air spaces between the dielectric and the conducting sheets cause changes in the effective dielectric constant and thus modify the velocity of waves in the medium. This effect probably could be largely eliminated by painting the dielectric sheets with conducting silver paint.

It will be of interest here to examine the performance of a spherical reflector without correction. The condition will be that the diameter of the aberration circle at the focus of the spherical reflector shall be less than the half-power width of the diffraction disc. It may be shown that this condition is equivalent to about 1/4 the Rayleigh Limit.

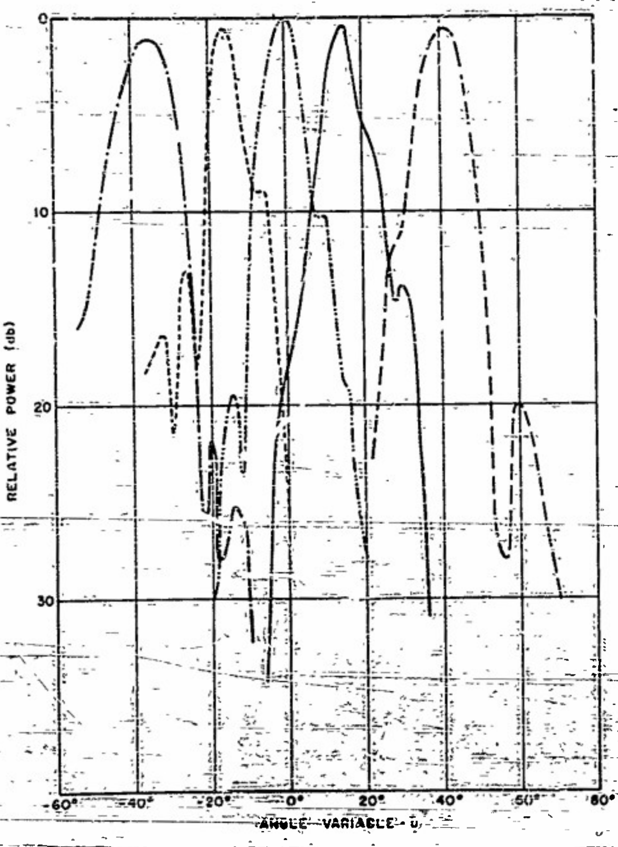

Figure 10 - Berti System antenna patterns (H-plane)

The diameter of the least circle of aberration in a spherical reflector is given to good approximation by[8]

$$\underline{DLC} = \underline{H}^3/16\underline{f}^2,$$

where $\underline{H}$ is the height of the marginal ray and $\underline{f}$ is the focal length. The diameter of the aperture is $2\underline{H}$; the focal length is very closely given by

$$f = \underline{R}/2.$$

The diameter of the diffraction disc at half power is

$$\underline{A} = 1.02\, f\lambda/2\underline{H}.$$

Let us now set the diameters of the two circles equal. It is required to find the maximum permissible diameter $2\underline{H}$. The result is

$$2\underline{H} = 128\lambda(\underline{f}/2\underline{H})^3,$$

where $(\underline{f}/2\underline{H})$ is the focal length to diameter ratio. Table 1 gives the maximum diameter of the aperture of a spherical reflector which satisfies the condition that the aberration be equal to 1/4 the Rayleigh Limit.

A comparison of the uncorrected spherical reflector with the Concentric and Berti Systems is afforded by Tables 2 and 3. The Concentric System is compared with a spherical reflector with and without a stop in Table 2. The Berti System employing a double-layer pillbox is compared with the uncorrected double layer pillbox in Table 3. It is evident that correctors yield little or no improvement. It may be seen with reference to Table 1 that this condition will prevail so long as the focal-length-to-diameter ratio of the reflector is close to 1 and the diameter is less than 100 wavelengths.

---

8 A. Bouwers, op. cit., pp. 7, 8.

TABLE 1
Diameters of Spherical Reflectors Satisfying 1/4 Rayleigh Limit

f/2H	2H
3.0	3456
2.0	1024
1.0	128
0.5	16

TABLE 2
Comparison of Spherical Reflector with Concentric System

	Beam Angle	Gain Reduction	Half Power Width	First Side Lobe	Half Power Width E-Plane	First Side Lobe E-Plane
60″ Hemispherical reflector with concentric lens H-Plane	0°	0 db	4°	18 db	4°	26 db
	27°	0 db	4°	18 db		
	41°	½ db ?	4°	15 db		
	49°	2 db	5°	12 db		
60″ Hemispherical reflector with plywood stop H-Plane	0°	0 db	3.4°	19 db	3.4°	26 db
	17°	0 db	3.3°	19 db		
	29°	0 db	3.4°	18 db		
	45°	2 db	3.6°	12 db		
60″ Hemispherical reflector with no stop H-Plane	0°	0 db	2.5°	14 db		
	30°	0 db	2.9°	18 db		
	45°	0 db	3.0°	14 db		

TABLE 3
Comparison of Berti System with Uncorrected Double-Layer Pillbox

	Beam Angle	Gain Reduction	Half Power Width	Side Lobe
With Concentric Lens H-Plane	0°	0 db	8°	10.3 db
	16°	½ db ?	8°	8.8 db
	35°	1 db ?	11°	21 db
	42°	1 db ?	11°	11 db
No lens H-Plane	0°	0 db	5.3°	20.5 db
	30°	0 db	5.3°	20.5 db
	45°	0 db	5.3°	19.5 db

DISCUSSION

Budenbom: (BTL) Did your spherical reflector have a 60-inch aperture?

Dunbar: (SRI) This was an X-band reflector with a 60-inch aperture, but it had an effective aperture of 20 inches.

Budenbom: We at Bell Telephone Laboratories are working on a circular reflector with correction at the edge of the aperture similar to that used by Mr. Chait. I was trying to get a comparison on beamwidths or aperture efficiency.

Kelleher: (NRL) Could you tell us what criterion you used in determining what size aperture could be used with what f/D ratio?

Dunbar: We can use the circle of confusion to define spherical aberration. We make the circle of confusion equal to the half-power width of the Airy disk.

Kelleher: Have you tried to relate that condition which might be considered as a received condition to the transmit condition using a point source and evaluating the phase error over your aperture?

Dunbar: Yes, it turns out to be the same.

Kelleher: Dr. M. L. Kales here at NRL did some similar work. I believe he reached the same conclusion that the circle of confusion condition and phase error condition gave the same results.

Chait: (NRL) I believe the conclusion we reached was that the optimum phase error condition and the circle of least confusion occurred at the same focal point. If we were to plot the size of the circle of least confusion and the maximum amount of phase error as a function of focal point, the curves might not necessarily coincide.

Sletten: (AFCRC) I would like to give some information to the BTL people. We used a corrected line source with the same size spherical reflector as that employed by Mr. Dunbar. In the same plane we were able to get beamwidths of less than 2°. However, we illuminated only one-half of the sphere; so in the other plane our beamwidths were about 4°. We think that for a perfect correction, a sphere of that size should produce a 2-degree beam.

A RAPID-SCAN, CIRCULARLY SYMMETRICAL PILLBOX ANTENNA

Walter Rotman
Air Force Cambridge Research Center

ABSTRACT

A directional antenna for microwave applications, capable of high-speed scanning and using several novel techniques, has been designed and tested. Construction is of the waveguide-fed, double-layer pillbox type, but with a circular radiating aperture instead of the customary linear one. A sketch of the antenna with the emerging rays indicated is shown in Figure 1.

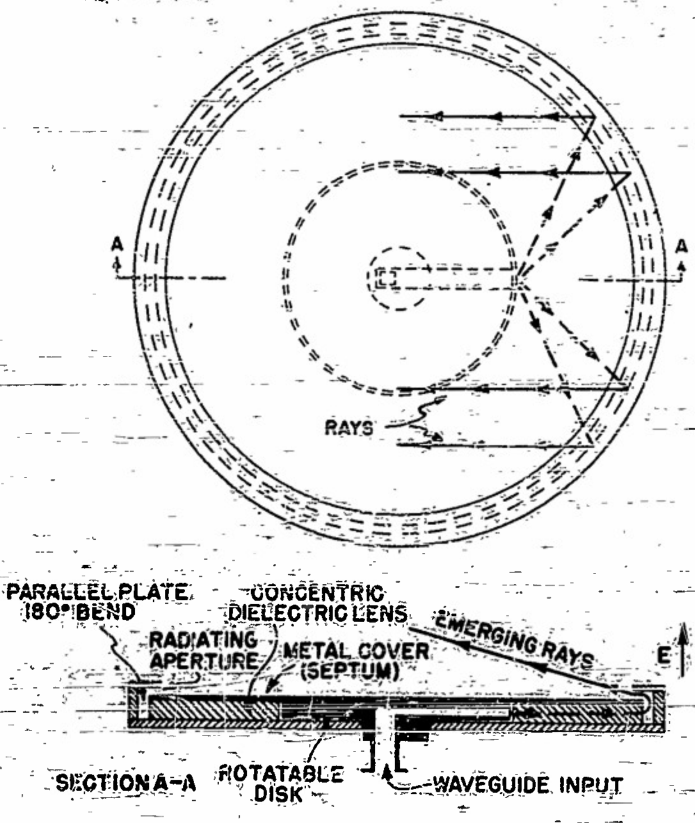

Figure 1 - Double-layer concentric pillbox

The operational basis of the antenna is derived from the fact that radiation from a point source may be approximately collimated by a suitably located spherical reflector or, in parallel plate structures, by a circular cylindrical reflector. For such a cylindrical reflector the limitation upon the degree of collimation is principally imposed by spherical aberration, which may be partly eliminated without destroying axial symmetry by introducing a circularly-symmetric dielectric lens between the parallel plates. Alternately, geodesic principles of the type described by Myers[1] may be employed to markedly reduce the spherical aberration. The following remarks apply only to the dielectric lens corrector, however.

If the structure is made in the form of a double-layer pillbox, the lens may be enclosed within the same layer as the point source feed. The collimated beam then passes through the pillbox bend into the alternate layer or top of the pillbox. In place of the customary linear aperture, however, a circular aperture radiating over the upper surface of the pillbox is used. Circular symmetry of all reflecting and refracting elements is thus preserved. Furthermore, a circular aperture, lying in the horizontal plane and radiating over a metal plane, produces a much narrower beam in

[1] Myers, S. B., "Parallel Plate Optics for Rapid Scanning," Journal of Applied Physics, 18: 221, February 1947

elevation than would be obtained from an equivalent linear aperture. Control of the surface characteristics of the metal plane by dielectric loading or corrugations or both permits changes in elevation pattern without affecting appreciably the pencil-beam characteristics of the azimuthal pattern.

This antenna possesses characteristics which make it adaptable to several applications:

1. Complete axial symmetry of all stationary portions. Hence, the antenna is capable of high-speed scan through either 360° or any sector thereof by simple rotation of the relatively small central hub.

2. Narrow azimuthal pattern and shaped elevation pattern.

3. Adaptability to flush mounting. The pillbox, except for transmission line input, is in the form of a circular plate only one or two inches thick at X-band and may be made an integral part of any flat surface.

4. Simultaneous scan in several directions. Since (if all bends and transitions are perfectly matched) no reflected energy is incident upon a transmitting waveguide point source, a multiplicity of sources may be used simultaneously without mutual interference.

Experimental and theoretical studies to determine the properties of the antenna have been conducted and are now being analyzed. A model has been built and successfully tested.

***

DISCUSSION

Spencer: (AFCRC) I would like to comment on the Myers Radiation Laboratory report. A lot of the work described by Myers was done by other people. A large part of it was stimulated by a suggestion from Dr. Chu. A feed source could be moved around the base of some object such as a jardiniere. Energy would travel in geodesics around the side walls and be radiated from a diameter across the top. Considerable work has been done in proving or disproving this idea. I think that I succeeded in showing that such a system had inherent spherical aberration. This is evident if we consider that this surface can be pushed down to form a two-layer parallel-plate system with a circular reflector. There appears to be some correction when we use a cylindrical surface since the wave fronts would turn up and you can defocus. Charley Robinson found that he could insert a layer of dielectric and correct some of the spherical aberration. This is in agreement with a statement of Dr. Kingslake of Eastman Kodak Company who says that no matter where you put a dielectric you obtain the opposite sense of spherical aberration from that of the reflector.

Kelleher: (NRL) Mr. Sakiotis of NRL has worked on what we might call the Myers' geodesic problem. He used a type of analysis essentially different from that employed by Myers. He tried to minimize phase error across the entire aperture, whereas I believe that Myers' analysis was more valid in the center of the aperture. I have a question for Mr. Rotman: Was this structure a cylinder or a cone?

Rotman: (AFCRC) It was a portion of a right circular cylinder.

Kelleher: It was my idea that Myers' results, described in the Journal of Applied Physics article, indicated the best cylinder to be one with a zero height.

Rotman: Myers showed that the best solution is one in which the height is approximately 1/3 of the radius. For a cylinder of zero height he compares a 30-inch aperture with a 60-inch aperture. The 60-inch aperture is superior, of course, when we use only the center 30 inches.

Kelleher: One further question: Just how did you support your plates? That was one of our problems which we felt must be solved before we could build Mr. Sakiotis' model.

Rotman: With our semicircular structure we supported the plates with metal bars at the edges. We were fortunate to find a spot where we could put metal supports. For our 360-degree model, we expect to use nonreflecting metal posts which have been developed both at our laboratories and at Bell Telephone Laboratories.

Warren: (RCA) What was the effective aperture of your system?

Rotman: We used 75% of the physical aperture; for the geodesic type we used approximately 60%.

FOSTER SCANNER DEVELOPMENTS

J. C. Foster and W. M. Telford
McGill University

BASIC PRINCIPLE OF THE FOSTER SCANNER

In its most elementary form the Foster Scanner may be considered as a line source pivoted and moving at uniform speed in such a manner that when it has moved through a given angle it snaps back to the original position. The source must be placed on the surface of a cone and this cone revolved inside another cone. Suitable barriers and an exit slit in the outer cone are necessary additions.

REQUIREMENTS OF THE PRESENT SCANNER

This scanner which is being developed under Subcontract No. 2-7-1316 from the National Research Council is intended for a Canadian Army application. The system requires a double beam — one above the other — each scanning 20 degrees and both obtained from a single reflector. The speed of scan is approximately 15 scans per second for both beams, and the beamwidth must be equal to or less than 1 degree in both planes. No dimension of the equipment shall be longer than 78 in. It should be as light as possible and should operate at a wavelength of 1.87 cm. Several possibilities were suggested, but it was decided to construct the scanner with the following features:

1. A single waveguide slot array to be fed through a rotating joint on the rotor shaft
2. A 40-degree developed cone to have a 14-degree vertex angle when rolled into a cone
3. Two exit slits 180 degrees apart to introduce the radiation into separate horn feeds energizing a single reflector; each feed to be slightly off the focal line of the reflector
4. Rotor and stator cones to be fabricated as far as possible from sheet metal.

DATA ON SINGLE-SLOT AND ON THE 100-SLOT ARRAY

The data on a single slot has been obtained from bench measurements of short sections. It was decided to use shunt slots in the array. The conductance of a single slot is given by $G/G_0 = \sin^2\theta$ for the tapered-mouth arrangement used. The illumination across the array matches a somewhat arbitrary symmetrical gabling function, and it was matched by using ten groups of ten slots each. The amplitudes are given by Table 1.

TABLE 1
Illumination Values for the Array

Slot Number	1-10	11-20	21-30	31-40	41-60	61-70	71-80	81-90	91-100
Amplitude	.30	.40	.55	.80	1.0	.80	.55	.40	.30

The spacing of slots was 230 degrees which gave a 10-degree squint angle and made maximum use of inner cone space. The theoretical pattern was computed for a 100-slot array 58-1/4 in. long (without end load). The beamwidth was .72 degrees at half power, and the side lobes were less than 5 percent in field strength. Experimental patterns were taken at 16,050 megacycles at which the beamwidth was .74 degrees at half power, and the side lobes were 10 percent in field strength or 20 db down. The angle of squint changes by 1 degree for a 1.7-percent frequency change.

ASSEMBLY OF SOURCE IN THE ROTOR

The channels for leading the radiation from the array to the inner cone space were extruded by the Aluminum Co. of Canada by a process which was relatively inexpensive. The shaft which supported the inner cone was purposely made hollow to take a waveguide feed line. The array was fed from waveguides passing through a hole in the wall of the shaft. The rotor joint connected to this waveguide was mounted on the end of the shaft.

METHOD OF CONSTRUCTION OF ROTOR AND STATOR

The rotor and stator skeletons were made of 65ST machined ribs. A channel was built into the rotor opposite the array in order to obtain a counter-balance effect. All tooth barriers (three sets) were machined together at one time on a milling machine to eliminate any difficulty in meshing the teeth. The sheet metal skins for the rotor and stator were rolled into half cones, assembled on the frames, and riveted with Cherry rivets. The tolerances on the teeth were .031 in. between the teeth and the skin and .037 in. between adjacent teeth as two tooth barriers were meshed.

CONSTRUCTION OF THE REFLECTOR

The reflector was an asymmetrical parabolic cylinder which was cut along a line 6 in. from the vertex line to avoid feed obstruction; in its final form it was 60 x 90 in. It was made of sheet metal with riveted construction and weighed about 135 lbs. One feed horn was placed 2 in. inside of the focal line and 45 degrees below the axis; the other was placed 2 in. outside the focal line and 15 degrees above the axis.

DISCUSSION

Foster: (McGill) I have always felt that the main problem was to make the thing. Anyone can see that it will work. We would like to be academic but we cannot in this case. A main problem is to get a scanner made. The extruded material made within the past few years by the Aluminum Company of Canada together with the idea of cutting all of the teeth at one time has removed any vestige of trouble about making the teeth. The other change has been to employ aircraft techniques; thus avoiding lengthy machine work on a large lathe. We have the two best organizations in Canada working on that. We have one set in already and it looks pretty good. We thing the future models will be even better.

Miller: (NRC) Dr. Foster has been handling this scanner under contract from us and he is ahead of our schedule. There is one problem related to this scanner which I would like to mention. We have two feed horns energizing a single reflector. Naturally both could not be on the focal line. If we used a normal reflector and put the two feed horns in the focal plane and displaced from the focal line, we would get poor beam characteristics. However, since we were using a half parabola this restriction to the focal plane was no longer necessary. Dr. Gruenberg of our laboratories developed a theory which indicated correct positioning for the two feeds. The results, when applied to the experimental reflector obtained from McGill University, were highly satisfactory. A space between the two feed horns was a little over two beamwidths. The side lobes were about 26 db down in both cases.

Kelleher: (NRL) Has Dr. Gruenberg published this information in any form? The use of a half parabola presents a different picture when the feed is moved in approximately along the axis. With the feed at the focal point we get a wavefront normal to the axis. If we move in and out along the axis of the half parabola, our average phase front is no longer normal to the axis. Did this fact have to be considered in Dr. Gruenberg's work?

Miller: I don't know about that detail. Perhaps Dr. Gruenberg has the answer.

Gruenberg: (NRC) The essential thing in the analysis is that in the full parabola you have a cubic phase error, whereas in the half parabola you have a quadratic phase error plus a linear term; and you can compensate for that by defocussing. You can get an optimum direction along which the feed can be moved. That direction is in line at about 20 degrees to the axis.

Kelleher: I believe that answers my question. Your feeds were not along the axis of the reflector.

Adams: (NRL) We, like Dr. Foster, have been interested in obtaining a scanner for some time. We reported on our r-f work at the previous symposium. I would like to announce that we have a scanner now. It may be seen on the roof of Building 50. We also have representatives from American Machine and Foundry Company who will be glad to explain their machining techniques.

AIRBORNE SCANNER FOR NIGHTHAWK

W. C. Wilkinson
RCA, Princeton, N. J.

This antenna is part of Nighthawk, an experimental airborne high-resolution radar set being developed for BuAer for use in short-range air-to-ground search. The system operates at 35,000 Mc. It will have a range resolution of about 6 feet by the use of a 10-millimicrosecond pulse and an azimuth resolution of about 0.4 degree by the use of a 5-1/2-foot aperture.

System needs which determine the target specifications of the antenna are:

Frequency	35,000 Mc
Horizontal beamwidth	0.3 - 0.4 deg.
Horizontal scan angle	25 - 45 deg.
Horizontal scan rate	10 - 30 per sec.
Vertical beamwidth	0.5 - 2 deg.
Vertical train angle	0 to -45 deg.
Three-axis stabilization:	
roll	±15 deg.
pitch	±5 deg.
yaw	±45 deg.
Pulse length	10 millimicroseconds

Because of the wide scan angle and relatively high scan rate, it is thought that the Foster type of scanner is best suited for this job. To produce 30 degrees or 75 beam-widths of scan, the scanner will be about 6 feet long and 15 inches in diameter. The feed will be either a slotted-waveguide linear array or a pillbox, the choice being made on the basis of mechanical tolerances and space available. The Foster scanner will feed a half-parabolic cylindrical 12-inch reflector of 6-inch focal length for vertical focusing to a narrow beam 1.8 degrees wide. The complete antenna will be mechanically stabilized for airplane motion and will be housed in a radome about the same size as that of the AN/APS-20 (8 feet in width and 3 feet in depth). The entire antenna will be rotated for elevation train.

Expected problems are: maintenance of parallel sheet spacings, fabrication of barriers for the scanner, asymmetrical feed for vertical dish, and general construction difficulties. A form of tuned spacer will be used to reduce rigidity requirements in the flat sections of the scanner. A sample spacer tested in waveguide had a VSWR of 1.3 or less over the magnetron frequency range (about 2 percent) and a loss of 0.2 db. It is proposed that two or more choke barriers be used instead of the commonly used meshing waveguide-beyond-cutoff type. This will relieve some of the mating tolerances between the stator and rotor and will place the close tolerances in the choke dimensions. Preliminary measurements indicate approximately 20 db for the combination of two simple quarter-wave chokes.

Fabrication of the stator-rotor assembly has been started, and it is expected that flight tests of the system will begin sometime this fall.

DISCUSSION

Dunbar: (SRI) Has there been any attempt made to prevent the longitudinal propagation of energy in the long choke grooves?

Wilkinson: (RCA) We have not done anything along those lines as yet. There is some indication that we have the effect you mention. Our experimental work has involved feeding from one long-tapered horn into another long-tapered horn through a short section in which we put the chokes. There is some indication of unusual effects. This type of choke groove was described in a Radiation Laboratory report. They did not mention this effect which you have brought up. We expect to do further work on our experimental model in an attempt to resolve this problem.

Feiker: (GE) Brown at Syracuse had this idea at one time, but he never did try it out.

Foster: (McGill) The best way to handle the problem is to push the energy down the drain as fast as you can.

Abbey: (NEL) Dr. Tomiyasu of Sperry has done considerable work with longitudinal chokes and has developed a choke which eliminates this difficulty.

Wilkinson: I have a question I would like to direct to Dr. Foster. Some of your previous work under a USAF contract indicated vibrational problems in your fabricated structure when high speeds were attempted. The structure, as I recall, was welded and then some machine work was done. It appears that perhaps this present model requires no machining. Is this true?

Foster: This model which you refer to fell into the hands of a bad machinist and he ruined it before anyone could stop him. The model was not balanced. If you are going to do any machining you might as well have a casting. The idea now is to put the model together so that no machining is necessary.

FOSTER SCANNER DEVELOPMENTS

G. E. Feiker
General Engineering Laboratory
General Electric Company

Two Foster scanners are presently under development for use in search antenna systems. These are of two different types, the first a double-beam scanner and the second a single-beam scanner. The first type is illustrated in Figure 1. A traveling-wave line source attached to the rotor collimates the azimuth beam at an angle to the line source equal to half the scan angle. During half the scanning cycle the beam is scanned in azimuth through the exit horn A and during the remainder of the cycle through horn B. These horns are displaced on either side of the focus of an asymmetrical slat-type reflector in such a way that the beams scan sequentially in azimuth at different elevation angles.

Design work has been completed and a prototype is under construction. Barriers have been matched in parallel plates to less than 1.06 VSWR over a 2-degree bandwidth in the X-band. The line source, consisting of 20 groups of 4 slots each, was designed to approximate a Dolph distribution. The experimental pattern is shown in Figure 2. The design figure for side-lobe level was 30 db; first side lobes varied between 23 db and 28 db. The input VSWR was less than 1.05 over the band.

The second Foster scanner under development is of the feed-through type fed from an external pillbox, as shown in Figure 3. Since the system will employ coherent MTI,

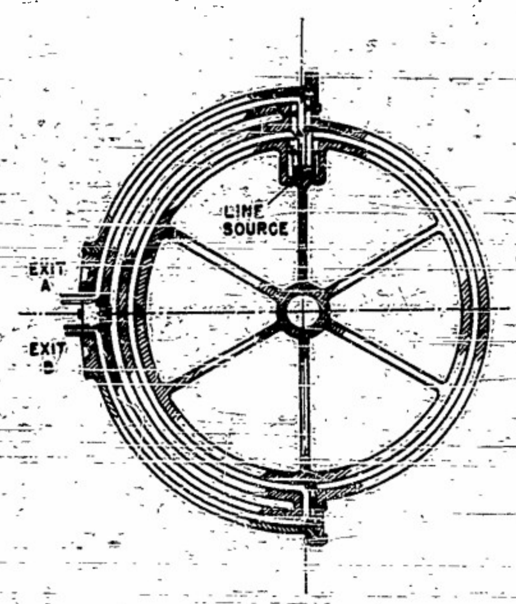

Figure 1 - Double-beam Foster scanner

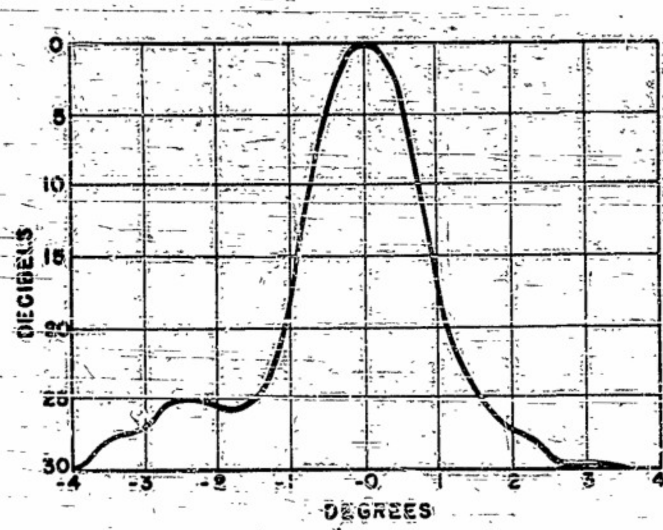

Figure 2 - Radiation pattern of line-source array

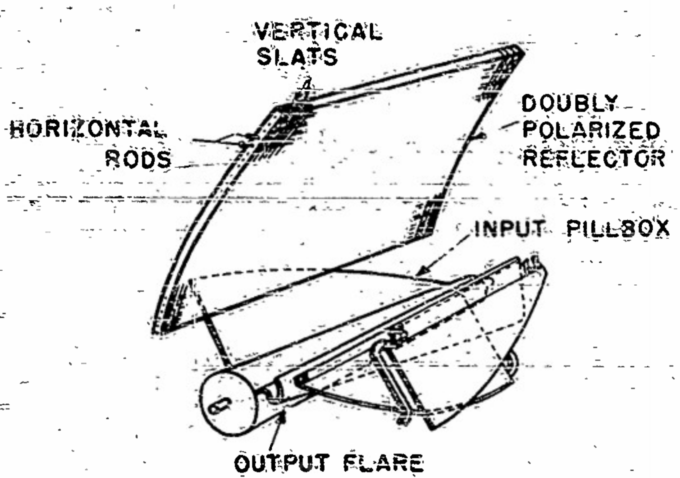

Figure 3 - Single-beam Foster scanner antenna assembly

any reflections during scan must be exceedingly small. Accordingly, the scanner has been designed so that the barriers are never parallel to the wavefront. This design is illustrated in Figure 4 which shows the developed view of the scanner. An output flare has been added in order to center the scan about the normal to the exit horn. This flared section has been rolled up, as shown in Figure 3, to keep the exit horn parallel to the scanner axis. As illustrated in this figure, the scanner output horns and separate tracking feeds illuminate a common reflector having two reflecting surfaces. The front surface collimates the vertical polarization from the search feed, and the rear surface collimates the horizontal polarization from the track feeds.

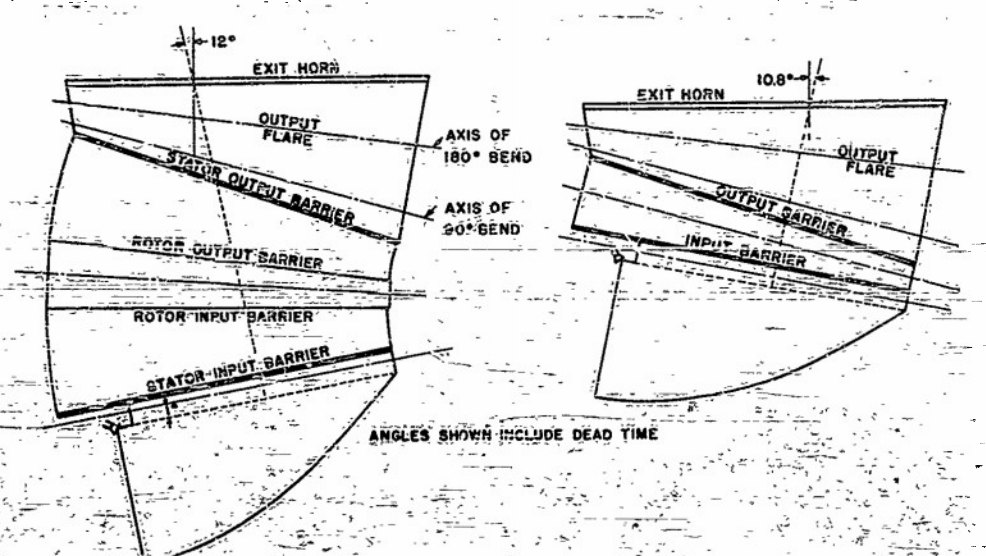

Figure 4 - Plane developments of scanner at ends of scanning cycle

ON THE MANGIN MIRROR *

Roy C. Gunter, Jr.
Clark University, Worcester, Massachusetts

INTRODUCTION

In view of existing effort in the field of radar scanning antennas, it seemed that the next logical step was the design of a multiple element system, probably a separated doublet; the writer, however, suggested that it might be well to examine certain other phases of the general problem before embarking on a specific design problem. The point was raised that the possibilities of high and low index spheric and aspheric singlet dioptric systems had been considered; catoptric systems such as the parabola, sphere, etc., had been extensively investigated; but an equally extensive study had not been made of catadioptric systems. A philosophical examination of the catadioptric system shows that the corrector plate may be placed in one of three possible positions: (a) in front of the mirror, (b) coincident with the mirror surface, or (c) behind the mirror. Combinations of these are also possible. System (a) had been studied by Stanford Research Institute and others and reported under the generic terms of Schmidt, Bouwers, etc. System (c), while at first glance appears ridiculous, is actually a distinct possibility if one admits the various folded systems of the Schmidt type. System (b), however, apparently has been little considered, and accordingly it seemed advisable to investigate it. Since this system is classically known as a "Mangin Mirror," this term will be retained.

THE MANGIN MIRROR

Fundamental Considerations

Prior to the introduction of the paraboloidal mirror by the Germans, the spherical mirror was widely used in searchlights. An obvious disadvantage was the spherical aberration which caused a broadening of the beam as the reflector was "opened up," i.e., used at high relative apertures.

An attempt to improve the performance of the spherical system was first made by A. Mangin[1,2,3,4,5] in 1876. In essence, his corrector consisted of a negative spheric lens in contact with the surface of the mirror, as shown in Figure 1.

* This work was supported by the U.S. Signal Corps via Contract No. DA36-039-SC-5459, with the Stanford Research Institute

[1] A. Mangin, Memorial de l'Officier d'Ingenieur, Paris (1876)
[2] A. Mangin, Assoc. Franc. pour l'Avancement de la Science, p. 339 (1878)
[3] A. Blondel, Theorie des Projecteur Electriques, (A. Lahure, Imprimeur-Editeur, Paris, 1894), p. 32 et. seq.
[4] Dictionary of Applied Physics (Macmillan and Co., Ltd., London, 1923), Vol. IV, p. 524
[5] L. C. Martin, Technical Optics (Pitman Publishing Co., New York, 1950), Vol. II, pp. 253,4

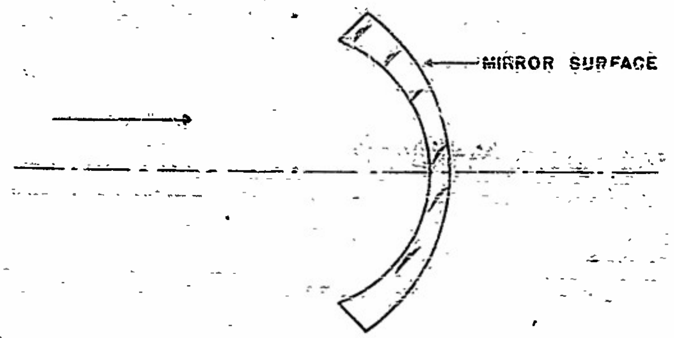

Figure 1 - The Mangin Mirror

In practice, the corrector was ground and polished, and then the rear surface was silvered. Such units were demonstrated to be sensibly free from spherical aberration, and coma was quite low. The system never received much favor, largely because of the steep curve on the front surface and the consequent excessive thickness of glass at the margins. Further, the paraboloid, while harder to make in one sense than a spheric, was essentially a simpler system.

The fact remains, however, that Mangin did show it was possible to correct a spherical reflector for both coma and spherical aberration, and for very large relative apertures at that. Unfortunately, details of Mangin's work are to be found only in obscure French Government pamphlets; hence, it was decided that the quickest way to assess the advantages of the system was to actually calculate it out. To this end a radius and aperture were chosen for the mirror surface that would give approximately an f/1 system, and then the curvature of the front surface was varied. It should be borne clearly in mind that this is not "bending" the lens in the strict optical sense of the word inasmuch as the paraxial focal length was not kept constant.

It has been pointed out that one of the prime difficulties with the Mangin system is the excessive marginal thickness. Considering the wavelength region in which we are working, it occurred to the writer that it might be feasible to adopt a basically different fabrication technique. This would involve spinning the spherical reflector and then spraying on the correction coating. The coating would then be finished to a zero center thickness ($t = 0$). In an analysis one should consider the effects of varying the radius of the first surface and the index of the dioptric material. Although the investigation was directed toward finding a zero center thickness, it seemed advisable to investigate, to a limited extent, the effect of finite center thickness. The following sections comprise a discussion of the aberrations—spherical, coma, and astigmatism—which are of greatest interest to the designers of rapid-scanning radar antennas.

Spherical Aberration and Coma

While there do exist relatively simple analytical expressions that will give the primary spherical aberration with satisfactory exactness for systems at high f-numbers, such expressions are not, in general, satisfactory for f-numbers in the vicinity of unity or less. Because of this, an exact trigonometrical ray-tracing procedure was used to determine the spherical aberration (LA'). Angles were carried out to an accuracy of $\pm .0001^{\circ}$ but with six decimal figures carried along routinely to avoid any rounding off errors. Since the amount of calculation in such a ray-tracing procedure is extensive, only the results will be reported.

Tables 1, 1A, 2, and 3 show the variation in LA' and Coma as the chosen parameters are varied. The units used are relative units.

As the purpose of this investigation was not to come up with a design for an optimum system but rather to explore the possibilities of a principle, a somewhat simplified measure of coma (sagittal) was employed. This is not the true OSC' as referred to by Conrady.[6]

[6] A. E. Conrady, Applied Optics and Optical Design (Oxford University Press, London, 1929), p. 370 et. seq.

TABLE 1

LA′ — For Various Values of R_1; n = 1.52, t = 0, R_2 = -4

R_1/R_2	LA′ h = .866051	LA′ h = 1.224769	LA′ h = 1.500000	Paraxial Focal Length
.6	-.028196	-.062719	-.118692	+3.061212
.64	-.011255	-.033691	-.052525	+2.826863
.66	-.005092	-.014343	-.029056	+2.731785
.68	+.00152	-.002639	-.009425	+2.647968
.70	+.004826	+.007550	+.007491	+2.573526
.74	+.012811	+0.25856	+.035902	+2.447094
.80	+.022805	+.046268	+.070335	+2.298850

TABLE 1A

Coma — For Various Values of R_1; n = 1.52, t = 0, R_2 = -4

R_1/R_2	Coma h = .866051	Coma h = 1.224769	Coma h = 1.5	Paraxial Focal Length
.6	-.004171	-.005197	+.014833	+3.061212
.64	+.019259	+.030909	+.043324	+2.826863
.66	+.025954	+.049134	+.068245	+2.731785
.68	+.032187	+.062871	+.090987	+2.647968
.70	+.038026	+.075668	+.111915	+2.573526
.74	+.048797	+.104199	+.149387	+2.447094
.80	+.062762	+.128425	+.197135	+2.298850

TABLE 2

LA′ and Coma — For Various Values of n; h = 1.5, t = 0, R_1 = +.68R_2, R_2 = -4

n	LA′	Coma	Paraxial Focal Length
1.35	+.037533	+.156861	+2.394366
1.52	-.009425	+.090987	+2.647968
1.75	-.068204	+.007771	+3.092031
2.20	-.215988	-.139797	+4.594596

TABLE 3

LA′ and Coma — For Various Values of t; h = 1.5, n = 1.52, R_1 = -.68R_2

t	LA′	Coma	Paraxial Focal Length
0	+.009425	+.090987	+2.647968
.04	-.005412	+.096446	+2.608319
.08	+.001782	+.101690	+2.569567
.16	+.006188	+.113096	+2.494711

The technique is an application of the Sine Condition in the presence of spherical aberration. Details of this technique may be found in Jenkins and White.[7] The governing equation is:

$$\text{Coma} = \text{spherical aberration} - (f'_p - f'_m), \qquad (1)$$

where $f'_m = h/\sin\theta'_m$ and θ'_m = closing angle for the last surface, f'_p being the true paraxial focal length measured from the second principal surface. Detailed discussion of these aberrations as well as astigmatism will be withheld until the discussion.

[7] F. A. Jenkins and H. E. White, Fundamentals of Optics (McGraw-Hill Book Co., Inc., New York, 1950) pp. 135,6.

Astigmatism

To investigate the astigmatism the equations of Coddington[8] were used. These are:

$$\frac{n\cos\phi}{s} + \frac{n'\cos\phi'}{s'_t} = \frac{n'\cos\phi' - n\cos\phi}{r} \tag{2}$$

$$\frac{n}{s} + \frac{n'}{s'_s} = \frac{n'\cos\phi' - n\cos\phi}{r}. \tag{3}$$

In both equations, ϕ and ϕ' are the angles of incidence and refraction, respectively, of the chief ray at each surface. Image and object distances are measured along the chief ray. These equations are not really accurate for wide apertures, but they do furnish a first approximation. In the final analysis of an actual design for wide aperture systems trigonometrical ray tracing would be employed.

Tables 4 and 5 show the effect of varying R_1 and the index. Figure 2 is a graphical presentation of the results of Table 1 for $R_1 = .70R_2$. Because of time limitations, no attempt was made to check the effect on astigmatism of an increase in center thickness. It is not anticipated that such a procedure would be fruitful unless the thickness is increased excessively.

TABLE 4
Astigmatism — For Various Values
of R_1; $t = 0$, $R_2 = -4$, and $n = 1.52$

R_1/R_2	Astigmatism ($S'_s - S'_t$) $\theta = 8°$	$\theta = 12°$	$\theta = 20°$*
.66	+.050069	+.113311	+.328592
.70	+.045764	+.103922	+.297019
.74	**	**	+.248131

* θ = semi-field angle
** not calculated

TABLE 5
Astigmatism — For Various Values
of n; $t = 0$, $R_2 = -4$, and $\theta = 20°$

n	Astigmatism ($S'_s - S'_t$) $\theta = 20°$
1.52	.297019
1.75	.367310

DISCUSSION

Critical evaluation of the performance of any image-forming system is generally effected by comparison first with an absolute standard, such as Rayleigh Limit, and then

8 These equations are generally attributed to Coddington. A derivation of them may be found in G. S. Monk, Light, Principles and Experiments (McGraw-Hill Book Co., Inc. New York, 1937) first edition, p. 424.

with existing systems designed to do the same job. Accordingly, we discuss our modified Mangin system (henceforth abbreviated MMS) first in terms of the Rayleigh Limit and then by comparison with its existing counterparts.

System Aberrations vs. Rayleigh Limit

While the statement of the Rayleigh Limit in terms of path difference is fundamental, the statement of optical aberration tolerances in this manner is inconvenient. It can be shown that the Rayleigh Limit may be restated in terms of spherical aberration, coma, and astigmatism as follows:[9]

$$\text{Tolerance for LA}' = \frac{4\lambda}{n' \sin^2 \theta'_M} \tag{4}$$

$$\text{Tolerance for Coma (sagittal)} = \frac{\lambda/2}{n' \sin \theta'_M} \tag{5}$$

$$\text{Tolerance for OSC}' = \frac{\lambda/2}{n' H' \sin \theta'_M} \quad \frac{\text{coma (sagittal)}}{H'_K} \tag{6}$$

$$\text{Tolerance for focal range} = \frac{\lambda}{n' \sin^2 \theta'_M} \tag{7}$$

where θ'_M is the closing angle, n' the index of image space, and H'_k = height of the image determined by the intersection of the principal ray and the paraxial image plane.

If we choose an antenna of diameter 72 inches, then 1.5 ru (relative units) = 36 inches, or 1 ru = 24 inches. These antenna dimensions may, of course, be varied at will, subject to the problem at hand, with consequent redefinition of the ru. Let us in addition choose λ = 3 cm. The λ in relative units then becomes 3/2.54x24 = .0492 ru. With these factors pinned down we can compute the Rayleigh Tolerances. This is shown in Table 6 for LA'.

TABLE 6
Rayleigh Tolerance for LA' (t = 0)
at h = 1.5

R_1/R_2	LA' (ru)	R.T. (ru)
.6	-.118692	.2191
.64	-.052525	.186835
.66	-.029058	.175055
.68	-.009425	.165212
.70	+.007491	.156853
.74	+.035902	.143405
.80	+.070335	.128690

It is thus clear that satisfying the Rayleigh Tolerance for LA' is easy. Indeed, a zero value of LA' may be obtained but, as anyone conversant with this field knows, (a) such a choice almost certainly will prove unwise when the other aberrations are considered, and (b) a reduction of LA' below about one-quarter the tolerance provides no appreciable gain in the amount of energy focussed within the image. Table 6 is important, however, in that it shows the latitude available in picking R_1 for minimum coma or astigmatism.

9 A. E. Conrady, loc. cit., pp. 136, 137, 393

The measure of coma used in the section on the Mangin Mirror is valuable because it is (a) a relatively simple and quick way of assessing the variation of sagittal coma with system parameters and (b) does provide an excellent method if we wish to judge the variation of coma in terms of focal length. To judge the coma in terms of the Rayleigh Tolerance one may use the OSC′ of Conrady.

$$OSC' = 1 - \frac{\theta'_p}{\sin \theta'_M} \left[\frac{S'_{3p} - S'_{pr}}{S'_3 - S'_{pr}} \right], \qquad (8)$$

where

θ'_p = the closing angle of the paraxial ray obtained by an artifice in ray tracing,
θ'_M = the closing angle of the marginal ray,
S'_{3p} = back focus for the paraxial ray,
S'_3 = back focus for the marginal ray, and
S'_{pr} = distance of exit pupil point from last surface.

It is clear from Table 2 that it is possible to obtain zero coma by correct choice of index, the index for this condition being about 1.76 when $R_1 = 0.68R_2$. There are reasons to believe, however, that the utilization of $n = 1.52$ may be advantageous; so OSC′ has been computed for three selected values of R_1 with $t = 0$. The results and comparison with the Rayleigh Tolerance for OSC′, and hence sagittal coma, appear in Table 7.

TABLE 7
OSC′ for Selected Values of R_1/R_2;
$t = 0$, $n = 1.52$, $R_2 = -4$

R_1/R_2	OSC′	Rayleigh Tolerance for OSC′
.60	-.00176	.034581
.66	-.02656	.030910
.70	-.043097	.029259

As the upper and lower rim ray method was not used to calculate coma or astigmatism, the data required for an exact determination of H'_k was not available. Instead, a simpler, but more stringent tolerance, was placed on OSC′ by the use of $H'_k = 1.5$, the full aperture. The ratio of the true Raleigh Tolerance to that indicated in Table 7 is about 8:7. The results shown in Table 7 are, as usual, both pleasant and (as expected) unpleasant. Pleasant because it is clear that the coma can be held well within the Rayleigh Tolerance by proper choice of R_1 and unpleasant becuase the "proper choice" (a) does not coincide with the minimum value of spherical and (b) occurs at a rather steep curvature.

If an actual design were to be worked out, an endeavor would be made, of course, to arrive at the best compromise of R_1, R_2, t, and n. It is fairly clear from Table 3 that there is little to be gained by increasing the center thickness t from zero.

Let us refer to Figure 2 to study the astigmatism when the front surface is the stop. If the feed is caused to move circularly midway between the S and T surfaces, its radius would be 2.628 ru for $\theta = 20°$. While this is not exactly midway for $\theta = 12°$, it is not too far off, the radius being 2.591 for $\theta = 12°$, a difference of .04 ru or 0.96 inches for the assumed antenna dimensions. This might well be tolerated as it is most advantageous, as we shall see, to use the full focal range tolerance at maximum field angle. The center for the feed rotation would then be the exit pupil point located about 12.6 inches behind the antenna. Actually, if the feed were caused to move circularly with the vertex of the antenna as a center and the paraxial focal length as a radius, it is highly possible that the defocussing produced might well be acceptable. This possibility exists since astigmatism produces, in general, a symmetrical diffusion wheras coma does not.

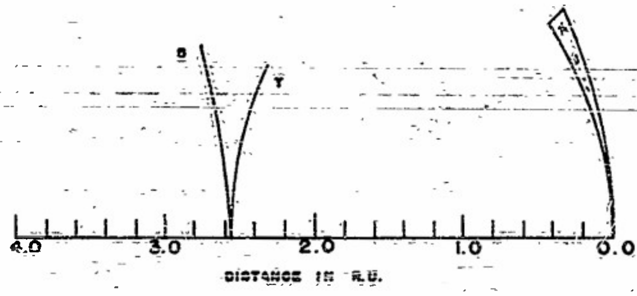

Figure 2 - Astigmatism for a Mangin Mirror $R_1 = .70R$, $R_2 = -4$, $T = 0$, $N = 1.52$

The Rayleigh Tolerance for the astigmatism may be determined by assuming that the chief ray is the optical axis rotated and θ'_M is then the angle between the ray from the upper (or lower) margin and the chief ray at the point where the feed is located. To a sufficiently close approximation this angle turns out (from graphical methods) to be 32° for $\theta = 20^\circ$, $\theta = 12^\circ$, and $\theta = 6^\circ$. Thus, the astigmatism allowed may be derived from Equation 7.

$$\text{Tolerance for astigmatism} = \frac{\lambda}{n \sin^2 \theta'_M}$$

$$= \frac{.0492}{(.5299)^2}$$

$$= .1752 \text{ ru} \qquad (7a)$$

Referring to Table 4 or Figure 2, we see that this tolerance is reached at about 14°. Hence, this particular system reaches the Rayleigh Tolerance for astigmatism at a full field of 28°. Inasmuch as θ'_M is approximately the same for $R_1 = .66$, $.70$, and $.74R_2$, it may be said that while the field may be expanded slightly by going to a less steep curvature, but keeping the front surface as the stop, the gain will probably not balance the marked increase in coma. Inspection of the Petzval condition indicates that some slight improvement might be achieved, but it will probably be found that the astigmatism is the basic limiting factor in this otherwise satisfactory system. If an astigmatism of about twice the Rayleigh Tolerance may be accepted, it is demonstrably possible to bring the coma and spherical aberration of this system well within the required limits without resorting to other than a simple spherical mirror and in-contact corrector plate, and with no artificial stop.

Comparison with Comparable Existing Systems

There are many optical systems with which the MMS might be compared. However, it seems logical to limit this comparison to systems in which there is a single optical "operator." If we thus exclude systems with separated "operators," there is left, of the simple systems, but the spherical reflector, the paraboloidal reflector, and the simple lens. Comparison of their relative performance may be made most easily by a chart of the form shown in Table 8. The comparison is made at f/1 for $\lambda = 3$ cm with stop at the lens or reflector.

In addition it should be noted that for normal values of the index, the central thickness of a simple lens at f/1 would be several times that of the marginal thickness of the MMS.

TABLE 8
Comparison of the Aberrations of the Simple Lens, Spherical Reflector, and Paraboloidal Reflector with the Modified Mangin System

	Simple Lens	Spherical Reflector	Paraboloidal Reflector	Mangin Mirror
Spherical Aberration	cannot be made less than R. T. for normal values of N	< R.T.	Zero	< R.T.
Coma	can be made zero	> R.T.	≫ R.T.	< R.T.
Astigmatism $S'_s - S'_t$ at 20°	≈0.1 f	≈0.1 f	coma so great that hides effect of astigmatism	≈0.1 f
Maximum Relative Aperture	0.5	0.5	0.0	≈0.5

A study of Table 8 shows that the MMS is clearly superior or equal to the others as regards coma and spherical aberration. It is understood, of course, that if an aberration may be reduced to appreciably less than the Rayleigh Tolerance, there is no significant merit in taking the aberration to zero. As regards astigmatism, the four systems are effectively equal. It would then seem that on a strictly aberration basis the MMS embodies a closer approach to perfection than the other three. The facts, however, that there may be some loss due to the dielectric in the MMS and that the ultimate f number for a paraboloidal reflector is zero (coma, etc., disregarded) as against about 0.5 for spherical surfaces must be taken into consideration.

It would appear that the Bouwers', Maksatov, Schmidt, and Bennett[10] systems all have merit, and from a purely aberration point of view they are probably better corrected than the MMS. The Bennett system (s) is essentially that of Maksatov, but all surfaces are concentric (or nearly so) with the focal surface coincident (or nearly so) with the first surface of the corrector plate. In addition the Bennett system utilizes a second corrector in contact with the mirror. From an over-all antenna point of view these systems are, in general, much more complex mechanically as well as optically than the MMS. The Bennett system in addition, while exceptionally well corrected because of its concentricity, utilizes very thick corrector elements. One-way corrector element thicknesses of from 20 to 217% of the focal length were employed. The comparable element thickness for the MMS is about 6% of the focal length.

The writer would like once again to bring attention to a method of construction which, while difficult (if not impossible) at optical wavelengths, becomes quite possible at radar wavelengths. This is the spinning of the spherical reflector, spraying or coating of the corrector material (probably polyethylene) on the reflector surface, and subsequent machining to specifications.

[10] H. F. Bennett, "Catadioptric Lens Systems," U.S. Patent 2,571,657 (1951) filed April 27, 1945, Serial #590,598.

Conditions Pertaining When the Paraxial Focus is at the Center of Curvature of the First Surface

During the course of this investigation, the results of Table 1 were graphed. It then became apparent that when $R_1 \approx 0.67R_2$, the paraxial focus and the center of curvature of the first surface were nearly coincident, the center thickness being equal to zero. A theoretical study was then made to find the analytical relation between R_1, R_2, and in such that exact coincidence would exist. The derivation proved quite simple and is given here as a matter of interest:

$$\frac{n}{s} + \frac{n'}{s'} = \frac{n'-n}{R}, \quad \text{the general paraxial formula.} \tag{9}$$

Assuming $s = R_1$, we will work for $s_3' = \infty$.

$$\frac{1}{R_1} + \frac{n'}{s_1'} = \frac{n'-1}{-R_1}\text{; solving for } s_1' \text{ we get} \tag{10}$$

$$s_1' = -R_1 ;$$

$$\therefore s_2 = +R_1 . \tag{11}$$

For the mirror, $$\frac{1}{s} - \frac{1}{s'} = -\frac{2}{R} \quad \text{is the general paraxial formula} \tag{12}$$

$$\therefore \frac{1}{+R_1} - \frac{1}{s_2'} = -\frac{2}{-R_2}$$

and $$\therefore s_2' = \frac{R_1R_2}{2R_1-R_2} = s_3$$

Utilizing (9) again for the third surface, (13)

$$\frac{n'}{\frac{R_1R_2}{2R_1-R_2}} + \frac{1}{s_3'} = \frac{1-n'}{+R_1} \quad (R_1 \text{ is + since direction of light is reversed});$$

solving for $\frac{1}{s_3}$, we get,

$$\frac{1}{s_3'} = \frac{1-2n'}{R_1} \frac{2n'}{R_2} . \tag{14}$$

If R_1 is to be the paraxial focal length then $s_3' = \infty$.

$$\therefore 0 = \frac{1-2n'}{R_1} \frac{2n'}{R_2}, \text{ and simplifying} \tag{15}$$

$$R_1 = \frac{1-2n'}{2n'} R_2 . \tag{16}$$

For $n' = 1.52$ we have,

$$R_1 = \frac{1-3.04}{3.04} R_2 = -.67105R_2 \quad . \tag{17}$$

In this derivation, R_1 and R_2 stand for the absolute values of the radii of curvature. If we recognize that R_2 is actually negative, then Equation (17) becomes,

$$R_1 = +.67105R_2 \quad . \tag{18}$$

It will be noted that it is in very close agreement with the value interpolated from Table 1.

As in any preliminary investigation of this sort, a termination line must be drawn. It was thus decided by the writer that a single study would be made of the possibilities inherent in Equation (18) and then leave further detailed analysis for the actual design phase, if such there be. Accordingly, the astigmatism OSC′ and spherical were determined either by direct calculation or by interpolation, with the results appearing in Table 9. Figure 3 is a graphical sketch of the system discussed in Table 9 showing the sagittal and tangential intercepts with the meridional plane.

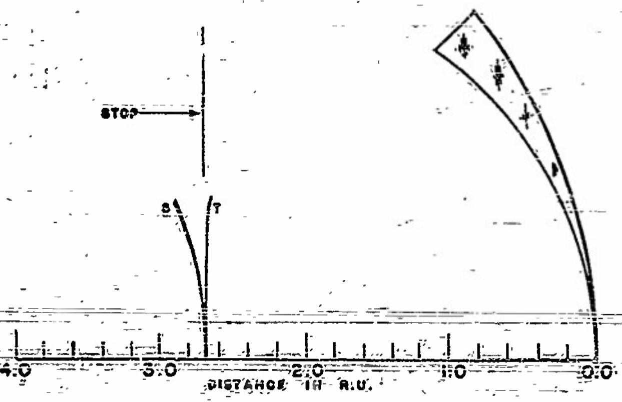

Figure 3 - Astigmatism for modified Mangin system. $R_1 = .671053R$, $R_1 = -4$, $T = 0$, $N = 1.52$, stop at R_1

TABLE 9
Variation of Aberrations when Stop Is Moved to Center of Curvature of First Surface

Aberration	Stop Determined by MMS	Stop Located at Center of Curvature of First Surface	R.T.
Astigmatism	.320	.167	.175
OSC′	.030	.037	.030
Spherical	.018	.019	.170

Examination of Table 9 and Figure 3 reveals the effects of moving the stop. These effects are: (a) the most prominent change is the large reduction in astigmatism, (b) coma and spherical aberration are relatively unaffected, (c) if the same f-number is to be preserved the edge thickness must be about doubled, and (d) the field curvature has changed from positive to very slightly negative. There are several other obvious factors involved in the choice of an artificial stop. These, however, are more of a mechanical engineering nature and will not be discussed in this report. It is clear, however, that by proper movement of the stop, the astigmatism can be reduced to about the Rayleigh Tolerance for the desired field. Inspection of Equation (8) also shows that by proper placement of the stop the sagittal coma may be reduced to a minimum. The two positions, incidentally, should be approximately the same.[11]

DISCUSSION

Dunbar: (SRI) We have some experimental results obtained from a pillbox of 30-inch aperture operating at 0.85 cm. It is a one-layer pillbox of 1/8-inch spacing employing a polyethylene lens. The feed horn is in the aperture; so it obstructs to some extent. On-axis the beamwidth was 1°, and the first side lobe was 16 db. At 11 beamwidths off, the beamwidth had increased to 1.3°, and the first side lobe was still 16 db. At 16 beamwidths off, the conditions were the same. At 27° off we had 1.5-degree beamwidth, and the first side lobe was raised to 14 db. Because we are in a parallel plate system this data gives no information on astigmatism. The 27-degree position is far in excess of the value calculated on the basis of permissible astigmatism. The increase in beamwidth is probably due to some coma coming into the system, but the pattern did not show any coma lobe.

Budenbom: (BTL) I would like Dr. Gunter to define what he means by relative aperture and to discuss the units used in his tables.

Gunter: (Clark) The relative aperture corresponds to the reciprocal of the f-number — that is, the f/D ratio.

Spencer: (AFCRC) On the question of f/D ratio, we have a practical consideration of turning radius which limits us to values less than 1. This is due to the fact that the turning radius should be determined by the diameter rather than by the focal length.

11 A. E. Conrady, loc. cit., p. 350

FEED STABILIZATION SYSTEM

K. S. Kelleher and H. H. Hibbs
Naval Research Laboratory

The scanner to be described in this talk is a wide-angle system capable of sweeping a pencil beam over a greater angle than any existing scanner with which we are familiar. If anyone requires an antenna which will scan a narrow beam through 120° in one plane, this, I believe, is the solution.

The system for which this scanner has been designed is a target-acquisition radar which will be used in conjunction with gun fire control systems. It has generally been considered that the antenna should scan a beam over a hemisphere. A more accurate description might be the scan over the truncated hemisphere as shown in Figure 1. The scanner must provide the coverage shown here once every four seconds.

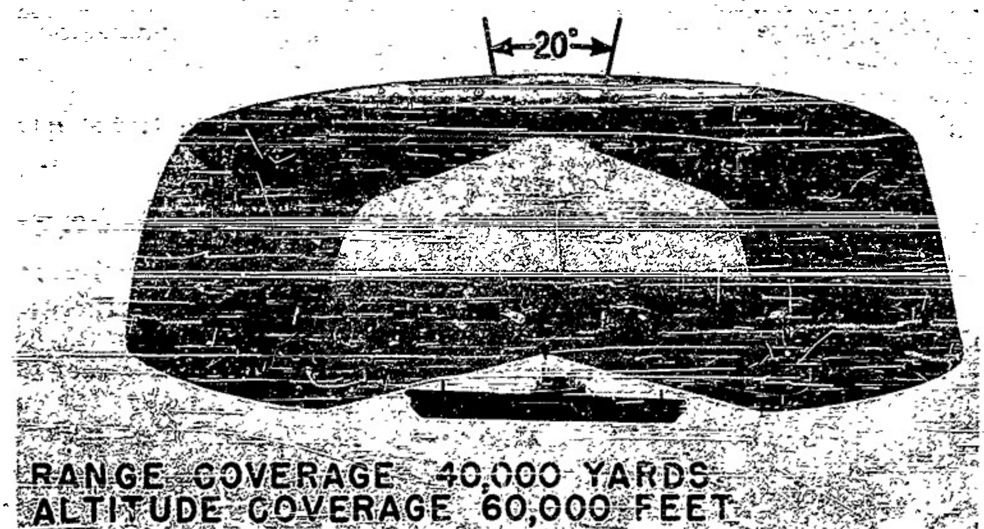

Figure 1 - Truncated hemisphere coverage

Many solutions for executing this coverage have been proposed in the past two years. Various industrial laboratories have formally proposed four different ones. Radio Division I and II of NRL have proposed, between them, five different solutions. At the present time, it appears that every one of these proposals could be successfully employed on a large ship. However, if we assign the single further condition that the topside weight be less than 500 lb, most of these proposals are unusable. The reason for this is fairly simple. The system must be stabilized, and the weight of conventional stabilization is prohibitive.

One of the best of the proposed systems is shown in Figure 2. It is a BTL proposal based on the Schmidt scanner described at the last symposium. It employs a cylindrical reflector and double-layer pillbox. The feed system within the pillbox is an organ pipe.

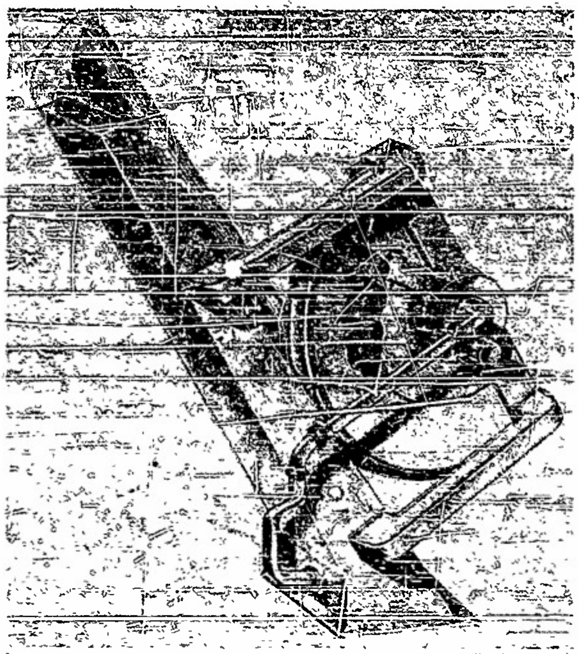

Figure 2 - BTL target acquisition system

This is due to the fact that stabilization is accomplished by scanning the antenna beam in order to hold it fixed on the horizon as the ship rolls and pitches. Since a roll of the order of ±30 degrees is expected, the antenna system must be capable of scanning through 60 degrees just in order to produce stabilization. The first problem in feed stabilization is then not the feed but the reflector.

The most interesting feature of this scanner is the reflector. Figure 4 shows cross-sections of the reflector in the two principal planes. In one plane it is a parabola and in the other it is a circle. The surface is formed by rotating the parabolic curve about a line parallel to the latus rectum, as indicated by the arrow. Note that the reflector will not be a symmetrical one. Since almost any type of scanning feed will present obstruction to reflected radiation, it is well to use a half dish in the manner shown here. Figure 4(b) indicates how a feed can be scanned through 120° using the symmetry of the circle. The change in arc length subtended by the rays from the feed indicates a change in beamwidth as the antenna is scanned.

Its output can be seen at the point where the pillbox plate is cut away. This system has the desirable feature that the antenna beam and the rate of scan can be varied during the scan cycle. Unfortunately, this system must also be stabilized, and is, therefore, too heavy for the application we are interested in.

Figure 3 shows a model of the system which we feel will do the job. Its tentative parameters are about the same as the BTL system. Its reflector is somewhat smaller, and it eliminates the pillbox weight and loss. The biggest weight saving, however, develops from the fact that instead of stabilizing the entire structure, only the feed is stabilized.

Feed stabilization has been considered by workers in this field for many years. It is usually immediately recognized that this can be achieved only when the reflector or lens used as an objective is a wide-angle scanner.

Figure 3 - NRL target acquisition system

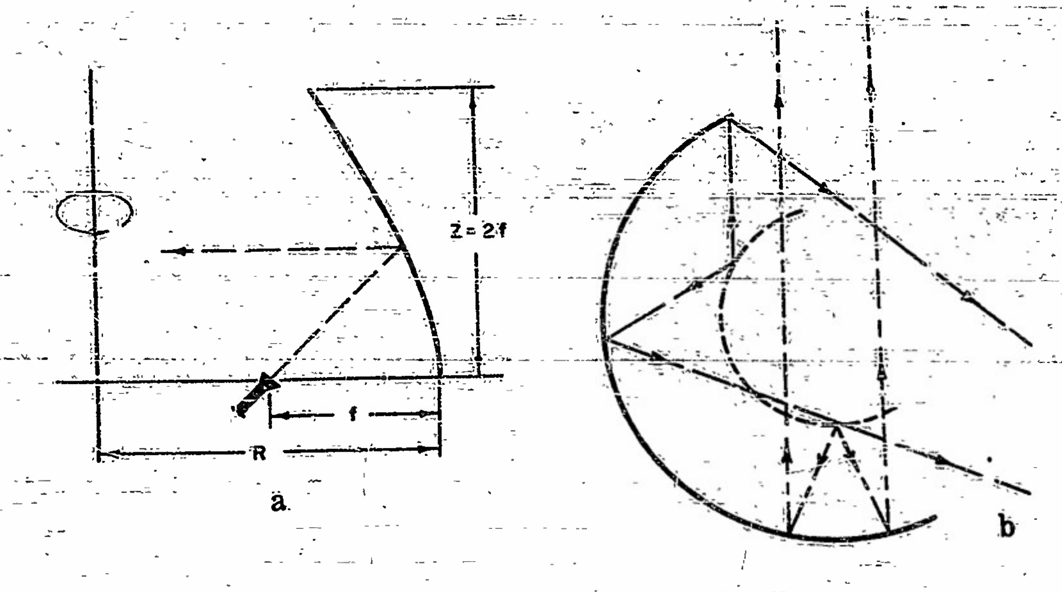

Figure 4 - Cross-sections of reflector

An investigation has been made of the ratio of f to R, and an experimental model with near optimum ratio has been built.

A considerable amount of work has been done on this X-band model of the reflector (Figure 5). In this case, the f/R ratio was 0.46. Identical parabolic curves were cut from sheets of 1/16 in. brass. These sheets were assembled so that they touched a circular arc on the base. Ordinary window screening was then applied to form the reflecting surface. The result was as though a single parabolic curve were swept through 130 degrees.

Figure 5 - Model of X-band reflector and feed

We are in the process of constructing another X-band model which is somewhat larger and which is generated by a curve sweeping through 180 degrees. The feed shown on Figure 5 is one of those which we have tried. Note that the outputs from the organ-pipe channels increase in size from one end of the aperture to the other. The metal plate is employed to direct the energy into the asymmetrical reflector.

Figure 6 shows experimental results when normal horns are used to feed the reflector. The upper curves are patterns in the plane of scan, while the one plotted 10 db below is a pattern in the other plane. The change in the upper patterns is due to the use of various feed horns—that is, to the use of various areas of the reflector. As expected, the patterns with best lobes are those with the broadest beams. The side lobe level for the narrowest beam is 17 db. This, we feel, is adequate for our purpose and superior to those obtained from existing scanners which have provided satisfactory operation. It has been possible to obtain a pattern in the plane of scan with a beamwidth of about 4.0 degrees and side lobes of about 20 db. Unfortunately, patterns in the other plane then had broader beams.

The pattern obtained in the horizontal plane is very good. The side lobes are low, and the 4.5-degree beamwidth represents a very efficient use of the aperture width. It has been possible to decrease the beamwidth in this plane slightly at the expense of higher side lobes. In general, the patterns obtained in this plane are about equal to those obtained from a paraboloid. This is due in large measure to the fact that the cross section of the reflector in this plane is a parabola.

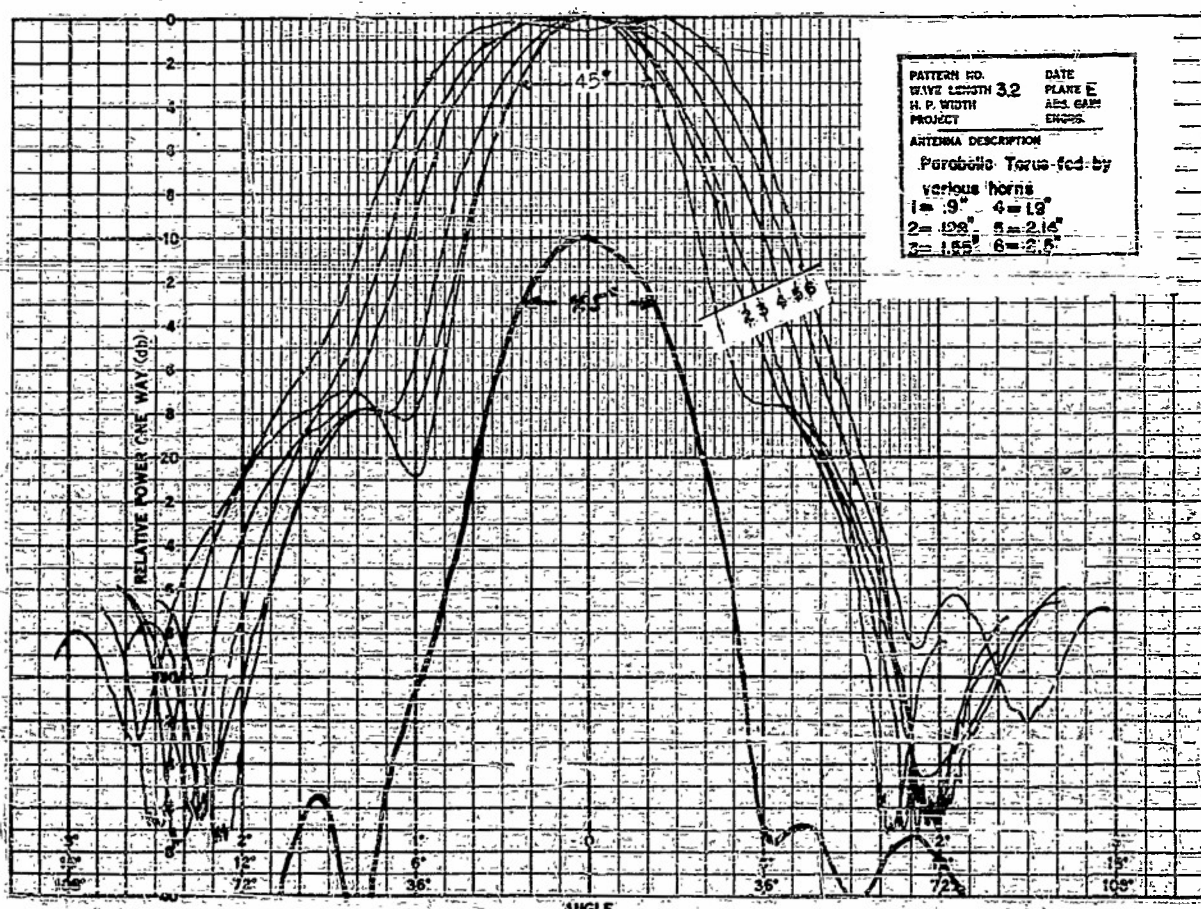

Figure 6 - Patterns from parabolic torus

The patterns shown here are among the first we obtained. We have since taken hundreds of patterns in an investigation of unusual feed systems. We have not decided exactly which system to use, but we feel that we can always fall back on these particular patterns.

The methods of obtaining feed stabilization (Figure 7) are of some interest. Our first thoughts were centered around the system shown in Figure 7(a). The semi-circle here indicates a cross section of the reflector in the vertical plane. The feed system is a ring scanner which will be discussed in detail this afternoon. It provides a method for feeding any of the five horns which lines up with the inner feed arc. In the present position, one horn is about to enter and another is leaving the feed arc. Stabilization can be achieved by merely holding the feed line to the inner arc horizontal. Any horn is then initially fed when it lies in the horizontal plane. The initial radiated beam will then always begin its scan in the horizontal plane. This beam will accordingly never be directed below the horizon and will never begin the scan at a point above the horizon; therefore, stabilization is achieved.

Figure 7(b) indicates the method of stabilization with which we are now concerned. It consists of four feeds with an r-f switch and an organ-pipe sector of feed channels. Stabilization is achieved by holding the first channel horizontal so that the beam at the beginning of the scan cycle is again in the horizontal plane. This second solution is now preferred for several reasons. The most significant reason is that a similar feed system occurs in the BTL scanner, and we hope to use their results in our design.

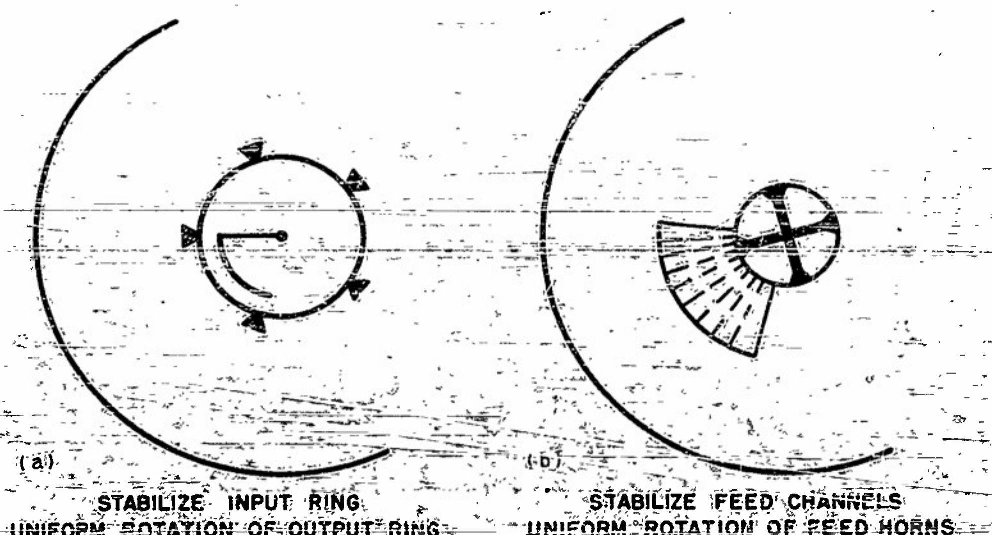

Figure 7 - Methods of obtaining feed stabilization

Figure 8 shows details of the feed system which indicate the close relationship between the two systems. The BTL system is mounted in a pillbox; its extent, therefore, appears to be somewhat greater than that which is actually used. The only difference between the two is in the arc length occupied by the output channels. The BTL arc, I believe, subtends 110 degrees while the NRL system would occupy 70 to 80 degrees.

I hope everyone will understand the feed system from a consideration Figure 8. Energy is introduced through the circular guide in the center. The transition from circular guide to rectangular guide together with the four feed horns acts as an r-f switch. Energy goes into the one of the four channels which is not shorted; that is, it goes through the channel which is feeding the organ pipe. As the four waveguides rotate, each of the four is fed in

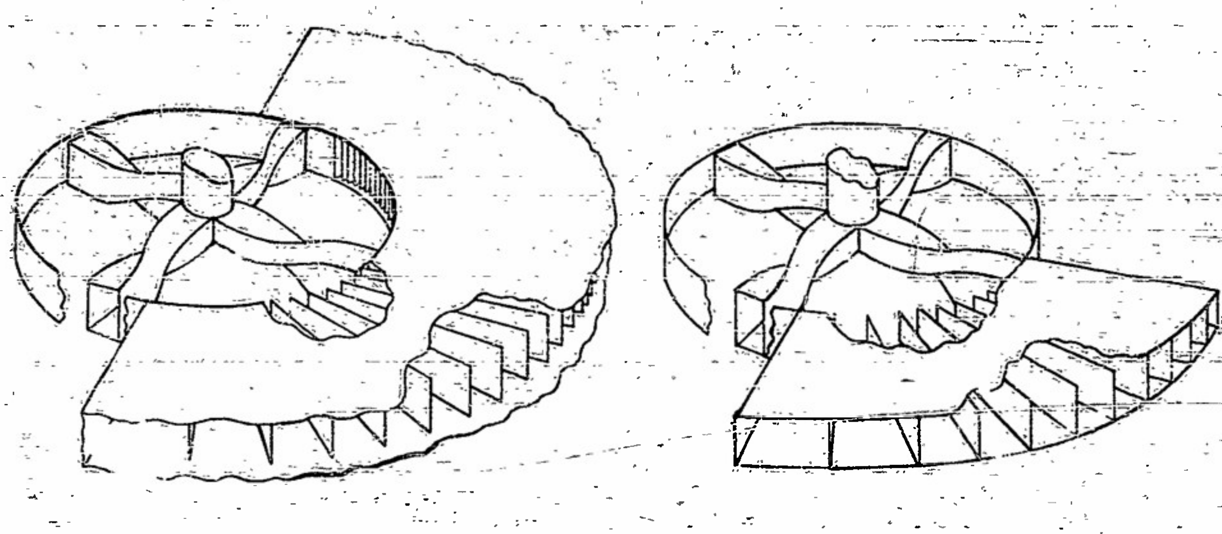

Figure 8 - Organ-pipe feed systems

turn, and each feeds the organ pipe. Feed energy is then made to sweep along the organ pipe aperture.

I would like to take this opportunity to thank Dr. Wheeler and Mr. Lince of BTL for their very helpful cooperation and for their permission to use some of their figures in my paper.

Figure 9 indicates what occurs as the antenna rotates and the ship holds a fixed position of roll. The first beam remains horizontal, but the plane of scan is not vertical. Correction for azimuth and elevation position must then be introduced in terms of the antenna position and ship's position.

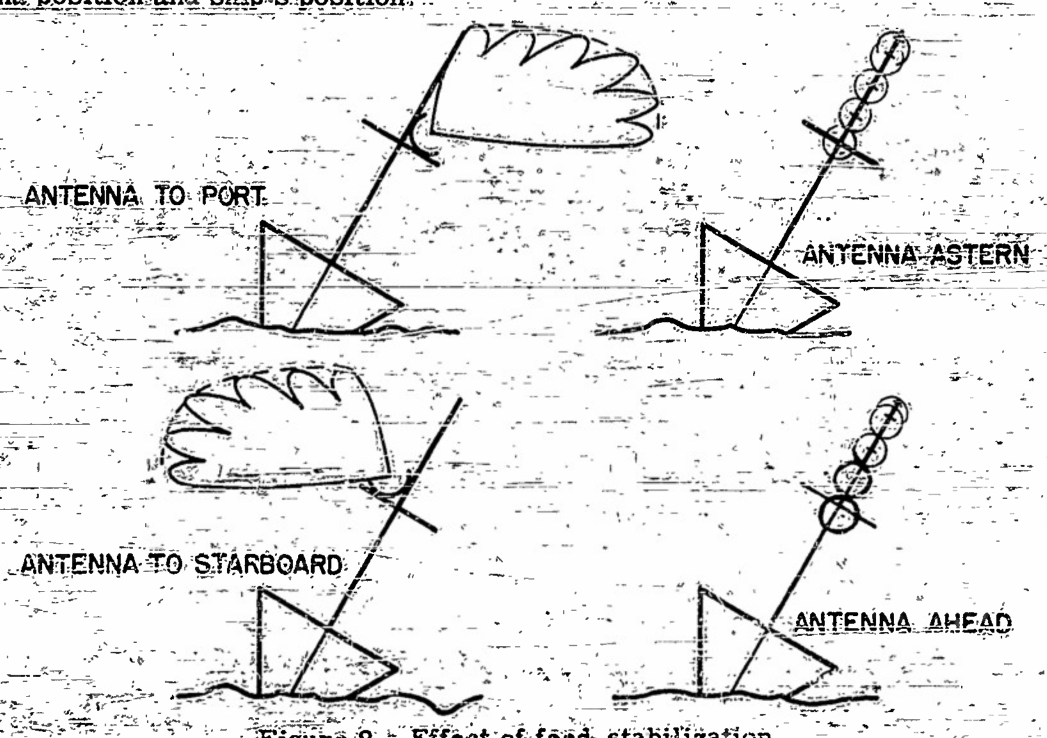

Figure 9 - Effect of feed stabilization

Figure 10 shows the proposed scanner dimensions. The reflector will be about 11 feet by 5 feet. The feed arc has a radius of about 3 feet. We expect to get a on-horizon beam of 3.5 degrees by 3.5 degrees with a corresponding gain of 33.5 db. The beam in the scan plane will increase in width with increasing elevation up to a maximum width of 11 degrees. A rough estimate of the weight has been given to us as 250 lbs without pedestal and about 500 lbs with pedestal.

Figure 11 introduces some philosophy on wide angle scanners. It offers a comparison between the lens, the parabolic cylinder, and this new reflector. The comparison is based on concepts of effective aperture. That is, how large must these antennas be in order to produce the same beamwidth or the same gain?

The mathematics employed here is quite simple. In the fundamental case of the simple aperture or lens, we have the effect pointed out by Dr. Spencer at the last symposium: The effective aperture d is related to antenna size A by a cosine factor. A similar relation occurs for the parabolic cylinder, but here the antenna size A must be even greater by an amount 2Δ to insure that energy is not lost past the reflector. The length of Δ depends on the focal length of the system. In order to obtain usable numbers, f was picked equal to d/2—that is, it was equal to one-half of the line segment. To avoid crowding, the drawing shows f much larger than this value.

This particular representation indicates the lens to be superior to the cylinder. However, this superiority is somewhat offset by the fact that the feed displacement for the lens is greater than that for the cylinder.

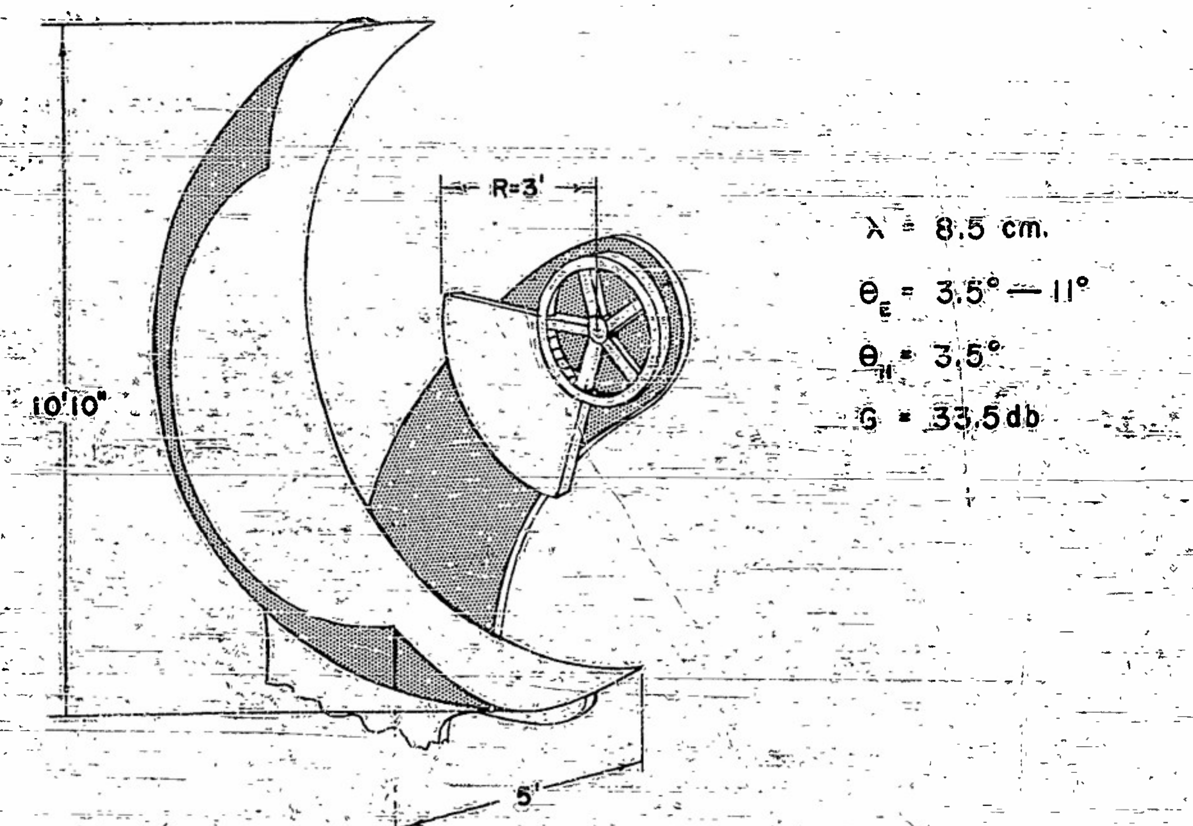

Figure 10 - Dimensions of proposed NRL antenna

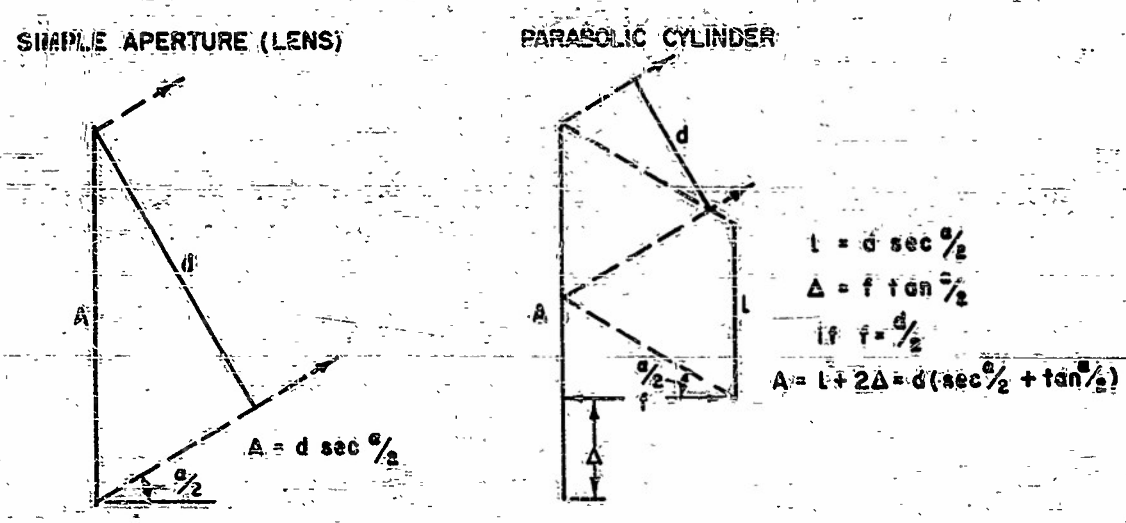

COMPARISON OF ANTENNA SIZES:

ANTENNA	120° SCAN	90° SCAN	60° SCAN	REMARKS
LENS	2.00 d	1.41 d	1.15 d	LENS LOSS
PARABOLIC CYLINDER	3.73 d	2.41 d	1.73 d	PILLBOX LOSS
NEW REFLECTOR	1.78 d	1.75 d	1.69 d	NO ANTENNA LOSS

Figure 11 - Comparison of wide-angle scanners

If we consider antenna size alone, the table shown in Figure 11 is applicable. At very wide angles the new reflector is superior to the other two. At smaller scan angles, the lens appears superior. This, of course, assumes that a lens could be built capable of scanning through 60 degrees.

The remarks are included in the table since they relate to the efficiency of the system. There appears to be loss inherent in the lens and the parabolic cylinders which utilize pillboxes. It was established at the last symposium that the normal lens has a loss of 2 to 3 db compared to a reflector. A figure of 1 db for pillbox losses is probably reasonable. Fortunately, we will have a discussion of pillbox losses later in the program.

From the considerations covered in this talk, it appears that this new reflector might be a useful component in scanning systems designed for wide-angle coverage.

In conclusion, the authors would like to thank Mr. Maag of our section for his work on this project and Mr. Coleman for his assistance in preparing the slides.

DISCUSSION

Spencer: (AFCRC) Could you restate for my benefit the shape of your reflector?

Kelleher: (NRL) The reflector might be called a parabolic torus—that is, a doughnut-shaped surface. Consider a doughnut, and replace the ordinary circular cross section by a parabola. A section of this doughnut then forms our surface.

Spencer: This surface is reminiscent of what we used to call the barrel reflector.

Kelleher: Yes, it is related, although I believe the barrel reflectors were used to produce cosecant beams whereas this produces a pencil beam.

Dunbar: (SRI) I am interested in the last slide shown by Mr. Kelleher. The fact that the parabolic cylinder reflector and the torus do not use their entire surface at all times is not bad. In many cases it is good because it is necessary to obtain a scan. Many people seem to think it is bad because we are wasting some of the surface. It is a price you must pay in order to obtain scanning. A similar loss in gain is obtained from the fixed lens aperture because with scanning the aperture decreases by the cosine of the scan angle.

Kelleher: Thank you. That is the point I wanted to make with that last slide. The lens appears to be good at smaller angles, but it would seem that for wide-angle scanning you can use only about 1/2 of your aperture in almost any system, lens or otherwise.

* * *

FEED SYSTEMS AND SCANNING LOSS

Mr. H. T. Budenbohm, BTL, Whippany
(Chairman)

AN ORGAN-PIPE ANTENNA

P. H. Smith
Bell Telephone Laboratories

ABSTRACT

The Bell Telephone Laboratories is in the process of developing a radar set for picket submarines which is intended to provide accurate range, height, and azimuth data on aircraft. This radar will operate in the X_B-band.

The antenna for this radar is being designed to generate and scan a narrow pencil beam rapidly in elevation at a linear rate while at the same time rotating slowly and uniformly in azimuth to provide either complete or sectoral azimuth coverage.

This antenna is unique in that it will represent the first application of a metal-plate lens to submarine service and also in that it is to be mounted on a platform which is fully stabilized against roll and pitch above the deck of the submarine.

The metal-plate lens portion of the assembly serves in the usual way to collimate the relatively wide-angle primary radiation from an electrically scanning "point source" into a scanning pencil beam. The scanning point source is generated by an "organ-pipe" scanner housed in a water-tight weldment and located at an appropriate distance and position behind the metal plate lens assembly.

Physically the metal plate lens will be 5-1/2 ft wide and 7-1/2 ft high and will be composed of 73 horizontal metal plates of 61S aluminum 1/8 inch thick. The contour of the front surface of the lens will be cylindrical, with the axis of the cylinder horizontal. The curvature in the vertical plane minimizes coma aberrations as a result of scanning off-axis approximately ± 12-1/2 beamwidths.

The lens has an f over d ratio of 1.1 and is zoned on its inner surface. Both inner and outer edges of the individual lens plates are tapered to reduce surface reflections.

Due to the fact that this lens is to be subjected to unusually severe mechanical stress in crash dives it was necessary to locate the lens plate separators a maximum of 12 inches apart. The lens plates will be anodized and painted to resist corrosion.

The "organ" scanner portion of this antenna is composed of a total of 44 cast feed horns stacked vertically so that the locus of their individual apertures follows the zero-coma feed circle whose radius is 50 inches.

The electric plane dimension of the horns is horizontal to provide horizontal polarization, and the horns are flared only in this plane. At any instant the total energy emerges from a maximum of 3 and a minimum of 2 feed horns.

In the final design it is planned to cast together groups of 8 feed horns to provide maximum mechanical resistance to hydrostatic crushing forces of 800 lbs per square inch on the sides of the scanner housing when the submarine is at maximum depth. This total force amounts to approximately 180 tons or 4 tons per feed horn.

The radiation pattern of the scanner horns produces a 12-db illumination taper for the lens. Minor lobes of the primary feed pattern in the horizontal plane are down about 25 db from the peak intensity. In the vertical plane they are down about 13 db at the center of scan. These larger lobes are the result of the space-phase relationship necessitated by stacking the horns with their magnetic dimension in the vertical plane. Closer spacings would improve this but would necessitate narrower horns more nearly approaching cutoff.

The 44 scanner horns are excited through 44 separate waveguides folded together in a compact assembly. All waveguides are approximately the same length and are made by bending a continuous piece of waveguide. The folding arrangement for the waveguides provides a U-shaped bend in each run which permits design changes in individual waveguide lengths to be readily made as may be required.

The input ends of all 44 waveguides are brought together in a 9-inch diameter circle at the center of the scanner. A small feed horn subtending an arc equivalent to two waveguide apertures is located on the axis of the circle and rotates at speeds of from 2 to 8 rev. per sec.

A low-loss dielectric water-sealing cover plate is planned for the scanner horns. The outer surface of this cover is to be machined with 44 horizontal water-matching grooves, each one-quarter wavelength deep and covering 50 percent of the total aperture of each horn. Such a surface has been found to minimize reflection from sea water which comes in contact with the cover plate and thereby minimizes the tendency for the waveguide components to spark over when the antenna is hit by a water wave or is submerged.

DISCUSSION

Berkowitz: (Sperry) Could you explain the reason for the H-plane taper of the feed horns?

Smith: (BTL) That is a means of obtaining a uniform phase front across the horn. I believe it is described in Southworth's work.

Chait: (NRL) What happened to your impedance when the antenna comes out of the water, if your Rexalite is stepped to provide a match in the water?

Smith: A similar antenna was matched in air, and we found very little difference when it was submerged. As the antenna approached the water we were troubled by the reflection at the water surface. When it is entirely within the water, however, it does not know whether it is in water or air. Energy reflected into the waveguide is cancelled by the two surfaces each having equal reflection and being spaced a quarter wave apart.

ORGAN-PIPE SCANNER DEVELOPMENT

G. E. Felker
General Engineering Laboratory
General Electric Company

An S-band organ-pipe scanner is under development for use as a rapid scanning primary source for an asymmetrical paraboloidal reflector. The scanner configuration, shown in Figure 1, consists of 20 waveguide channels of equal electrical lengths diverging from a feed circle. The feed horn, which illuminates $2\frac{1}{2}$ channels, is designed to scan at a 17-cycle-per-second rate. The scan angle is plus and minus five beamwidths at an f/D ratio of 0.75.

Primary patterns of the organ pipe are illustrated in Figure 2. The impedance locus during the scanning cycle is shown in Figure 3. Maximum pulling rate is approximately

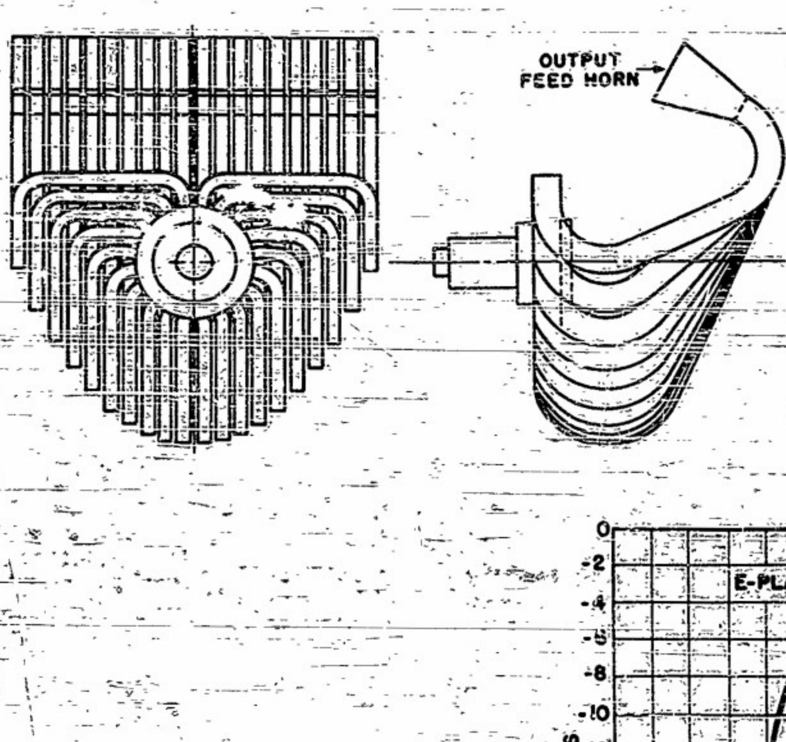

Figure 1 - Organ-pipe scanner

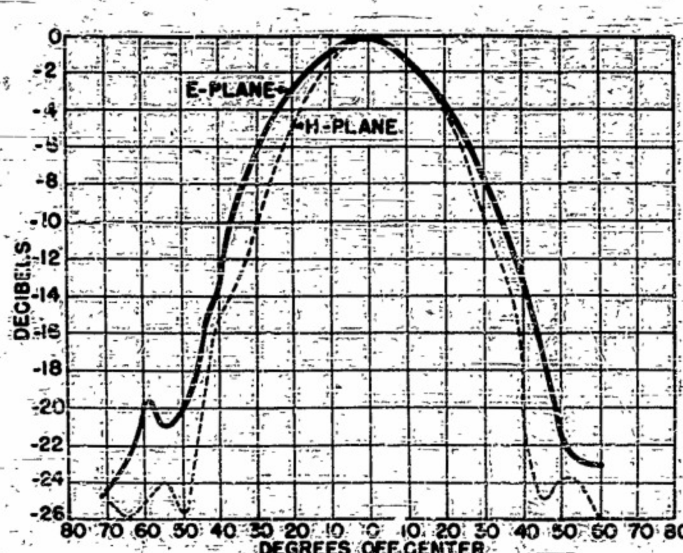

Figure 2 - Primary feed patterns (organ-pipe scanner)

400 Mc/sec[2] for a magnetron pulling figure of 12 Mc/sec. This will be reduced by a factor of three by the long-line effect in the 50-foot feed line to the transmitter.

High-power performance appears to be very promising. Tests made on an X-band sample indicated satisfactory operation at powers up to 400 kw at .001 duty factor without pressurization.

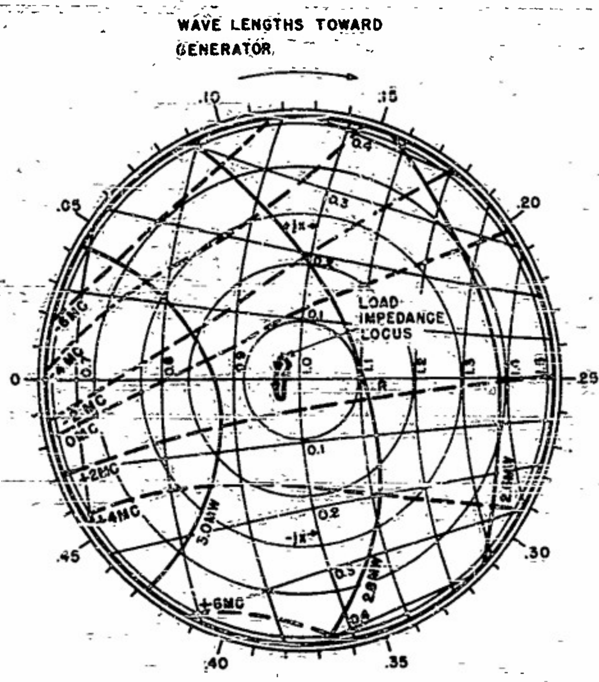

Figure 3 - Impedance variation with scan (organ-pipe scanner)

* * *

SCANNERS AT A.S.R.E.

H. M. Bristow
Royal Naval Scientific Service
Admiralty Signal and Radar Establishment, England

INTRODUCTION

This lecture was read for the Chief Scientist, A.S.R.E., from a paper by B. W. Lythall, A.S.R.E. Extension, Nutbourne.

The scanning unit to be described is part of an S-band radar system, at present under development, known as Postal. The unit consists of five separate and identical scanners in close proximity. It will be used in the focal zone of a fourteen-foot-diameter lens of unity f-number. A mounting which carries the lens and scanning unit will be rotated continuously in azimuth.

SCANNER DEVELOPMENT

Each scanner is essentially a device which simulates a horn feed moving along a linear path of about 18 in. in a sawtooth manner at about 20 cycles per second; it must also be capable of handling the required power. It has been clear for a long time that the main difficulties are not so much in the general design of a rapid-scanning feed, but in the development of such a feed subject to the particular restrictions imposed by the choice of the radar parameters for "Postal."

There are two features which impose severe limitations on the design.

1. Because five scanners are used, the beam swing required from each is small. Hence the width of the feed horn is significant compared with the distance through which the horn has to move during one scan cycle: thus with many simple single feed systems the dead-space is prohibitively large.

2. As the scanners are stacked diagonally, the maximum dimension of the mechanism in the direction perpendicular to the feeding plane must not exceed about 6-1/2 in., except where permitted by the offset of one scanner relative to the next.

There is a description in the Proceedings of the 1949 U.S.N.E.L. Antenna Conference of a proposed organ-pipe scanner for Postal in which the dead-space is reduced by using two feed horns with a self-commutating arrangement attached between the feed and the rotating joint. The layout of this device was considerably improved later, mainly by the adoption of a cylindrical commutating plate instead of a plane one; this enabled the axial length of the system to be considerably reduced. The restricted space inside the feed circle still posed considerable problems, however, and effort was transferred to a more sophisticated design of scanner.

Principle of Present Scanner

Figure 1 will help to explain the basic mechanism of the present scanner, which consists of a fixed waveguide feed and a fixed "stator" similar to the organ-pipe, between which is a rotating disc of waveguides, afterwards called the "rotor." The rotor consists of a number of "horns," each of whose throats subtends an angle of, say, θ at the center of rotation. The mouths of the horns, however, each subtend an angle of $[n/(n+1)]\,\theta$, where n is the number of stator waveguides embraced by a horn mouth. If the rotor turns through an angle θ between pulses, it will be found that as each pulse is transmitted, a horn is aligned with the feed and illuminates a group of n waveguides in the stator; the successive groups for successive pulses are stepped along the stator by one waveguide per pulse. In order to avoid serious reception losses each horn contains n waveguides, which on transmission are, of course, aligned with the illuminated group of waveguides in the stator.

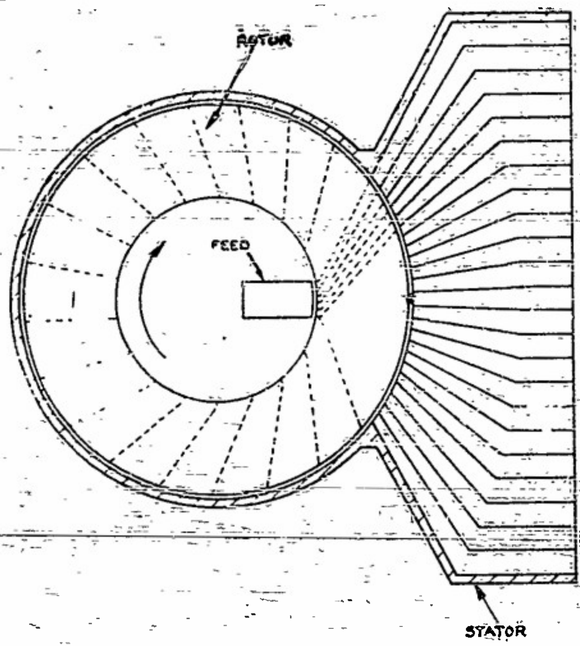

Figure 1 - Simplex noninterlaced scanner, schematic

The dead-space is effectively one pulse interval, since although the last pulse is transmitted correctly, reception of reflected signals from it is progressively inhibited as the target range increases.

Even in this somewhat symbolic form the design appears to have several attractive features.

1. The layout is essentially planar, leading to a "pancake" form very suitable for stacking scanners in Postal.
2. There is only one moving component and most of the constructional difficulties are also in this same component.
3. The dead-space is limited to one pulse interval and there is no additional mismatch presented to the transmitter during this pulse.

Interlacing and Duplexing

Some extensions of the principle have been developed for the revised radar parameters of Postal. Figure 1 is drawn with n = 5 and with 19 pulses transmitted per cycle. The present values for Postal are n = 8, and 25 pulses per cycle. Since the inner circumference of the rotor is determined, not by the length of scan, but by the number of pulses per cycle and the width of the waveguide feed, an "interlaced" rotor is employed to keep the inner diameter of the rotor to a reasonable size. The principle of interlacing is illustrated in Figure 2. The horns of the rotor are overlapped by half their width so that half of one horn is also used as half of the next. Thus the inner diameter of the rotor is approximately halved and the number of vanes in the rotor is also halved. There is, however, an additional pulse wasted in the dead space, as will be seen from Figure 3. There is no additional mismatch presented to the transmitter during this pulse.

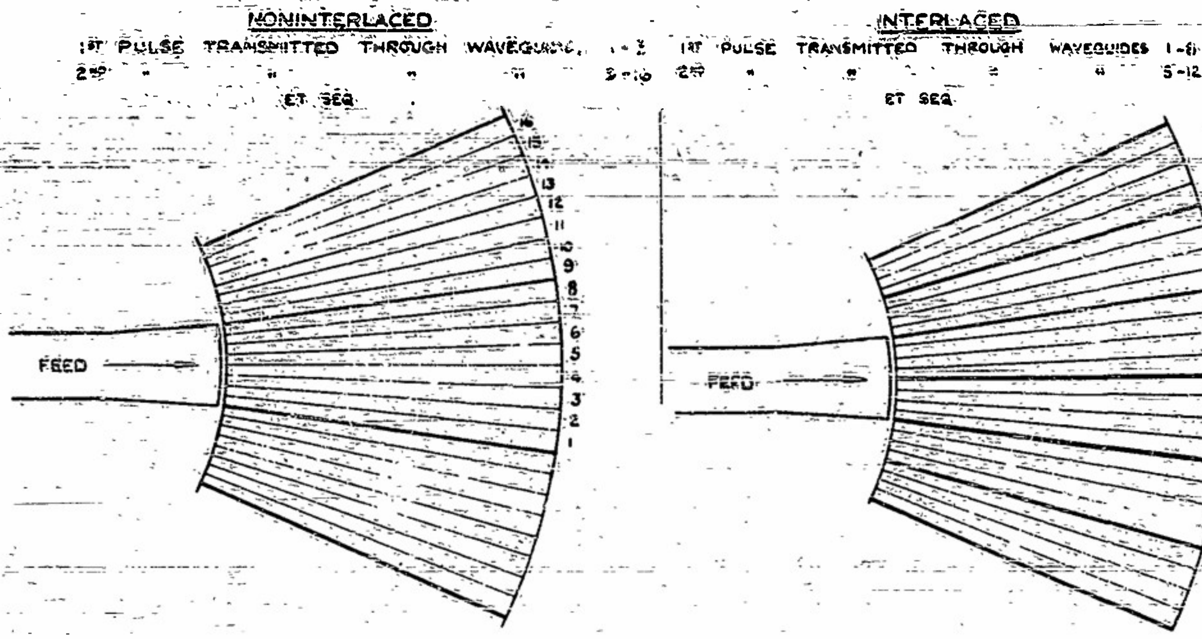

Figure 2 - Principle of interlaced rotor

After preliminary measurements of the impedance of individual curved waveguides, it was decided to increase the outer diameter of the rotor considerably. It is then possible to use a "duplex" rotor in which there are two complete sets of waveguides in the rotor circumference. Although the number of walls in the rotor is now doubled, the rotation speed is halved and the total inertia is in fact slightly reduced. Moreover the rotor is now inherently balanced. The curvature of the rotor waveguides is considerably reduced, while their length remains of the order of a wavelength, as desired; the angle of divergence of the stator is also reduced, so that the path length correction required in the stator is very much reduced and can therefore be expected to be reasonable over a much broader band. A scale plan of the present system, using an interlaced duplex rotor, is shown in Figure 4.*

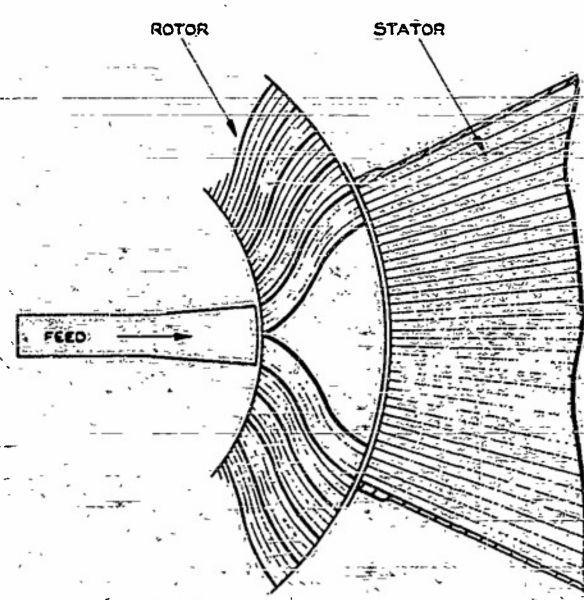

Figure 3 - Interlaced rotor (additional pulse wasted)

* The stator contains two additional waveguides at each end to accept possible leakage of energy down the sides of the rotor horn.

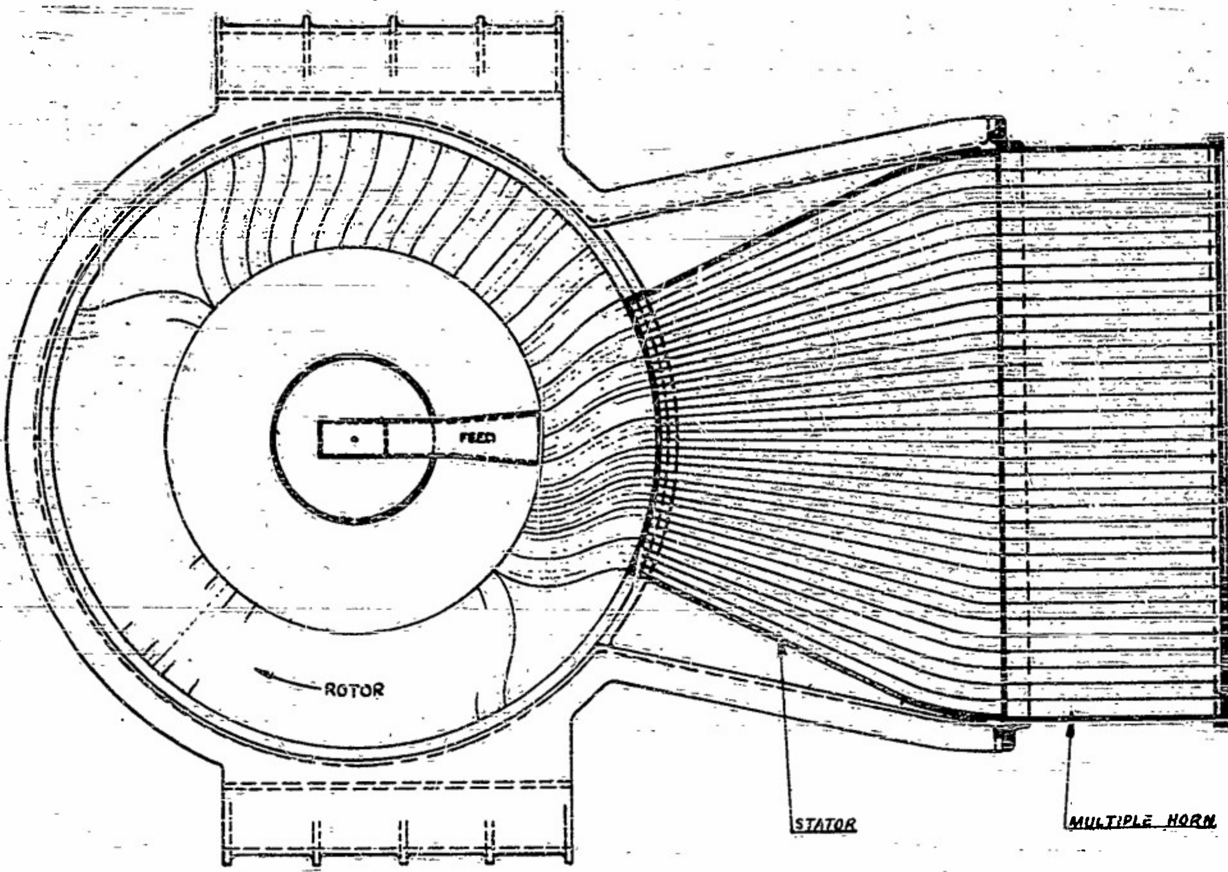

Figure 4 - Duplex interlaced rotor, schematic

Design Problems

The main problems expected to occur were the power handling capacity of the feed rotor and rotor-stator gaps, which inherently cannot be choked; the impedance matching of the curved rotor waveguides; the path-length correction and pressure sealing of the stator; and the difficulties associated with the limited H-plane dimension of the output. The first two problems are the severest.

Power-Handling Capacity

It is impossible to provide proper chokes at the rotor gaps, since the thin H-plane wall of one waveguide is also the wall of the next guide; thus it was expected that power breakdown might prove a serious limitation. A linear model of the feed-rotor and rotor-stator gaps was made up (Figure 5(a)) all to the dimensions of the input rotor waveguides. In order to ease fabrication of the final rotor and to reduce weight, the waveguide walls had to be as thin as possible and were set at 0.028 in. With this wall thickness it was found that cylindrical pillars fitted to the free edges of the walls increased the power-handling capacity very considerably, and with 3/32 in. diameter pillars and a gap of 1/16 in. the breakdown power was slightly above 1.3 Mw at atmospheric pressure. Thus, assuming no serious reflections occur beyond the gaps, it is thought that with the design pressure of 30 lbs/sq in. in excess over atmospheric pressure, the device should be reasonably safe at the working power of 2 Mw, although the safety factor is not as high as is desirable.

The breakdown power was not significantly different when the waveguide walls were fully misaligned, or when two gaps were used in series.

The reflection from 3/32-in. diameter pillars was found to be small enough to ignore, although the 1/8-in. diameter pillars used at the outer gap in the experimental model were matched by transverse pillars, forming lips 0.055 in. deep around the outer rims of the rotor side-plates 3/32 in. pillars are now proposed for all gaps. Measurement of the impedance of gaps and pillars presented some difficulty, since not only must the test waveguide be flanked with other waveguides to obtain the correct radiation impedance through the gap, but these waveguides must be fed with the same power as the test waveguide.

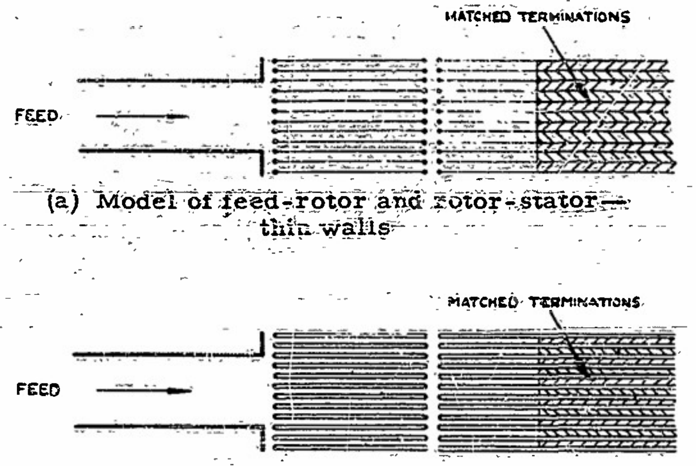

(a) Model of feed-rotor and rotor-stator— thin walls

(b) Model of feed-rotor and rotor-stator— thick walls

Figure 5 (a and b) - Test rig for breakdown measurements

An alternative method, described later, of manufacturing the rotor would use thick walls, as shown in Figure 5(b). A model using 0.080 in. walls did not breakdown until the power reached 1.5 Mw, even though the waveguides were narrower.

Impedance of Rotor Waveguides

The circumferential positions of the two ends of each of the rotor waveguide walls are fixed by the basic principle of the scanner. It is clear that the guide walls between these two sets of points must be faired or "streamlined" to produce the smoothest curves with no constrictions or extreme curvature, but once this has been done there is little further impedance adjustment that can be done. It has been found from measurements on isolated waveguides with typical profiles that generally a total length of about an integral number of half wavelengths is to be preferred, even though the taper and curvature are not uniform throughout the length. This is convenient in the duplex rotor, where the curves are also less drastic than in the simplex case.

It is clear, however, from isolated measurements that some of the curved waveguides may need matching, and this will have to be done by inserting posts into the narrow sides. Attempts at matching isolated curves over the required frequency band have proved quite satisfactory. The method of insertion of the posts is discussed in the section dealing with methods of manufacture.

There is no analytical set of curves which satisfies all the required initial conditions. The curves were therefore first smoothed by hand until a reasonable-looking set was obtained. They were then drawn out ten times full size and the irregularities further smoothed out. Coordinates of these curves were fed into a jig-borer for manufacture of the engraving templates, and further residual irregularities were then shown up. The coordinates were therefore further smoothed analytically, and then the master templates were made.

Stator: Path Length Correction and Pressure Sealing

The difference in electrical length between the longest and shortest stator guide is now only about one third of a wavelength with the duplex rotor, and the maximum variation in length across an eight-guide group is only one quarter wavelength. The small path length correction required should thus be able to be accomplished with adequate bandwidth by the use of dielectric blocks (e.g., of polythene). The correction is in fact needed more to correct the squint of the scanner beam than to improve its shape and side lobes.

Consideration is being given to the use of long lengths of expanded dielectric rather than short lengths of solid dielectric. The weight appears to be less, and the bandwidth of the impedance transformation should be much higher. It is not yet known, however, whether the electrical constants of the material can be made sufficiently consistent.

It is hoped that the correcting blocks may be used also as the pressure seal at the throat of the final output flare. (A dielectric window across the whole stator is undesirable because it introduces another gap which cannot be choked.) It may be possible to grow a soft metal gasket on to the metallized surfaces of the dielectric blocks; if this fails, simple metallized blocks may be used, since the mechanical impedance presented to the high-pressure air will probably be so high that the leakage will be small. Another possibility is the use of a multiple gasket made of copper-plated P.V.C. rods.

Limited Dimension of Output Flare

The H-plane dimension of the final flared scanner mouth is limited by the stacking of the scanners and is not sufficient for the most desirable illumination taper on the lens. Narrowing of the beam from the limited aperture by the use of transverse pins (after Pao at M.I.T.) or by using a box-horn is therefore being considered in spite of the higher side-lobe energy characteristic of such devices.

Transverse pins have been found to produce a satisfactory beamwidth, but since the simple horn is extremely well-matched, the addition of pins introduces a severe reflection which it has proved difficult to remove.

Leakage through the rotor gaps will cause some energy to travel down waveguides adjacent to the eight which are being fed. This will produce an effectively larger E-plane aperture and a narrower E-plane beam from the scanner; however, this reinforcement is absent on one side of the radiating aperture, and there will be some variation of the radiated pattern. This has been noticed in experiments, but it is hoped that it will be tolerable.

Manufacturing Methods

The rotor, and to a lesser extent, the stator, clearly present the main manufacturing problem. The first models, like the experimental model, will be fabricated with vanes of 0.028 in. sheet brass held in curved slots milled in the two side plates. The slot cutting is done with a high-speed end-mill mounted on an engraving machine. Figure 6 shows the engraving of the two side plates of the first experimental rotor quadrant.

The brass vanes are pulled through the slots and soldered into place; the pillars are soldered into position, maintaining the free edges of the vanes reasonably plane.

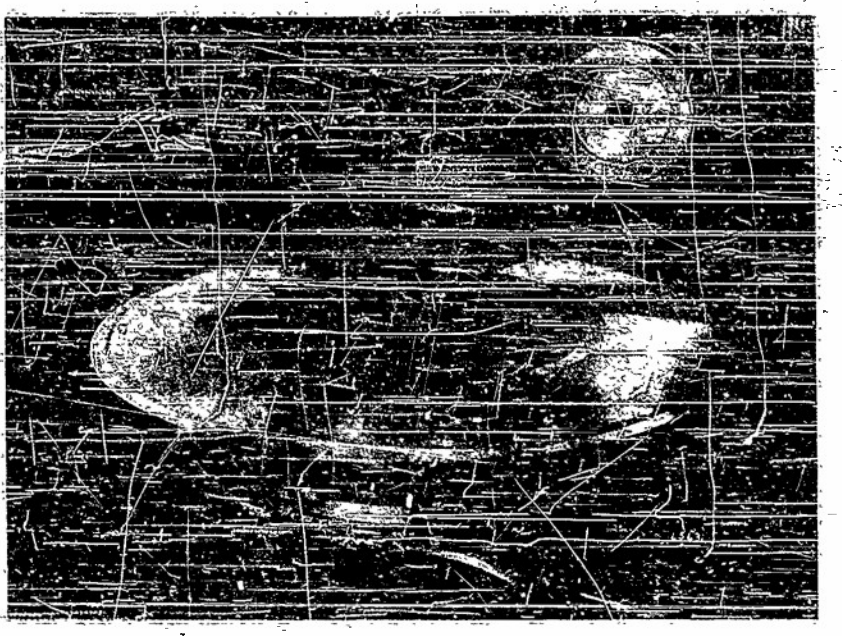

Figure 6 - Experimental model rotor showing engraving of side walls

In production, any matching posts in the rotor waveguides would be inserted in holes jig-drilled into the side plates before assembly. Difficulty arises, however, in the experimental determination of the positions and dimensions of such posts, since the side plates must be drilled from the outside where there is no really accurate indication of the position of the vanes.

Another method of manufacture using electroforming techniques is being explored, in which copper-plated light-alloy vanes are assembled in a perspex or wax jig and copper side plates are "grown" on to the vanes. In this case the vanes will be thicker (0.084 in.) and the first experimental quadrant, now being made, will be split along the central plane and made in two halves so that the matching posts can be inserted and soldered in from the inside of the waveguide.

Possibilities of low-pressure die-casting are being investigated, but the tooling is extremely complex, and it is doubtful whether the stator can be similarly made. The two previous methods, of course, apply equally well to the stator.

GENERAL PROGRAMME

The work described has led to the design of an experimental model scanner, which after many delays, has now been received from the contractors. It is shown in Figures 7 and 8. The rotor consists of rather more than a quadrant of the full circle since this contains all possible unlike waveguide paths of the set. There are two feeds so that either any eight adjacent rotor waveguides can be fed at once, or any single guide can be fed individually. The rotor can feed either into the stator or into a batch of twelve straight, matched waveguides which can be indexed so that the centre eight of these guides can be aligned with the particular set of rotor waveguides being illuminated by the feed. The rotor can also be indexed at intervals of half a waveguide. Thus the impedance of each individual rotor guide can be measured, as well as the scanner impedance for all rotor positions.

Figure 7 - Experimental model scanner with matched loads mounted and stator on bench

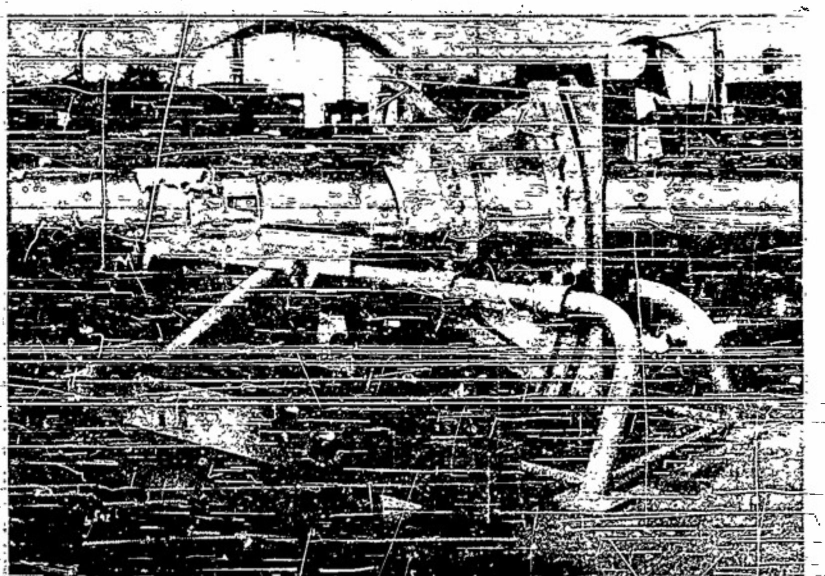

Figure 8 - Experimental model scanner with stator mounted and matched loads in foreground

This apparatus has only recently arrived in the laboratories, and it is hoped that a large quantity of information will be obtained from it in the next few months. After the first measurements, the main object will be to determine any necessary matching posts in the rotor, in order not to hold up production of the complete scanners. Measurements to date have shown that it will probably not be necessary to match at least half the rotor vanes.

The complete model scanner for the trials programme has been fully engineered and designed, subject to detailed modifications in the light of results on the experimental model, and it is hoped that this will form the production prototype. A section of this scanner is shown in Figure 9 and an outline sketch is shown in Figure 10. The whole unit is contained in a pressure tight light-alloy split casting, the rotor is held in two light-alloy spiders and rotates on two 6-1/2-in. ball races. A sketch of the five-scanner assembly is shown in Figure 11.

The author wishes to acknowledge the prominent part taken in the development of this scanner by D. G. Hanan (engineering Development and Design) and R. A. Ballard (Experimental Development).

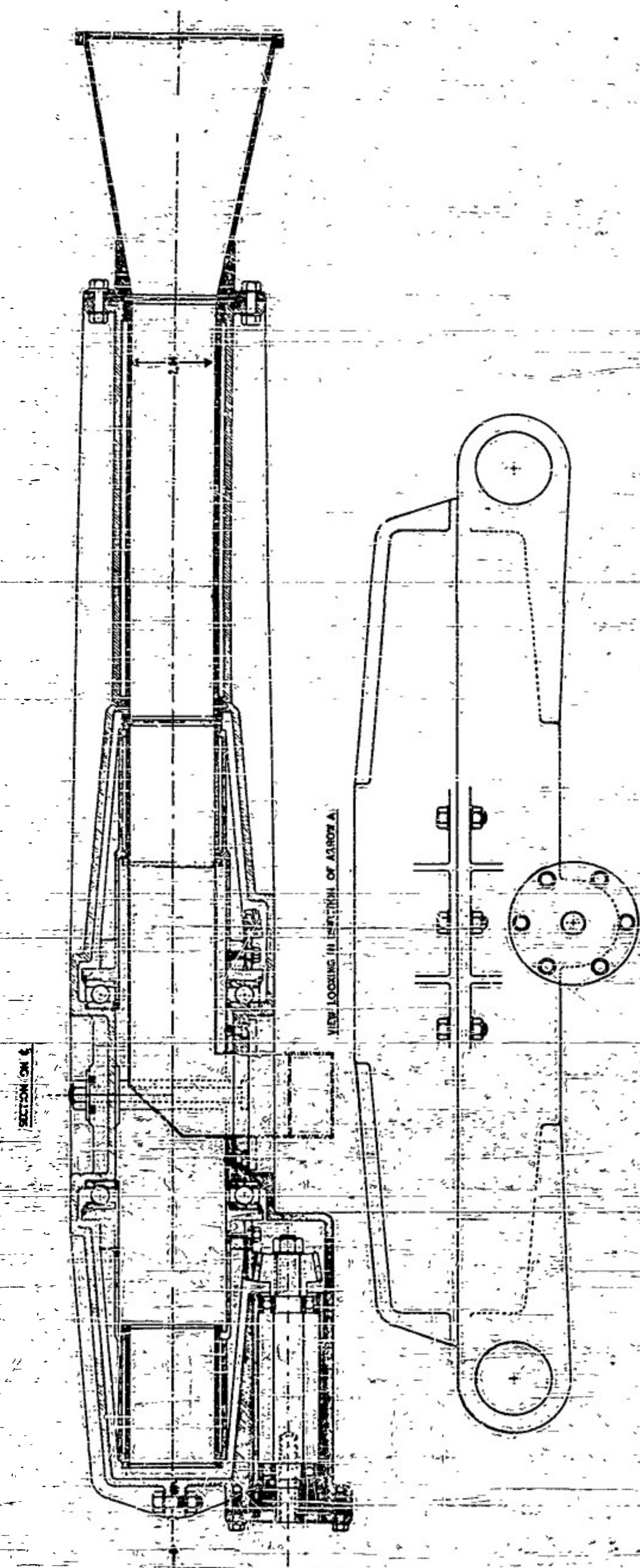

Figure 9 - Section of pressurized scanner

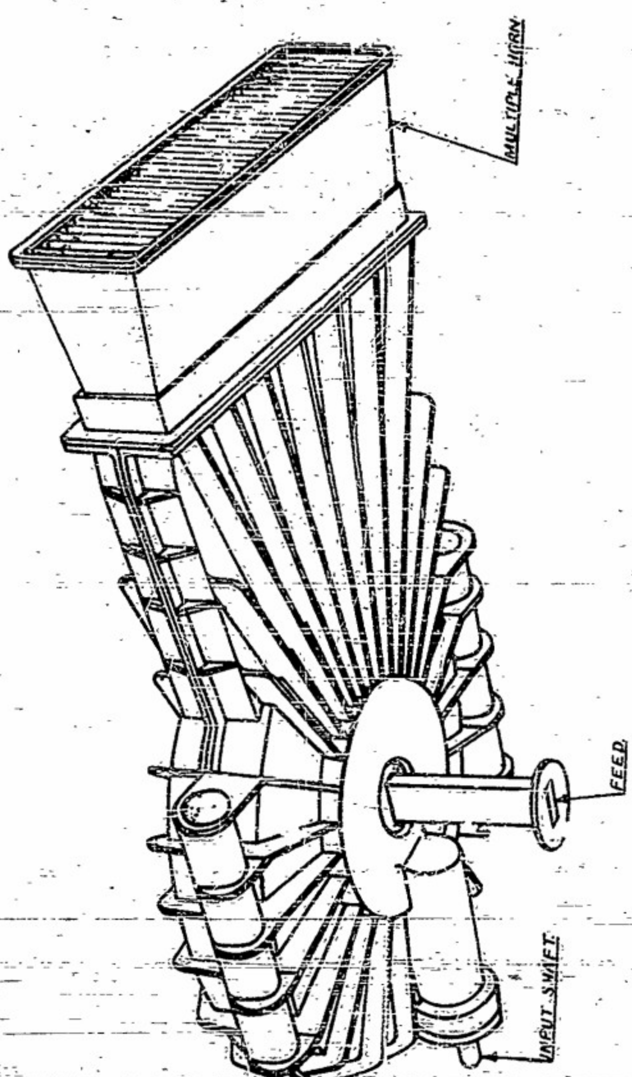

Figure 10 - Single scanner

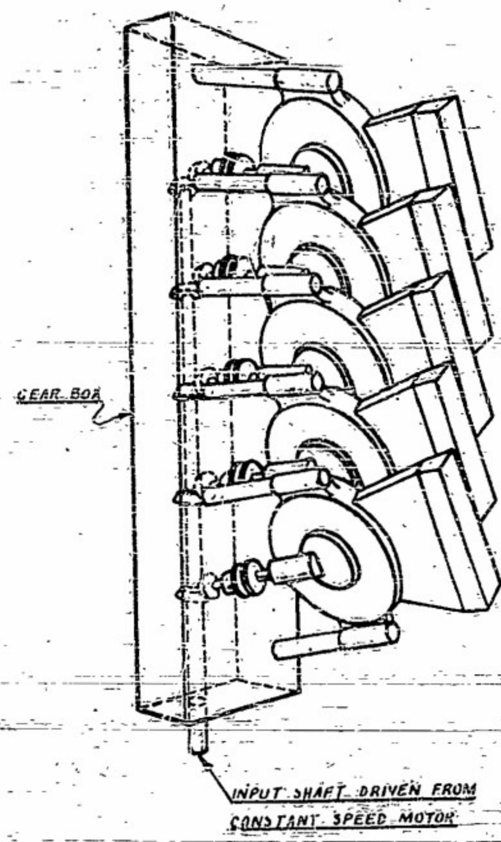

Figure 11 - Scanning unit

DISCUSSION

Rush: (GAFB) Could you clarify your statement that there was one pulse wasted in the system? Is that one pulse for every pulse sent out or one pulse for the entire scan?

Bristow: (ASRE) It is one pulse for the entire revolution of the scanner.

Sheitelman: (BuShips) Can you tell us what this device is used for?

Bristow: This is a radar for appraisal of the air situation. It is supposed to give vertical coverage up to 22-1/2 degrees and an azimuth scan rate of about 5 rpm.

Budenbom: (BTL) What is the wavelength of this system?

Bristow: It is an S-band set.

RING SCANNER WITH APPLICATIONS

W. F. Gabriel
Naval Research Laboratory

"Ring Scanner" is a name which has been arbitrarily chosen for the particular type of multiple-channel, waveguide ring switch with which we are concerned. This device was developed as a solution to the problem of obtaining a rapid, repetitive, feed-horn motion along an arc of a circle.

The most important element in a waveguide ring switch is the mechanism used to accomplish the switching action and, in the case of the Ring Scanner, this mechanism consists of a right-angle waveguide pin bend. The use of pins in waveguide bends first came to our attention through the work of Louis D. Breetz of NRL. Figure 1 shows a drawing of the pin-bend apparatus used by Breetz. It is reproduced from his NRL Report 3795. This particular device is a special type of rotary joint and contains two pin bends. Each bend consists of a set of five straight pins or "fingers" which are set so as to simulate a right-angle E-plane waveguide bend. The simple sketch to the right in Figure 1 shows a side view of the pin bends as they are about to pass through one another. It will be noted that there is no choke arrangement at the free ends of the pins, this omission being due to the particular application with which Breetz was concerned. A VSWR of about 1.2 over a 10-percent band was obtained with these pin bends, and it was found that they carried about 200 kw of power at X-band.

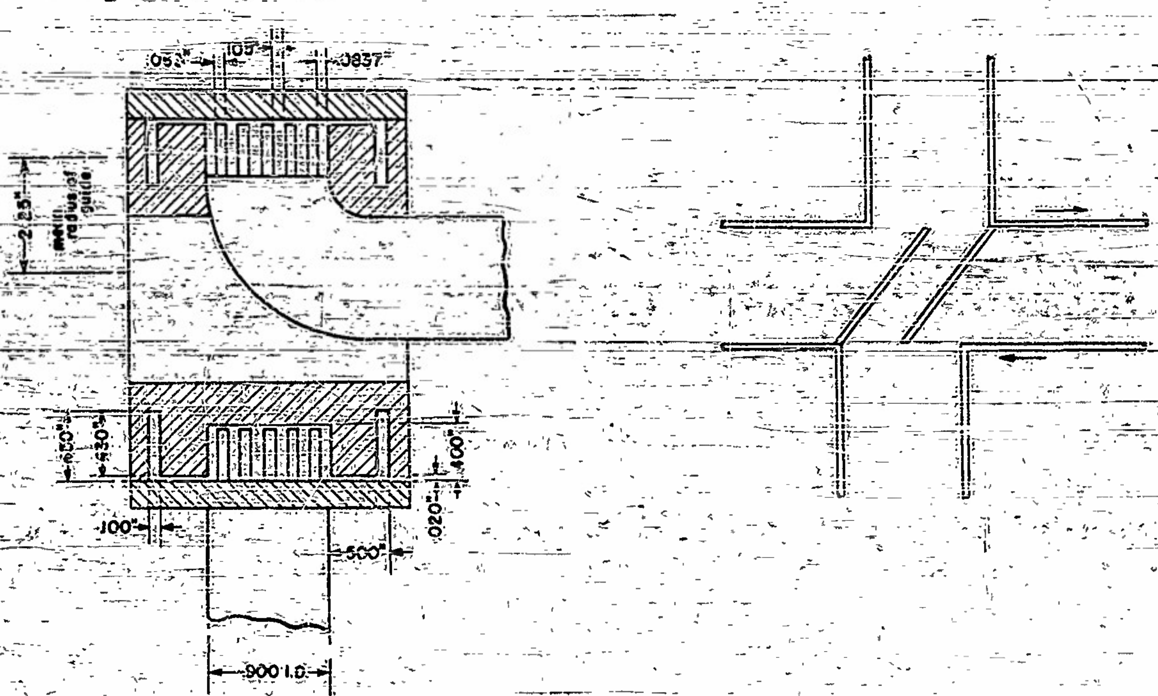

Figure 1 - Breetz pin bend apparatus

The simplicity of the pin-bend idea was very appealing, of course, and it was subsequently decided to develop a pin bend suitable for certain scanning applications. Figure 2 shows a photograph of the final model arrived at. Essentially, it consists of an ordinary double-mitred, right-angle, H-plane bend in which a portion of the solid side wall has been removed and replaced by closely spaced choke pins. This choke-pin bend was only slightly inferior to a solid-wall bend in terms of VSWR. Its success may be attributed to two factors: First, when the pins are arranged in an H-plane bend in this manner they are parallel to the guide-wall current paths and therefore do not interrupt those currents to any appreciable extent (that is not the case in an E-plane pin bend); second, the quarter-wavelength "choke-tail" on the free ends of the pins aids in approaching the short-circuit impedance which is desired at those points.

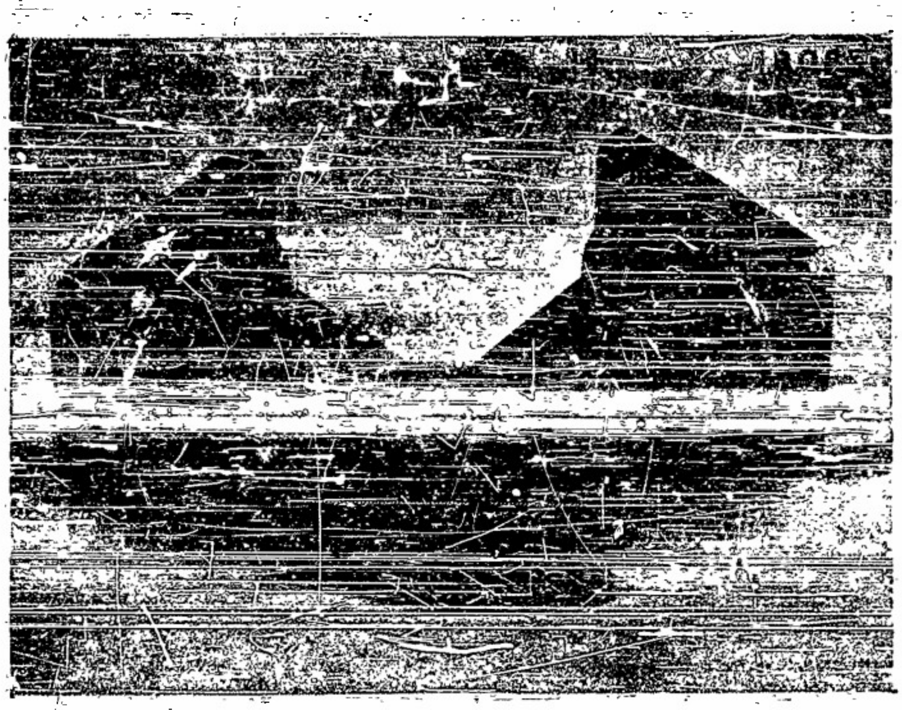

Figure 2 - Double-mitred H-plane choke-pin bend

Having obtained a successful pin-bend design, the next step was to apply it in a waveguide switch. Figures 3 and 4 show photographs of the waveguide switch which was constructed utilizing the H-plane choke pin bend. It is composed of two similar parts which can move relative to one another. Each part forms half of the common waveguide section in which the switching operation is carried out and supports one pin bend. Figure 5 is a simple schematic top view of the switch illustrating its operation. VSWR data taken on this particular switch is presented in graphical form in Figures 6 and 7. It will be noted in Figure 6 that the VSWR of a single H-plane choke pin bend is less than 1.1 over an 11-percent frequency band. Figure 7 is a plot of the switching cross-over mismatch; it shows that the minimum distance within which a waveguide branch can be switched from "on" to "off" is 1.5 inches, using standard 1 x 1/2-inch X-band waveguide. This distance, of course, is the "dead-time space" associated with the switch.

To test its power handling capacity, the switch was inserted between a 4J52 magnetron and a high-power dummy load. No sign of breakdown was observed for any position of the switch except, of course, at cross-over; thereby indicating a power handling capacity in excess of 100 kilowatts. Maximum power-handling capacity is not known at the present time.

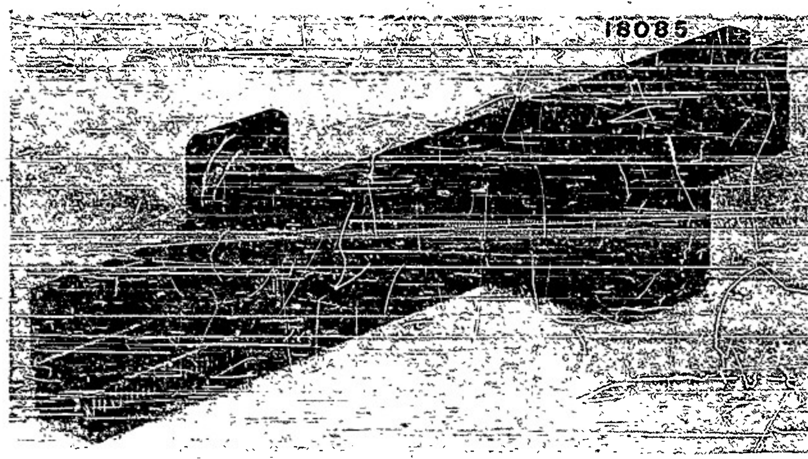

Figure 3 - H-plane pin bend waveguide switch

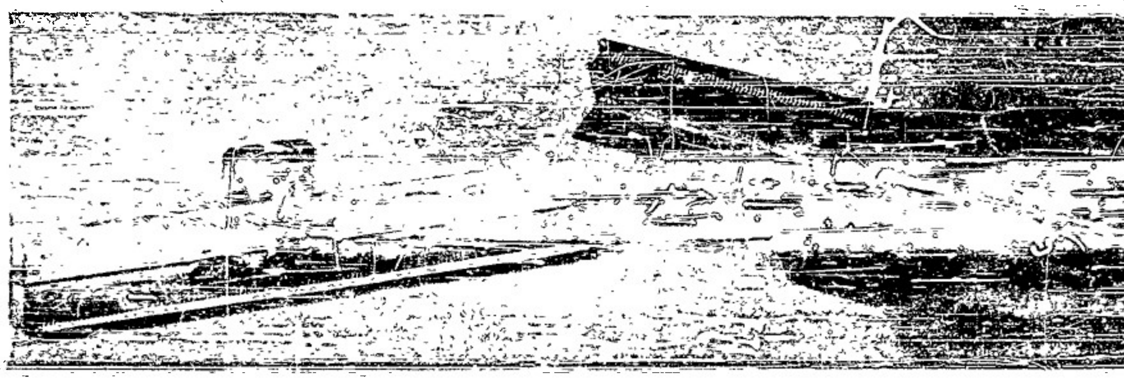

Figure 4 - Waveguide switch disassembled

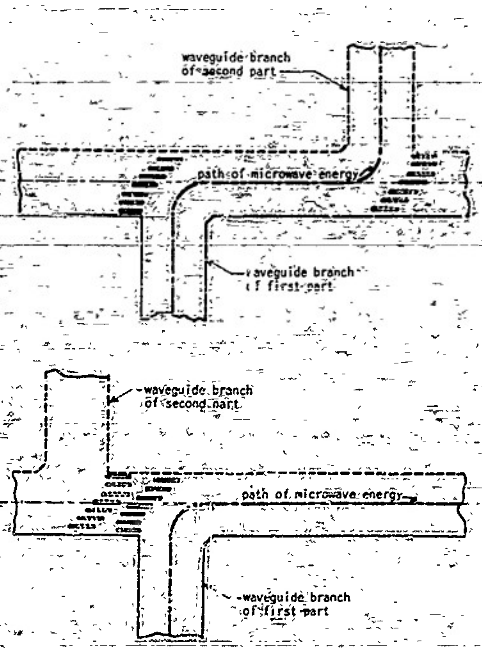

Figure 5 - Simple schematic illustrating
switch operation

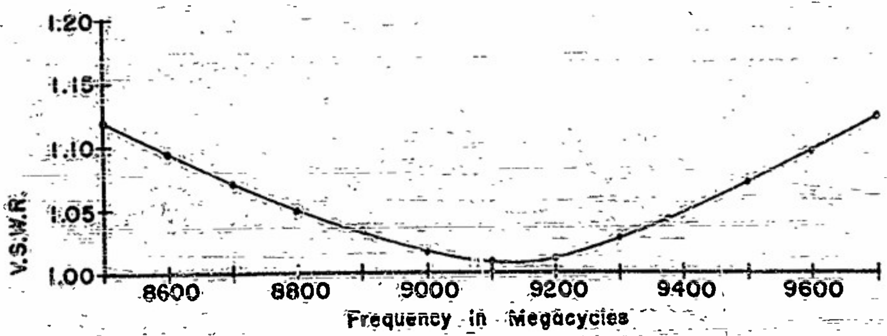

Figure 6 - VSWR of H-plane choke-pin bend

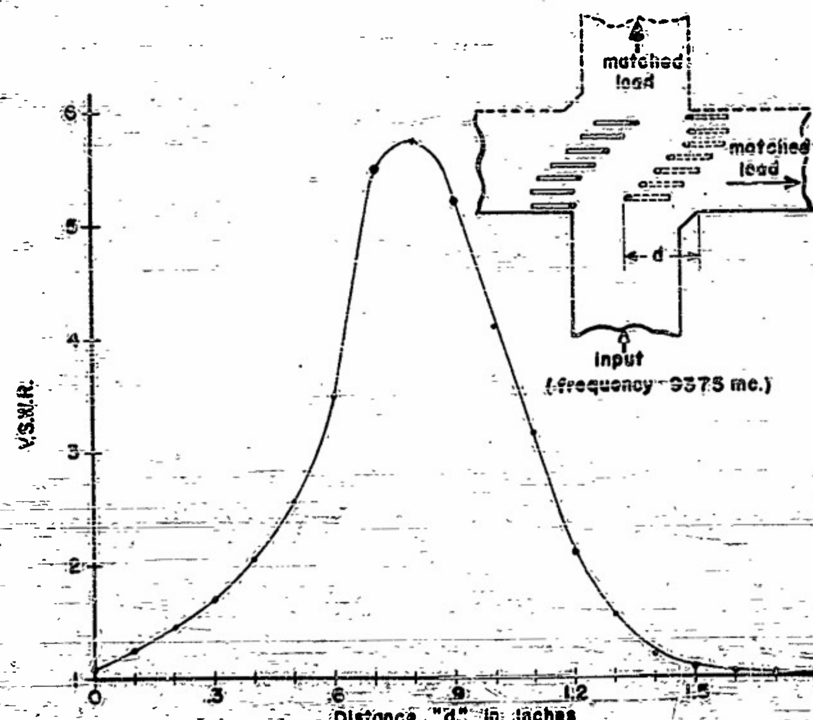

Figure 7 - VSWR during switching crossover

One of the problems which comes up in designing a two-piece waveguide section such as this is the longitudinal choke. Ordinarily, half-wavelength choke grooves are unsatisfactory because of the fact that they act like another waveguide of different wave velocity coupled to the main guide; consequently they cause changes in the normal phase and amplitude distribution along the main guide if a distance of more than a few wavelengths is involved. Also, there may be appreciable reflection of energy if the choke grooves are interrupted or terminated by a mismatch; conversely, there is appreciable radiation of energy out the ends of the choke grooves if they are not terminated properly. One method of reducing or eliminating these effects is to use a serrated choke which discourages longitudinal propagation of energy. Such a choke was used on the switch under discussion and may be clearly seen in Figures 3 and 4. The design is patterned after that used by Speery Gyroscope Company for their Transvar coupler, and consists of a row of closely spaced quarter-wavelength pins. It effectively breaks up longitudinal choke propagation and yet provides good choke action. However, it has the disadvantage of higher attenuation losses than the ordinary choke groove. An X-band waveguide channel 18 inches in length was constructed, utilizing this type of pin choke, and it was found to have an attenuation of 0.2 decibels per foot at 9375 megacycles.

The satisfactory operation of the foregoing straight-section pin switch led to the design of a complete Ring Scanner, shown in Figure 8 with the top cover removed. It has a diameter of about 20 inches and was designed to feed four organ-pipe levels in a two-dimensional "TV" type scanner. Figure 9 shows schematic views of this particular ring scanner. Here you can clearly see the input, the common waveguide section or "feed trough," the four output branches on the wheel, and the plumbing down to the appropriate output feed horns. The active scan angle (angle during which the output feed horn receives energy) is 82 degrees, and the switching dead-time angle is 8 degrees.

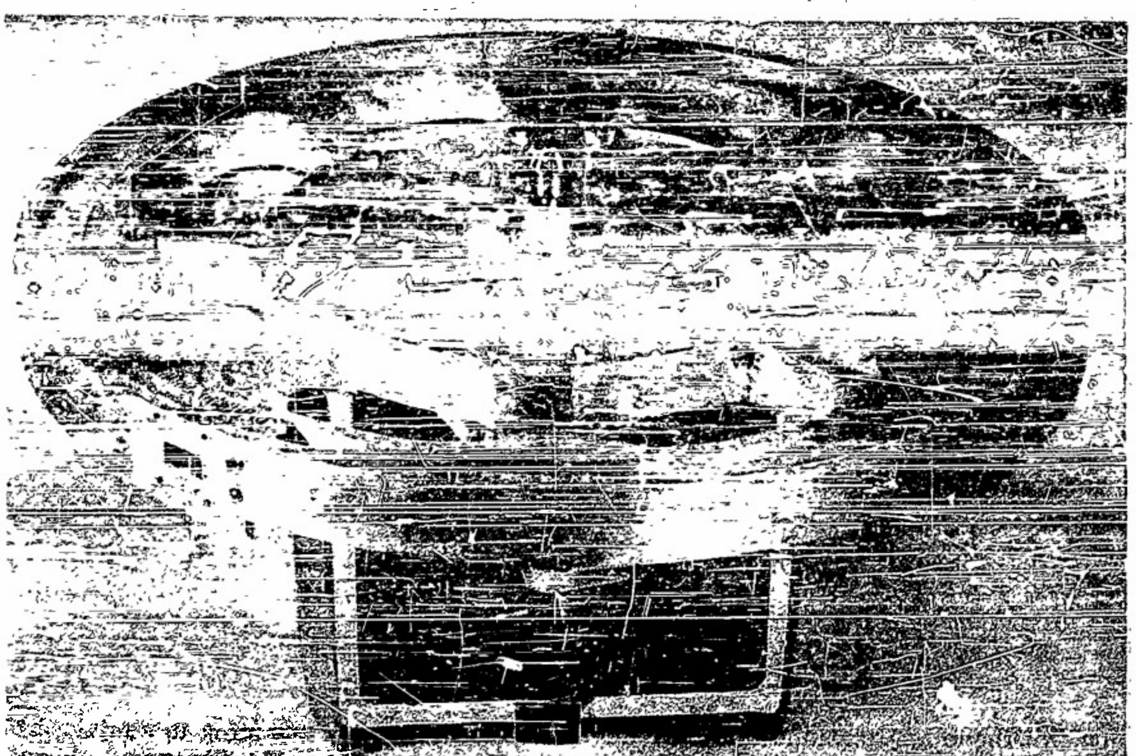

Figure 8 - Ring Scanner with cover plate removed

Preliminary measurements on the present model have shown that all of the pin bends are functioning as expected, but the choke design employed requires some alterations. The choke consists of a regular groove choke slotted at 1/8-inch intervals, and it appears to be radiating a little and also supporting longitudinal propagation to some extent. Its total losses amount to about 0.5 decibels per foot at 9375 megacycles. It would be very desirable, of course, to find a nonpropagating type of choke which has considerably lower attenuation losses, because this is the principal difficulty encountered to date in the Ring Scanner. However, even with the relatively high losses of present chokes, the Ring Scanner could be satisfactorily applied to several types of scanning problems because the length of the common waveguide section is not great enough to make the total losses objectionable.

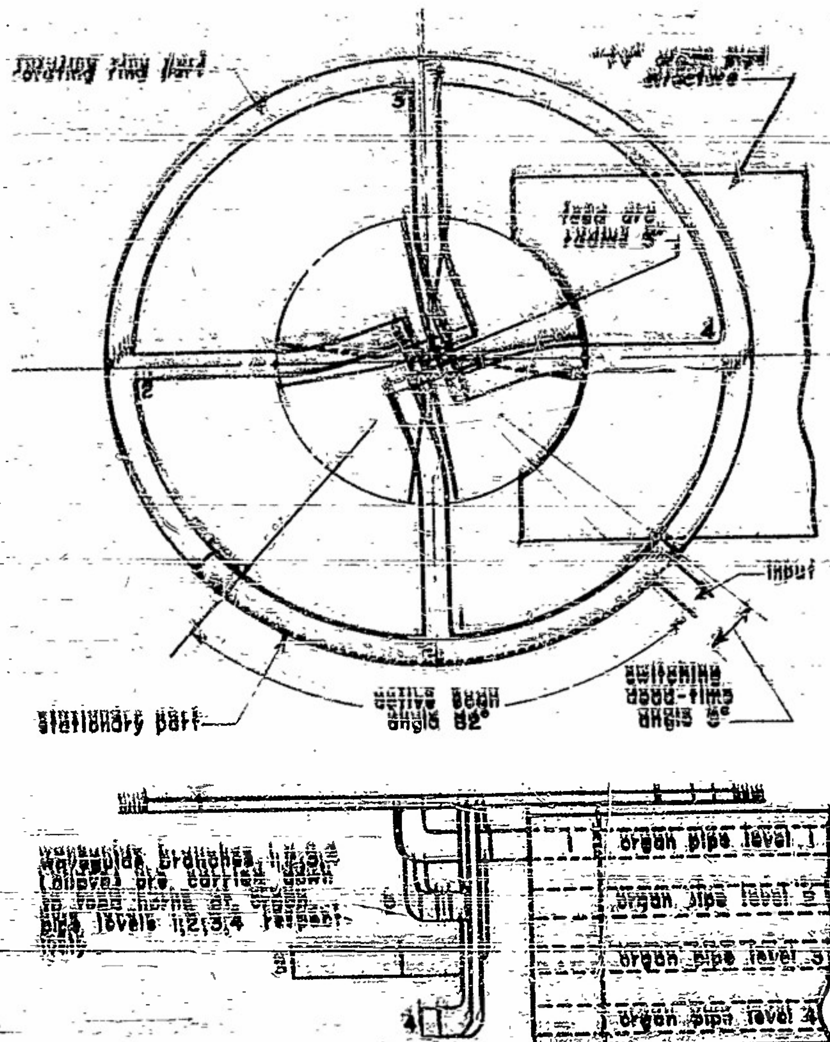

Figure 9 - Schematic views of Ring Scanner

One of these applications is small-angle, two-dimensional scanning in conjunction with an organ-pipe structure, for which the present model was designed. Figure 10 shows an artist's sketch of a proposed Ground Controlled Approach radar system. It consists of a fourteen-level, light-weight organ-pipe structure fed by two Ring Scanners whose wheels are attached to a common shaft. It operates in the following manner. Energy is fed to one of the two Ring Scanners which, in turn, feeds it to whichever organ-pipe level is being scanned; when that level has been swept, the fast-acting switch is triggered and shifts the energy to the other Ring Scanner which is in position to scan the next level. In other words, while one Ring Scanner is feeding a given organ-pipe level, the other is switching over so that it will be ready to feed the next level. In this manner, the switching dead time of the two Ring Scanners is completely eliminated and only that of the fast acting switch is present. (This proposal for cutting down switching dead time was advanced by Ralph E. Hiatt of the Air Force Cambridge Research Center.) The switch could conceivably be made with either gas-tube elements or ferrite elements similar to the Luhr's ferrite switch. The system could easily have an area scan repetition rate as high as ten to fifteen times per second if it were desired, since only free rotation is involved. The small drawing near the bottom illustrates a single Ring Scanner unit feeding two GCA systems pointed in different directions. This is possible because of the fact that the Ring Scanner is a multiple-channel switching device and, therefore, can have several inputs and associated outputs. Each system would be independent of the others and, if desired, could operate at a different frequency.

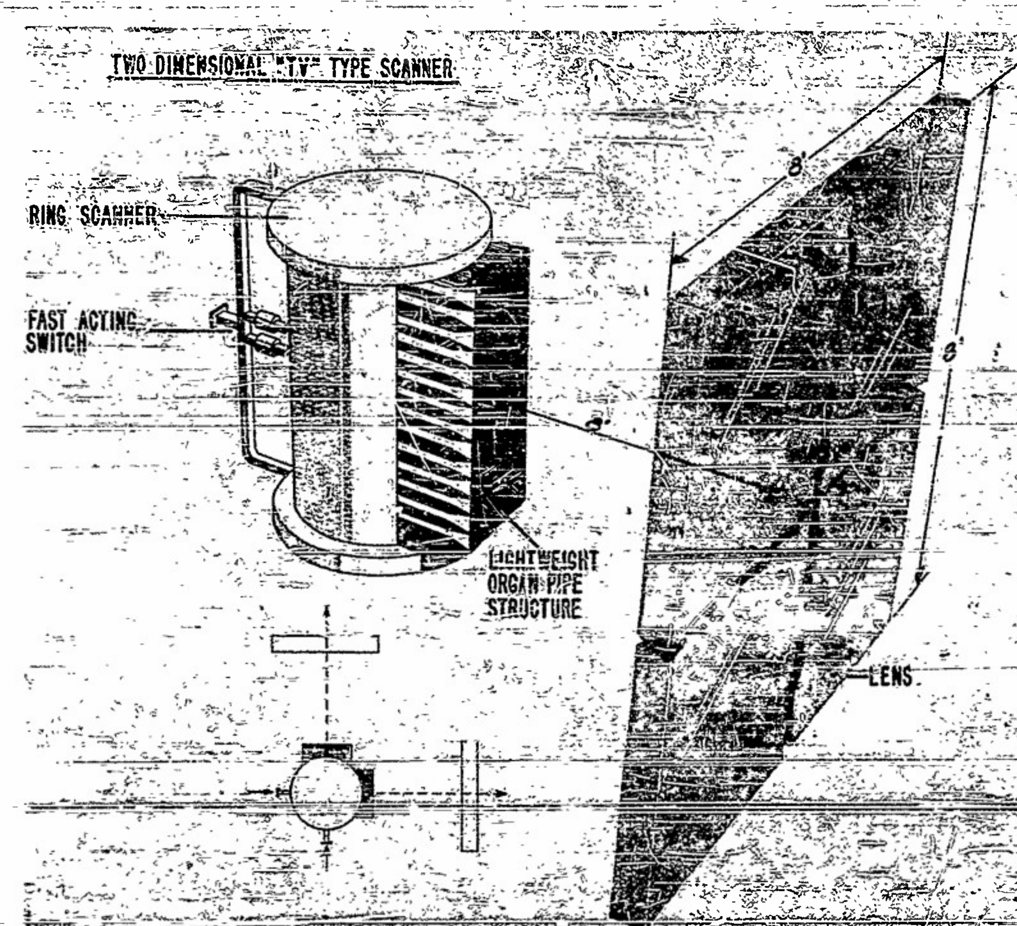

Figure 10 - Artist's sketch of GCA radar proposal

Another application of the Ring Scanner would be that of feeding various types of microwave optical systems such as the Schmidt lens scanners, concentric lens scanners, virtual source scanners, Luneberg lens scanners, surface-of-revolution scanners, etc. As a typical example, let us consider the feed required for a Schmidt lens system in which the scan angle is to be about 40 degrees and switching dead time less than 10 percent. Figure 11 shows a schematic view of the Ring Scanner required, and Figure 12 illustrates how it would be mounted with respect to the Schmidt lens pillbox. Since the scanning wheel carries eight feed horns, it would have to rotate at a speed of only 225 rpm in order to obtain a scan repetition rate of 30 cps. Figure 13 is a photograph of a model which illustrates a proposal for scanning an 84-degree sector by combining two such systems.

If a surface-of-revolution optical system were available, this 84-degree coverage might be obtained by using only one Ring Scanner instead of two. Figure 14 shows a cross-section view of what such a system might look like.

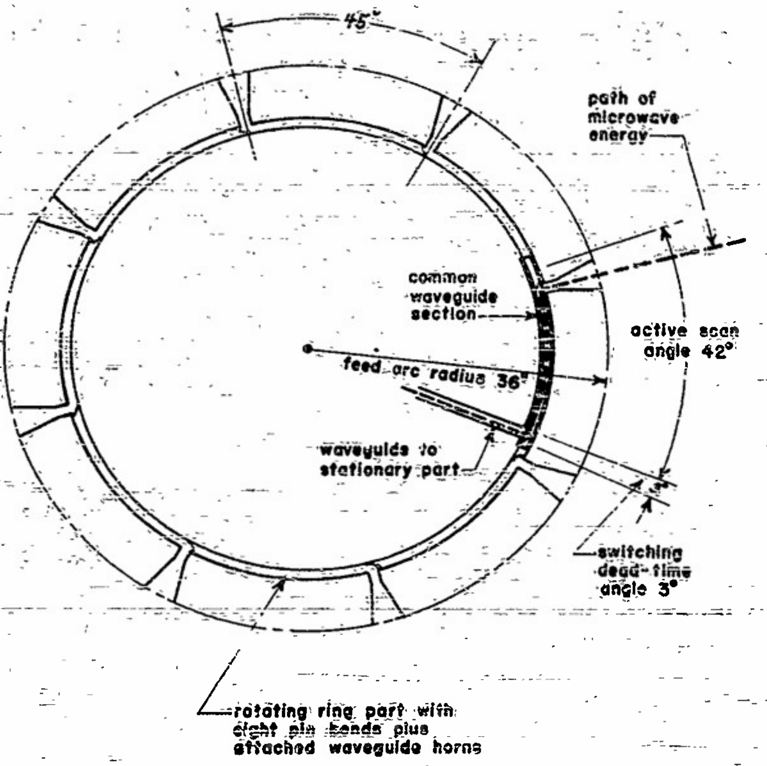

Figure 11 - Schematic of Schmidt System Ring Scanner

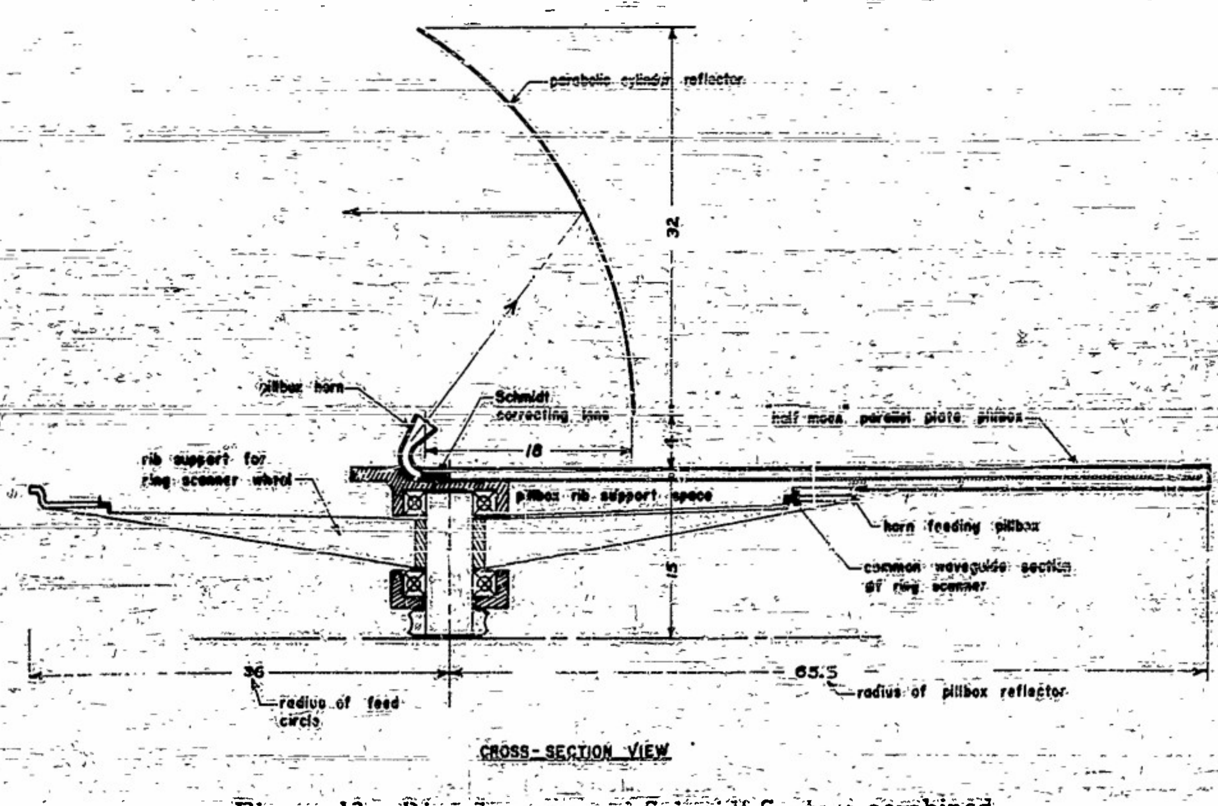

Figure 12 - Ring Scanner and Schmidt System combined

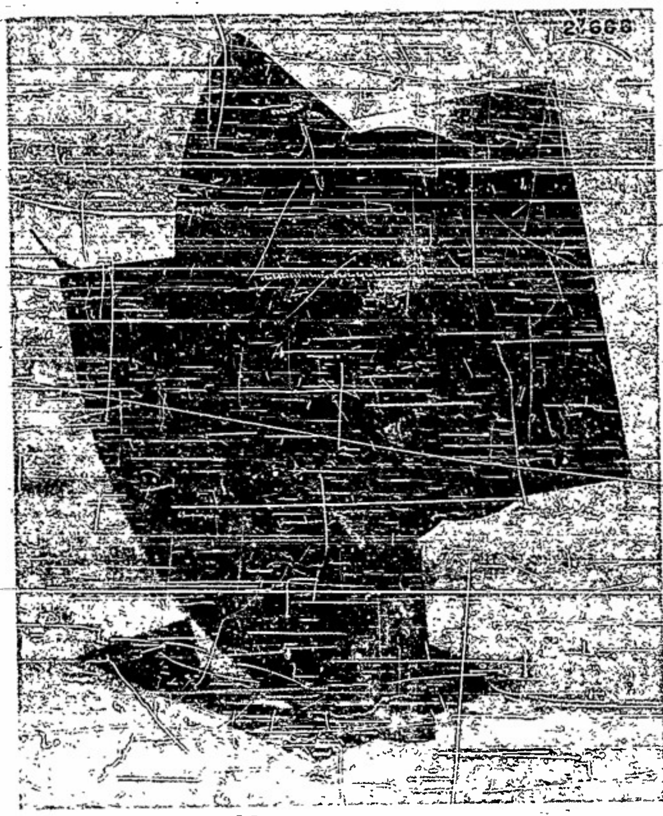

Figure 13 - Model of Schmidt System proposal for 84-degree scan angle

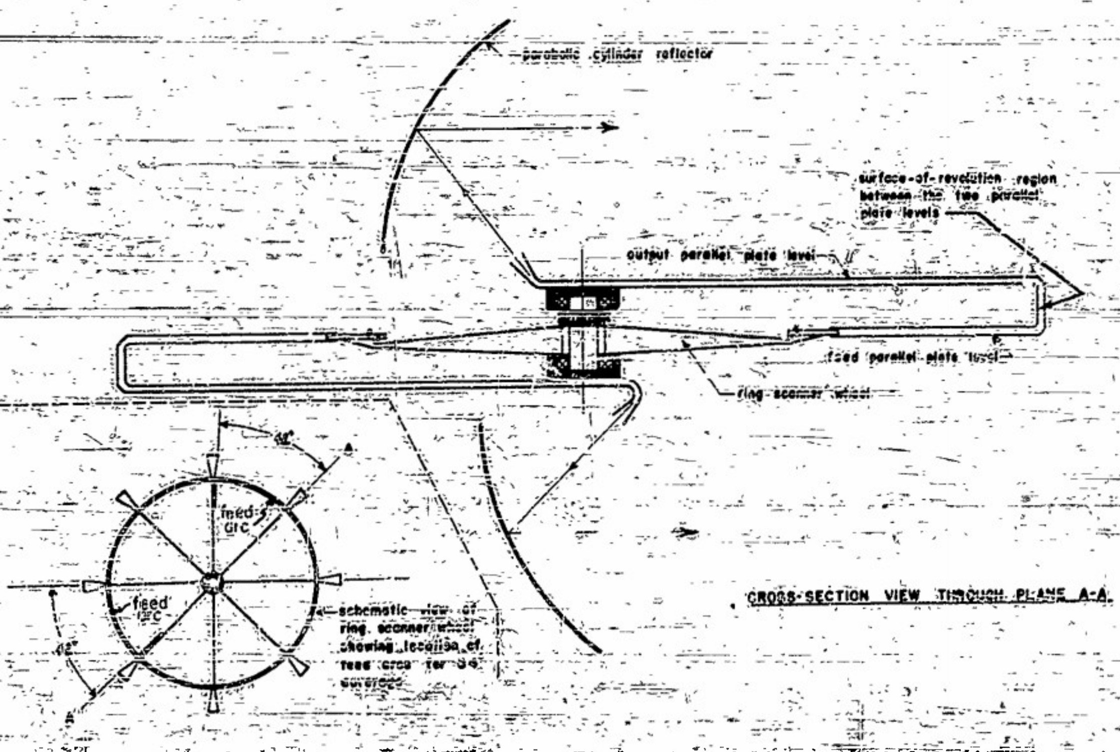

Figure 14 - Single Ring Scanner feeding two microwave optical systems

The last application to be discussed is known as the Concentric Circle Scanner. Figure 15 is a drawing of a proposed X-band Concentric Circle Scanner. The heart of the device is a Ring Scanner, of course, and in this drawing you can see the input waveguide feed and five output branches which go to five feed horns located at different radii. If the input were to be held stationary and the scanning horn wheel rotated, each horn would be fed over the same angle, and a pie-shaped sector would be scanned. If, however, the input is also rotated in the same direction as the scanning wheel, various scanning effects can be obtained. For instance, by rotating the input at the same speed as the scanning wheel, you could pick out any of the five horns and scan it continuously. Then again, by rotating the input at exactly 4/5 the speed of the scanning wheel, each horn will be fed for one complete revolution of the scanning wheel; thus giving a full solid-angle scan consisting of concentric circles (thus the name). These scan circles are complete except for switching dead-time spots. However, the switching dead-time spots can be made to precess by rotating the input a little faster than exactly 4/5 the speed of the scanning wheel. In fact, by selecting the proper speed ratio of the two wheels, the dead-time spots can be made to vanish altogether. Of course, this doesn't make the switching dead-time vanish; it merely causes it to occur between complete scan circles.

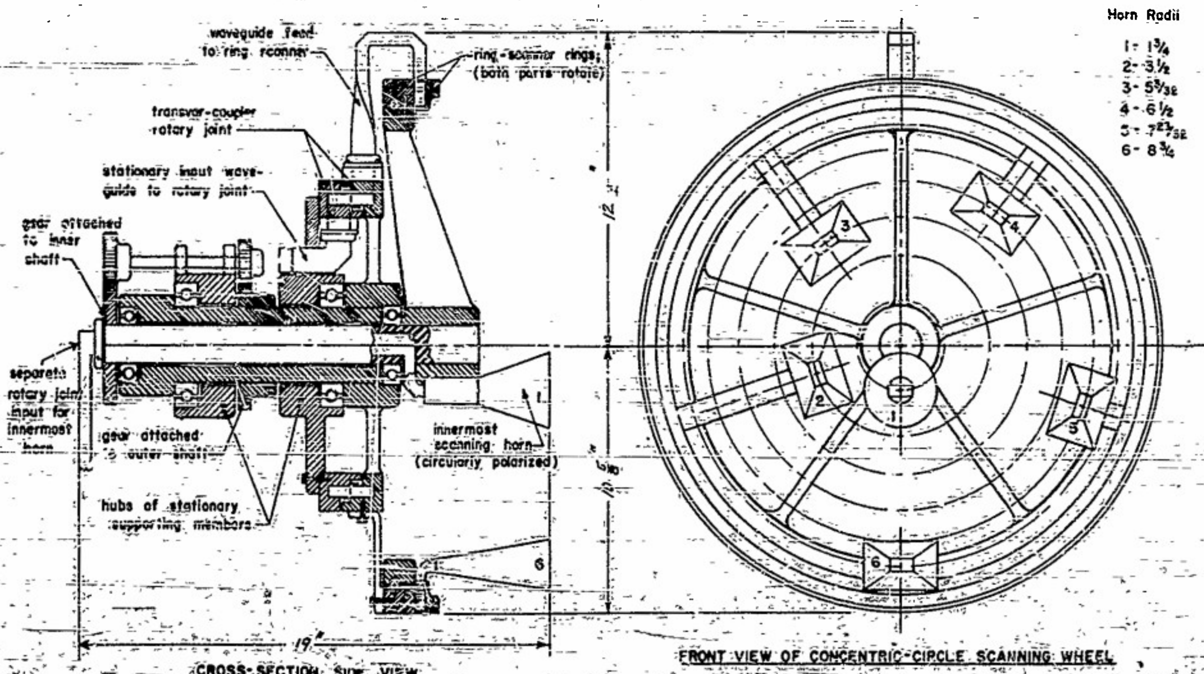

Figure 15 - X-band Concentric Circle Scanner proposal

Due to the fact that the input to the ring scanner is rotating, it becomes necessary to employ a rotary joint here. In this particular proposal, the Sperry Gyroscope Company Transvar Coupler rotary joint was considered, because it permits a simple construction for this scanner and yet feeds over a full 360 degrees of rotation.

You will note that the center horn is not fed by the ring scanner like the other five, but is fed separately through the supporting shaft for the scanning wheel; also, it is circularly polarized rather than linearly polarized like the other horns. The reason for this is that this was a proposal for a combination tracking radar and look-through search radar for use with either a gun fire control system or target missile guidance system. The scanning wheel was to rotate at 1800 rpm; thus giving a tracking signal of 30 cps and a solid-angle, look-through, search scan with a repetition rate of about 5.5 times per second. Figure 16 shows an artist's sketch of a Concentric Circle Scanner.

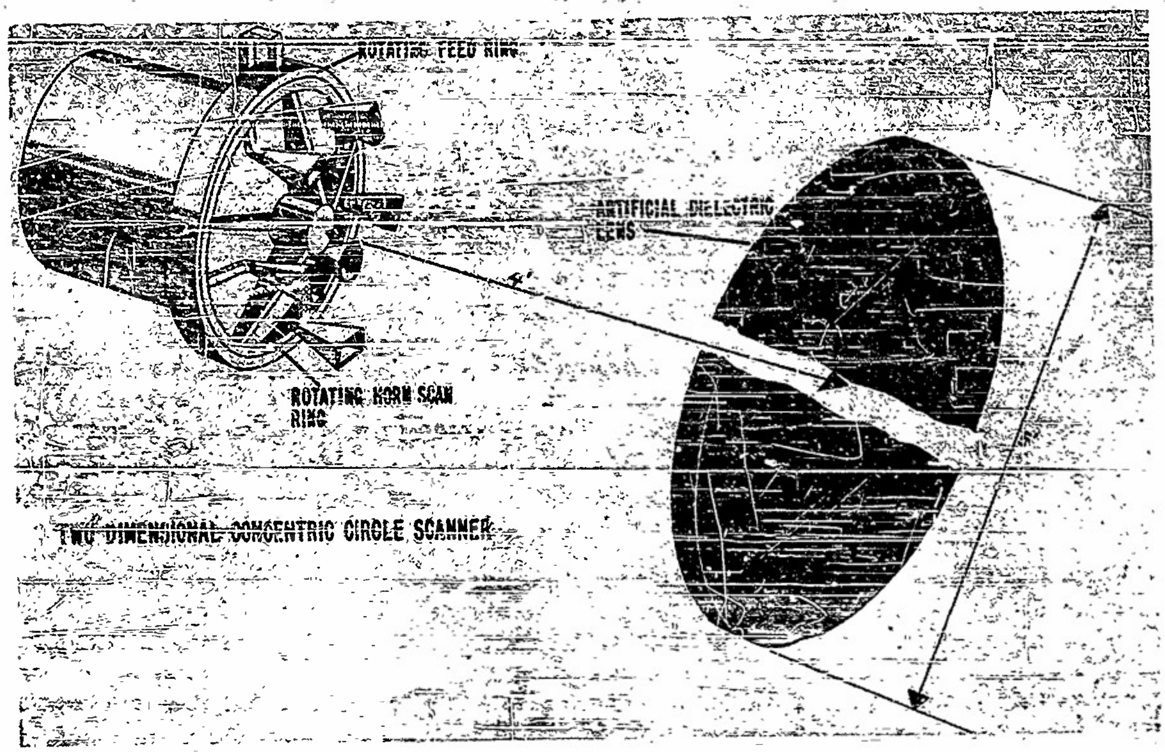

Figure 16 - Artist's sketch of Concentric Circle Scanner

The author wishes to acknowledge the assistance of Kenneth S. Kelleher in working out the foregoing applications of the Ring Scanner.

DISCUSSION

Budenbom: (BTL) What spatial angle does your ring scanner angle of 80° correspond to?

Gabriel: (NRL) I had indicated a ring scanner used in conjunction with the Schmidt system. For that antenna we expected a scan angle of 40° to 45°. To reach the 84° shown on the slide it was necessary to use two Schmidt scanners.

MARK 25 MOD. 6 SCANNER

M. Burlingham
Reeves Instrument Corporation

We, at Reeves Instrument Corporation, have been working on an automatic tracking and missile flight control radar.

The Mark 25 Mod. 6 Scanner was developed because the specifications required a system using a 7 1/2-foot lens, a system which would be able to acquire and track a target and to guide a beam riding missile. This scanner is matched to a VSWR of 1.2 or better over a 300-megacycle bandwidth and has a loss of less than 1 db. The scanner waveguide components, including the 3-high-speed rotary joints, are capable of withstanding pressures above 30 lbs/sq in., although the operating pressure is set at 15 lbs/sq in.

Figure 1 shows a side view of the scanner which has an over-all length of 28 inches and a maximum diameter of 20 inches. To produce the desired scanning, a dc motor, under the control of an amplidyne speed regulating system, drives a horn-type radiator through a gearing system. The horn moves in such a manner that the radar beam, after passing through the lens, will move in either a spiral pattern for target acquisition or a conical pattern for target tracking and missile guidance.

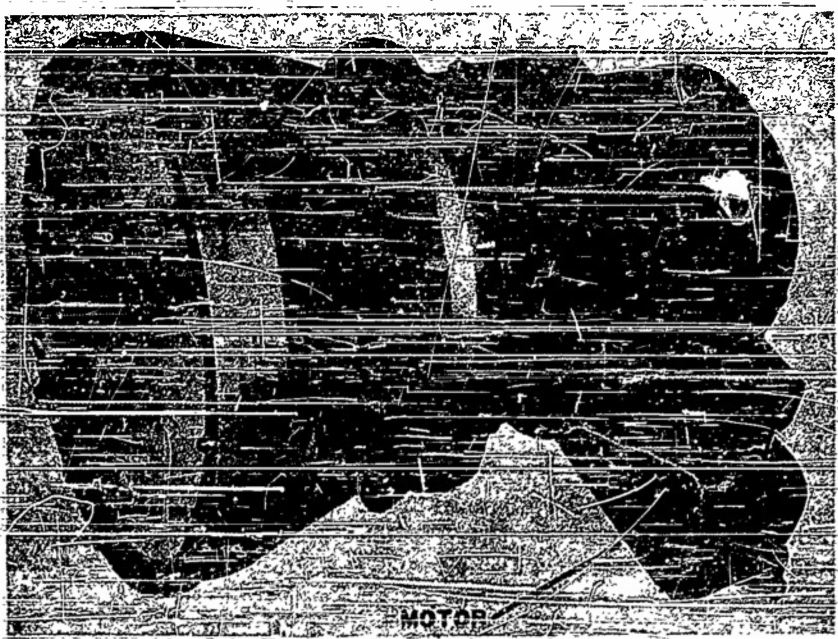

Figure 1 - Side view of scanner

Figure 2 is a rear view of the scanner with the rear cover removed. The rotary joint is one of three necessary to bring energy from the stationary waveguide run to the horn. This particular joint permits conical scanning. The instantaneous train and elevation position of the horn in scan is derived from the output of the three two-phase 30-cycle reference generators. The solenoid operates the clutch which controls the type of scanning—conical or spiral.

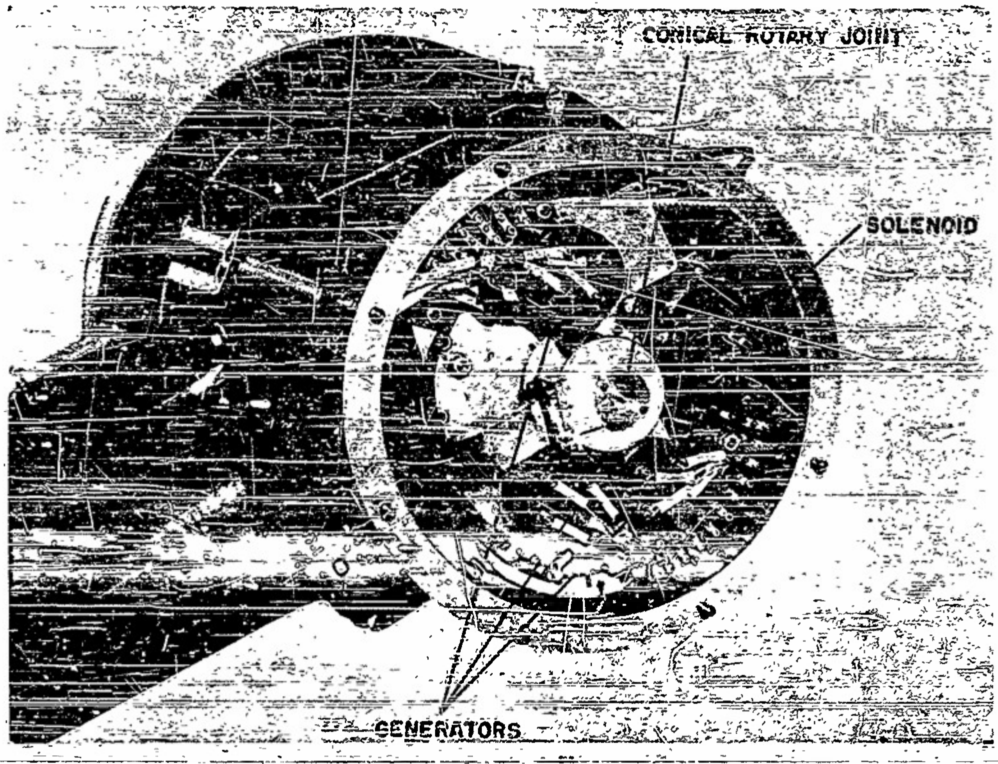

Figure 2 - Rear view of scanner

Figure 3 is a front view of the scanner with the front housing and the Fiberglas cover removed. The remaining two rotary joints are partly visible. The rotary joint in back of the horn is necessary to allow the radar beam to remain vertically polarized. It permits horizontal orientation of the horn's longer dimension. The other rotary joint, in conjunction with the rear conical rotary joint, permits spiral scanning.

Figure 4 illustrates all of the microwave components of the scanner. A flexible waveguide connects the scanner housing to the rear conical rotary joint. The gooseneck assembly, the secondary T-head, and the horn assembly are the rotating microwave components of the scanner. The gooseneck assembly is attached to the secondary T-head by means of the spiral rotary joint. The horn assembly is attached to the secondary T-head by means of the polarization rotary joint. Since the longer dimension of the horn must remain stationary, a gear train, the first gear being nonrotating and the last one being attached to the horn assembly, is employed.

Figure 3 - Front view of scanner

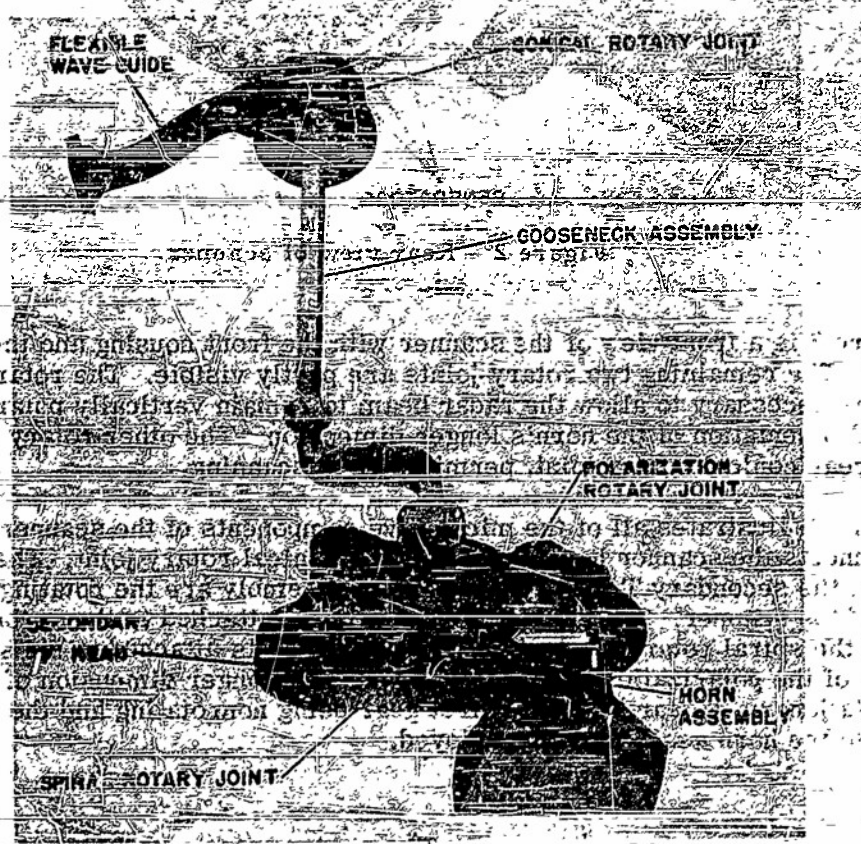

Figure 4 - Microwave components of scanner

With the help of Figure 5, it can be shown how spiral or conical scanning is accomplished. In (a) the scan drive motor rotates the T-head about the primary center line at a speed of 1800 rpm. With the clutch in the spiral position, as shown in (b), the T-head rotates about its own axis (the secondary center line) at a speed of 144 rpm; the resultant horn motion consists of the sum of these two rotating motions.

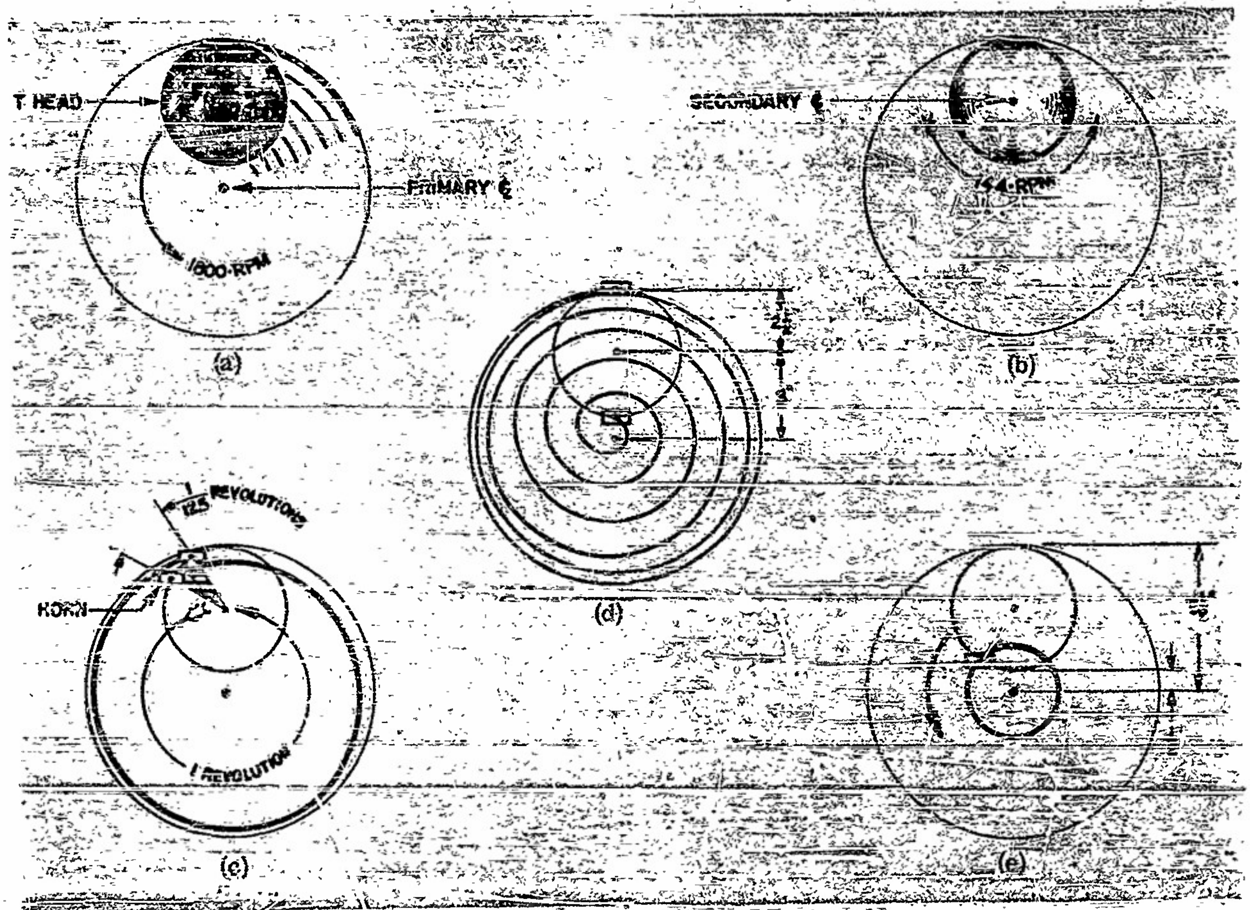

Figure 5 - Scanner rotation

For every rotation of the T-head about the primary center line in (c), the horn which is attached to the T-head moves less than 1/12 of a turn about the secondary center line. Thus it takes 12-1/2 turns of the assembly for the horn to make one complete revolution.

The axis of the horn in (d) is 2-1/2 inches from the axis of the T-head, and the axis of the T-head is 3 inches from the primary axis. Thus the horn describes a spiral with an inner radius of 1/2 inch and an outer radius of 5-1/2 inch. In conjunction with the lens, this provides a solid field-view angle of 7 degrees.

With the clutch in the conical position (e), the T-head does not rotate about its own axis. Thus the resultant motion consists of the fixed-radius rotation of the horn about the primary center line. Provision is made to adjust the radius of rotation between a minimum of 1/2 inch and a maximum of 5-1/2 inches.

The function of the clutch in Figure 6 is to cause the secondary T-head to rotate about its axis for spiral scanning or not to rotate about its axis for conical scanning. Choice of scans may be had by throwing into the system, by means of the clutch which is splined to the follower, either the spiral or the conical driver. Note that the conical driver is equipped with a single tapered recess, but the conical clutch half is equipped with a single tapered tooth to permit predetermined fixed-radius positioning of the horn in conical scanning. Because there is relative speed between the two drivers, springs had to be incorporated between the two halves of the clutch to take up the initial shock when shifting from one position to the other.

Figure 7 is a typical high-speed, pressurized rotary joint employed as the rear conical rotary joint. Note the size of the rotary joint by comparing it with its standard X-band flange.

Pressurization is achieved with the help of a lapped, nitrited nitralloy surface which rotates against a low-coefficient-of-friction carbon graphite (graphitar) surface. The nitralloy surface is locked to half of the rotary joint, and the graphitar surface is keyed to the other half of the rotary joint.

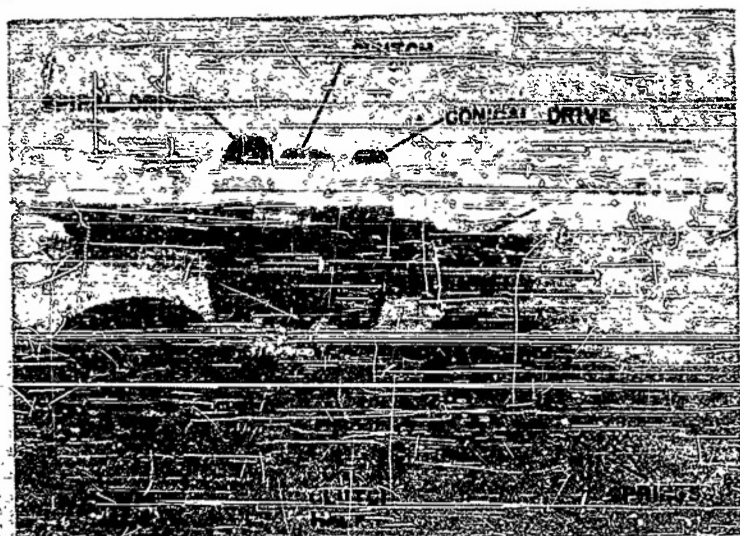

Figure 6 - Scanner clutch

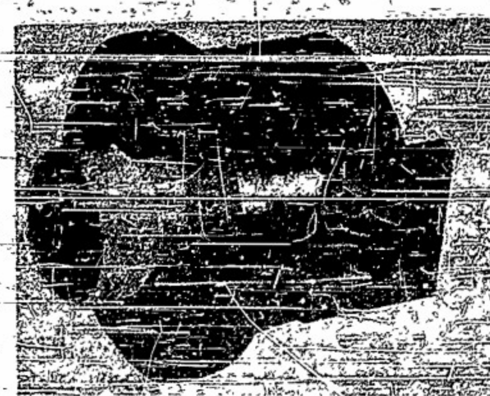

Figure 7 - Scanner rotary joint

DISCUSSION

Dunbar: (SRI) What speed is used with the high-speed rotary joints? Is it possible to get 3600 rpm?

Burlingham: (Reeves) Our highest speed has been 1944 rpm.

Dunbar: Would your bearings take a higher speed?

Burlingham: I see no reason why they could not be rotated faster, although we have not attempted this.

Budenbom: (BTL) Could these joints hold the pressure that might be required in an aircraft system?

Burlingham: There is a certain amount of leakage. We replenish the air at all times.

Budenbom: You think that with the addition of an air bottle that we might be able to use this joint?

Burlingham: Yes, I believe you may be able to do that.

* * *

CASSEGRAIN SYSTEM WITH DIAMETRIC SCANNING

H. H. Hibbs
Naval Research Laboratory

Since the idea for a diametric scanning antenna was a product of our last scanning symposium, this seems like a good time to talk about it.

The possibility of scanning an objective across its diameter, while at the same time have the diameter rotate about the axis of the objective, was first suggested to us by Mr. Small who until a few weeks ago was associated with the Antenna Research Branch of NRL, but is now with NEL in California.

It was decided that an antenna of this type might have possibilities as a track-through scan radar. I will attempt, in the short time that I have, to describe some of the work done to date on this system.

The organ-pipe feed system shown in Figure 1 was designed and constructed to satisfy the requirements for diametric scanning. A symmetrical design was used so that the feed system could be rotated about an axis which is perpendicular to the screen. Mr. Bartelt of the Bureau of Ordnance suggested that we use a wavelength of 1.8 cm. The feed circle is at the rear and in the center of this structure; this enables us to rotate the feed horn and organ-pipe feed about the same axis.

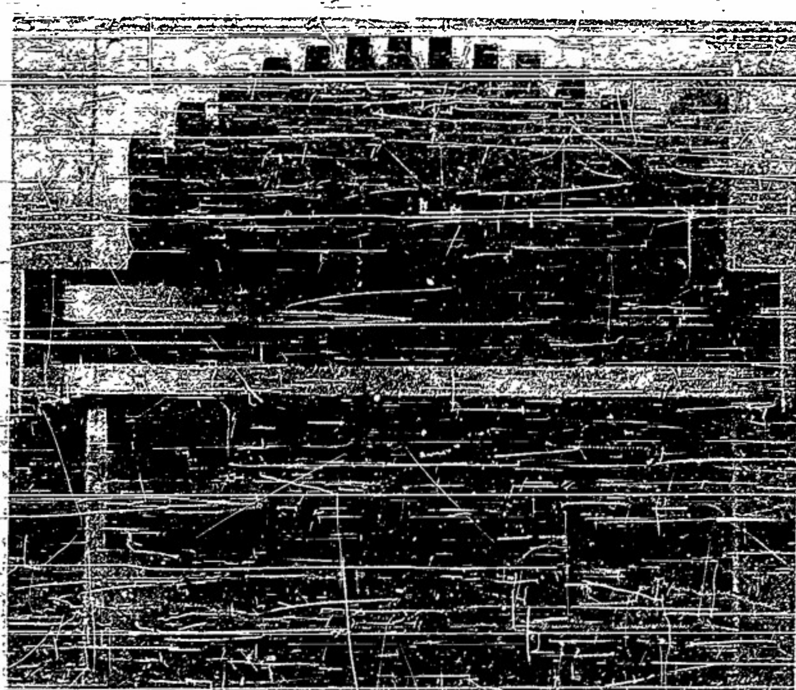

Figure 1 - Organ-pipe feed system

The microwave energy is transmitted from a rotating feed horn in the feed circle through the waveguide channels and out the aperture which is across the center line. The waveguide channels are looped over to form trombone sections thus making each path length equal. The feed horn scans completely across the aperture and then returns to the starting point. Three of these channels are fed at one time to produce a 10-db beamwidth of 28 degrees. The box horn was added to give the same beamwidth in the H-plane.

For mechanical simplicity in achieving the diametric scan, we decided to try a Cassegrain System. Figure 2 shows our first model which utilized on existing parabolic cylinder. The organ-pipe feed was placed at the rear, and the box horn was inserted through a slot in the center.

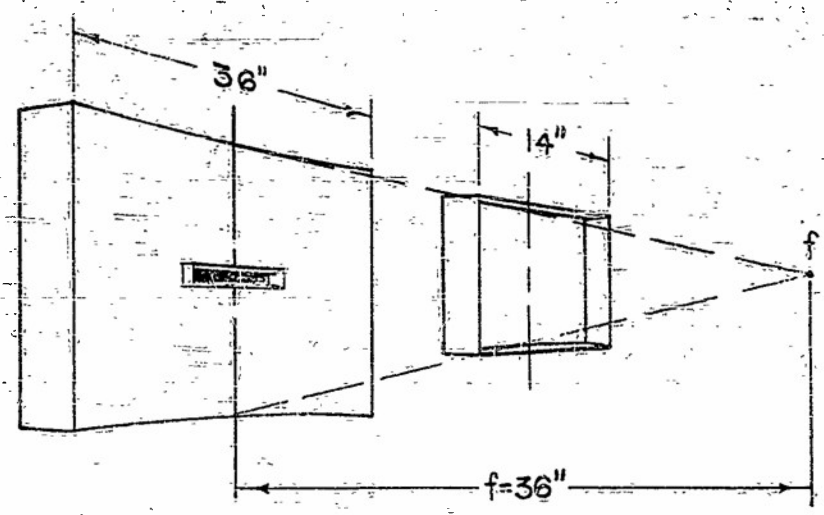

Figure 2 - Cassegrain System

The hyperbolic cylinder was so designed that if placed at a point which would properly illuminate the parabolic cylinder it would produce a virtual source at the focus of the major reflector. As you can see, our major problem here is the blocking caused by the hyperbolic cylinder, and it is no doubt the cause of the high side lobes.

Figure 3 is one of the best patterns obtained with this setup. We have a 3-db beamwidth of 1.85 degrees, and the highest side lobe is 18 db down. With this data we were ready to proceed with a two-dimensional model.

Figure 4 shows the Diametric Scanner and Cassegrain System as you will see it on exhibit. As yet we have no conclusive data on this model. The organ-pipe feed is placed at the rear of the reflector and can be rotated with the center of the reflector. The hyperboloid is supported by Fiberglas tubes and can be positioned with adjusting screws. By different combinations of rotational speeds of the scanner and scanner feed horn, many unique scans may be obtained - from a sectoral scan through a spiral scan to a diametric scan.

We have this model rigged with lights to demonstrate the different scan possibilities, and it will be on exhibit in Building 52.

In conclusion, I would like to give acknowledgment to Mr. Kelleher for his assistance on this project.

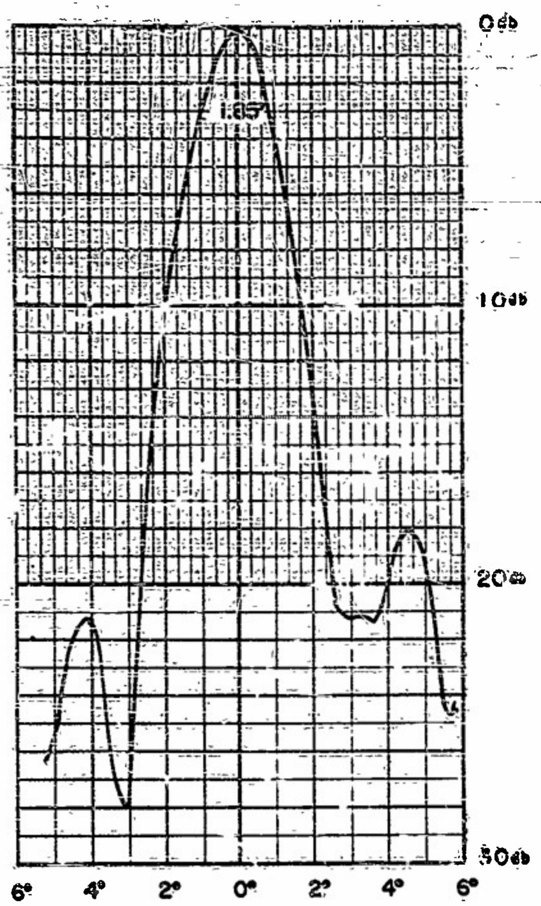

Figure 3 - Antenna pattern

Figure 4 - Diametric Scanner and Cassegrain System

DISCUSSION

Thomas: (Gi. Martin)	I would like to ask Mr. Bibbs if he feeds three alternate waveguides?
Hibbs: (NRL)	Yes, that is right. There is a space between each waveguide.
Thomas:	Does that produce high lobes?
Hibbs:	In the primary pattern the lobes are 10 to 12 db; the secondary pattern shown on the slide had 18-db lobes.
Spencer: (AFCRC)	Did your photograph show the hyperboloid mounted in front of the reflector? I was wondering if the waveguides feeding it would not spill energy past its edges.
Hibbs:	We have to work out proper phase to tilt the beam from the ends of the organ pipe toward the hyperboloid.
Spencer:	I presume that if you make the hyperboloid larger you will have more trouble with aperture blocking.
Hibbs:	We do have a larger hyperboloid but have not had the opportunity to evaluate it.
Rowland: (Pick.&Burns)	Would it be possible for you to make the hyperboloid in the form of a grating and then rotate the polarization between the hyperboloid and the dish so that the reflected rays would not be affected by the hyperboloid?
Hibbs:	That might be a good thing to try.
Kelleher: (NRL)	Someone has suggested that I mention the fact that this is a no-dead-time organ pipe. The scan sweeps from left to right and returns from right to left; it is usable at all positions. The conventional organ pipe has a split beam at the dead-time sector. One further thought, this paper was included at this point in the program because of the fact that this scanner will produce a conical scan, spherical scan, and other types of scan depending on the relative rotation rates of the feed horn and the organ-pipe system.

EFFECTS OF VARIABLE INTEGRATION TIME AND DETECTOR CHARACTERISTICS OF SCANNING LOSS CALCULATIONS

J. E. Corbin
Bell Telephone Laboratories, Whippany Laboratory, Whippany, New Jersey

Many radar systems have had poor range performance in portions of their scanned fields because of excessive scanning losses. The process of scanning involves time factors that effect the range performance of the associated radar because of the presence of integration or memory in the system. The parameters with which we are concerned are scanning frequency or frame time, antenna beam angle and pulse repetition frequency. When other requirements permit sufficient latitude, these characteristics must be juggled to obtain the best range performance in all portions of the scanned field.

To predict radar range and evaluate scanning loss, it is necessary to know the time through which integration occurs. This time has been assumed to be a constant for the usual cathode-ray tube and human observer. However, when we compare the scanning loss measurements for a number of radar systems with calculations based on a six- to eight-second integration time and the square-root integration law, we find disagreement. The square-root relation can be stated as follows:

$$P_m \cong \sqrt{\frac{n_t}{n_s}} \qquad (1)$$

where

P_m is the minimum detectable received power,

$n_t = n_s + n_n$ is the total number of sweeps in a beamwidth during the integration time,

n_s is the number of sweeps in which signal power is presented during the integration time, and

$n_n = n_{noise}$ is the number of sweeps having only noise presented at the range being considered during integration time.

The results indicate that a change in the integration concept must be made if reasonably accurate predictions of radar range and losses due to scanning are to be made.

The conclusions drawn from the measurements is that the integration time (τ) for detection on a cathode-ray tube by a human observer is not a universal constant but bears some functional relationship to the pulse repetition frequency of the form

$$\tau = a + bf^{-1} + cf^{-2} + \ldots\ldots$$

The assumption that b = 1250 and that all other constants equal zero produces a fairly satisfactory first-order approximation. Thus the relationship takes the form of $f\tau = 1250$.

Figure 1 is a plot on semi-log paper of measured curves of scanning loss versus scanner speed in rpm. Superimposed on these curves are two asymptotes, one having zero slope representing the maximum loss, and the other having a square-root slope obtained from the usual relationship. Integration time τ for the system is defined as the time associated with the scanning speed at which these asymptotes intersect.

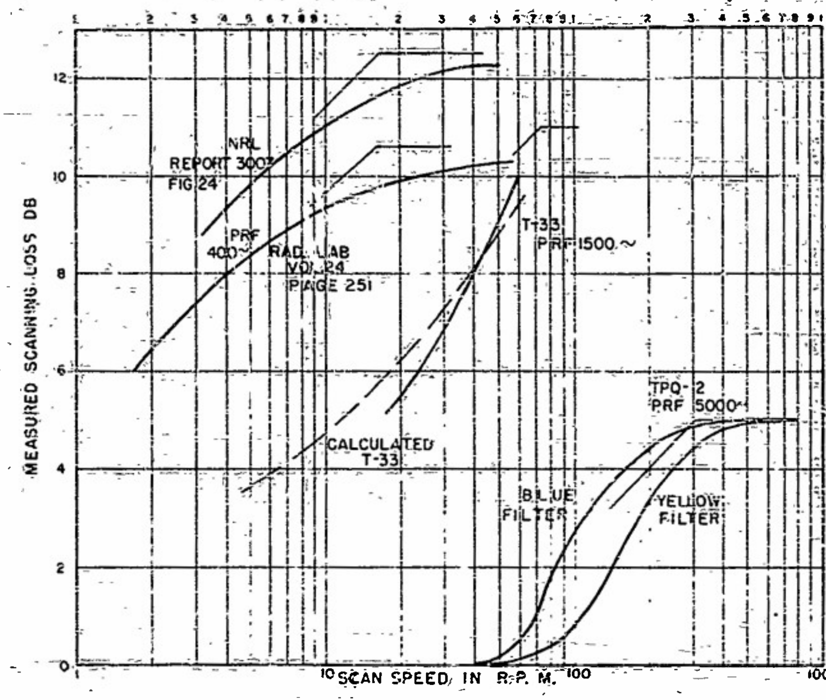

Figure 1 - Scanning loss vs. antenna speed

The data exhibited in curve form on Figure 1 came from several sources measured at different times. However, the general experimental procedure used in obtaining the data was the same. In some cases, actual radar reflection from a fixed target was used and in other cases a simulated radar echo was used. In all cases, however, the curves represent averages of a number of observers. This type of measurement yields data that fluctuate considerably and is subject to uncertainties of the order of plus or minus one db.

The corner speeds shown on Figure 1 produce a range of constants from 930 to 1650. It is easy to see that small changes in the choice of these corners will close this range considerably.

To obtain scanning-loss data, the radar under test is modified by inserting an attenuator and an auxiliary i-f amplifier of suitable bandwidth into the i-f system. The auxiliary amplifier raises the gain following the attenuator to allow the desired noise level to be displayed on the indicator. The attenuator is adjusted by the operator to obtain detection of a strong steady local target in the portion of the scanned field under test. Scanning losses are determined by comparing the attenuator settings to those obtained with the antenna not scanning but pointed directly at the same target. A block diagram of the radar modification is shown in Figure 2.

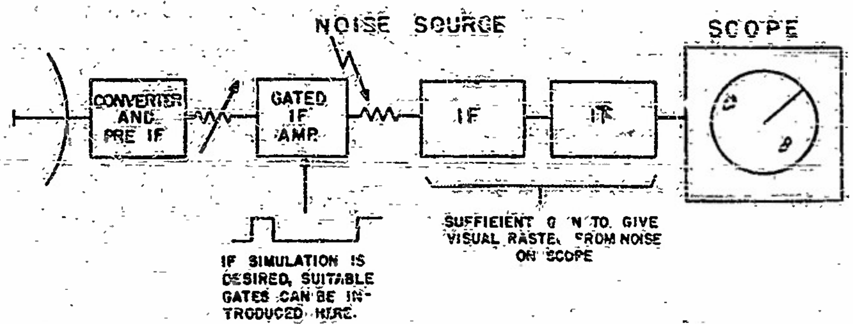

Figure 2 - Radar system modification for scanning loss measurements

A comparison of the measured and computed integration time τ is plotted on Figure 3. The time referred to here as the integration time is concerned with look-to-look integration. For slow scanning speed only the pulses received during a single pass of the antenna are integrated. The next pass of the antenna occurs at too long a time after the last look to contribute to the signal information presented during the last pass. As the antenna scanning speed increases, the pulses on target per pass decrease, and as a result the scanning loss increases until a speed is reached where the succeeding look contributes signal information stored at the last look; thus the contributing number of pulses remain constant. The empirical relation appears to agree wit.. the measured data much better than the concept of a constant integration time.

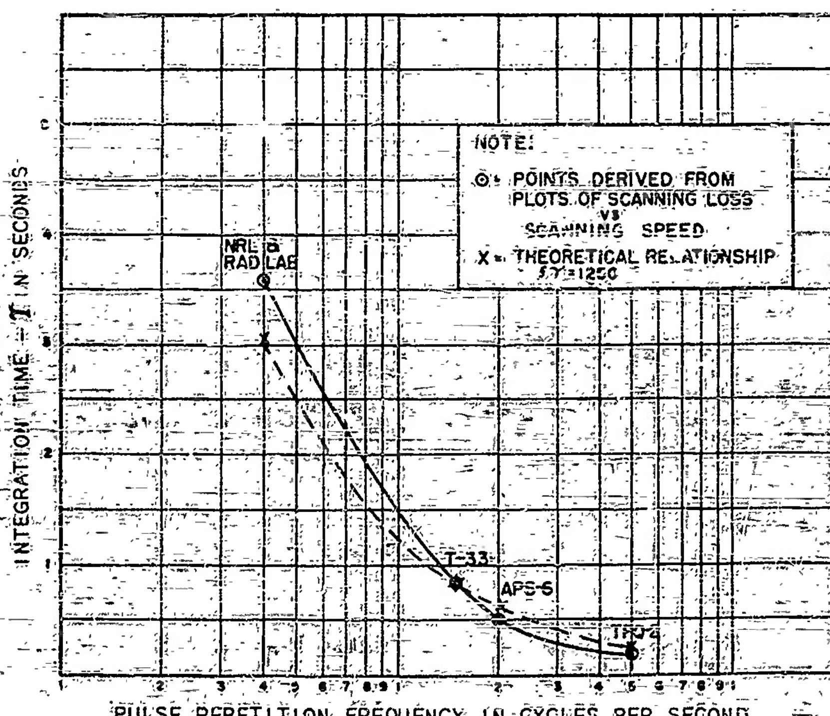

Figure 3 - Integration time vs. pulse repetition

Along with the above modification, the nonlinearities in the second detector must be included. In the usual experimental setup scanning loss is measured by the attenuation of the signal at intermediate frequencies. It is not necessarily true, for example, that a two-db change of a signal attenuator in the intermediate frequency transmission path represents a two-db change in signal-to-noise ratio in the video path.

Figure 4 is a plot of a universal detector characteristic published by Fubini and Johnson in the December 1948 IRE Proceedings. This curve illustrates the degree of compression in going from the video circuit to intermediate circuits when the signal and noise powers are of the same orders.

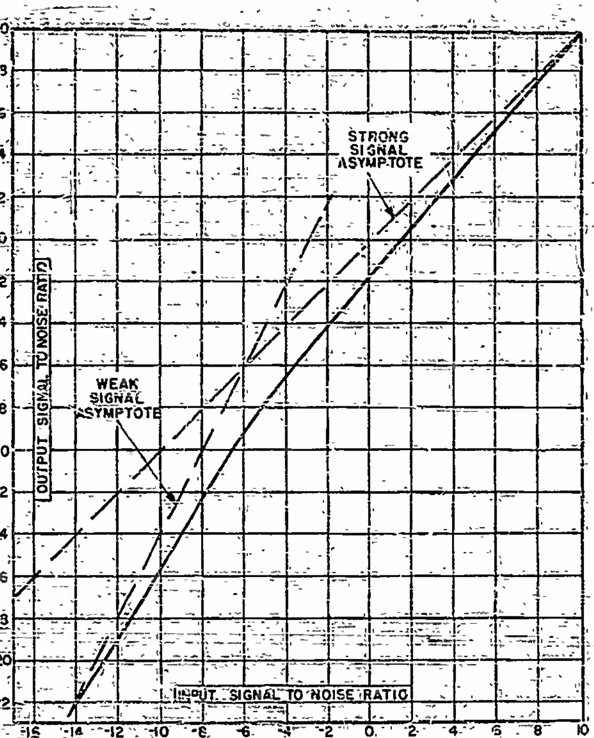

Figure 4 - Universal detector characteristic from Fubini-Johnson, I.R.E. Proceedings, Dec. 1948

The following procedure indicates how these concepts might be used in the computation of scanning loss for a proposed system.

First, estimate integration time τ for the system pulse repetition rate involved, using the empirical relationship $f\tau = 1250$, where f is repetition rate in cps. Then determine the scanning losses, using the appropriate relation in Equations (2) and (3). The noise and signal quantities n_t and n_s are evaluated from the geometry of the scan.

$$L = \frac{Nn_t}{n_s} = 35.3 \frac{n_t}{n_s} \tag{2}$$

N = total pulses generated in time τ (becomes fixed at 1250),

n_s = total sweeps containing signal in time τ

n_t = total sweeps presented on indicator which could superimpose noise on indicated target position in time τ.

For a simple PPI scan, this relation reduces to

$$L = \sqrt{\frac{6\tau R}{\theta}}, \text{ for } R \leq \frac{60}{\tau}, \qquad (3)$$

where R is antenna scan speed in rpm and θ is antenna beamwidth in degrees.

For $R \geq 60/\tau$ a limiting loss of $L = \sqrt{360/\theta}$ is assumed.

For complex scans where the frame time of the scan is less than τ the quantities N, n_t, and n_s may be redefined for convenience in terms of a frame. The scanning loss may then be determined on a per-frame basis from the scan geometry. If the frame time of the scan is greater than the integration time, the values of N, n_t, and n_s must be determined for the full time τ as defined above. The losses thus calculated apply to the video. To obtain the losses as applied to r-f or i-f, the detector characteristic must be taken into account. A curve such as the one shown in Figure 4 is convenient.

The procedure is to estimate the threshold video signal-to-noise ratio (S/N) v when spotlighting the target. A good estimate of (S/N) v for current radars is -14 db. Using this value of (S/N) v the corresponding i-f signal-to-noise ratio can be determined from Figure 4. For example, the maximum scanning loss for a spiral scanning system was calculated from the geometry of the scan to be 22 db. This results in a variation of the (S/N) v from -14 db at spotlight to a value of +8 db at the point of maximum loss. In the i-f, where scanning loss measurements are made, this would correspond to an S/N range of -9 db to +8 db.

By the use of these simple relations, much better agreement between measured and calculated losses have been obtained.

DISCUSSION

Dunbar: (SRI) Could you discuss the comparison between a moderate number of pulses in a beamwidth and one pulse per beamwidth in a system which scans very rapidly? That is, could you compare 5 pulses in a beamwidth to 5 successive pulses acquired in a very short time?

Corbin: (BTL) If your time between scans is less than the integration time, there should be little difference. What scan time will you consider?

Dunbar: Scan period of 4 to 6 seconds.

Corbin: That is much greater than any integration time. On the TPQ-2 we had an integration time of 2/10 second.

Wilkinson: (RCA) I would like to compare the case where we might scan 30 frames per second to that in which we scan 5 frames per second, assuming that we have the same number of hits.

Corbin: The scanning loss should go down for the slower frame rate. The exact point at which a change would occur depends on your system. If we stay above the knee of the curve, nothing will happen. If you have a lot of look-to-look integration, nothing will change. You have more pulses per beamwidth and less looks. Once you pass the point where the frame-to-frame integration stops, you slow the scan down and have more pulses in a beamwidth. The scanning loss becomes less and then drops down eventually to the searchlight condition for zero speed.

Wilkinson: What I wanted to know was where is the point where the frame-to-frame integration drops off?

Corbin: We have defined it by $f\tau = 1250$.

Wilkinson: I have a slightly different question. Suppose we permit the target to move so that between frames it moves more than the spot diameter, but very little more?

Corbin: The loss goes up. I believe it was analyzed in an NRL report. They claimed no loss was suffered if the target moved less than 1/2 its size. Integration continues out to the point at which there is no overlapping at all. The trace left on a scope by a moving target has some integration value.

Warren: (RCA) Do you think that the knee of your curve would correspond to the spotlight value if you reduced the pulse repetition rate by the same factor with which your beamwidth corresponds to the total scan angle?

Corbin: No, I do not think so. I think it depends on the cathode-ray tube buildup.

Varela: (NRL) I would like to point out that in Mr. Dunbar's single-pulse case there is a loss due to the fact that you cannot realize all of the antenna gain. The beam moves off target during the time interval between the transmitted and the received pulse.

Gunter: (Clark Un.) An effect, similar to that of taking a photograph of a cathode-ray tube over a long period of time -- as mentioned by Mr. Corbin, exists in aerial photography.

Blake: (NRL) It appears to me that you have destroyed the concept of an integration time which might depend on the PPI and the observer and have substituted for it an integration number. I suppose you realize this is revolutionary. Have you applied this result or attempted to explain it by any mechanism?

Corbin: I do not believe that this is revolutionary. Previous range formulas used by some people are related to this figure.

* * *

LOSSES IN THE AN/TPQ-2 SCANNER *

R. E. Honer
State Engineering Experiment Station
Georgia Institute of Technology

ABSTRACT

A theoretical and experimental investigation was conducted to determine the causes of unexplained power losses of the order of 4 db in the antenna system of the AN/TPQ-2 Mortar-Locating Radar. The antenna consists of two Lewis-type scanners feeding a common waveguide lens. The program of investigation consisted of studies of the losses in the r-f system, the explanation of the losses, and consideration of methods for the reduction of these losses. The losses in the system were measured by the short-circuit method and checked by the substitution method. These losses are itemized and discussed.

The investigation resulted in the following conclusions concerning the AN/TPQ-2 scanner.

1. Particular attention must be given to rigidity of the parallel plate medium since this controls the effects of temperature upon losses.

2. The dielectric lenses must make good contact with the surfaces of the parallel plates.

3. Shorting barriers between the plates must make good contact and be parallel to the electric field.

4. Cracks and surface roughness contribute appreciable to the losses.

* Evans Signal Laboratory, Contract No. DA 36-039-sc-5469

DISCUSSION

Budenbom: (BTL) Since this scanner was developed by Western Electric Co., we have significant evidence that this session was not organized in a smoke-filled room.

Foster: (McGill) BTL should not feel badly. This scanner is something in the nature of unfinished business on their part. One was made at Radiation Laboratory at the same time, and it did not have that much loss.

Honer: (Ga. Tech.) We are not connected with BTL but we think that this is a good scanner. It seemed that development work on it was suddenly dropped in 1945. I think that our work has indicated that some improvements can be made on this scanner. It does not appear to be too difficult to construct. It may have applications in some instances. I think that further investigation of temperature and buckling effects in parallel plate media should be carried out.

Budenbom: I recall considerable concern at the Bell Laboratories when this 4-db figure was discovered some years ago. Perhaps the gentleman from Evans Signal Laboratory has more information on this.

Ducore: (SCEL) Some years back, RCA developed for us a scanner which used this Lewis-type scan. The scanner was formed by electroform process. Perhaps Mr. Wilkinson of RCA has information on this scanner.

Wilkinson: (RCA) As I recall, it was less than 4 db. Data on that scanner was given at the last symposium. We used an electroformed parallel-plate structure in which the barrier was an integral part of the parallel sheets. We used a similar type of lens. We plated the lens and placed an absorbing cloth between the plated lens and the parallel-plate conductor.

LUNEBERG LENS AND SCANNING ELECTRONICS

Dr. L. C. Van Atta, Hughes Aircraft
(Chairman)

SPHERICAL LUNEBERG LENS

Henry Jasik
Airborne Instruments Laboratory, Inc.

A countermeasures system known as the high probability intercept system is under development at Airborne Instruments Laboratory for the Bureau of Ships. One of the major components of this system is an instantaneous direction finder which is capable of obtaining directional information without scanning. To accomplish this, it is necessary that multiple overlapping beams receptive to both polarizations be used to cover the entire 360 degrees of the azimuth plane. For the first developmental system, 15 beams each 24 degrees wide in azimuth were required at S-band. In order to achieve some additional gain, it was desired that the elevation beamwidth also be 24 degrees.

The brute-force approach to this problem would be the use of 15 pyramidal horns, each with an aperture 15 inches in diameter and having an over-all length of about 30 inches. To mount these horns aboard ship would require an unwieldy structure having a volume of about 30 cubic feet. In order to reduce the over-all size required, it was thought that it might be more efficient to use one aperture 15 times rather than having 15 individual apertures. This philosophy led us to consider the possibility of using a spherical Luneberg lens with 15 feeds.

The Luneberg lens* is a symmetrical lens having a variable refractive index given by the relationship

$$n = \sqrt{2 - \left(\frac{r}{R}\right)^2},$$

where r is the radius coordinate and R is the outside radius of the lens. Although considerable work has been done on the two-dimensional lenses of the variable refractive index type and of the geodesic type, little work has been done on the spherical type of lens.

In looking for ways to achieve the variable refractive index required for the lens, a number of possibilities were considered. From the standpoint of expediency, it was decided that the simplest way to build the developmental model would be to use an artificial dielectric consisting of pyrex glass balls arranged in a symmetrical lattice structure. The spacing of the lattice would be varied in such a manner as to achieve the desired refractive index along the radius. Our computations were considerably aided by the use of some data on spherical particles arranged in a cubical lattice that had been obtained at the Air Force Cambridge Research Center †.

Before building the complete lens, a slice of the central section was constructed and tested between parallel plates in order to check the computations. Figure 1 shows a photograph of the two-dimensional lens between parallel plates having a rectangular lip on the edge of the plates. The lens, which was 14 inches in diameter and 1/2 inch high, was fed by a short section of rectangular waveguide. Figure 2 shows the structure with the top

* Luneberg, R. K., "Mathematical Theory of Optics," Brown University, 1944
† Corkum, R. W., "Isotropic Artificial Dielectric," Proc. I.R.E., May 1952

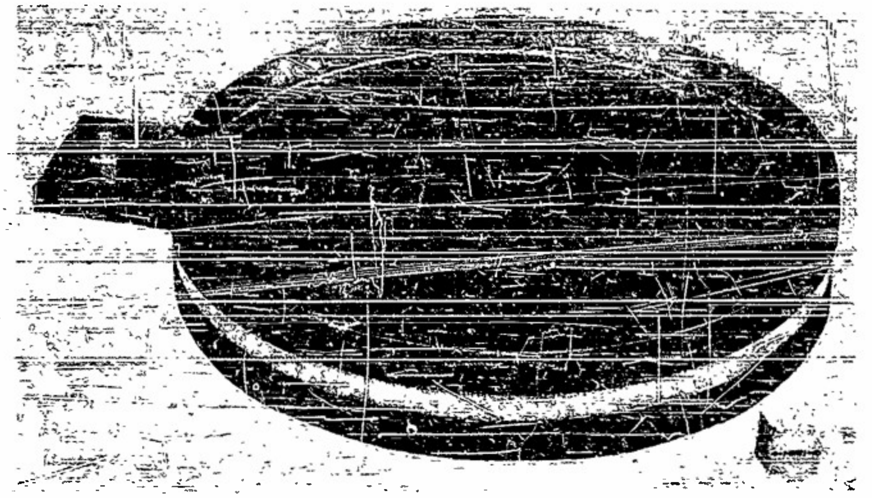

Figure 1 - Two-dimensional Luneberg lens between parallel plates

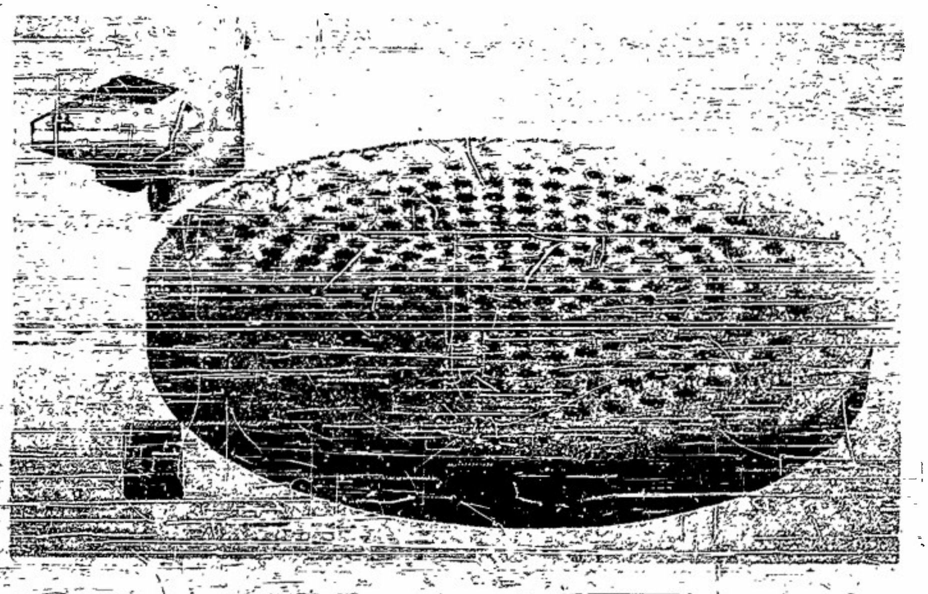

Figure 2 - Two-dimensional lens with top plate removed

plate removed. Here, the construction of the lens is readily visible. The glass balls are laid out in a circularly symmetrical pattern with the number of balls per unit volume decreasing from the center out to the edge. This results in a variation of refractive index according to the relationship given above. Figure 3 shows a close-up view of the lens proper. All of the glass balls with the exception of those in the outermost row have a diameter of 1/2 inch. In the outermost row, the size was reduced to 3/8-inch diameter so that the spacing between the glass balls did not become too large.

Phase-front measurements made on the two-dimensional lens indicated that the structure was operating as predicted. At 3000 Mc, the wave front in the forward direction was plane to within one sixteenth of a wavelength. The radiation patterns at 3000 Mc are shown in Figure 4.

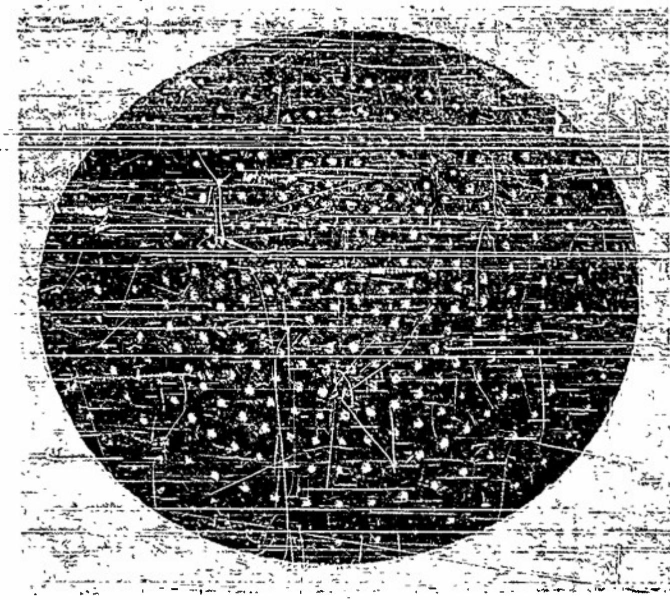

Figure 3 - Close-up view of lens

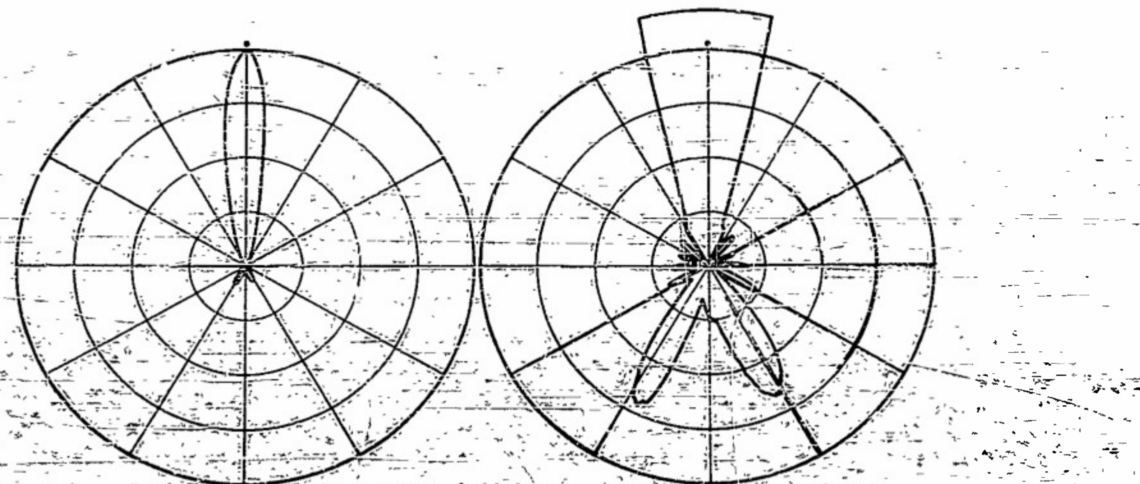

Figure 4 - Horizontal plane radiation power pattern of Luneberg lens antenna with rectangular lip (polarization-vertical)

The pattern on the left was taken at a standard gain setting while the pattern at the right was taken with the gain increased by 10 db. The main beam is smooth and symmetrical, and the close-in side lobes are fairly low. The main difficulty was the large amplitude of the back lobes, which were only 12 db down from the main beam. These back lobes were of considerable concern and raised the question as to whether the same difficulties would be encountered with the spherical lens.

One explanation was that the reflection from the edge of the parallel plate aperture could be responsible for the back lobes. Because the aperture possessed cylindrical symmetry, the reflected wave would tend to be focused in the backward direction. The backward lobes would be down from the main beam by the order of magnitude of the reflection coefficient.

To check this hypothesis, another set of parallel plates having a conical flare at the edge of the aperture was built. This flare was 3 inches long and 3 inches high and provided a considerably better match than the abrupt aperture transition previously used. Patterns at 3000 Mc were again taken at a standard gain setting and with the gain increased 10 db as shown in Figure 5. These patterns show that the back lobes were reduced considerably and were now about 17 db below the main beam. The shape of the main beam was essentially the same as before (Figure 4). This test showed that the back lobes were primarily due to aperture reflection and not to the design of the lens.

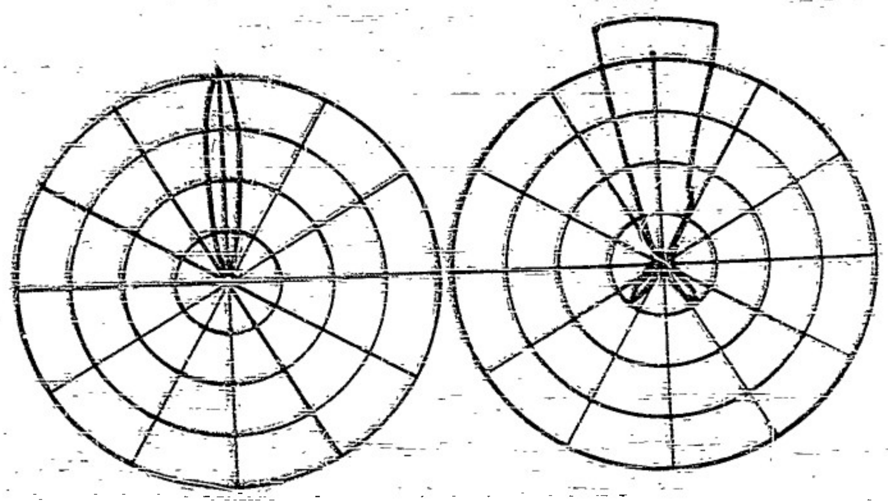

Figure 5 - Horizontal plane radiation power pattern of Luneberg lens antenna with conical flare (polarization-vertical)

Because of the favorable results obtained with the two-dimensional lens, design and construction of the complete spherical lens was undertaken. Figure 6 shows the completed lens. The individual slices were housed in a cylindrical structure for convenience, although the glass balls are contained within a spherical volume. Spacecloth with a plate back of it is used at the top and bottom of the lens to reduce reflections from the supporting structure.

It is of some interest to present the results obtained with a single feed. A simple dipole backed by a corner reflector was used as the primary feed. With the feed oriented in turn for each of the two polarizations, patterns were taken for the two principal planes. The results at 3000 Mc are summarized in Table 1.

It can be seen from the beamwidths obtained that the lens is reasonably isotropic because essentially the same results were obtained for both polarizations in both principal planes. The horizontal patterns of the lens with a single feed are shown in Figures 7 and 8. As before, the patterns on the left were taken with a standard gain setting while the patterns on the right were taken with the gain increased 10 db. The side-lobe level is quite acceptable from the standpoint of the system used for the direction finding application. As a matter of fact, the side-lobe level could be somewhat higher before any serious systems problem

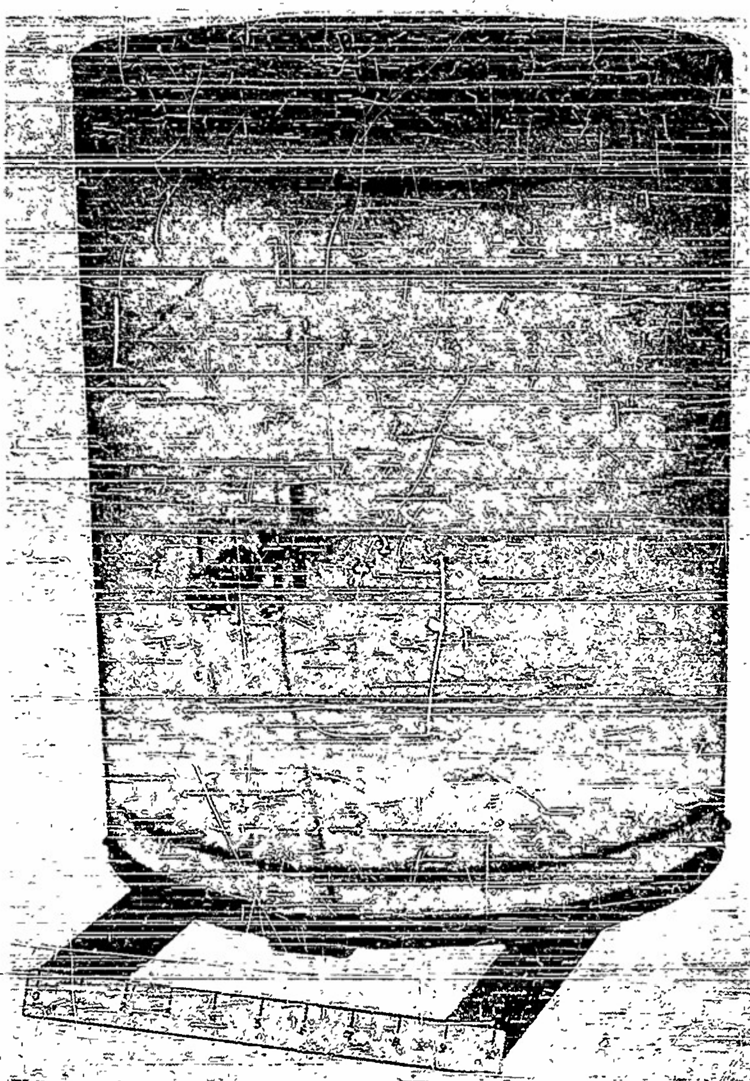

Figure 6 - Spherical Luneberg lens

TABLE 1
Pattern Characteristics for Single Feed

	Beamwidth at 3 db down	Beamwidth at 10 db down	Side-lobe level db down
Horizontal plane			
Vertical polarization	17	26	16.5
Horizontal polarization	18.2	28	18
Vertical plane			
Vertical polarization	18.5	32	23
Horizontal polarization	18	28	18

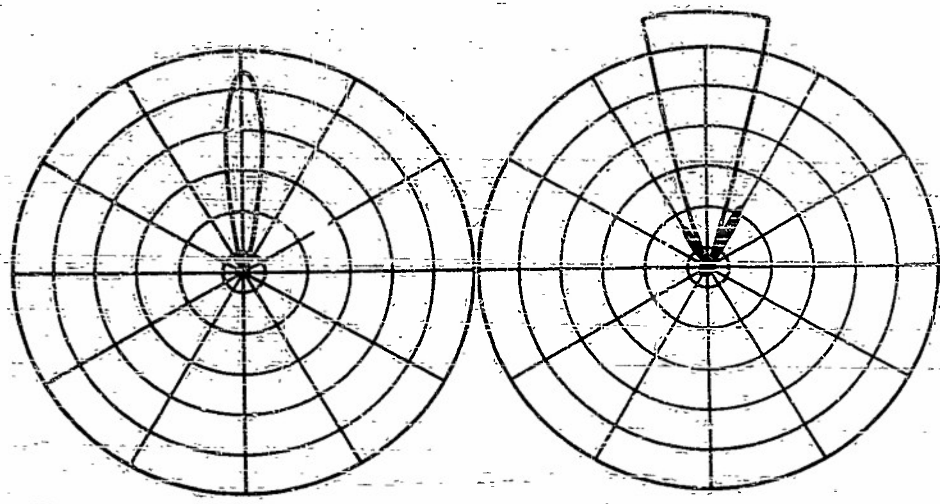

Figure 7 - Horizontal plane radiation power pattern (horizontal polarization) of spherical lens antenna with single feed

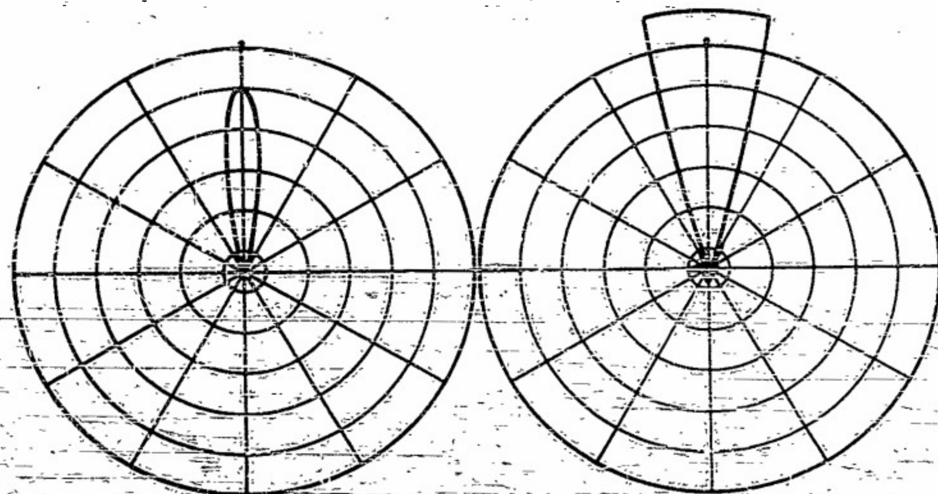

Figure 8 - Horizontal plane radiation power pattern (vertical polarization) of spherical lens antenna with single feed

would be encountered. It will be noted, however, that the beamwidth obtained was considerably narrower than the 24 degrees originally required.

The beamwidth was less than the value that had been originally estimated for two reasons. The first was the narrowing obtained because of the end-fire effect due to the lens having depth as well as breadth. The second is the tendency of the Luneberg lens to accentuate the wide-angle radiation of the primary feed, thereby bringing up the illumination level at the edges of the aperture.

The narrower beamwidths lower the crossover level between adjacent beams more than desired. In order to bring the beamwidth back to 24 degrees, it was decided to reduce the diameter of the prototype antenna to 11 inches instead of 14 inches.

To determine how the 11-inch prototype antenna would perform from 2700 Mc to 3300 Mc with a complete set of feeds, data were obtained on the 14-inch experimental antenna in the region from 2200 Mc to 2700 Mc.

The problem of locating feeds completely around the periphery of the lens was not as serious as it might appear at first. For one thing, the antenna is a complete sphere and the feeds occupy only a strip of the sphere. Actually, even this strip is only slightly blocked because of the feed polarization. Because the antenna needed to be receptive to both polarizations, the feed was mounted at 45 degrees. This resulted in the rather fortunate circumstance that the feeds on opposite sides of the lens were perpendicular to one another and were thus essentially transparent to one another. The dipoles were backed by a grating of 45-degree elements that acted as reflectors for the individual dipoles. Figure 9 shows the lens with a single dipole oriented at 45 degrees and the 45-degree reflecting grating mounted around the lens. Figure 10 shows a detail view of the experimental grating. In order to determine what effect the grating had, patterns were taken with and without the grating blocking the forward half of the lens. The only result was a negligible change in beamwidth and an increase of 1 db in side-lobe level.

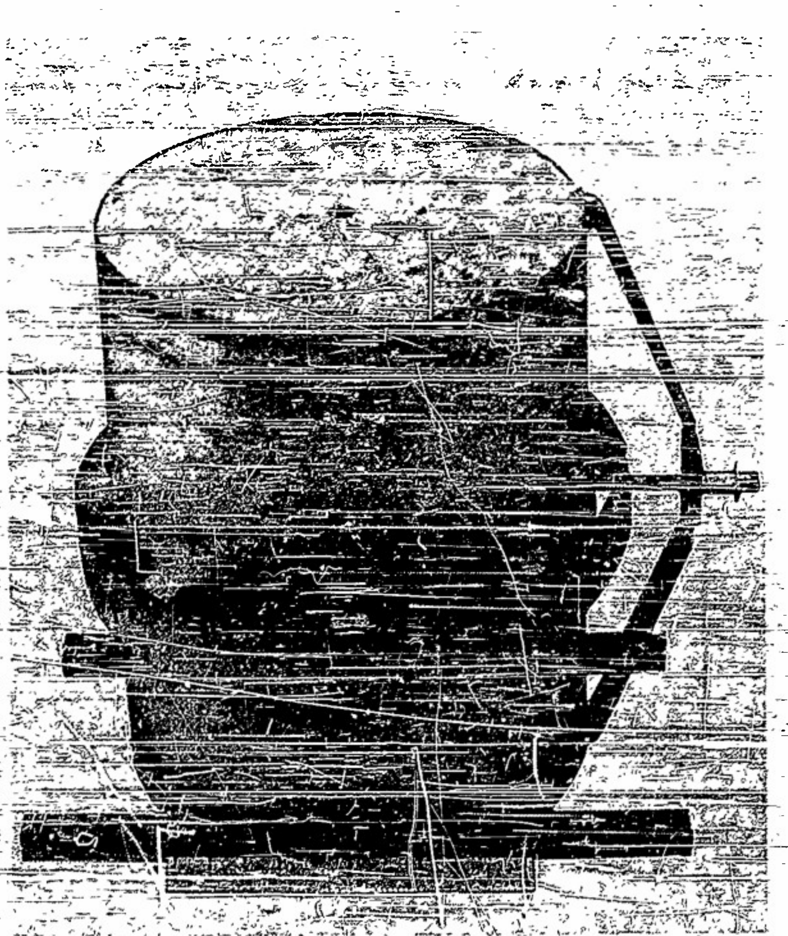

Figure 9 — Spherical Luneberg lens with 45-degree dipole and 45-degree reflecting grating

To determine the performance of the complete antenna, 15 feeds and feed cables at 45 degrees were mounted on the lens. Data were taken down to 2200 Mc with the experimental antenna to determine the performance of the scaled prototype antenna. The results are shown in Figures 11 and 12. The horizontal plane half-power beamwidths vary from 28 degrees to about 21 degrees over the band, while the cross-over level varies from 2.0 db down to about 3.5 db down. The vertical-plane beamwidths are slightly narrower than those in the horizontal plane. The side-lobe level varies from 14 db down at the low end of the band to about 22 db down at the high end of the band. The side-lobe level at the low end of the band is partially due to the broadening of the primary-feed illumination pattern as the frequency goes down and partially due to the cumulative effect of the other feeds and cables.

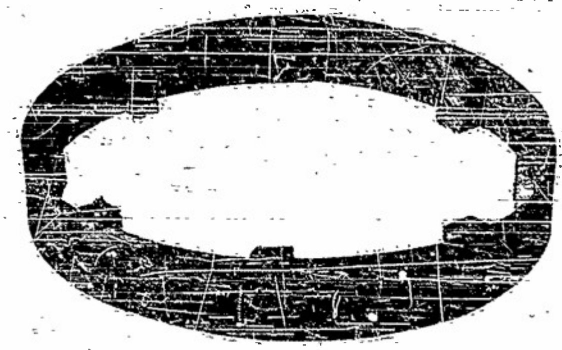

Figure 10 - Detail view of 45-degree grating

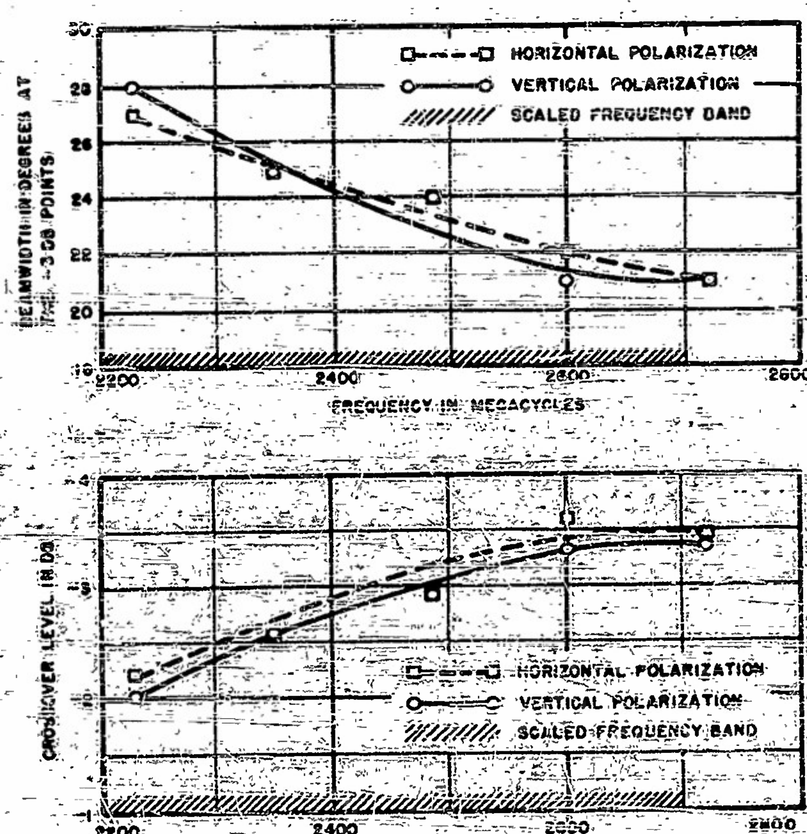

Figure 11 - Azimuth plane beamwidth and cross-over level for complete spherical lens

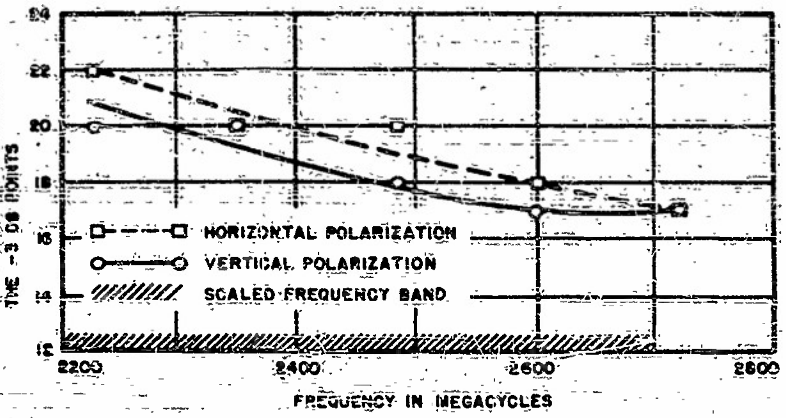

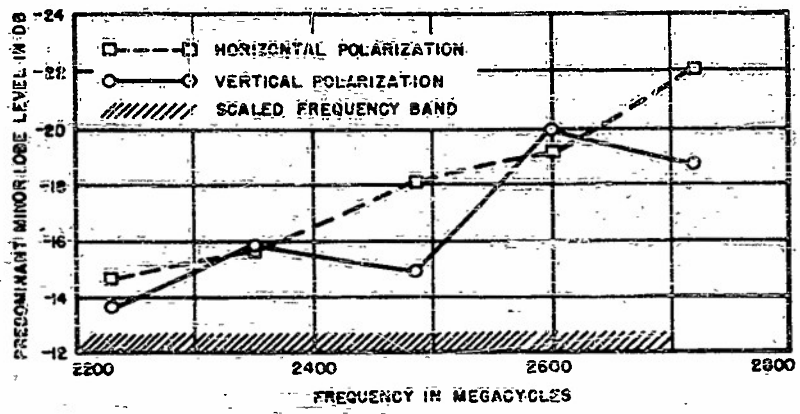

Figure 12 - Elevation plane beamwidth and horizontal plane minor lobe level for complete spherical lens

The over-all electrical performance of the antenna was considered quite acceptable in terms of the system performance required. The volume of the prototype antenna will be less than 2 cubic feet so that a very substantial saving in space will be gained over the 15-horn array.

As a matter of interest, some measurements were made on the experimental lens to determine its performance over an extended frequency range. The primary feed was changed and patterns were measured as the frequency was varied from 1000 Mc to 7000 Mc. As might be expected, the beamwidth decreased as the frequency increased. Above 5500 Mc, however, the patterns were not satisfactory because some secondary beams of large amplitude started to form. It is not definite whether these were due to the lattice spacing or due to the diameter of the individual glass balls. The variation of the beamwidth with wavelength for the 14-inch diameter lens was found to be proportional to the inverse 1.2 power of the frequency. Since a plane aperture would vary as the inverse first power of the frequency, it is believed that the more rapid variation of the beamwidth is due to the end-fire effect that is present with the spherical lens.

Some thought has been given to the possibility of modifying the lens to maintain its beamwidth constant over a wide frequency range. Preliminary computations indicate that this can probably be done by using the lens to generate a slightly curved wave front that will have a compensating effect with frequency. The modified wave front shape would be obtained by changing the law of variation of refractive index from its present form to a slightly revised form.

DISCUSSION

Question: Do you have a photograph of that 15-feed system?

Jasik: (AIL) No, I do not. It was a haywire arrangement. We are building a prototype now.

Question: Are the 15 feeds displaced around the entire surface?

Jasik: Yes, they are spaced every 24 degrees around the equator. Since it is going to be used on shipboard against aircraft, it might have been better to drop the feeds slightly below the equator to point the beam upward. This would have improved the feed blocking.

Question: Have you tried a radome over the entire system?

Jasik: Yes, we have, and a cylindrical radome does not appear to be too critical. The cylindrical radome over the spherical lens scattered the reflections more than they would have been had the radome been spherical. I believe this antenna will be one of the first Lunebergs to go into a system. It is not the first spherical Luneberg, however. I believe Hughes Aircraft Company built a spherical lens some time ago, using a different technique.

Question: How was the dielectric constant determined?

Jasik: We used the results obtained at Cambridge Field Station by use of a cubical lattice. We postulated that what counts is the density of the balls per unit volume rather than the spacing between balls, provided that the balls were small enough. We computed a position of the balls from the density concept in various radial steps. To simplify fabrication, this position was made to correspond to the desires of our machine shop. As a matter of interest, it took about a day and a half to drill all of the holes required in the lens. I do not think that this construction would be useful in a production model, but we feel that it is ideal to prove a philosophy and a design technique.

Jones: (RRDE) Do you consider the possibility of using hollow metal spheres as obstacles?

Jasik: Yes, but when metal spheres are used, the permeability goes down as the lattice spacing is increased. I believe the Cambridge data shows you reach a limit in the refractive index of about 1.29 which is less than the 1.41 that is required. The glass spheres are relatively inexpensive and easy to obtain and are possibly somewhat lighter.

Gruenberg: (NRC) Do you have any idea of the loss in this lens?

Jasik: No, we have not, but we did make an estimate of the loss for a wave passing through a sphere filled completely with the pyrex material. The result was 3/10 to 4/10 of a db. Since we did not have the sphere completely filled, and since our measured gain of 17 to 18 db is ample, we felt that the losses were nothing to worry about.

Van Atta: (Hughes) In regard to the scattering by the obstacles—if it were appreciable, it would show up in the side lobes from the system.

Riblet: (Mic.Dev.) Can one infer from the data you have given that the inherent bandwidth of this system is of the order to 5 to 1?

Jasik: From the standpoint of the range over which this system can perform, it is good from 1,000 to 5,000 megacycles. This range could be extended up to 10,000 or 15,000 megacycles by reducing the obstacle size and the spacing. Of course there is no lower limit. The problem confronting us here is that of keeping the beamwidth constant over a frequency band of about two to one. The structure was developed on the basis of geometrical optics and so is of course independent of frequency.

Carnine: (Melpar) Could you give references on the general derivation of the Luneberg lens?

Jasik: The first derivation was given in Luneberg's Notes, published by Brown University. I believe this is the only place in the literature where it is done completely. The basic operation of the lens has been discussed in many places in the literature. In this country, work has been done by Cambridge Research Center and by NRL. The work in Canada will be discussed in the next talk. There has been a paper in the British literature on a horizontally polarized lens.

Hiatt: (AFCRC) Do you have any information on the coupling between various feeds?

Jasik: Yes, the coupling between two adjacent feeds was of the order of 24 db. This decreased for the other feeds. The diametrically opposite feed had a coupling figure of less than 40 db.

Kelleher: (NRL) In answer to the question of the gentleman from Melpar, there is another derivation of the Luneberg lens which is somewhat simpler. It has not been published yet. Dr. Eaton of NRL has worked out the solution and will give a paper at the West Coast IRE meeting.

Jasik: Mr. Kelleher, does that include the more general case?

Kelleher: Yes, I believe that is so. Dr. Eaton obtained an integral equation similar to that of Luneberg's, and he has a neater solution to that equation.

THE TIN HAT, A MODIFIED LUNEBERG LENS

F. G. R. Warren
RCA Victor Company, LTD.
Montreal, Canada

In my title, I have described the subject of this paper as a modified Luneberg lens. I am sure that most of you are familiar with the various forms of the Luneberg lens which have been constructed for microwave use; so I will go over the background only very briefly. The Luneberg lens is an optical device in which the index of refraction of a sphere of transparent material varies from unity at the surface to the root of 2 at the center according to the relation $n = \sqrt{2 - r^2}$. In ordinary optics this exists only in theory, but in microwave optics we are able to make both two- and three-dimensional versions since we have a number of ways of obtaining a variable index of refraction.

Further, R. F. Rinehart has derived a parallel-plate system in the shape of a surface of revolution which is the path-length analogue of the two-dimensional, variable-index solution. However, when we calculate the exact equivalent of the Luneberg lens as a surface of revolution, parallel-plate system of unit index of refraction we find that the system is vertical at the edges. If we represent the system by the generator of the surface of revolution which is the mean surface between the plates, the Rinehart solution is of the form of the broken curve in Figure 1. To use the system as a microwave lens the emerging rays must be brought into the horizontal plane. If a curved lip is added to the Rinehart solution, this adds extra focusing properties which somewhat degrade the performance of the lens. This has been done at the Air Force Cambridge Research Laboratories where it has been shown that this defect may be largely rectified by pushing the feed horn up in between the plates of the system. This, however, should be avoided if possible; especially if rapid scanning is to be accomplished by moving the feed about the circumference of the system.

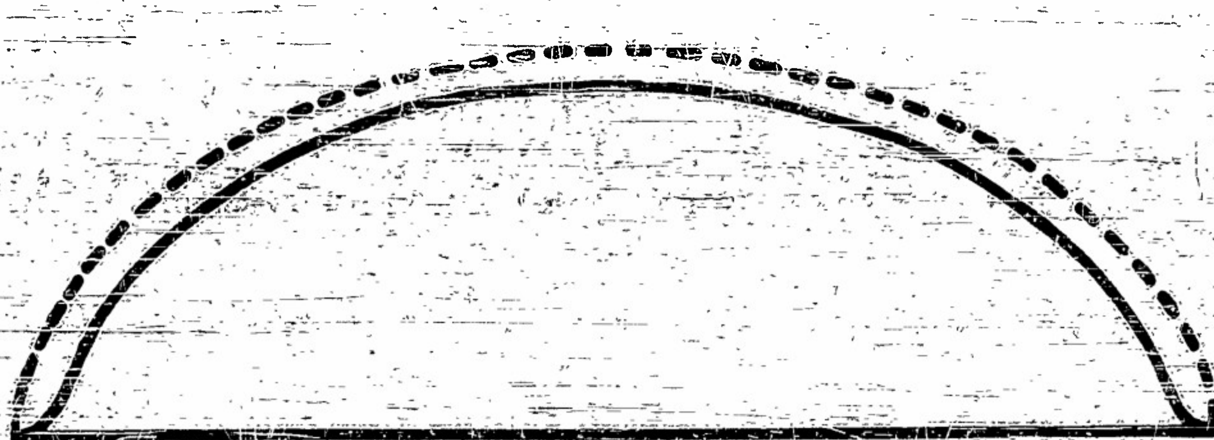

Figure 1 - Comparison of generating curves for Tin Hat and for Rinehart and Parker form

The work I am describing began with an attempt to derive the shape of the surfaces which would give a parallel-plate system having horizontal edges and yet would focus perfectly; that is, a system which would give a beam of parallel radiations from a point source on the circumference. At this point I might say that this work was undertaken as a part of a study under contract to the Defense Research Board in Canada. Much of the work, both theoretical and experimental, was done by Mr. S. E. A. Pinnell who is co-author with me of two reports on the project which are available through the Defense Research Board.

We visualized the system we wanted as having in general the shape of a helmet, for which reason we christened it the "tin hat." Analysis showed that the vertical edges of the Rinehart solution were a necessary consequence of requiring focusing across the entire aperture—that is, focusing even of rays which travel entirely in the narrow region near the circumference. If we were willing to forego the focusing requirement for these extreme rays, we could put a curved lip within this region and still construct a system which focused all other rays. One attempt to find an analytical solution for the central surface to go with any given lip was successful in giving a formal solution, but this was itself an integral equation which we could not solve in any useful case. We were able, however, to find the shape of the required central surface to go with the given lip by returning to basic principles and building up the required surface by means of a polygon type of approximation to the generator of the surface. The slope of each straight element of the polygon was determined by requiring that a particular ray emerge from the system parallel to the diameter drawn through the source point. The calculations are all made in terms of the mean surface between the actual parallel plates and are based upon the assumption that the radiation travels along geodesics on the mean surface. The number of straight elements chosen was sufficiently large that on construction a smooth surface would be obtained. Obtaining a sufficiently accurate surface by this means is a bit laborious, but on the other hand the process is very flexible.

The comparison between the shape of the generator of the mean surface of the Rinehart form and that of the tin hat is shown in Figure 1. The broken curve represents the Rinehart solution, while the solid curve is the tin hat with a lip comprising the outer 10 per-cent in radius. It should be pointed out that the tin hat is not a unique shape since for each different lip there exists a complementary central surface.

A model antenna 9.5 inches in diameter was constructed on the basis of the calculations made, and radiation patterns were measured with the pattern-measuring facilities at the laboratories of the National Research Council of Canada in Ottawa. Figure 2 shows a horizontal pattern measured at a wavelength of 1.25 centimeters. Patterns are on a linear voltage scale but a db scale is marked at the left. The half-power beamwidth of this pattern is 3.1 degrees. This agrees closely with the calculated beamwidth, assuming a reasonable illumination taper. The sidelobes in this pattern are all below 20 db. Because the device uses path-length focusing, it should be insensitive to frequency. To investigate this property, radiation patterns were also measured at a wavelength of 0.887 centimeters. A typical horizontal pattern at this wavelength is shown in Figure 3. The half-power beamwidth is 2.4 degrees, with sidelobes below 24 db. Again this is in agreement with the calculations; the change in beamwidth being in the ratio of the wavelengths. Vertical patterns had also been calculated in both cases, and it had been shown that because of the end-fire type directivity introduced by the dimension of the aperture in the direction of propagation the vertical half-power beamwidth would be considerably less than that corresponding to the height of the aperture. Thus, although the vertical spacing of the plates was only 0.4 centimeters, the vertical half-power pattern width at a wavelength of 0.86 cm was calculated to be 36 degrees, and at a wavelength of 1.25 cm the calculated vertical half-power width was 45 degrees. Experimental values were

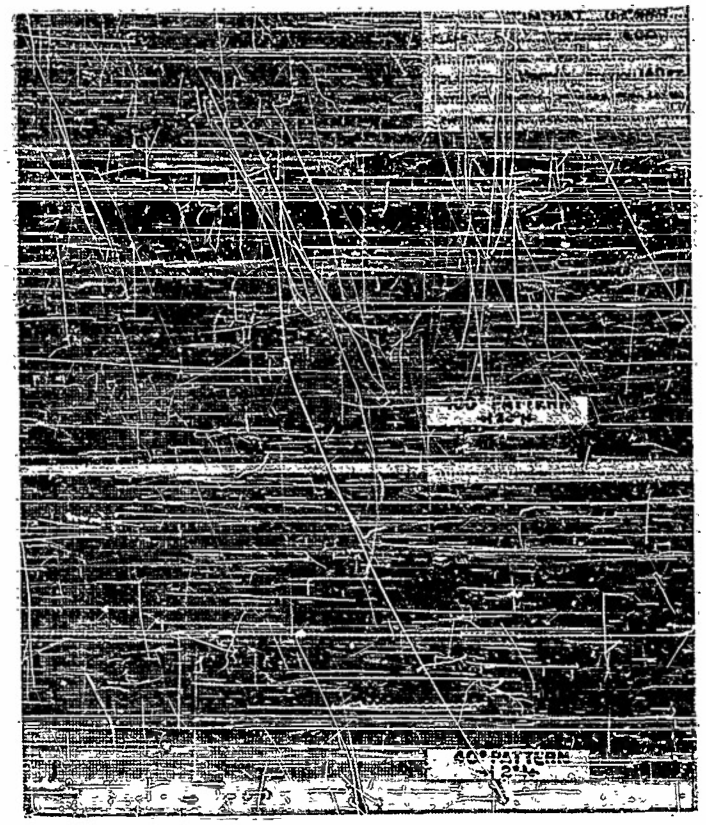

Figure 2 - H-plane pattern of 9.5 in. diameter tin hat at 1.25 cm wave-length

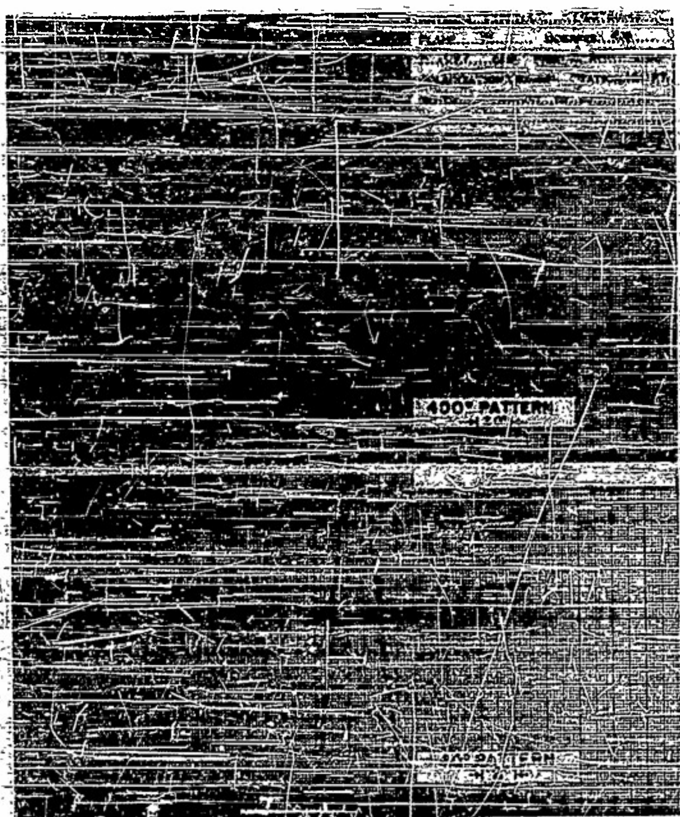

Figure 3 - H-plane pattern of 9.5 in. diameter tin hat at .887 cm wave-length

39 degrees at 0.886 cm and 45 degrees at 1.25 cm. These patterns were measured with simple waveguide feeds placed against the edge of the system and pointed toward the axis. No unusual precautions were necessary in locating the feeds.

The work done on this antenna suggested other possibilities, none of which have yet been brought to trial. I will discuss these briefly. In a 360-degree scanning model of the antenna we have been discussing, a single waveguide feed would revolve about the circumference of the system.

If we wish to scan through a smaller angle, say slightly less than 120 degrees, we could use three symmetrically located waveguide feeds in conjunction with a three-way waveguide rotary switch. Only one feed, that lying in a particular 120-degree sector, would be energized at any one time; and the beam would scan in a sawtooth fashion through a sector of 120 degrees, less switching loss, at three times the rate of rotation of the feed system. In the case of three feeds, the beam would pass almost entirely between the two inactive feeds so that aperture obstruction would be unimportant. If we wished to use more than three feeds to get a smaller angle of scan, the inactive feeds would cause serious obstruction of the aperture. However, without losing the optical advantages of using a surface of revolution we can construct a system for use in limited-angle scanning which avoids this obstruction of the aperture by the feeds. This is done by dividing the circumference into the aperture region and the feed region. In these two separate regions we use different lips, both of which are portions of surfaces of revolution about the axis of the system. They are so shaped, however, that the continuation of the feed circle does not interfere with the aperture. The center of the system is a complete surface of revolution which joins smoothly into the lip region. The methods of calculation used in deriving the shape of the tin hat are readily adaptable to calculating the shapes of the mean surfaces of these systems. Figure 4 shows a few of the possible shapes of this type of antenna. The form embodying a toroidal bend in the feed region is particularly interesting as it gives the shortest and lightest feed system. Because of the extra focusing introduced by the toroidal bend, the curvature of the dome-shaped section is less than that of the simple tin hat. You will see that it would also be possible to construct a modified Luneberg lens of the flat variable-index type which uses a toroidal bend around part of the circumference to separate the feed circle and aperture circle.

Systems of this type would be capable of a very rapid rate of scan through angles up to about 80 degrees. The scanning rate, in scans per second, is the rate of revolution of the feed system multiplied by the number of feeds used; the scanning rate, in degrees per second, is 360 times the rate of revolution of the feed system. The arrangement of the system with its rolled-under brim and ten-way rotary switch is shown diagrammatically in Figure 5. It scans through 36 degrees, less the loss due to switching time, at ten times the rate of revolution of the feed system.

Another variation of the surface-of-revolution type of focusing which can be handled by the same approach is that of phasing the aperture to elevate the beam maximum above the horizon. This would serve to give a measure of control over the shape of the vertical pattern. It is the only obvious way in which the beamwidth of the vertical radiation pattern could be increased--if this were desirable. The mathematical relations show that any elevation of the feed in this manner entails some decrease of the effective aperture. The higher the beam angle the smaller the portion of the aperture which can be properly phased. At 90 degrees elevation no finite length of the aperture can be properly phased by this method of focusing.

In summary, the main features of the work I have been discussing are as follows: Methods were derived for calculating the shape of the mean surface for a Luneberg-type,

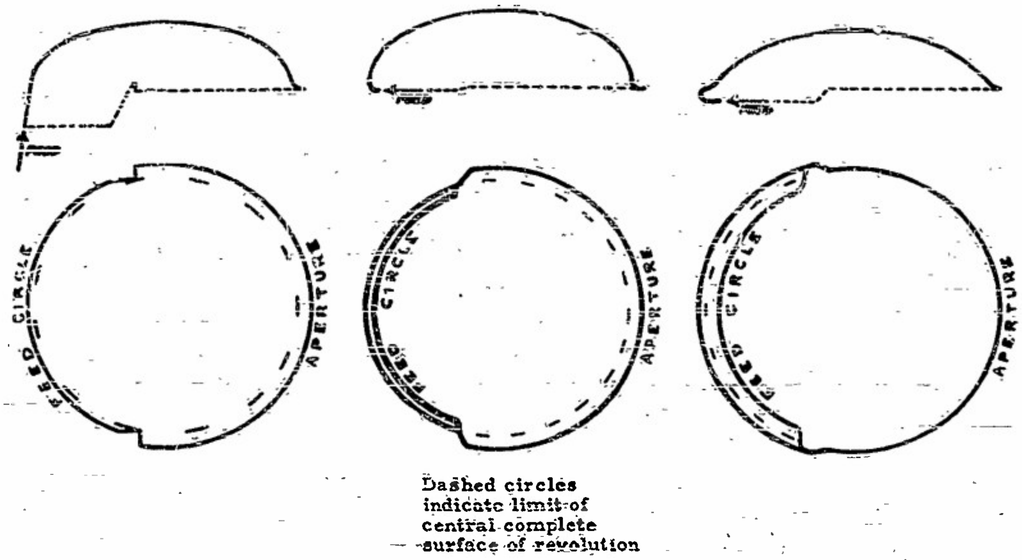

Figure 4 - Antenna forms with separate feed circle and aperture for use in limited-angle scanning

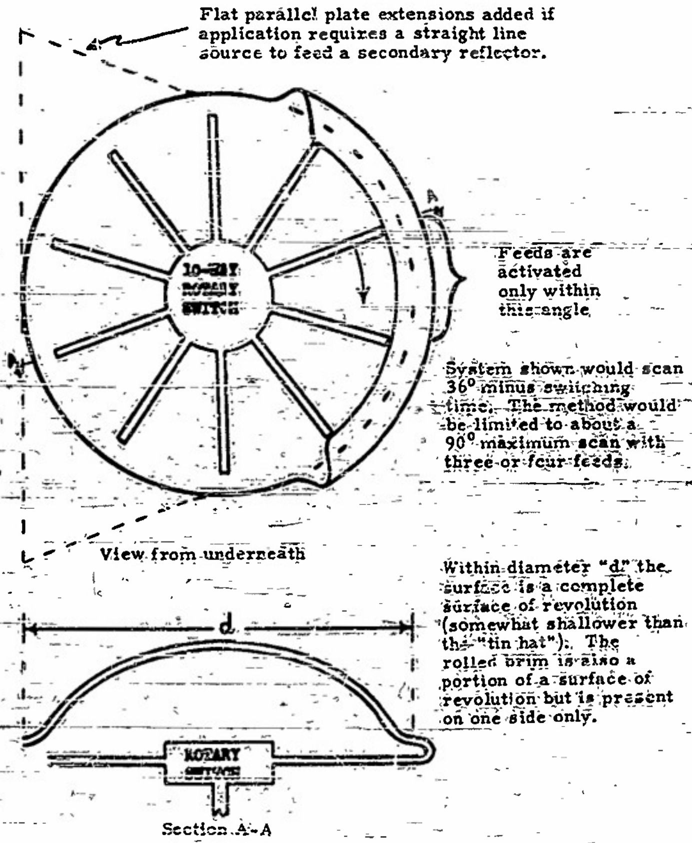

Figure 5 - Tin hat system with rolled-under brim

parallel-plate, surface-of-revolution lens corrected for the de-focusing effect of a horizontal lip. Calculations were made for a model which was constructed and tested at wavelengths of 0.887 cm and 1.25 cm. A new type of wide-angle, parallel-plate scanning antenna composed of portions of surfaces of revolution about the same axis was proposed. Full details of this work, including a number of related matters not discussed here, are given in two reports available through the Defense Research Board in Canada.

* * *

LUNEBERG LENS

G. D. M. Peeler
Naval Research Laboratory

We have designed a two-dimensional Luneberg lens using circular, almost parallel, conducting plates; the space between plates being filled with polystyrene. This lens uses the TE_{10} mode so that the proper index of refraction is obtained by making the plate spacing a function of the radius. Figure 1 shows a picture of the lens together with a sketch that exaggerates the curvature of the plates. For ease of construction, the top plate was kept flat and the bottom plate machined to give the proper plate spacing. The lens was designed for a wavelength of 3.2 cm, making the polystyrene thickness 0.91 inch at the center and 0.52 inch at the edge. The diameter is 36 inches. The flanges at the rear of the lens position a feed horn and were arbitrarily made to cover 90 degrees of the circumference. The extra rim at the edge of the top plate was added to make the aperture symmetrical; thus making the total thickness 1-7/8 inches.

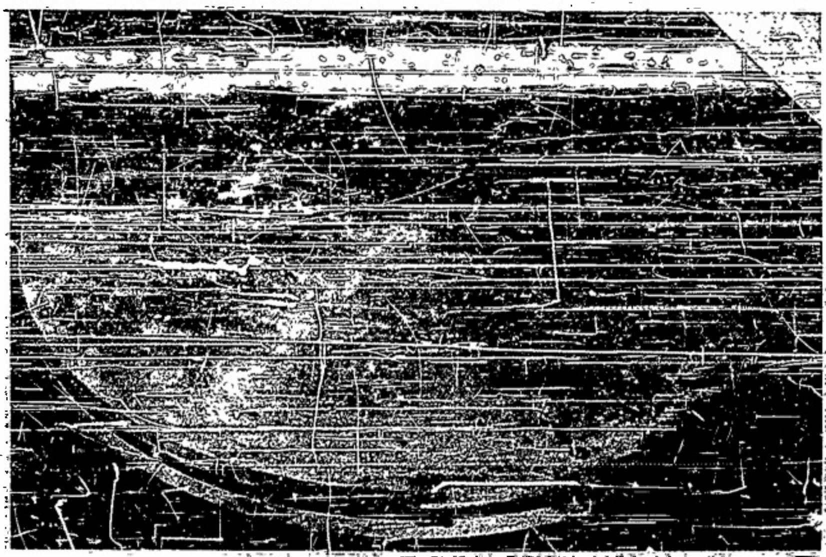

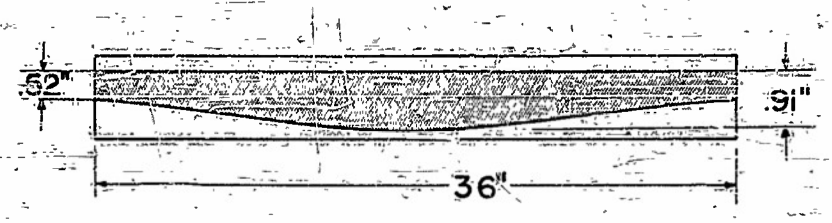

Figure 1 - Two-dimensional Luneberg lens

Provision is made for adding flares to this lens in order to obtain a more directive beam in the H-plane. One set of flares consists of plane sheets of 20-inch radius mounted on each side of the lens. These are designed to act as a box horn at the aperture. Another set, which we call the conical flares, has a plane section the same as the first set but with the addition of a section of a 45-degree cone to each flare to make the total aperture 12 inches.

The design of the lens can be understood by considering perfectly parallel plates separated by a dielectric which will propagate the TE_{10} mode. The index of refraction of this medium is given by

$$n = \frac{\lambda}{\lambda_g} = \sqrt{\epsilon' - \left(\frac{\lambda}{2a}\right)^2} \;, \qquad (1)$$

where ϵ' is the dielectric constant, λ is the free space wavelength, and a is the plate spacing. The design technique permits variation of the spacing between plates with radius in order to obtain the desired index of refraction

$$n = \sqrt{2 - r^2} \;. \qquad (2)$$

Equations (1) and (2) can be combined, and the plate spacing a can be found as a function of radius when the dielectric constant and the wavelength are taken as parameters

$$a = \frac{\lambda}{2\sqrt{\epsilon' - 2 + r^2}} \;. \qquad (3)$$

Inspection of Equation (3) for $r = 0$ indicates that ϵ' must be greater than 2 for this equation to have any meaning. The lens must operate above cutoff for the TE_{10} mode; when this condition is applied at $r = 1$ (the point most apt to be below cutoff), $\epsilon' > 2$ also results.

Figure 2 shows H-plane patterns with and without flares. The lens without flares has a pattern with a flat top and no side lobes as such, although there is appreciable amplitude at wide angles. The half-power beamwidth is 39 degrees. The addition of the plane flares increases the gain 3-1/2 db and decreases the beamwidth to 24 degrees. The conical flares give a beamwidth of 22 degrees and reduce the sidelobes slightly, but we believe that for most applications the improvement over the plane flares does not justify the larger structure.

Care must be taken to be sure that the addition of the flares does not destroy the focusing properties of the lens. Figure 3 shows no appreciable difference in E-plane patterns with and without the flares. These patterns, taken for the various feed positions, indicate constant gain; and they have sidelobes for the most part under 18 db. If the flares were used to support the feed instead of the flanges, 360-degree scanning could be obtained. The beamwidth is 2.2 degrees. Comparison of scales will show that the beam shift is equal to the feed horn shift; there were twice as many feed positions used without flares as with them.

The gain of the lens with the plane flares at 3.2 cm is 26 db, about what is expected from a consideration of the beamwidths.

Data taken over a 6-percent band of frequencies show that the patterns are much the same as those shown here for 3.2 cm.

Future plans for this project include developing smaller feed circle Lunebergs, as shown in Figure 4. Luneberg's solution requires the feed to be at the edge of the lens,

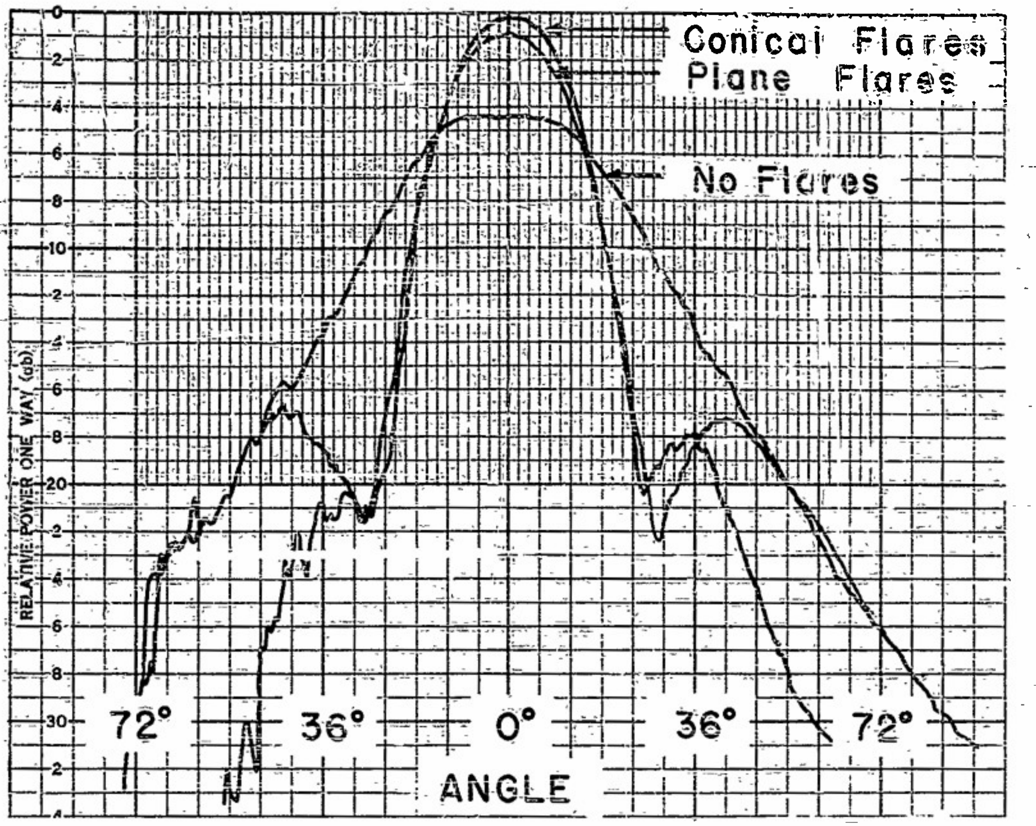

Figure 2 - Luneberg Lens—typical patterns (H-plane)

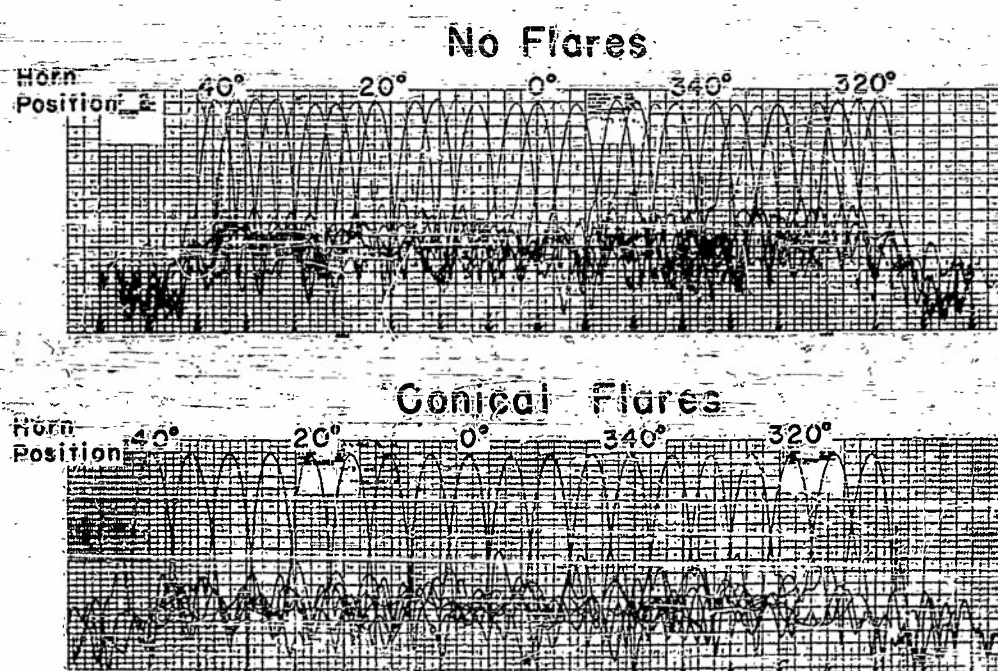

Figure 3 - Luneberg Lens—patterns for various horn positions (E-plane)

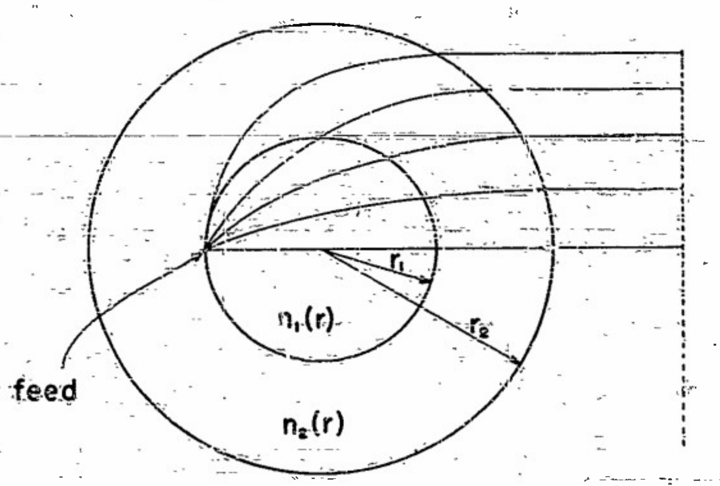

Figure 4 - Luneberg Lens — small feed circle

which is the case for the lenses developed to date. If the feed circle could be reduced, say to a radius of r_1, a lighter and more compact feed system could be designed which would permit easier and more rapid scanning. A lens with this smaller feed circle radius requires a different variation of index of refraction, and perhaps need not be called a Luneberg at all. Dr. Eaton of the Antenna Research Branch of NRL has solved the problem of determining the index of refraction for an arbitrary feed circle radius.

DISCUSSION

Wilkes: (APL) Could you explain how you bolted the two plates together ?

Peeler: (NRL) First, I should say that we used the TE_{10} mode so that the bolts are perpendicular to the E-vector. We first took data with no bolts, but we found that the polystyrene warped slightly after machining; so we were forced to add bolts, a few at a time, to continually improve the patterns.

Wilkes: Did you paint the polystyrene surfaces for good metal contact ?

Peeler: No, I did not. It should be possible to build a much lighter antenna if we were to do away with the metal plates and use painting as you suggested.

Question: How could the small feed circle be fed ?

Peeler If one were interested in a limited scan he could cut out a portion in the back; for a 360-degree scan, he could feed with a slot between the inner circle and the annular ring. The separation between the inner and outer regions of the lens would permit feed horn rotation or feed horn and inner ring rotation. For three-dimensional lens the scan might be limited to a sector of 90^0. For a full sphere, you must remove a part of the sphere.

* * *

360-DEGREE NONMECHANICAL SCANNER EMPLOYING A RINEHART-LUNEBERG LENS

R. S. Wehner
Hughes Aircraft Company
Culver City, California

In connection with a study of the problem of electronic scanning, under Air Force Cambridge Research Center Contract No. AF 19 (122)-454, Dr. M. J. Ehrlich and Mr. I. K. Williams of the Hughes Aircraft Company have proposed and partially investigated a new and interesting application of the Rinehart-Luneberg lens (1). In this application the lens is used as a principal component of a nonmechanical scanner in such a manner as to provide a possible practical solution to the aperture blocking problem—a natural means for extending the narrow annular aperture of a conventional Rinehart-Luneberg into a cylindrical or conical surface wide enough to permit the possibility of beam-shaping in the planes transverse to that of the aperture—and as a means for accomplishing wide-sector or full 360-degree scanning of a fan beam without mechanical motion of either the lens or its feed.

Consider the toroidal-bend aperture of a standard Rinehart-Luneberg lens (2) to be removed at its junction with the lens focal line and replaced by a cylindrical parallel-plate medium composed of many identical rectangular waveguides, arranged axially, narrow side abutting narrow side, as indicated in Figures 1 and 2. If any one of these waveguide apertures were fed so as to radiate into the lens, it would be apparent that the guide apertures lying along the opposite semi-circumference would be illuminated with the proper phase distribution to give rise to a plane wave (neglecting reflection and diffraction effects) providing that the individual rays were refracted so as to emerge parallel and coplanar. The toroidal bend accomplishes the latter function in the conventional Rinehart-Luneberg; here it is accomplished by the waveguide medium and by the slot arrays in each of the component guides.

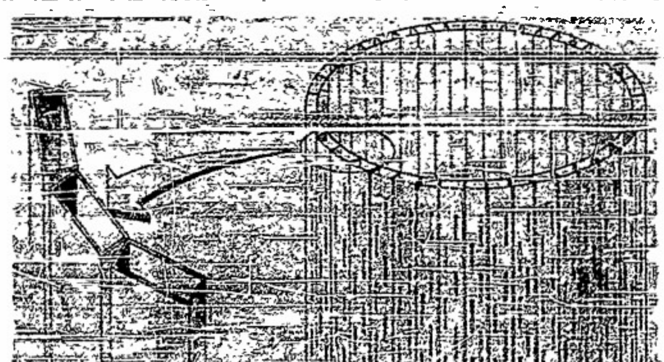

Figure 1 - Artist's sketch showing cylindrical surface composed of rectangular waveguides containing shunt slot arrays

It was expected that phase and amplitude changes in the refracted waves as a function of angle of incidence, internal reflections, and diffraction at the guide wall edges would complicate transmission from the Rinehart-Luneberg medium into the parallel-plate system. This matter was investigated experimentally using a 36-inch diameter Rinehart-Luneberg lens, formed of

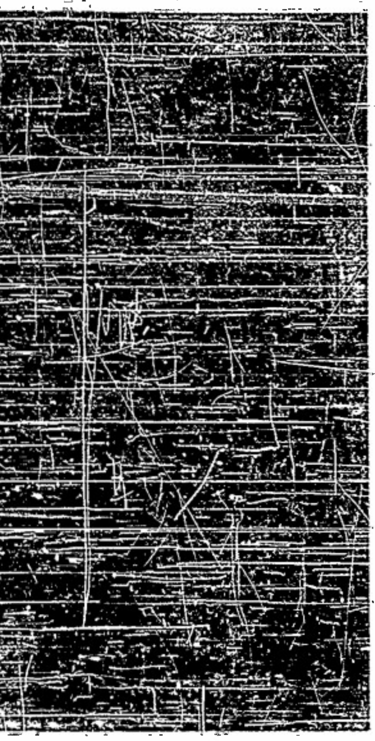

Figure 2 - Artist's sketch showing portion of Rinehart-Luneberg lens feeding parallel-plate medium composed of rectangular waveguides arranged to form cylindrical surface

aluminum spinnings, loaned to us by the Air Force Cambridge Research Center. Figure 3 shows the experimental setup, with the Luneberg lens fed by standard X-band guide and the lens feeding an array of 113 sections of standard guide, each terminated in a matched load. Figure 4 is a close-up of part of the system, with the upper spinning removed to show the guide apertures arranged along the focal line. (The toroidal bend was not removed for practical reasons.) Figure 5 shows the matched probe which could be inserted into the individual guide sections in place of their respective matched loads and also the AFCRC horn (3) which was used to feed the conventional Rinehart-Luneberg lens with open

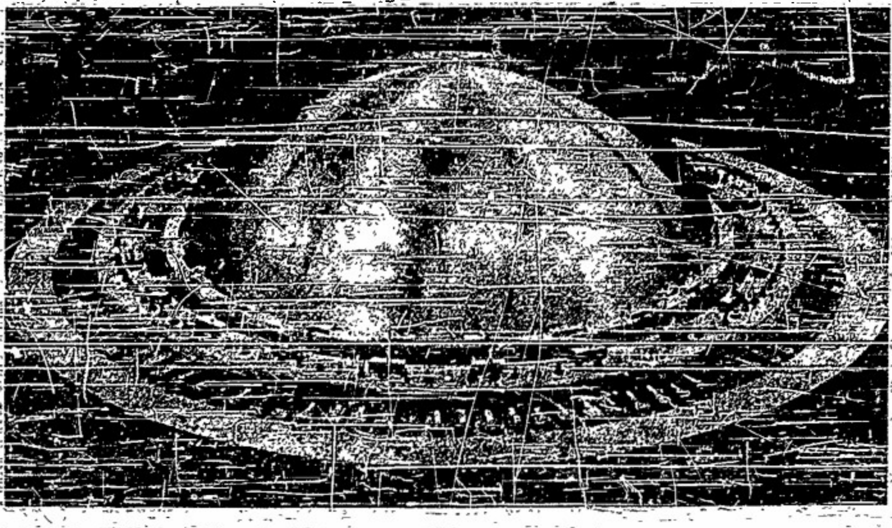

Figure 3- Photograph of 36-inch diameter Rinehart-Luneberg lens (with toroidal bend) feeding array of 113 matched X-band guides

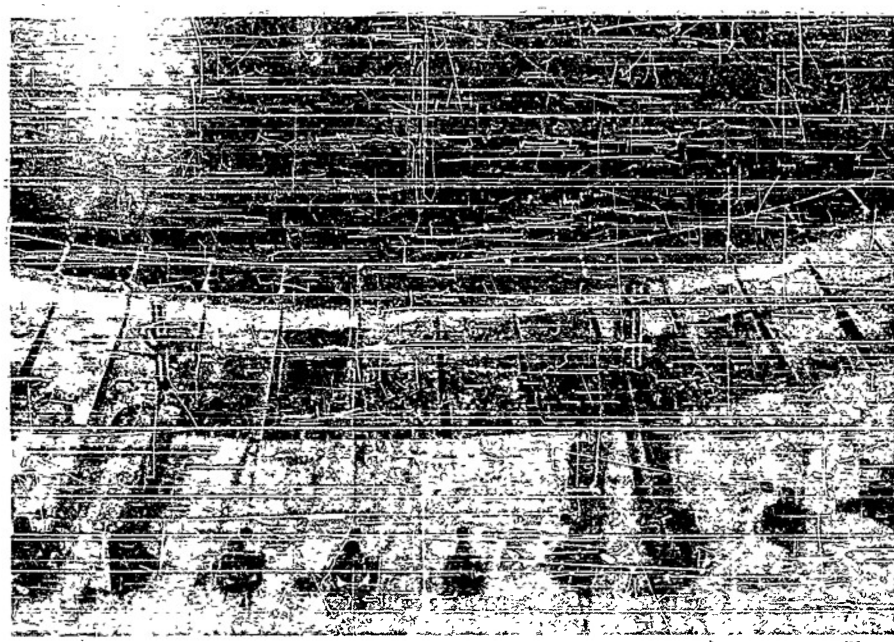

Figure 4 - Photograph of 36-inch diameter Rinehart-Luneberg lens (with toroidal bend) feeding array composed of X-band guides with upper surface of lens removed to show guide apertures along focal line

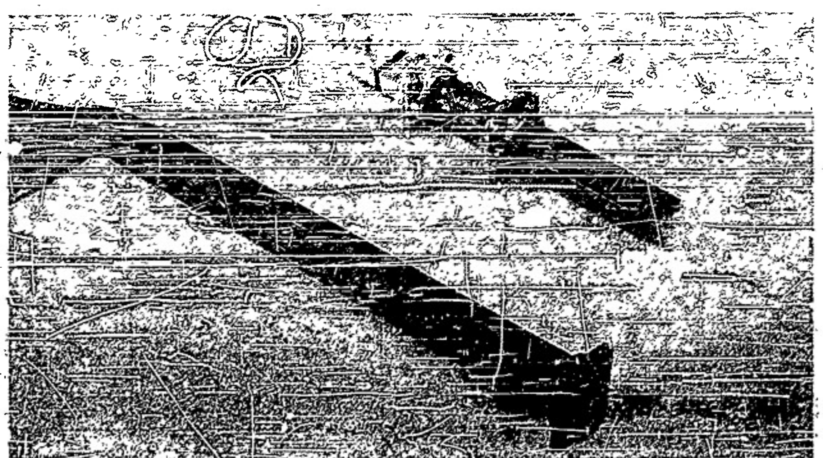

Figure 5 - Photograph of Air Force Cambridge Research Center feed horn used in study of open toroidal bend aperture and matched probe used in study of cylindrical waveguide-surface aperture

toroidal-bend aperture. Figures 6 and 7 show the measured amplitude and phase distributions over the waveguide array and toroidal-bend apertures as functions of angular position of the probe with respect to the direction opposite the feed. The general similarity of the two distributions is striking despite the more favorable illumination given the open aperture by the higher gain horn feed and despite the presence of obvious reflection and scattering effects in the data pertaining to the waveguide medium.

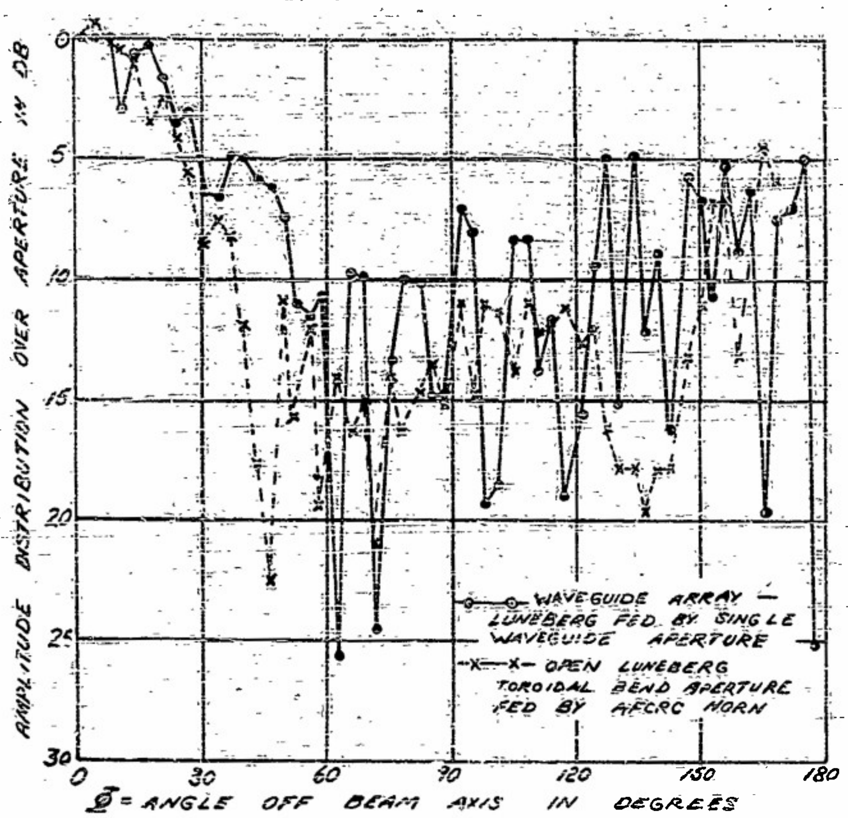

Figure 6 - Comparison of amplitude distributions over aperture of Rinehart-Luneberg lens feeding open toroidal bend and cylindrical array of X-band waveguides as measured at 9250 Mc

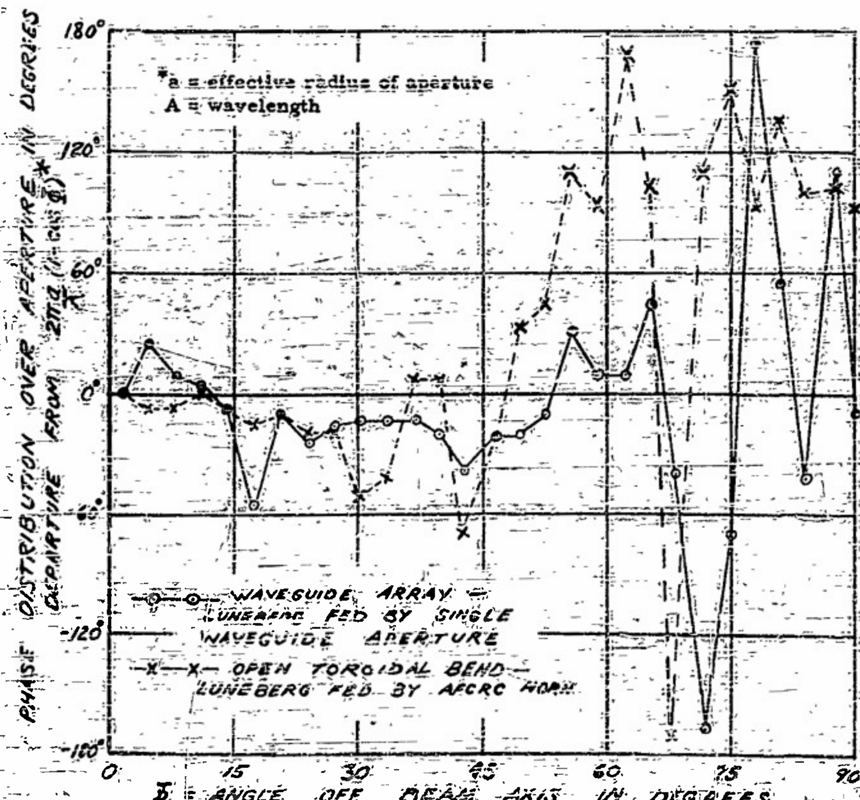

Figure 7 - Comparison of phase distributions over aperture of Rinehart-Luneberg lens feeding open toroidal bend and cylindrical array of X-band waveguides, as measured at 9250 Mc

The far-field pattern of the open-aperture lens, having the phase and amplitude distribution shown in Figures 6 and 7, was measured and found to be characterized by a 3-degree half-power beamwidth and a side-lobe level 22 db down. The corresponding pattern of the waveguide-array aperture was computed by approximate methods and found to have a 2.7-degree half-power width, with highest side lobes 10 db down. These results are only preliminary, and we have reasons for believing that the waveguide-array medium can be made equivalent or nearly equivalent in performance to the toroidal bend.

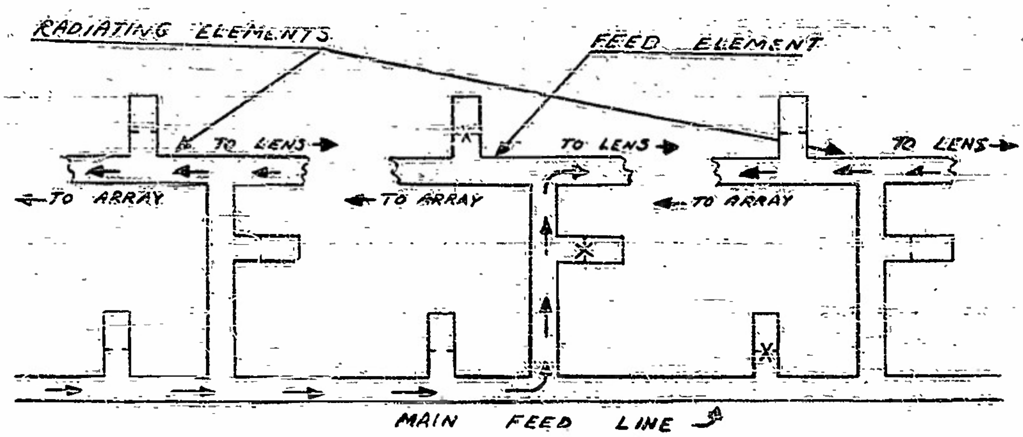

Figure 8 - Schematic diagram of proposed resonant switching system by means of which a Rineberg-Luneberg lens could be used to feed a cylindrical array of rectangular waveguides in an electronic scanner

To return to the electronic scanning problem, Figure 8 is a schematic diagram of one proposed feeding and switching arrangement by means of which any one of the waveguide elements could be made to serve as the feed for the Rinehart-Luneberg lens while the other guides function as radiating elements. This system involves a main circular feed line contained within the cylindrical waveguide surface and a system of switches in branch arms, three switches per element. In this particular arrangement, only the three switches associated with the element momentarily serving as the feed, indicated by the "X"'s in the figure, are fired at a given time; all the other switches are quiescent. Figure 9 is an artist's sketch of a possible method of incorporating this switching scheme into a Rinehart-Luneberg electronic scanner.

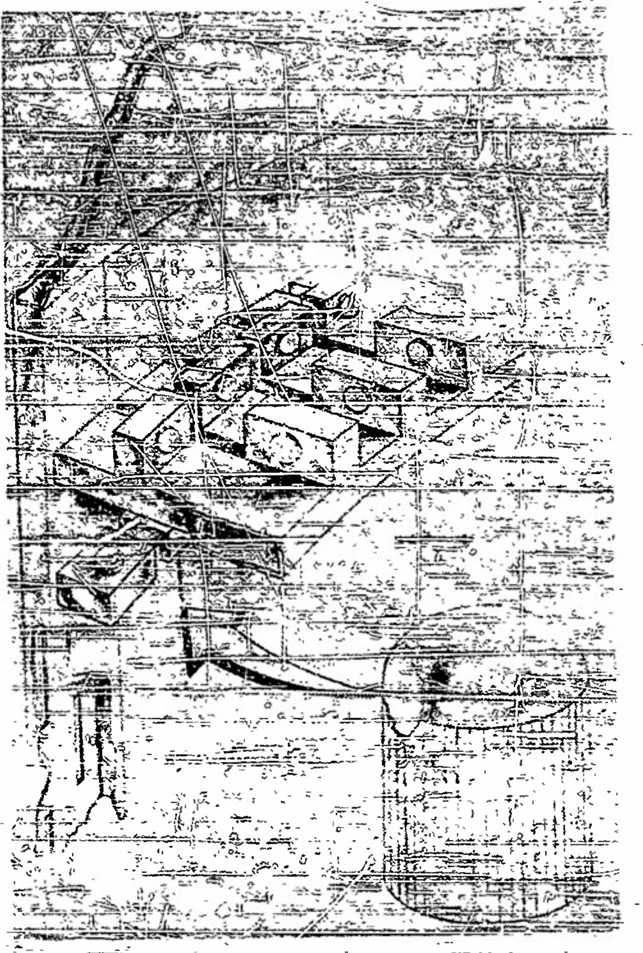

Figure 9 - Artist's sketch showing proposed feed and switching system for electronic scanner employing cylindrical waveguide-surface aperture fed by Rinehart-Luneberg lens

In conclusion, it is perhaps unnecessary to remark to this audience that no existing electronic switches (gas-tube, ferrite, or what-have-you) meet or even approach the requirements imposed by this type of radar scanner. However, the switch specifications, and the control system complexity, become much more reasonable if the scan angle is reduced from full 360 degrees to 90 degrees or less, so that a given element of the waveguide array need serve only as feed or as radiator and need not perform both functions.

REFERENCES

1. Rinehart, R. F., and Parker, F. D., "Parallel Plate Optics for Electrical Scanning," Case Institute of Technology, Final Report on Contract No. W28-099-ac-141, 30 June 1948

2. Kunz, K. S., Brammer, F. E., and Johannensen, J. D., "Final Report on Contract No. W28-099-ac-141," 30 September 1949

3. "Luneberg Horn Feed," United States Air Force Air Materiel Command Drawings No. X50C50466, dated 22 November 1949, and No. X50C50467, dated 18 July 1951

SCANNING AT R. R. D. E.

S. S. D. Jones
Radio Research and Development Establishment, England

Time being limited I intend to treat briefly items that have been published elsewhere, and conclude with a more detailed treatment of current work.

Our first venture into wide-angle microwave optics was to experiment with a variant of the Luneberg lens. The necessary varying refractive index was obtained by means of conducting sheets spaced in the direction of the magnetic vector, in such a way as to produce a quasi-refractive index varying according to the Luneberg relation. This variant, which had the defect of being limited to the production of a line source, is the only one we have examined experimentally. However, my former colleague, Brown, now of City and Guilds College, London, has developed the theory of a similar system which is capable of scanning a fan beam through 360° by moving the feed through a circle. Further information can be obtained from the references appended.

The only high-speed scanner that has been developed to the prototype stage is a Foster Scanner fed by a half pillbox. Its aperture is some 20 λ at "X" band, and it has been designed by my colleague, Slater, to scan over an arc of 40° at a speed of 25 cps (complete cycles). I have no information to give except that performance is entirely satisfactory. The design follows the information provided by Dr. Foster, and there were no snags. Considerable care was required both in machining of the light alloy castings which formed the cone and in dynamic balancing; fortunately, the National Gas Turbine Establishment found the latter problem a simple one.

We have recently been called upon to produce a lens to operate in the 8 centimeter band to the following specifications:

Beamwidth:	$<3^\circ$ to -3db
Scanning Angle:	$\pm 12.5^\circ$
Bandwidth:	$\pm$ 2-1/2%
Polarization:	Plane
Feed:	Point Source (moving for scanning) or line source (stack of horns suitably fed to synthesize CSC^2 beam).
Aperture Ratio:	Unity

We have considered both the Binormal and Kock types of lens. The former would give a better scanning performance; but, as plane polarization was specified an "eggbox" structure, which would be necessary to meet the Ruze conditions in both planes, seemed to be an unnecessary complication. We accordingly tried to meet the specification with the Kock type.

Our mechanical engineer wanted to use perforated plates to save weight and obtained some 16 s.w.g. sheet aluminum perforated with holes of 1/2-inch diameter in a face-centered hexagonal lattice. The ratio of hole to metal was 55%.

A few preliminary experiments showed that use of perforated plates offered an advantage more important than weight saving. Coupling between adjacent channels drastically modified the waveguide equation, and plate spacing was some 15% less than the value given by that equation for the desired refractive index of 0.5 (in fact, the lens was designed for n = 0.53 as, on account of some rather inaccurate preliminary experiments, a number of spacers which produced this value had been made before the lens was constructed). This reduction of plate spacing, by delaying the onset of second-order reflections, promised to improve the efficiency of the lens.

Figure 1 shows the construction of the lens. A combination of front and back steps was used so that the back surface of the lens lay approximately on a sphere centered on the focus.

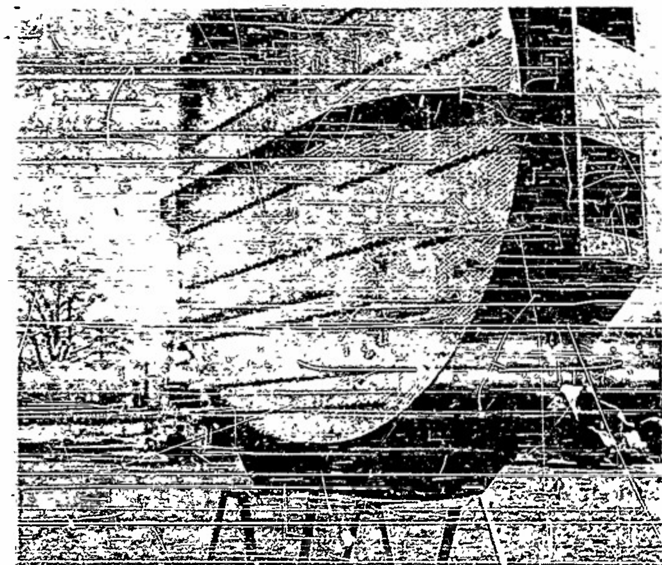

(a) Over-all construction of lens

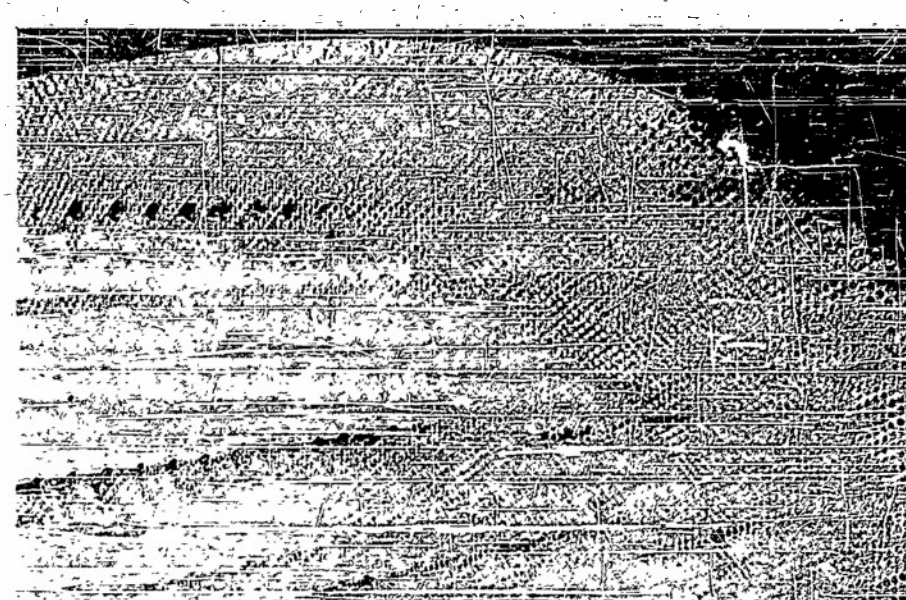

(b) Close-up of lens

Figure 1 - Kock-type lens

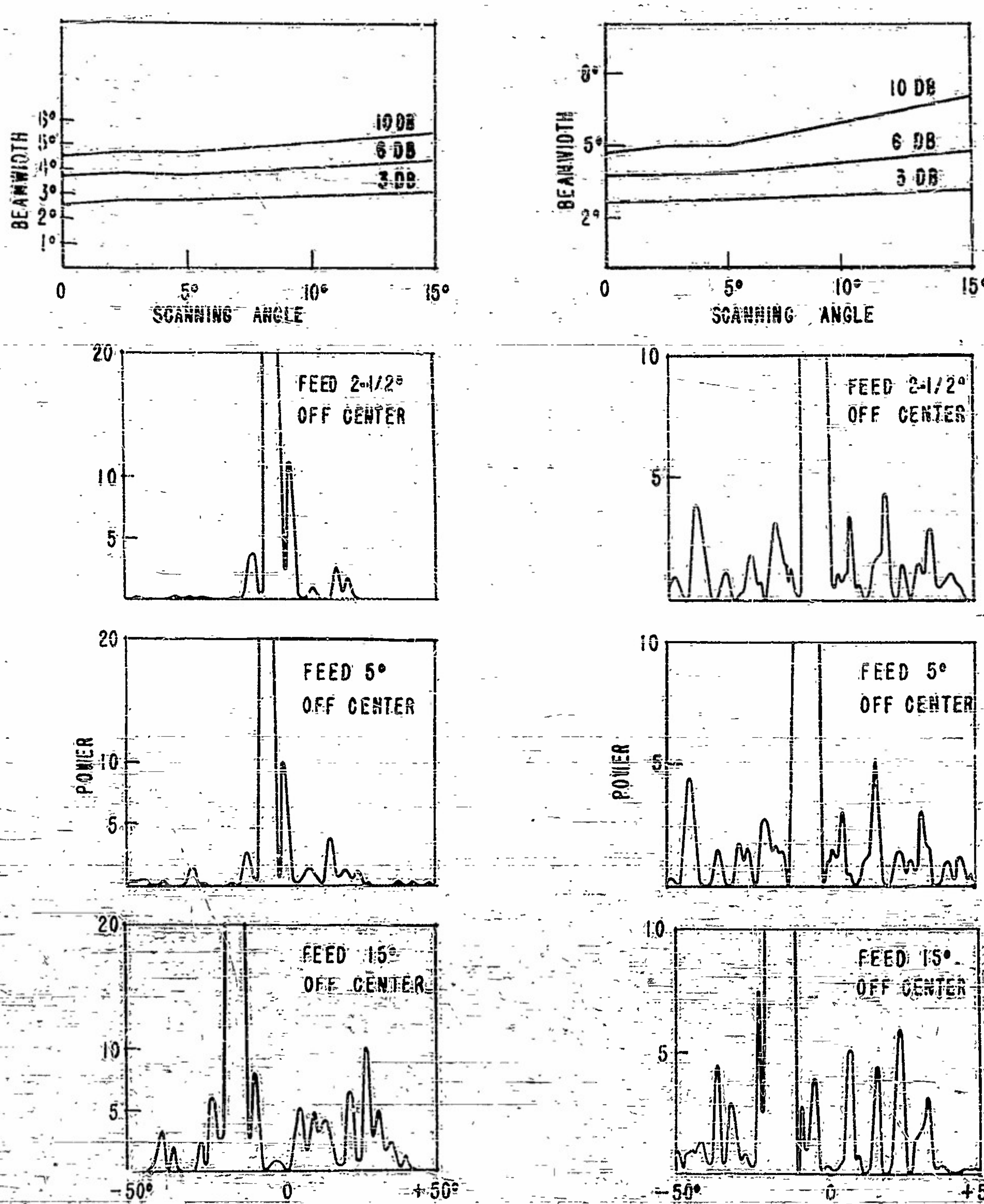

(A) E-Plane

(B) H-Plane

Figure 2 - Polar diagrams of 6' lens, λ = 8.2 cm, feed horn 5-1/2 by 4 in.

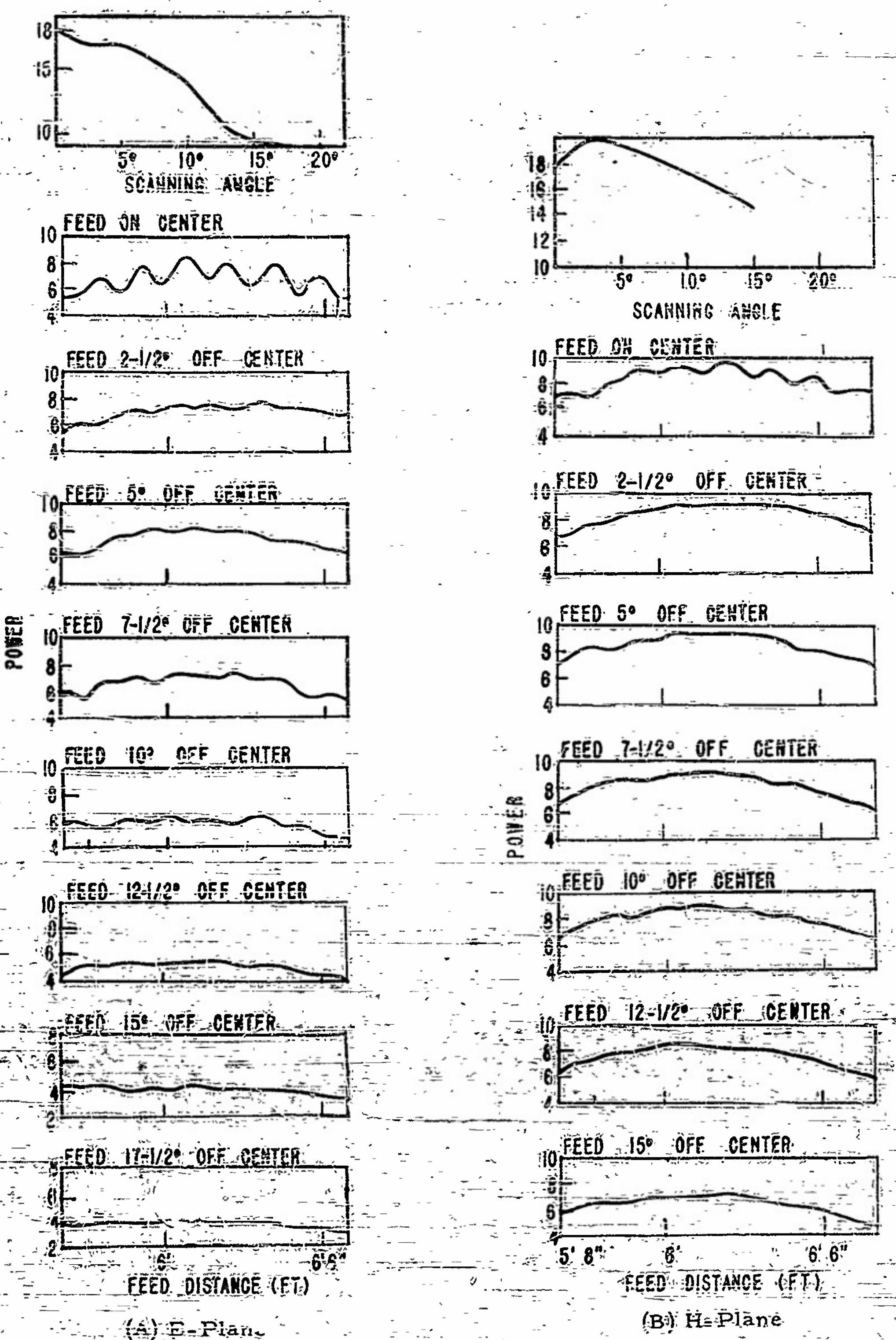

Figure 3 - Gain vs. feed distance of 6-foot lens.
λ = 8.2 cm, feed horn 5-1/2 by 4 inches

The remainder of the figures summarize the measured performance. Figure 2 shows radiation patterns at the design frequency, and Figure 3 gives a summary of the scanning properties in E-and H-planes. It will be seen that the optimum focal surface is very nearly a sphere centered on the center of the lens. The gain vs. scanning angle characteristic does not compete with the Binormal type of lens; but even so, it is sufficiently good for our present purpose, and the construction avoids the complication of the eggbox.

In all of these figures a primary feed horn giving a 10 db taper was used.

The efficiency of the lens system appears to be about 50%, though I think everybody here will understand my reluctance to be very confident in an absolute gain measurement. This rather high value would seem to indicate that front steps are slightly less harmful than the usual rear steps.

Finally, I would like to place on record my appreciation of the generosity of the U. S. Naval authorities in enabling the British representatives to attend this most valuable Conference.

BIBLIOGRAPHY

1. Luneberg, "Mathematical Theory of Optics," Brown University Press, p. 213, 1944

2. Jones, "A Wide Angle Microwave Radiator," Proc. I.E.E., Vol. 97, p. 255, 1950

3. Brown and Jones, Electronic Engineering, p. 357, Sept. 1950

4. Carlson and Heins, "The Reflexion of an EM Plane Wave by an Infinite Set of Plates," Quart. Applied Math. 4, p. 313, January 1947

5. Brown, "Proceedings of a Conference on Aerials for Marine Radar," Her Britannic Majesty's Stationary Office, February 1952

DISCUSSION

Budenbom: (BTL) Could you give a figure for the loss in gain on this lens?

Jones: (RRDE) The effective area was about one half of $4\pi A/\lambda^2$.

Kelleher: (NRL) That appears to be a very good gain figure. We had some discussion about lenses at the last symposium and I believe you have some information appropriate to that discussion. Your data appears to show a very broad maximum for your gain as a feed is moved along the axis of the lens.

Jones: Yes, it is very broad. It is what might be expected from the optics of the situation. The f/D ratio was 1 and there was a tolerance of ± 3 inches about the 6-foot focal length.

Kelleher: That is encouraging. The previous results seem to indicate that you might lose a large amount of gain if the feed were moved only slightly from the best focus point.

Jones: There was a ripple on the curve, and it is possible that bad impedance matching might give false gain data.

Budenbom: Your gain figure was no doubt quoted for the design frequency. Was there any attempt to broad band this lens?

Jones: No, it was a straightforward Kock design with steps on the front face. In regard to this 50% figure, I would like to say that it might be off by a db or so. We did not have access to a site which left us entirely free from ground reflections.

FERRITES AT MICROWAVES

H. N. Chait and N. G. Sakiotis
Naval Research Laboratory

One method of scanning involves the use of arrays of radiating elements such as dipoles, slots, or horns. The antenna beam is scanned by causing the relative phase between elements to vary with time in a prescribed manner. This has been accomplished in some antenna systems by mechanical methods. For example, in an Eagle Scanner the width of the waveguide feeding the array is changed, thus changing the guide wavelength which consequently varies the electrical distance between the elements of the array to provide the required scan. Unfortunately, this and other such schemes frequently result in mechanically complicated structures which are hard to construct, hard to maintain mechanically, and, most important of all, hard to move rapidly.

In recent years, attention has been directed toward the possibility of scanning by methods which avoid the use of mechanically moving parts. One approach to this problem involves a source whose frequency varies with time. This, as in an Eagle Scanner, changes the guide wavelength and thus can be used to produce an electrical scan. This line of attack is already being followed by Hughes Aircraft and others, and the major problem seems to be the development of variable-frequency magnetrons or klystrons.

Recently another method of electrical scanning suggested itself to us when a new type of waveguide switch was introduced by C. H. Luhrs. The design of this switch was based on the electromagnetic properties of certain ferrite materials. These properties have been the subject of recent papers by Kittel of BTL, Polder of Phillips Eindoven, and Rado of NRL. More recently, papers have been published by Hogan of BTL and Sakiotis, Simmons, and myself here at NRL describing some microwave applications of ferramic materials.

When we started our ferrite research program we found that these materials had characteristics quite unlike any other material currently used in microwave components. For lack of a better name, we call this material a ferromagnetic dielectric. This material has many interesting characteristics. Among others it is anisotropic in such a way that it could be made nonreciprocal—that is, one can make devices from it which will not obey the reciprocity law. Since there was so much unexplained in the literature we therefore embarked on an experimental and theoretical study of ferrites for use in the microwave region.

Since our primary aim has been the development of an electronic phase shifter, our investigations for the present have been confined to the measurement of the ferrite properties directly applicable to the design of such a gadget—namely, the phase shift and loss.

An idea of how ferrites operate can perhaps be obtained by considering the theory of operation of a Luhrs switch. Figure 1 shows a Luhrs switch as it is commonly used in an X-band waveguide setup. Notice that the output guide is rotated 90 degrees with respect to the input guide. The switch is located between these crossed guides. It consists of a section of dielectric-filled circular waveguide in which a piece of ferrite rod about 1/4 inch in diameter and 1-1/4 inches in length is axially located. It is similar to the arrangement

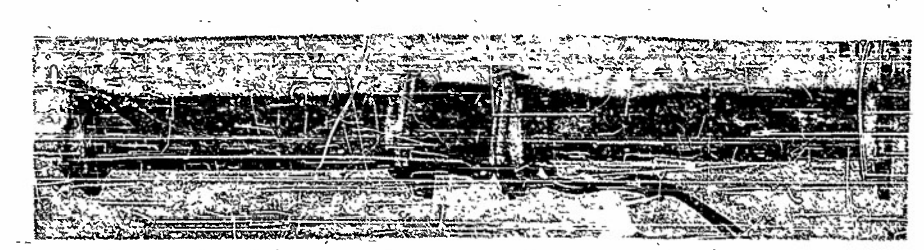

Figure 1 - Luhrs switch as used in X-band waveguide

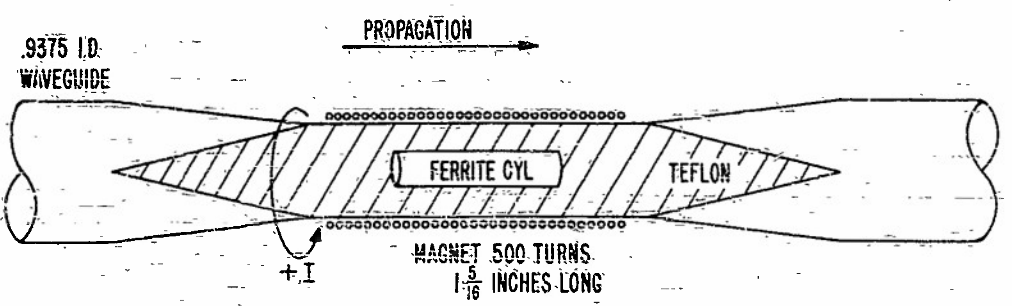

Figure 2 - Longitudinal section of a typical switch

shown in Figure 2. A coil of wire is provided to supply an axial magnetic field. When the proper current is fed to this coil, the polarization is rotated 90°, and power will be transmitted from one guide to the other with about 0.25 to 1.0 db of attenuation, depending on the particular switch and the ferrite in use. When the current is removed, attenuations of as high as 50 db have been measured.

This particular phenomenon can be explained by a consideration of the Faraday optical effect. Let us assume that the linearly polarized incident wave can be resolved into two circularly polarized components of equal magnitude, one right-handed and the other left. On application of the dc magnetic field, the ferrite becomes anisotropic in such a way as to have different indices of refraction for each of these components. Thus in passing through the material, a relative phase shift is introduced between these components, and this will cause rotation of the plane of polarization. With the proper field, the 90-degree rotation required by the switch may be obtained. It is evident from this that electronic phase shifting can be obtained by feeding such a device with energy having only one sense of circular polarization. The output phase can then be controlled by varying the field applied to the ferrite.

We then felt it was necessary to determine the factors which control the phase shift or rotation and the loss characteristics of the available ferrite materials. Figure 3 shows schematically our original measuring setup. Figure 4(a) is a picture of the actual setup for measurements in a circular waveguide and Figure 4(b) is the setup for measurements in a rectangular waveguide. Here we can measure all the characteristics of the ferrites in which we are interested. To simplify the actual measurements, the single-mode transducers have been replaced by double-mode transducers so that the input VSWR and the output ellipticity can be measured continuously without moving any part of the setup. The January 1952 issue of the NRL Progress Report contains a description of the work and the setup. We are determining how the physical dimensions and the shape of both the ferrite and the guide which contains it affect the phase and loss properties of all available ferrite materials. The effects are being studied for both longitudinal and transverse fields and combinations of both.

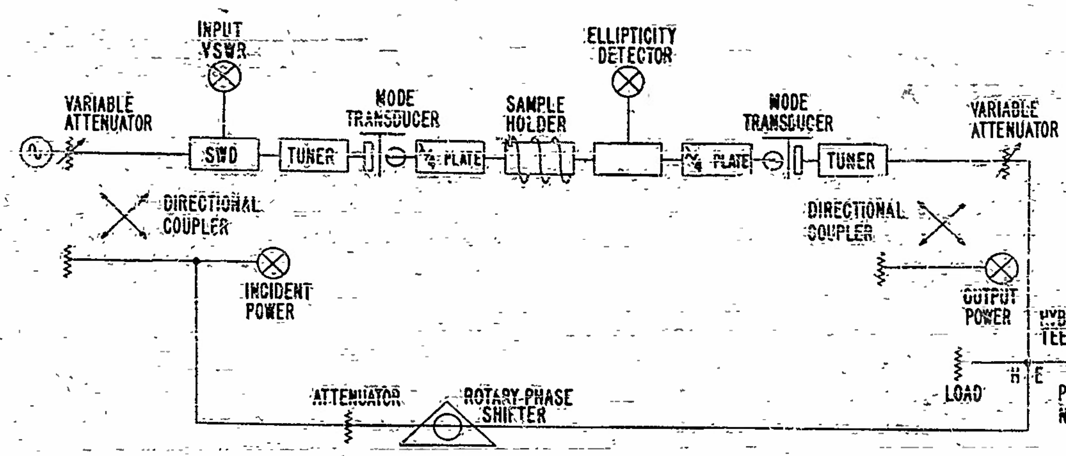

Figure 3 - Schematic diagram of original setup for measuring the characteristics of ferrites

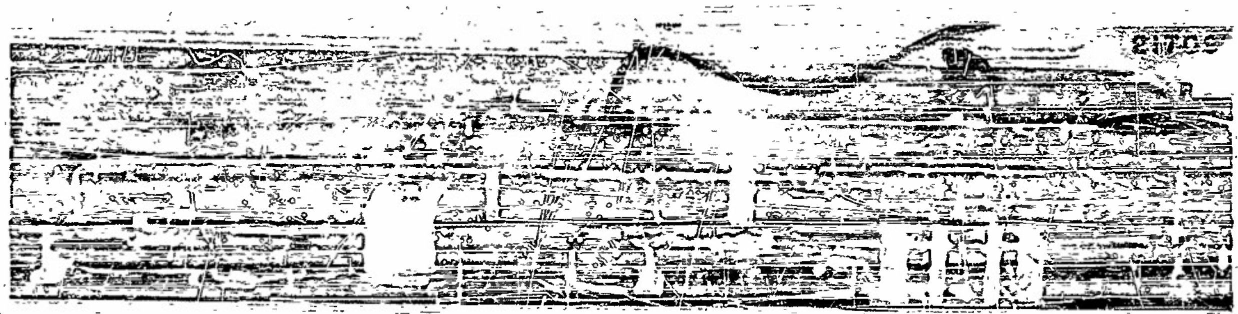

(a) Circular waveguide

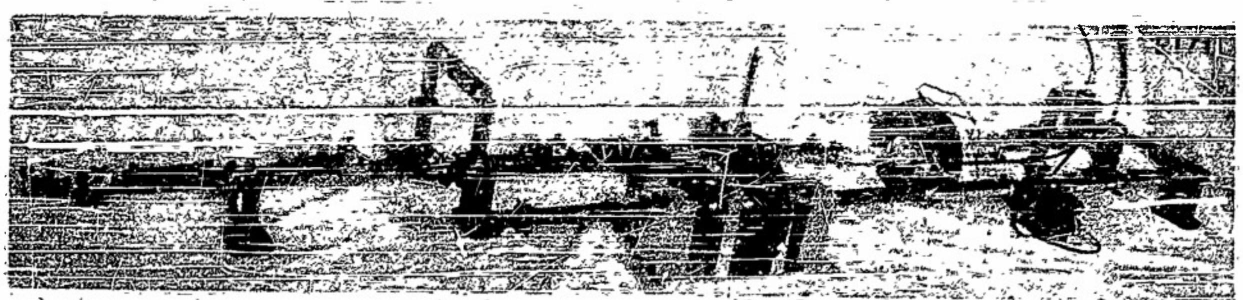

(b) Rectangular waveguide

Figure 4 - Actual setup for measuring the characteristics of ferrites

In coordination with our measurements, Dr. M. L. Kales of our branch has been conducting a theoretical study of the propagation modes in waveguide of arbitrary dimensions when the guides are filled or partially filled with ferrite. He is in the process of publishing a report giving some results of this investigation.

Once familiar with the properties of these ferrites, one finds many places in a radar system where they can be used; in fact, the number of applications is limited mainly by his own ingenuity. Ferrites in some form or other can be used to replace TR's, ATR's, modulators, switches, attenuators, phase shifters, wavemeters, matching sections, polarization changers, etc. There are, of course, many problems to be solved before these components can be used. Their power-handling capabilities, their bandwidth, and their temperature dependence are of prime interest.

I would now like to describe a few of the components which we are presently developing. As I mentioned earlier, we were very interested in building an all-electronic, variable phase shifter. Our first idea was to convert from linear to either right- or left-hand circular polarization, using some form of quarter-wave plate; then to do our phase shifting in a ferrite section; and finally to reconvert to linear polarization with another quarter-wave plate. We soon realized that the phase shift on transmission was different from that obtained on reception. This would be highly undesirable in an antenna array. Mr. Simmons of our branch suggested the addition of the two 45-degree ferrite rotators which made the unit bilateral. Figure 5 shows the schematic of this phase shifter which is an X-band model. An explanation of the operation of this device is included in the progress report article mentioned earlier.

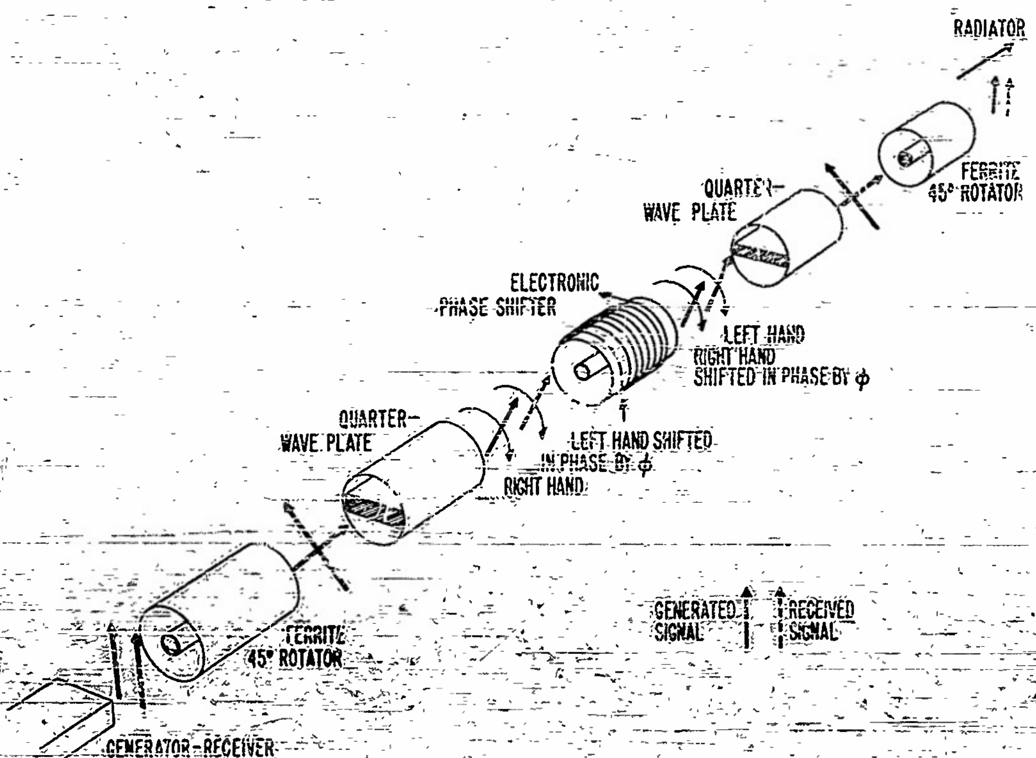

Figure 5 - Schematic diagram of phase shifter (X-band)

The performance of each of the units in this assembly has been checked. The 45-degree rotator was designed and built so as to rotate the plane of polarization 45 degrees when the ferrite is magnetically saturated. The insertion loss at saturation is about 0.20 db. The quarter-wave plates are of standard design. The design of the phase shifter is dependent on the total phase shift required. Figure 6 shows the phase shift and loss characteristics of a 70-degree variable phase shifter. As you can see, the loss is less than 0.30 db over the entire range of phase shift. Phase shifts of 360 degrees or more can be obtained if necessary. This, or any other similar phase shifter, is not limited by any mechanical motions since the phase shift is varied by changing the current passing through the coil. This can be done as rapidly as required in any existing scanning application.

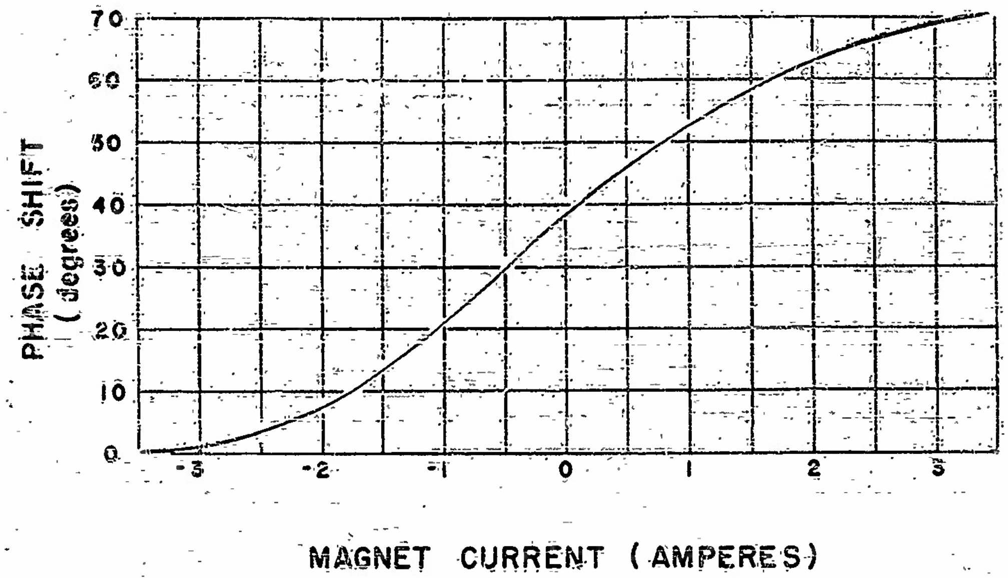

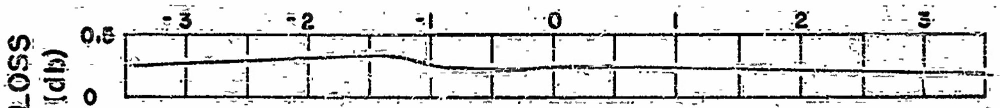

Figure 6 - Phase shift and loss characteristics of a 70-degree variable phase shifter

Another interesting device that may have many applications in scanning antennas is the movable ferrite slot. Imagine a nonradiating slot cut in a section of circular waveguide in an arrangement similar to Figure 7. Placing a cylindrical piece of ferrite in the center of this waveguide section will not materially affect the radiating properties of this

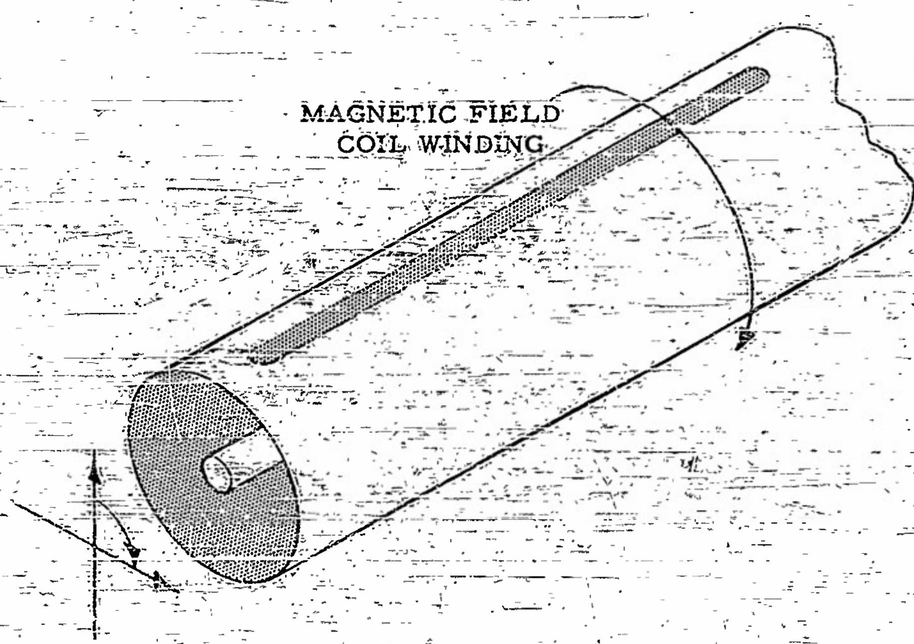

Figure 7 - Movable ferrite slot

slot. However, if an axial field is applied to this section of guide, the field in the guide is rotated and the slot can be made to radiate. Tests were conducted on the section of guide shown in Figure 8. The coupling loss was about 0.5 db whereas the decoupling in the unactivated position was 30 db or greater. An array of slots such as this one can be placed at the focus of any reflector or lens to present a movable point source to the objective; thus, the beam is scanned electronically. Such a unit is under development here at NRL.

Another moving point source can be developed using only Luhrs-type switches and two-mode transducers similar to the one shown in Figure 9. If the switch is placed in front of the transducer, power can be switched from one output to the other simply by placing a square wave of current on the solenoid wrapped around the switch. If a number of these elements are cascaded, we obtain the equivalent of the organ-pipe scanner. Such an arrangement is shown in Figure 10. The energy is switched consecutively from horns 1 to 5 by actuating the switches in the same order. The dead time will be negligible, since

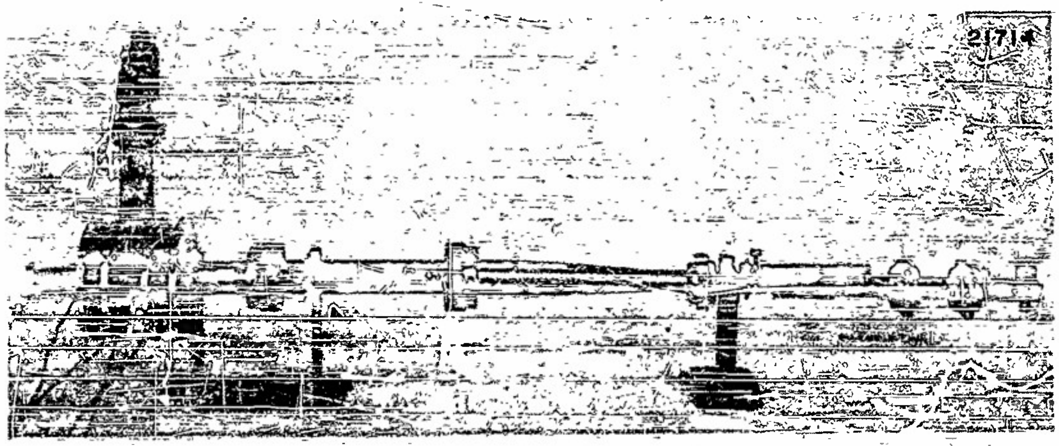

Figure 8 - Section of guide showing arrangement for making tests in which the axial field is rotated

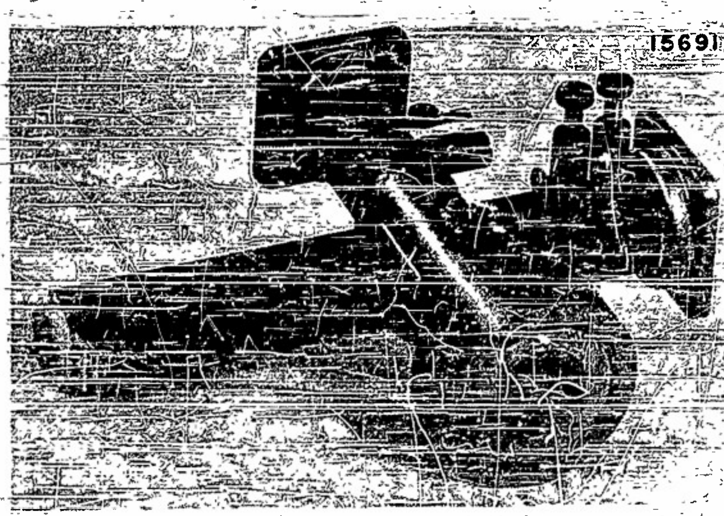

Figure 9 - Two-mode transducer

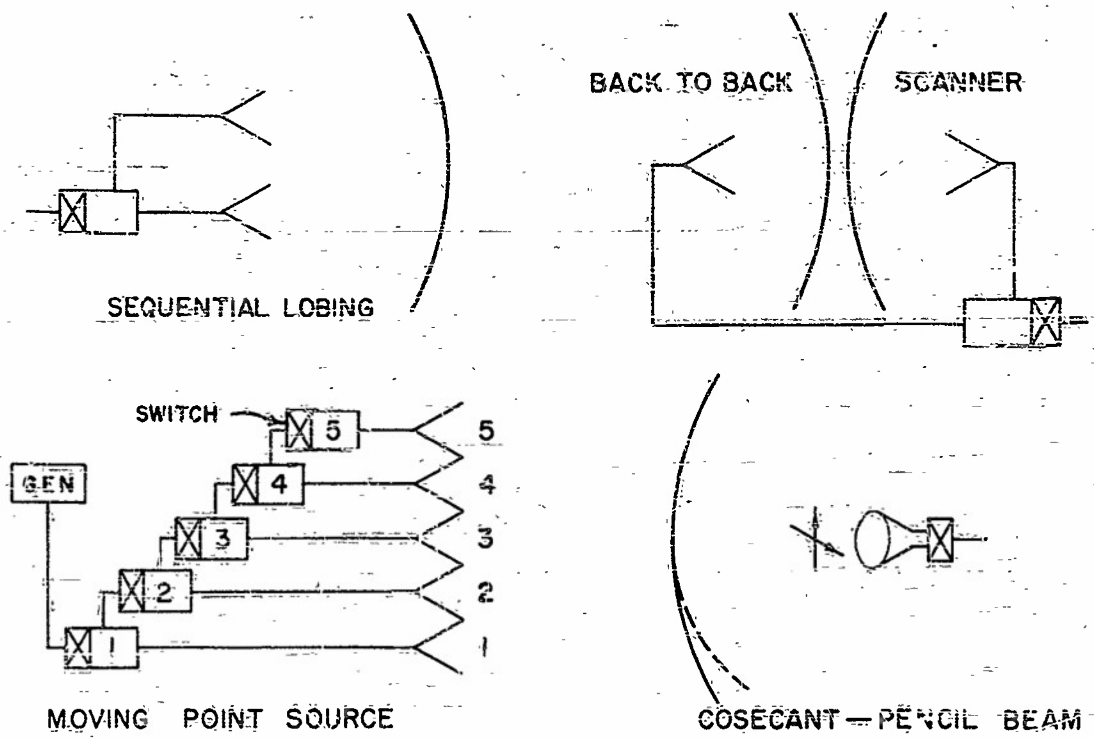

Figure 10 - Various applications utilizing Luhrs-type switches and two-mode transducers

the switching time can be made one microsecond or less. On this same slide are illustrated some other applications of the ferrite switch. The polarization rotation properties of the ferrite can be used to rotate the polarization of the energy coming from a horn; thus the antenna beam is changed from a pencil-beam to a cosecant-squared beam.

The last application I will talk about was suggested by Dr. Kales. It is similar to a BTL device developed for cw operation. We call it the "matchless matcher." Everyone here realizes the difficulty in isolating the antenna from the generator. There are cases where a scanning scheme has been discarded because of the pulling of the magnetron due to the variation in phase of the antenna reflection as this antenna scans. Figure 11 shows the typical arrangement of the "matchless matcher." When the magnetron fires, both the TR and ATR are closed. The output of the magnetron is rotated 45 degrees in passing through the 45-degree rotator, and then it proceeds to the antenna. If any power is reflected by the antenna, it comes back down the line, passes through the rotator, and is rotated another 45 degrees, making a total of 90. The reflected energy therefore cannot enter the input and must proceed up one of the two side arms. Since the TR and ATR are still closed, the reflected power proceeds to the upper arm and is absorbed in the load. By the time the target reflection arrives back at the antenna, both TR and ATR are open and thus the target energy proceeds to the receiver instead of the load.

We have just described a few of the many possible applications of ferrites in present-day radar systems. The field is relatively new. There is much more to be learned about ferrites at microwave frequencies, but of one thing we are sure: ferrites will have a place in the radar systems of the future.

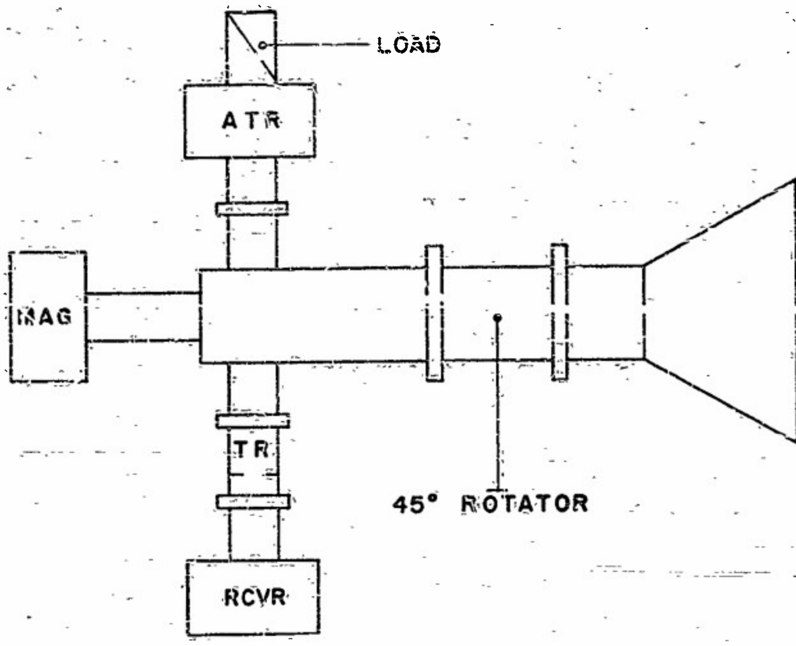

Figure 11 - The "matchless matcher"

DISCUSSION

Wilkes: (APL) How will you be able to handle power through this device?

Chait: (NRL) A switch has been operated at 15 kilowatts without any trouble. We intend to make power measurements in the near future. We have noticed a Cruft Laboratory report in which they measure loss in the ferrite as a function of the applied power. They found that the conditions improved as the power was increased.

Wilkes: Did you do anything about maintaining a constant temperature around the sample?

Chait: We have a water jacket around the waveguide to keep the ferrite at a constant temperature.

Wilkes: How do you conduct away the heat in the ferrite sample?

Chait: Our ferrite sample does not get hot. All our work has been done at low r-f powers.

Wilkes: We have used ac excitation with the Faraday cells which we have built. We have found considerable trouble from the heating of our samples. We are attempting to find a means for carrying away heat caused by hysteresis loss in the samples. These samples become very hot even with milliwatt r-f feeds.

Chait: We have used dc fields obtained from a few turns of wire through which we passed very high currents.

Wilkes: That would explain the absence of your difficulties.

Aiken: (Hazeltine) In regard to your waveguide switch—as you change the polarity of the magnetic field, does that change the polarization of the output wave?

Chait: Yes, as we go from zero current to saturation current, the polarization is changed.

Aiken: Then you must have high attenuation at zero current level?

Chait: No, not necessarily. That depends on the type and shape of the sample. Mr. J. P. Allen of NRL developed a circuit in which he used an early model of the Luhrs switch with high loss at zero current (about 2 db). He was able to actuate the switch at all times and so had little loss.

Aiken: Does the switch you describe completely cancel one sense of polarization so that there is a net 3-db loss?

Chait: (Mr. Chait used a slide to show that no loss of this type was necessary.) The switch changes the polarization from vertical to horizontal. If you have the means of coupling out either polarization there will be no loss.

Bernstein: (APL) What materials had been found useful in this investigation?

Chait: The particular material depended on the application for which it was required.

Bernstein: What is the lowest loss material you have found?

Chait: I do not think any one material stands out over any other. Luhrs used Ferramic A and D.

Bernstein: What material gives your lowest loss due to absorption?

Chait: The curve shown here was Ferramic D.

Aiken: Could we have a description of the ATR and TR action in the matchless matcher?

Chait: For a high-power source, the TR could be fired by leakage power. For a low-power source, it could be fired externally.

APPLICATIONS OF FERRITES TO MICROWAVE SWITCHES

Roy S. Anderson
Stanford Research Institute
Stanford, California

The requirement has long existed for a microwave switch capable of higher operating speeds than those realizable with conventional mechanical devices. Electrical devices can meet the requirement for higher speeds. This paper describes preliminary investigations of a switch which operates on the principle of changing electrically the propagation properties of waveguides. This is achieved by varying with an externally applied magnetic field, the electrical properties of a section of waveguide containing a ferromagnetic, semiconducting material — namely, a ferrite.

The Faraday magneto-optic effect * has been investigated in the microwave region by the use of ferrites as the optically active material (1, 2). (A Faraday switch has recently become available commercially (3).) The switch reported herein does not use the Faraday effect which depends upon magnetically induced anisotropic properties of materials. Instead, the electrical constants of ferrite materials are changed by the application of an external magnetic field. Miller (4) has applied this technique to suspensions of carbonyl iron powder in polystyrene. The use of ferrites instead of carbonyl iron is much more desirable, however, because of the relatively high loss of the carbonyl iron suspensions. More recently Reggia (5) has used the effect of magnetic fields on ferrites to control the attenuation in a coaxial transmission line.

The observations to be reported were made at 9430 Mc in standard X-band waveguide. The waveguide components consisted of a 2K25 klystron, an attenuator-strip load, a slotted section, and a tunable bolometer mount. Rectangular pieces of ferrite material were inserted into a section of waveguide to fill completely the waveguide cross section. No attempt was made to match the ferrite material into the waveguide.

An electromagnet of 6000 turns and 5000 ohms resistance provided the external magnetic field. Two coils, spaced one inch, were completely enclosed in a soft iron cylinder. Provision was made for the introduction into coils of either two cylindrical, soft iron pole pieces of 1 and 1/8-inch diameter or the waveguide section containing the ferrite. Three mutually orthogonal applied field directions were possible. The magnetic field could be oriented along the direction of waveguide propagation or in two directions in the plane of the waveguide cross section. These latter orientations were achieved by introducing the waveguide through rectangular holes cut for the waveguide cross section on a diameter of the coil casing cylinder. The transverse orientations were selected for the applied magnetic field to be either parallel or perpendicular to the waveguide E-field.

* This effect occurs with a material through which plane-polarized radiation passes when a magnetic field is applied to this material parallel to the direction of propagation of the radiation. Upon application of the magnetic field, rotation of the plane of polarization is observed.

The properties of the ferrite materials used in this investigation are summarized in Table 1:

TABLE 1
Properties of Ferrite Materials

Ferrite	μ_o	B_{sat} gauss	μ	ϵ
Steward F-6-23	13	600	0.27 - j 0.32	10.1 - j 1.27
Steward F-62-S	300	3500	0.64 - j 0.02	12.1 - j 0.84
SRI $NiOFe_2O_3$	3	--	0.44 - j 0.10	8.76 - j 0.36

The values quoted for μ and ϵ were obtained at 9430 Mc, using the method of measurement given by Birks (6). A laboratory Co-ferrite was also used, but no effect was observed upon application of a magnetic field.

The first magnetic field polarization attempted was in the longitudinal direction, that is, the direction paralleling the propagation. An effect for this orientation would correspond to the Faraday effect. With this polarization no significant change was observed in the transmission properties of the ferrites. However, in view of the large effect found for other magnetic field polarizations, it is believed that an effect may exist, although it is obscured because the flux density within the sample is much lower, relatively, than that for other magnetic polarizations. There are two reasons for this. In the case of a longitudinal field, the magnet pole pieces must be removed to allow insertion of the waveguide. This results in a considerable reduction in flux available to the sample. Further, for this polarization, the sample cross section is that of the waveguide, whereas for the other polarizations the cross section involves the much smaller sample thickness. A combination of these conditions causes a large reduction of the flux density available to the sample under longitudinal polarization.

More definite experimental results were obtained with the transverse polarizations. Consider the applied magnetic field parallel with the electric field. Figure 1 shows the effect on microwave transmission of varying the intensity of the magnetizing field applied to the two low-permeability ferrites. The sample lengths are almost equal. The general shape of the curves is almost identical and both indicate symmetry with magnetic field direction. One significant difference does occur, however. In the case of the laboratory Ni-ferrite a pronounced dispersion is observed. At approximately the same field strength an inflection occurs in the curve of the commercial ferrite F-62-S. It seems reasonable to attribute each of these deviations to an induced magnetic resonance—the Larmor precessional resonance. The point labeled 0 db is purely relative; the insertion loss is given on Figure 3. For purposes of reference, the flux density at 100 ma magnetizing current was measured to be 2×10^4 gauss.

The results produced when the same magnetic polarization was applied to the third ferrite are presented in Figure 2. The effect of changing sample thickness is illustrated. The increase in flux density in the sample resulting from a decrease in cross section appears of secondary importance to the effect of changing sample thickness. A comparison of these curves with those in Figure 1 will indicate that the results for the thicknesses used in Figure 1 will be quite comparable to those expected from the F-6-23 ferrite of similar thickness. From this it appears that the permeability of the medium seems to have little effect on the shape of the transmission curve.

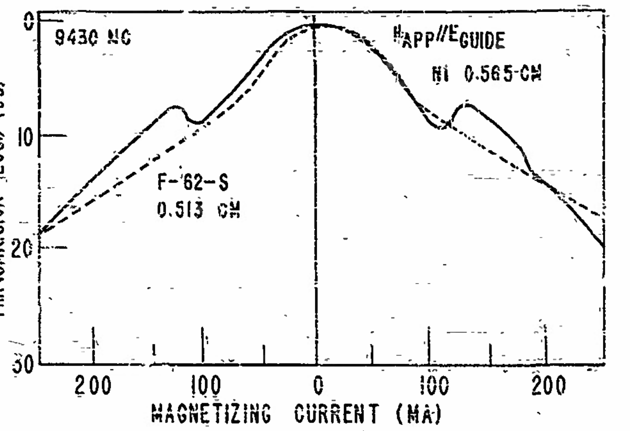

Figure 1 - Transmission of ferrites in transverse H-field—samples have nearly the same length

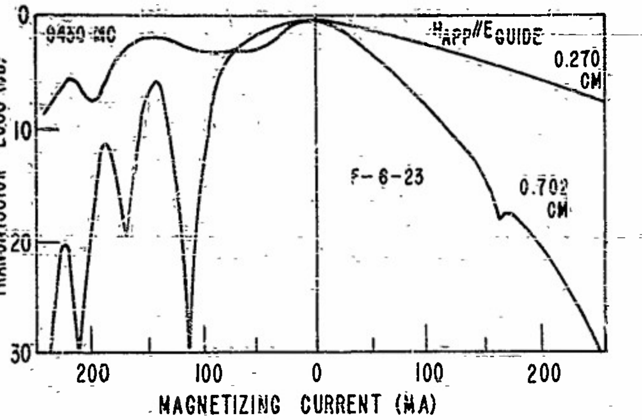

Figure 2 - Transmission of ferrites in transverse H-field—showing the effect of changing sample thickness

Of greater interest is the asymmetry of the transmission loss curve shown in Figure 2. One field direction appears to give quite normal results; the other shows pronounced absorptions superimposed on the general shape of the curve. No indication of the presence of these sharp responses has been found in reflection measurements of these materials. It must then be concluded that these are resonance absorptions. Since Larmor resonances cannot cause these particular responses, it is tentatively believed that these anomalies are explained by dimensional resonances similar to those reported by Brockman, Dowling, and Steneck (7). A displacement of the sample greater than a half wavelength had only slight influence on the transmission properties of the material. The magnetic history of the material seemed to have the most pronounced effect. This was evident from a change in the amplitude of the absorptions and also from an indication of absorption in the other half of the curve.

When the transverse magnetic field is rotated 90 degrees so that the field is now perpendicular to the waveguide E-field, a completely different effect is observed. Figure 3 presents these results. This field polarization indicates a transmission gain which increases with the applied magnetic field, as opposed to a transmission loss for the other polarization. Since these data are symmetric with field direction, only one direction is shown. The general form of these curves is that of a normal magnetization curve. A pronounced saturation is evident, in contrast to the results for the other polarization. The insertion loss of the sample without field is indicated on the appropriate curve. The high insertion losses should be expected since no effort has been made to match the samples into the waveguide. The effect of a change in thickness is also shown in this plot, the larger value for ferrite F-6-23 being associated with the thicker sample. The

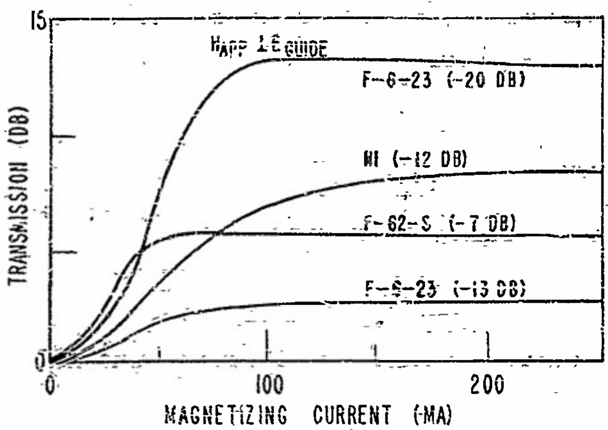

Figure 3 - Transmission of ferrites in transverse H-field–transverse magnetic field rotated 90 degrees

general shape of these curves is probably due to the effect of the steady magnetic field on the incremental permeability of the material. At saturation this value would be unity, and the magnetic behavior of the material then approaches that of free space. The dielectric properties of the ferrite must also be considered; they are responsible for deviations from free-space (loss-free) behavior.

The experimental results presented here were all taken on demagnetized samples and are analogous to normal magnetization curves. Hysteresis effects were evident, but for the sake of simplicity they have not been indicated in the data.

It must be emphasized that these are preliminary experimental results and interpretations. Further investigation will be conducted to determine reflection properties, electrical length (phase shift), the effects of alternating magnetic fields, and the suitability of other ferrite materials. Any general explanation of the behavior of ferrites under the influence of a magnetic field in waveguides which are propagating microwave radiation requires considerable investigation into the behavior of the field equations. Only recently has any work been done on this problem (8).

REFERENCES

(1). F. F. Roberts, "A Note on the Ferromagnetic Faraday Effect at Centimeter Wavelengths," J. de Physique et Le Radium, 12:305, March 1951

(2). C. L. Hogan, "The Ferromagnetic Faraday Effect at Microwave Frequencies and its Applications - the Microwave Gyrator". Bell Syst. Tech. J. 31:1, January 1952

(3). C. H. Luhrs Co., 297 Hudson St., Hackensack, N. J.

(4). T. Miller, "Magnetically Controlled Waveguide Attenuators," J. Appl. Phys., 20:878, September 1949

(5). F. Reggia, "Nat. Bur. Stand. Magnetic Attenuator," Nat. Bur. Stand. Tech. News Bulletin, 35:109, August 1951

(6). J. B. Birks, "The Measurement of the Permeability of Low-Conductivity Ferromagnetic Materials at Centimeter Wavelengths," Proc. Phys. Soc. London, 60:282, 1948

(7). F. G. Brockman, P. H. Dowling, and W. G. Steneck, "Dimensional Effects Resulting from a High Dielectric Constant Found in a Ferromagnetic Ferrite," Phys. Rev., 77:85, January 1950

(8). A. A. Th. M. van Trier, "Anomalous Wavetypes in Waveguides Containing Ferromagnetics," Bulletin Am. Phys. Soc., 27: No. 3, 31, May 1, 1952

DISCUSSION

Wilkes: (APL) Could you give the chemical formula for the ferrites used?

Anderson: (SRI) $NiOFeO_2$

Wilkes: With the nickel, that would correspond to Fe_2O_3.

Anderson: That is correct.

Rado: (NRL) In regard to the question of anisotropy, there are two related effects present. In one case you are dealing with an artificially produced anisotropy due to the external dc field, which is strong enough in some cases to overcome external anisotropy. In the cases which you have discussed, it is possible that the internal anisotropy is the stronger. Many of these difficulties arise from the fact that the waveguide problem has not yet been solved—unless Dr. Kales has solved them in the meantime. Because of the dimensional resonances it is difficult to interpret the data which you have when the dc field is at right angles to the ac magnetic field. This is a difficulty which exists over and above the mode properties. In the case of your second experiment in which the dc field was parallel to the ac field, you are probably saturating the material; in which case the incremental premeability is reduced, and consequently the losses are reduced and the transmission increased. The loss which is left will be determined entirely by the dielectric constant.

Anderson: Those were my impressions exactly.

Sakiotis: (NRL) May I ask why you expected symmetry in the asymmetrical curves?

Anderson: I do not believe you should expect an appreciable asymmetry in regard to the resonance points; there is no change in the E-vector.

Sakiotis: Chait has shown previously that when we reverse the axial field we get a different effect. I would expect that effect for all cases in which the r-f H-field and the dc H-field are crossed.

Anderson: But your effect depends on which index—either right or left hand—is affected.

Sakiotis: No. Using the same sense of polarization and reversing the field, you can get a different effect. In regard to these resonances, the absorption of the ferrite should not be blamed for all of the loss. It is possible that one can match into the ferrite but not match out of it. This means that you will see a low standing-wave ratio, but your loss may be reflected loss.

X-BAND LOW-LEVEL SWITCHES FOR HIGH-SPEED LOBING ANTENNAS

H. W. Lance
Bureau of Standards, Corona, California

INTRODUCTION

It is the purpose of this paper to describe the work done by and also that sponsored by the Missile Development Division of the National Bureau of Standards on X-band and low-level electronic switches suitable for use in high-speed antenna lobing. The three types of switches considered in this paper are shown in Figure 1.

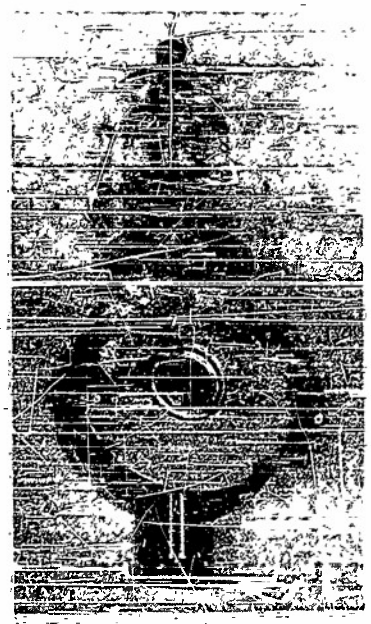

X7047

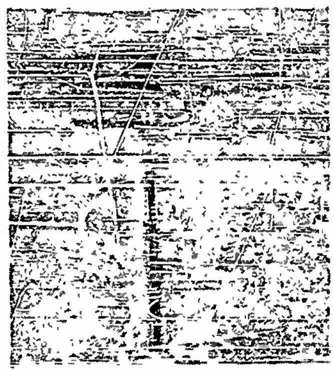

Gas discharge tube X208A
Waveguide Section

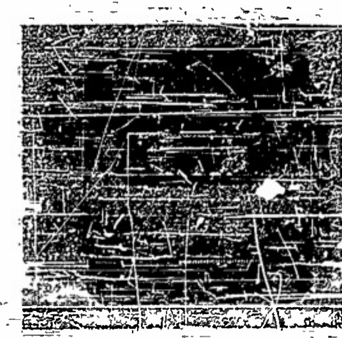

Polarization switch

Figure 1 - X-band low-level switches

The first of these is the X7047 combination switch and TR tube. This tube is the outgrowth of a suggestion made by MIT in 1945 and followed up by the Naval Research Laboratory(1). The suggestion was that a 1B24 TR tube might be modified by increasing the interaction of the keep-alive electrode with the electromagnetic field in the cavity so that it could be used also as a microwave switch. Soon after this proposal, a tube was made by Sylvania which demonstrated the feasibility of the idea. During the last few years, the National Bureau of Standards has sponsored and actively participated in developmental work on the tube. This work, together with the specifications which have been set up for the tube and the performance which has been obtained to date, are described briefly. In addition, a brief discussion is given of a radar in which the X7047 is used for antenna lobing.

Because of difficulties encountered in the development of the X7047 and because of a desire to have a tube which would operate over a greater bandwidth, work was started on the X208A. The initial work on this tube was done by Federal Telecommunication Laboratories, and it is now undergoing further development in the NBS Tube Laboratory. This is a switch only; where TR action is required, it must be obtained by a separate tube.

The third type is the polarization switch, in which the switching action is produced by means of a magnetized ferrite core. Several other laboratories are known to be interested in and working on this type of switch, and consequently a short summary of the results obtained by NBS to date are included.

THE X7047 COMBINATION TR AND SWITCH TUBE

After preliminary work had been done on this tube, a specification was drawn up incorporating the performance features which were considered to be both desirable and possible (2). Briefly, the requirements are that the tube must have a low insertion loss, a high attenuation (due primarily to reflection rather than to absorption) when switched, a low power requirement for switching, and other characteristics appropriate to good TR action, such as a short recovery time. Representative requirements, from the specification, are given in Table 1.

TABLE 1
Principal Performance Requirements of X7047

Frequency Range: 8490-9600 Mc (tunable)
Loaded Q: 350
Insertion Loss: 0.85-1.50 db
Attenuator Voltage -200 to -450 V
Attenuator Current: 0.75 ma
Attenuation at 0.75 ma: 35 db min.
Recovery time: 3 μsec max. (to within 3 db transmission)
Leakage Power (as TR): 30 mw max.
Transmitter Power: 100 kw max.
Life: 100 hr min.

(Insertion loss, recovery time, and attenuation limits at end of life: 2 db, 4 μsec, and 30 db respectively.)

Under development contracts at both Sylvania Electric Co. (3) and Bomac Laboratories (4), numerous variations in construction, fill, and processing were tried; and a few tubes were produced which fulfilled all of the requirements. However, most of them have been deficient in some respect. The most persistent shortcoming has been failure to meet the attenuation and recovery time requirements for a period of 100 hours. This is caused primarily by the interaction of the tube electrodes with the fill gas during the discharge. This interaction has two effects. First, it changes the composition of the fill and ordinarily results in decreased attenuation and longer recovery time. Second, it causes the formation of a deposit on the cathode which alters the impedance characteristics.

Up to June 1949, this deposit frequently was of a conducting nature and short-circuited the attenuator electrode (cathode) to the surrounding copper cone. About this time, a study of the problem was undertaken by the NBS Tube Laboratory (5). It was found that the deterioration of the cathode was enhanced by glow to arc transitions of the discharge, during which small bits of the cathode were melted and oxidized. Further study showed that this effect was much less prevalent when the cathode was made of 18-8 stainless steel instead of kovar, as was then the case.

The suggested change in cathode material was made, and the occurrence of short circuits was almost completely eliminated. However, another difficulty due to the formation of cathode deposits was encountered. In this case, the cathode was found to be partly covered with a nonconducting deposit which limited its effective area and forced the discharge farther into the abnormal glow region, thus increasing the potential difference required to maintain a fixed current in the tube. In extreme cases, the discharge could not be initiated by the available voltage. Recently this trouble has largely disappeared, due presumably to small dimensional and processing changes which have inhibited the formation of the cathode deposit.

The NBS Tube Laboratory is continuing work on the fundamentals of this problem, and in addition is studying the effectiveness of various parts of the glow discharge in producing attenuation, including attempts to determine electron temperature and density in the discharge by probe measurement techniques. This work is expected to contribute to better performance of future tubes. Meanwhile it is important to summarize the performance which is currently being obtained.

Tests on recent tubes have been made at both room temperature (25° C) and at higher temperatures typical of those encountered when operating the tubes in an enclosed space crowded with other electronic components (85° C, for example). Test results on tubes from two different production lots are shown in Figures 2 and 3. Both sets of curves have been included to show not only typical performance but typical variations from lot to lot. From the figures it is seen that during 100 hours of operation the attenuation may drop below 30 db, the insertion loss may exceed 2 db, and in some tubes the recovery time goes quite a bit above 4 microseconds.

Concerning the effect of ambient temperature, it is difficult to generalize from the data presented; but on the average, operation at elevated temperatures causes lower attenuation, shorter recovery time, and possibly a higher insertion loss.

It should be noted here that recovery time may be decreased by the application of a positive bias (25 to 100 v) to the attenuator electrode. However, operation in this manner is not a part of the specification, and in some tubes it is erratic. On recent tubes the keep-alive electrode has been eliminated, since it has been found that residual ionization from the switching process, at least if the tubes are switched at a frequency of 1000 cps or above, provides adequate keep-alive action.

Complete details on the X7047 are available in the form of numerous NBS memoranda and reports and contractors' reports.

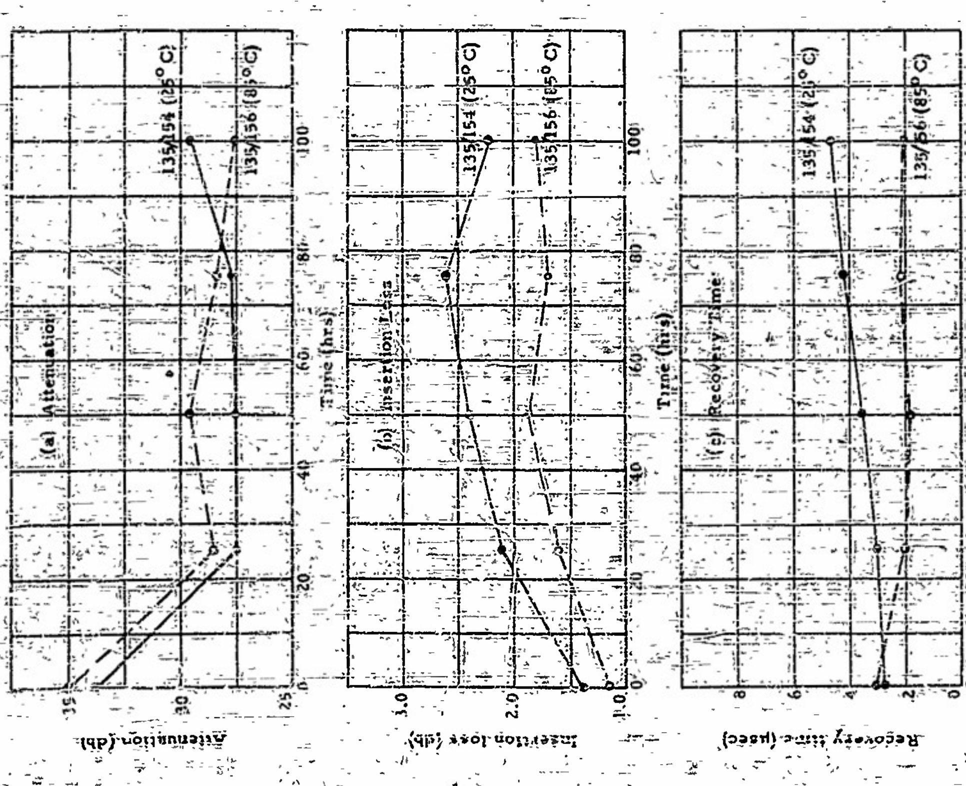

Figure 2 - X7047 (Series 135) typical performance

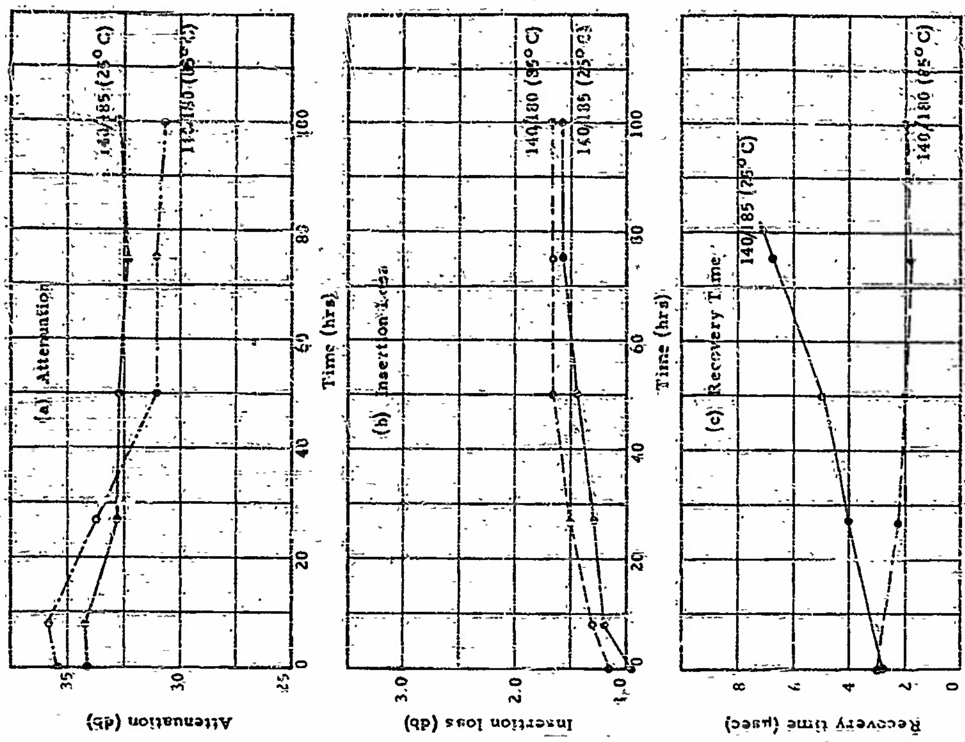

Figure 3 - X7047 (Series 140) typical performance

It should be mentioned in concluding the discussion of the X7047 that on a recent trip to England a survey of British TR and switch tube development yielded no information that a tube which will outperform the X7047 existed. However, two means of possible future improvement were suggested: that of separating the TR and switching functions so that each may undergo optimum development independently, as is already being done in the X203A, described in the following section; and that of utilizing a hard-soldered, gold-plated cavity with an active gas fill. This, it is felt, would almost certainly result in an improvement, but it would be a major developmental task.

A radar system in which the X7047 is used to produce high-speed lobing of the antenna has been developed by the NBS Missile Development Division. The microwave portion of this radar is shown schematically in Figure 4. As may be seen from the figure, the magnetron power output is divided into two equal parts and goes through separate duplexers to the antenna feeds. Both X 7047 tubes are fired by the magnetron pulse and then behave as ordinary TR tubes. Since the two feeds are disposed symmetrically to the left and right of the antenna focus, the transmitted power is beamed straight ahead.

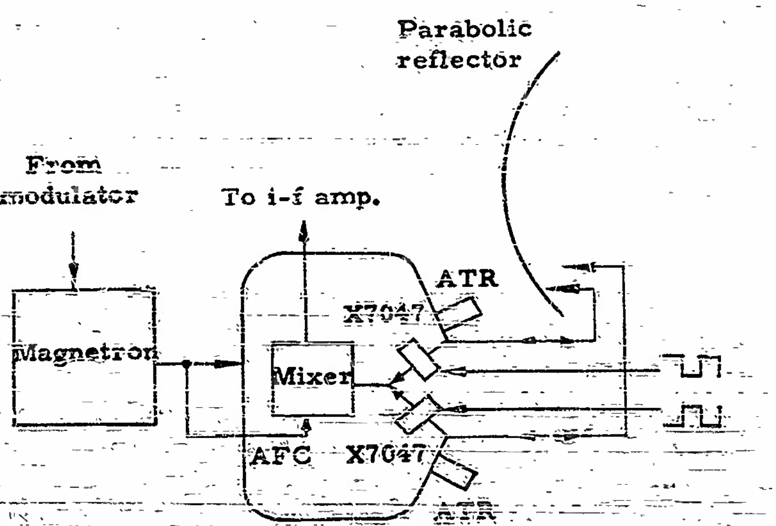

Figure 4 - Radar with high-speed lobing antenna

Since the X7047 tubes are fired by out-of-phase square-wave switching voltages, consecutive radar echoes are received alternately through the two feeds. Thus, the receiving beams are offset, corresponding to the displacement of the feeds from the focus of the paraboloid. The tubes, when switched, appear as short circuits across the wave-guide, and the position of the shorts is chosen so that good impedance matching is accomplished for the received signal.

For the normally used beam separations, the two antenna feeds must be placed rather close together, and the mutual feed coupling which results from this proximity may affect the shape of the antenna pattern. This is true because the signal received by the unused feed is reflected by the fired switch tube and may be coupled into the other feed on reradiation. This coupling may be reduced to a negligible value by a choke or a resistive strip placed between the two feeds. With the choke, an isolation of well over 30 db has been obtained over narrow frequency ranges; and with the resistive strip, between 25 and 30 db has been obtained over a 12-percent band.

The firing threshold of the X7047 is approximately equal to its leakage power as a TR tube, about 30 mw. Accordingly, it is not useful for high-level switching.

A switching frequency of 1000 cps has been used extensively. The maximum switching frequency and the possible effect on tube life of increased switching frequency has not been investigated carefully. In another application the tube has been used to modulate a microwave signal with modulation frequencies as high as 1 megacycle. At this frequency, however, the modulation percentage is limited by the recovery time of the tube. In any event, it appears that the highest switching frequencies likely to be encountered in radar practice may be used.

THE X208A SWITCH TUBE

Due partly to the difficulties encountered with the X7047 and partly to the desire for a tube which would operate without adjustment over a wider range of frequencies, NBS initiated in 1949 a switch-tube development contract with Federal Telecommunication Laboratories. Because the current required for a given attenuation increases with the bandwidth of the tube, a different scheme of switching had to be devised in order to obtain the required attenuation with the power which was available for switching. Since directional information from the antenna is needed only from targets at a selected range, it is sufficient to fire the switch tube only at times corresponding to the range of the desired target. Thus the switch need be on only for intervals slightly longer than the radar pulse.

Two switch tubes designed for pulsed operation were brought to the early developmental stage by FTL. One of these, the X208B, consists of a 1B63A TR tube in which the pair of cones not used for keep-alive action is pulsed with a dc discharge to produce attenuation. Although this tube demonstrated successfully the principles involved, it appeared to be more complicated and of less immediate interest than the other tube, and no further work has been done on it.

The second tube is the X208A which is a switch only and has no TR action. It is believed that the practice of separating the switching action from the TR action is a sound one, since the characteristics of each tube may then be fully utilized for the function it is required to perform. As shown in Figure 1, the waveguide structure and the gas discharge tube of the X208A are entirely separate, thus reducing the cost of manufacture and facilitating replacement. This tube was likewise carried to the early developmental stage by FTL. Typical performance of this tube is given in Table 2.

TABLE 2
X208A Switch Tube
Pulsed Operation - Typical Conditions

Peak Pulse Voltage: 2000 volts
Peak Pulse Current: 2 amp
Pulse Duration: 1 μsec
Repetition Rate: 1000 cps
Insertion Loss: <0.5 db
Attenuation: >30 db
Bandwidth: 8500 - 9600 Mc (for VSWR <2)
Fired VSWR: >20

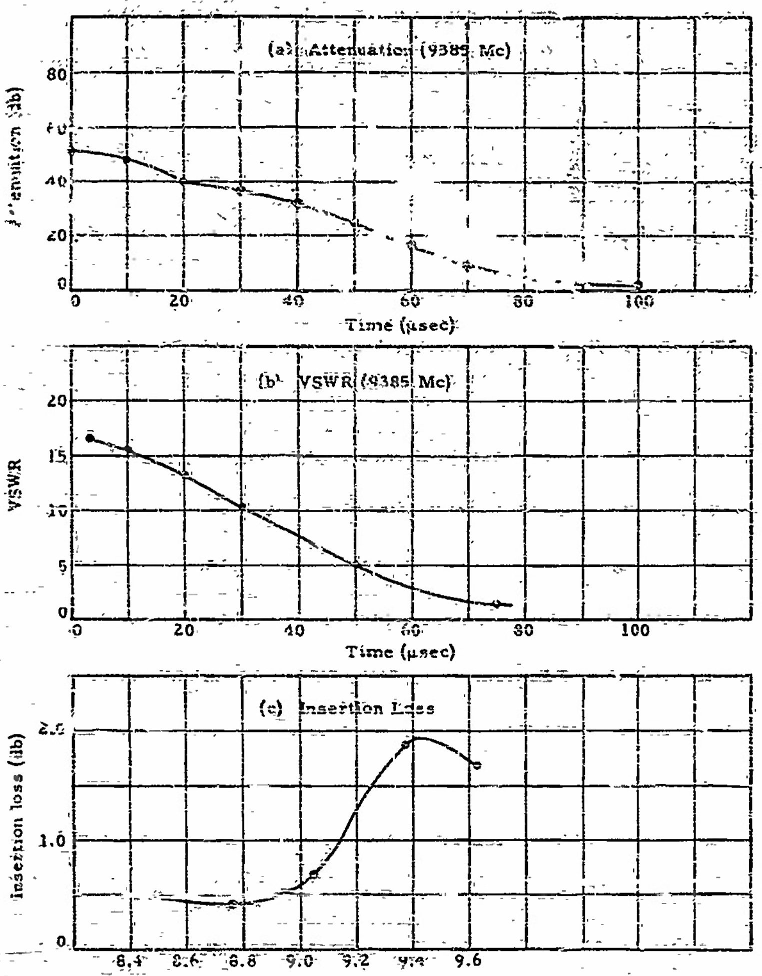

Figure 5 - X208A typical characteristics

Since there is no requirement for TR action, the tube is filled with pure xenon, thus giving it a long recovery time. In operation it is fired with a pulse of rather short duration; the period of high attenuation then persists for ten or more microseconds. This is demonstrated in Figure 5 where the attenuation and VSWR are shown as a function of the time elapsed since the firing pulse. The insertion loss over the 12-percent band is also given. This developmental tube had approximately the required initial characteristics, but it had a life of 30 hours or less. In fairness to FTL, however, it should be pointed out that the tube was produced at the very end of the contract, and adequate time for the improvement of its performance was not available. It is now undergoing further development in the NBS Tube Laboraotry where an attempt is being made to increase its life and possibly to improve some of its other characteristics.

POLARIZATION SWITCH

About a year ago our attention was called to a development by C. H. Luhrs (6) in which the microwave Faraday effect was used to produce a low-power X-band switch. This phenomenon is described by Beljers and Snoek (7) and by Hogan (8).

The simplest method of operating this switch is probably with a square-wave switching voltage, as is used for the X7047. However, it was desired to investigate the possibility of using it as a pulse-type switch. The original Luhrs switch had a response time of about 10^{-3} second, making it unsuitable for such operation. Studies at NBS by B. C. Wood (9) resulted in a switch which has a response time of about 3×10^{-7} second, which is probably faster than is required for antenna lobing. The response of the Luhrs switch was limited by eddy currents in the brass tube forming the circular waveguide section which acts as a shorted turn secondary for the driving coil. This was avoided in the NBS switch by use of a plastic tube covered with a thin conductive coating to form the waveguide wall. For maximum switching speed it is desirable to use a coating of as high a resistivity as is consistent with the allowable insertion loss.

A sketch of the switch is shown in Figure 6. Figure 7 shows the experimental pulser which was used in the development of the switch; and Figure 8 shows the pertinent voltage,

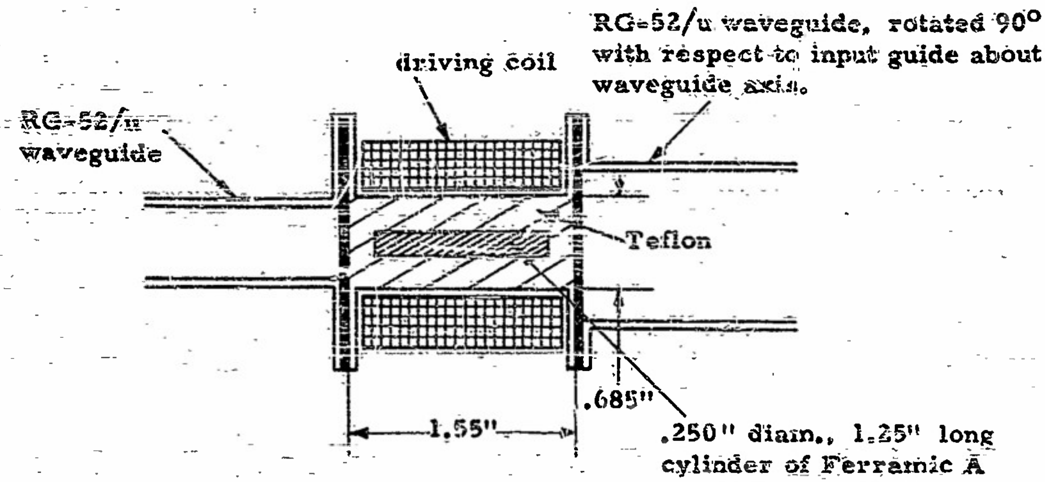

Figure 6 - Polarization switch

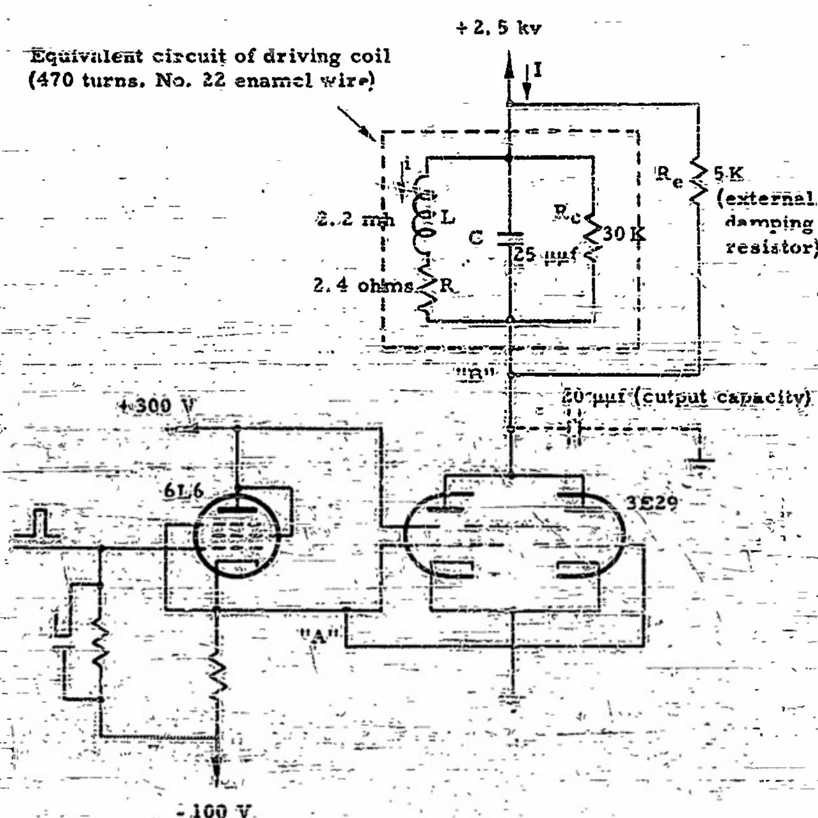

Figure 7 - Experimental pulser for polarization switch

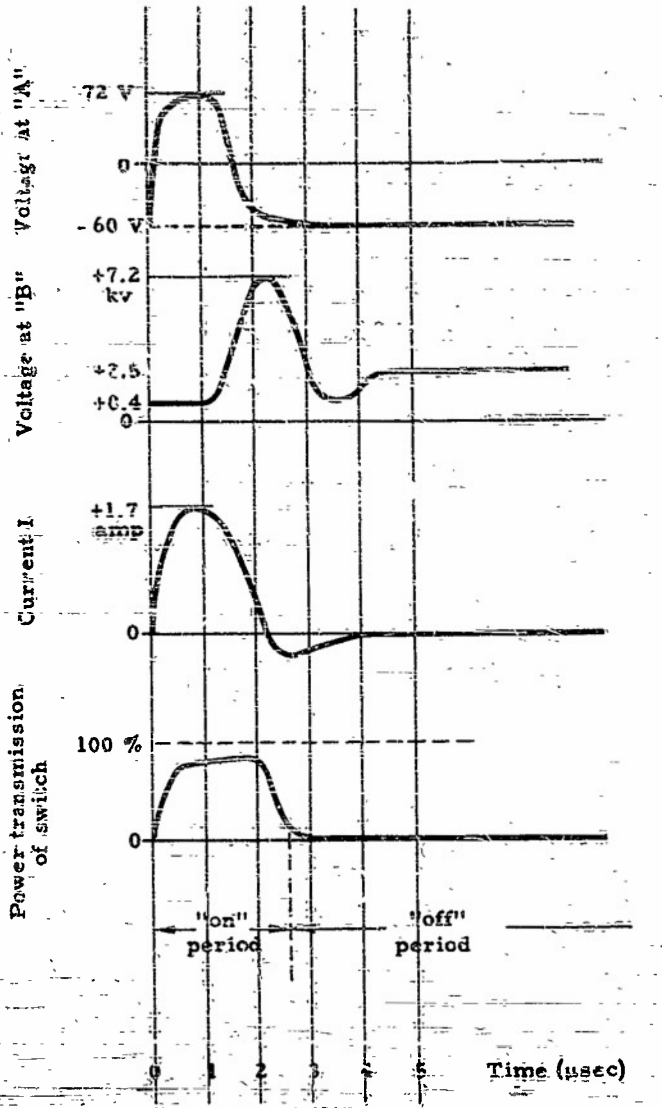

Figure 8 - Waveforms for polarization switch

current, and power waveforms. A small reverse current following the main pulse was necessary to demagnetize the ferrite material. In operation, with the switch between crossed guides, the correct amount of reverse current was determined by adjusting R_e of Figure 7 for minimum microwave transmission during the "off" period. Insertion loss of 0.8 db during the "on" period and attenuation of about 40 db during the off period were obtained. The input VSWR during the "on" period was less than 1.4 over a 5-percent band.

When the polarization switch is used at a Y-junction as in Figure 5, the minimum obtainable distance of the reflection point from the junction is about 1.2 wavelengths. This, of course, restricts the useful bandwidth of the system. The principal advantage to be gained by the use of a switch of this type for antenna lobing is the almost indefinite life which should be obtained.

This work has been done in connection with guided missile development for the Navy Bureau of Ordnance. The material on the radar system is confidential, the X7047 and X208A are restricted, and the polarization switch is unclassified.

REFERENCES

1. Sakiotis, N. G., Simmons, A. J., and Chait, H. N., Application of Ferrites to the Microwave Antenna Problem, NRL reprint, Jaunary 1952

2. Bureau of Ships Tentative Specification for Tube Type X7047 (TR and Low Level Attenuator), January 30, 1948

3. BuShips contract CS-1062 w/Sylvania Electric Co.

4. NBS contracts Cst 10218 and Cst 158 with Bomac Laboratories

5. French, Judson, C., Electrode Deterioration in TR-Type Tubes, NBS Report 13.2-50R, October 24, 1949

6. Luhrs, C. H., and Co., Hackensack, N. J., manufacturer of polarization switches.

7. Beljers, H. G., and Snoek, J. L., Gyromagnetic Phenomena Occurring within Ferrites, Phillips Tech-Rev., pp. 313-322, May 1950

8. Hogan, C. L., The Microwave Gyrator, B.S.T.J., pp. 1-31, January 1952

9. Wood, B. C., Application of Ferrites to Microwave Switching, NBS Report 15.3-74R in preparation

UNIFORM COVERAGE FOR VOLUME SCAN*

Hubert R. Shaw
North American Aviation, Inc.

If we wish to search a large volume of space with a radar beam of relatively small diameter, some orderly method of scanning the space is necessary. Many different scanning patterns are theoretically possible. However, the choice is limited first by the desire for reasonable efficiency of time and secondly by mechanical considerations.

One scanning method which has been frequently employed is the so-called "Palmer" or conical scan in which the radar beam is rotated rapidly in a circle and simultaneously moved slowly in a horizontal direction to produce a spiral. The resulting scan pattern is capable of almost infinite variation as the amplitude and pitch of the spiral are varied.

Another scanning method is the sine scan in which the radar beam is moved rapidly up and down with sinusoidal motion and simultaneously moved slowly in a horizontal direction.

It is the purpose of this paper to illustrate a number of these scan patterns and to present a new scan pattern which has significant advantages.

Figure 1 shows three conical scan patterns. A 2 to 1 pattern is shown in (a); it is so designated because the path of the spiral passes two beamwidths to the right and back one beamwidth per cycle as shown by the heavy line. Illustration (b) is designated a 3 to 1 pattern because the spiral passes three beamwidths to the right and back one, while (c) is designated a 3 to 2 pattern for a similar reason.

It may be of interest to note that spirals of this type are completely defined by the distance over and the distance back per cycle; that is, the diameter of the circle from which the spiral is derived is equal to one-half the distance over plus one-half the distance back.

In (d), (e), and (f) are shown the areas covered by the radar beam for each of the patterns above. These figures are obtained by moving a beam circle along the axis of the spiral. The darker areas indicate multiple coverage; the darker the area, the more times the beam circle passes over that area.

In all of these figures, it is assumed that a number of radar pulses occur during the time the beam moves one beamwidth so that the beam may be correctly considered to cover a swath whose width is equal to the diameter of the beam.

The 2-1 and 3-2 patterns appear useable as is, while the 3-1 pattern would require modification to close up the holes in the pattern before it could be used. Modification would consist of reducing the diameter of the small loop to eliminate the hole in the center and overlapping the pattern somewhat in the center to eliminate the hole in the center of the pattern.

*Presented by Virgil A. Counter, NAA

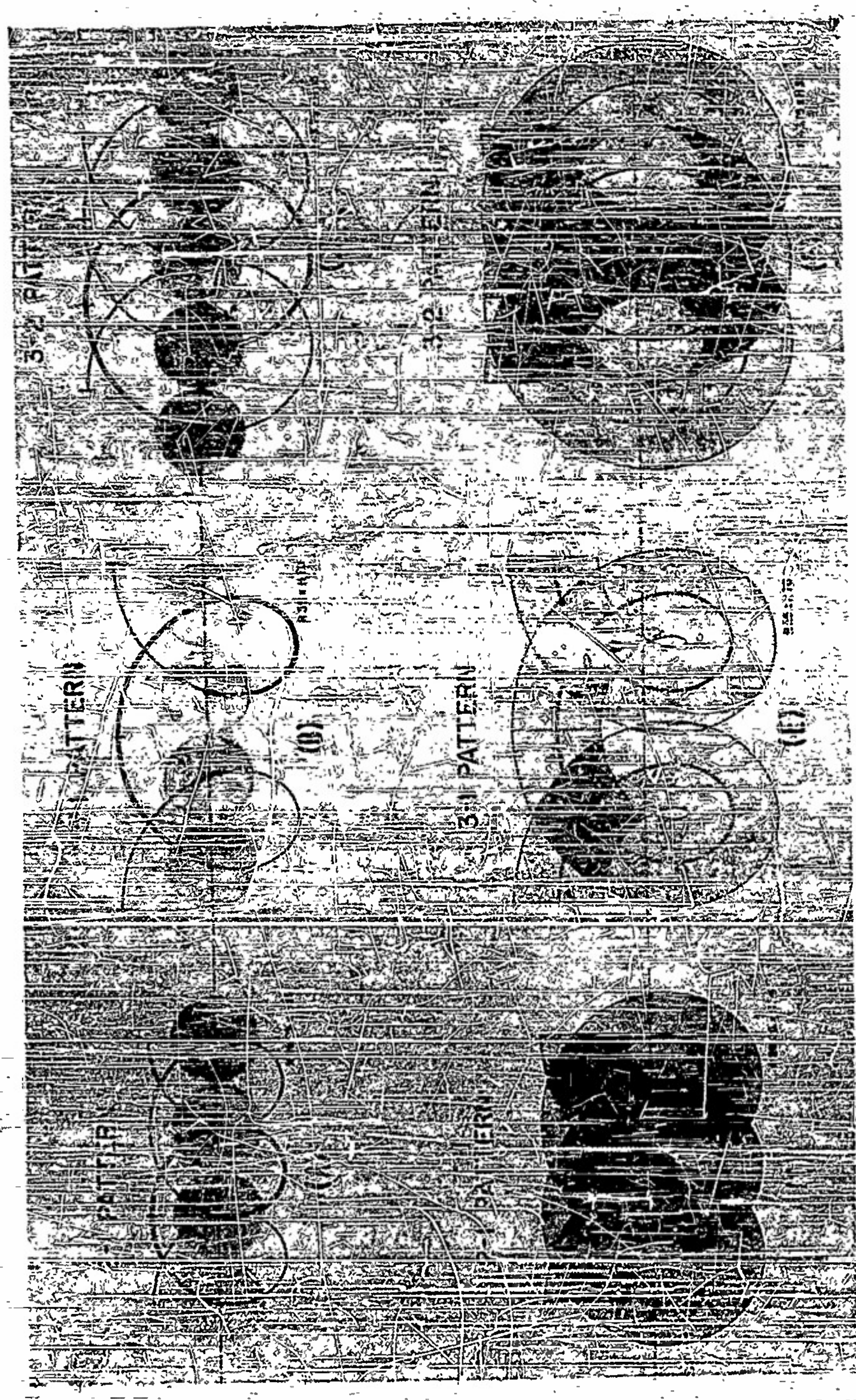

Figure 1 - Conical scan patterns

Figure 2 shows another set of patterns; this time in the "4" series. In (a) and (d) are shown 4-1 patterns; that is, over four beamwidths and back one. Patterns (b) and (e) are over four and back two, and patterns (c) and (f) are over four and back three. It is apparent that the only one of these patterns which is useful is the 4-3 pattern since the other two leave wide areas of no coverage.

Figure 3 shows the only pattern which is useful in the "5" series. Both of the patterns shown are 5-3 patterns. In one case the beam circles along the axis just touching each other, and in the other case the beams overlap by a half beamwidth. Pattern (b) appears usable as is, while pattern (a) again would require modification to close up the holes.

Figure 4 includes all the usable patterns in the 2, 3, 4, and 5 series, modified wherever necessary to close up any holes which may have been present in the original pattern. Dimensions have been added.

An exact evaluation of these patterns is extremely difficult because of the many factors involved. In general, it may be said that the greater the height of the swath the better, because fewer swaths are then necessary to cover a given number of elevation degrees. Also, the less the overlapping the better because overlapping represents excessive coverage of those areas which increases the time required to cover a given volume of space. In evaluating these patterns for the extent of overlap, only the central section should be considered. The right and left sides of the pattern indicate the coverage only at the beginning and end of the swath.

Another method of area scan, sine scan, is shown in Figure 5. With this method, the radar beam is moved rapidly up and down sinusoidally in elevation while it is moved slowly in a horizontal direction, thus producing the pattern as shown. Sine scan has several advantages: it is considerably easier to mechanize since the antenna dish is required to move only in one plane; also, as you see, the coverage is quite uniform. To provide a margin of safety, there is deliberate overlapping of adjacent cycles; aside from this deliberate overlapping, the areas of multiple coverage are quite small.

Both conical scan and sine scan suffer somewhat from the fact that the angular velocity of the beam varies over the cycle. Thus, the number of radar pulses which occur during the time the beam is changing position by one beamwidth is different at different parts of the cycle. In Figure 6, for example, is a case in which 50 radar pulses occur per scan cycle. The distribution of these pulses over the cycle is shown by the dots. Note that in this particular case a target on the scan axis and near the center of the swath would receive 5 hits and return 5 echoes while the radar beam is traveling one beamwidth. Now note that a target on the crest of the cycle would receive 13 hits and return 13 echoes while the radar beam is traveling one beamwidth.

By way of comparison, if a perfectly linear triangular wave (Figure 7) could be used for scanning, again with 50 pulses per cycle, 8 hits and echoes would occur during the time the beam is traveling one beamwidth at any point in the cycle.

Such a wave form can be approximated quite well be adding a small amount of 3rd harmonic to the fundamental sine scan with the waveforms additive at 90°.

As shown in Figure 8, the addition of 6 percent 3rd harmonic produces a waveform which has almost perfect linearity for the first 60° of the cycle, and the addition of 10 percent 3rd harmonic produces a waveform which is substantially linear for all but the last 10° of the cycle.

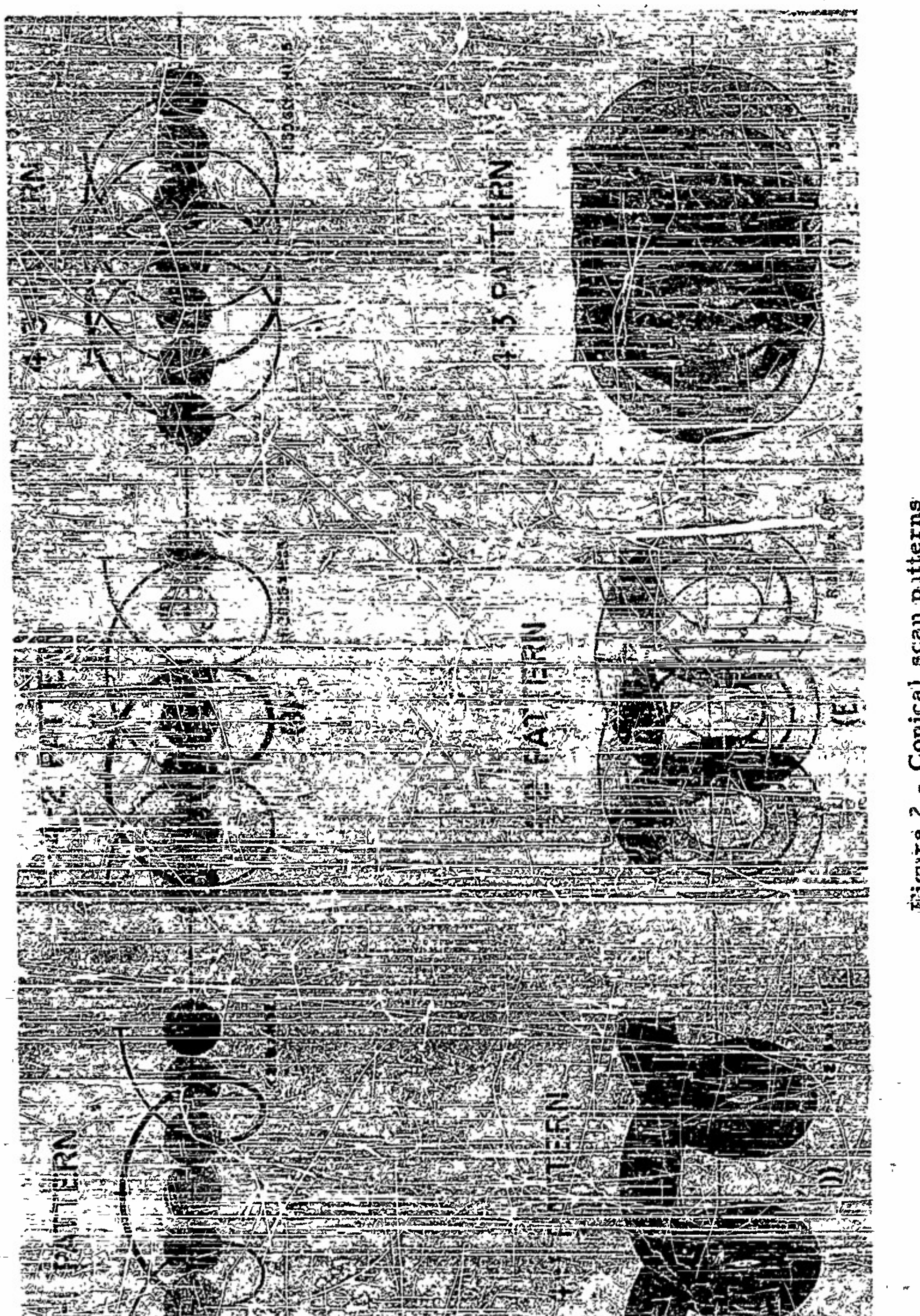

Figure 2 - Conical scan patterns

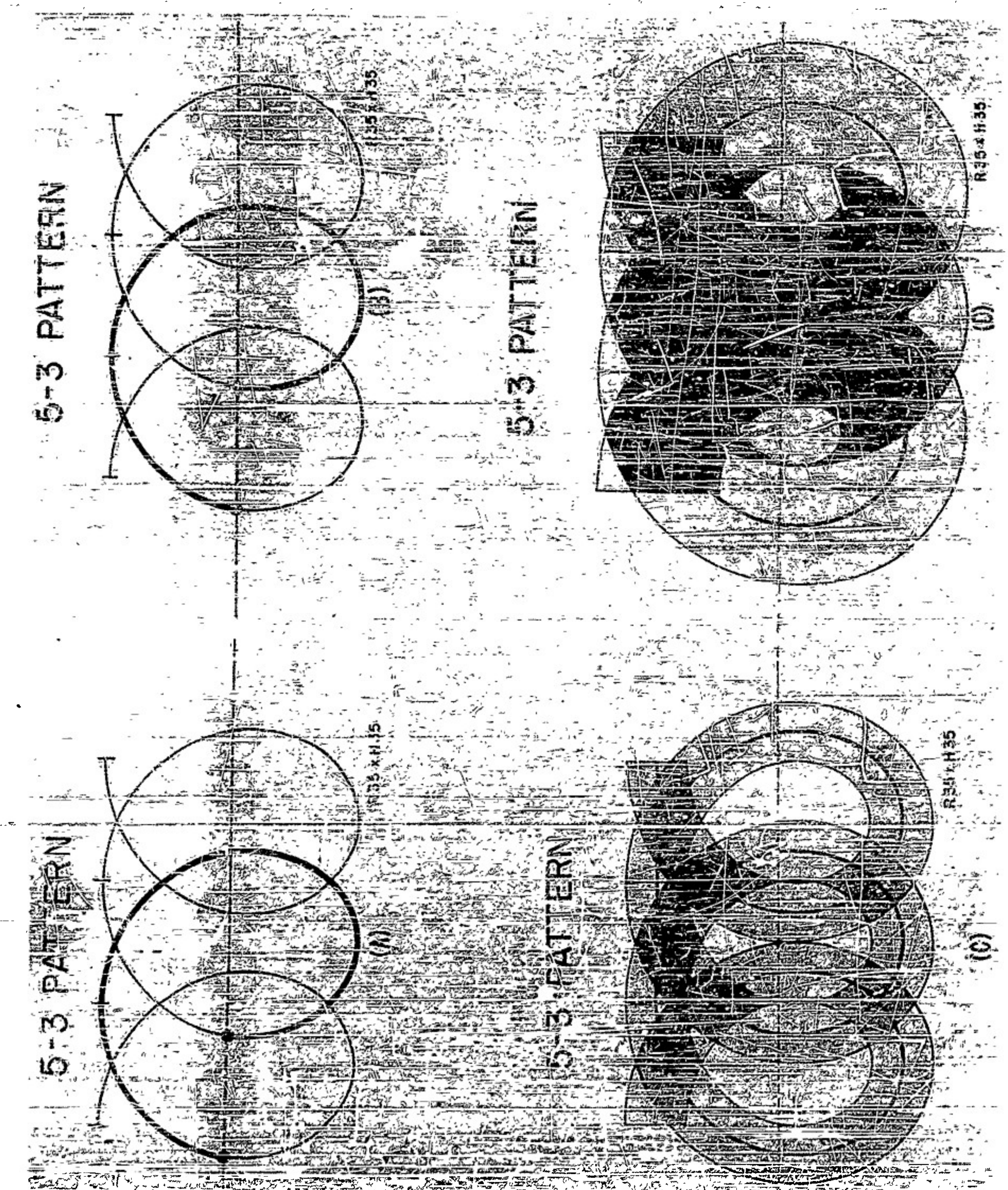

Figure 3 - Conical scan patterns

Figure 4 - Conical scan patterns

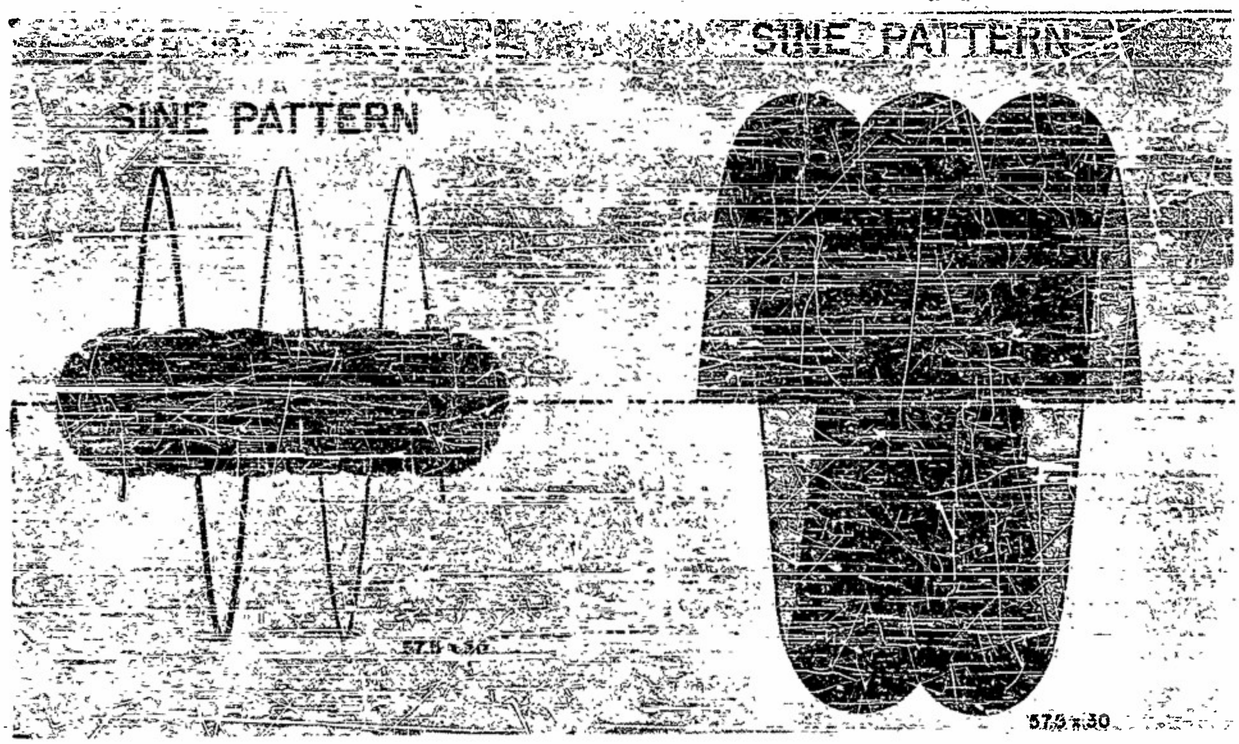

Figure 5 - Sine scan

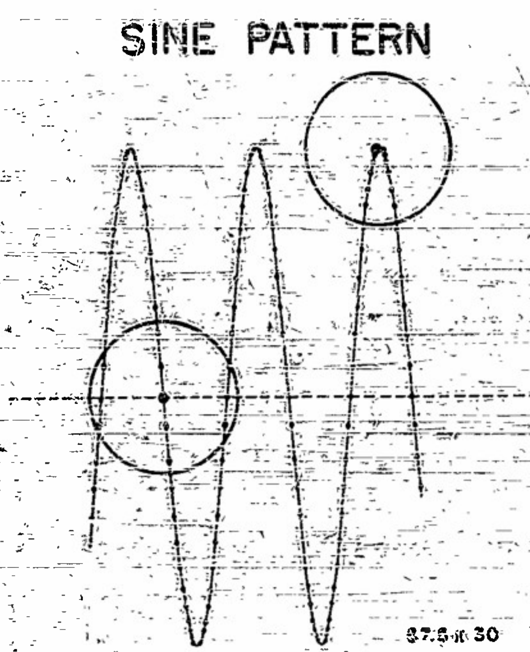

Figure 6 - Sine pattern showing distribution of pulses

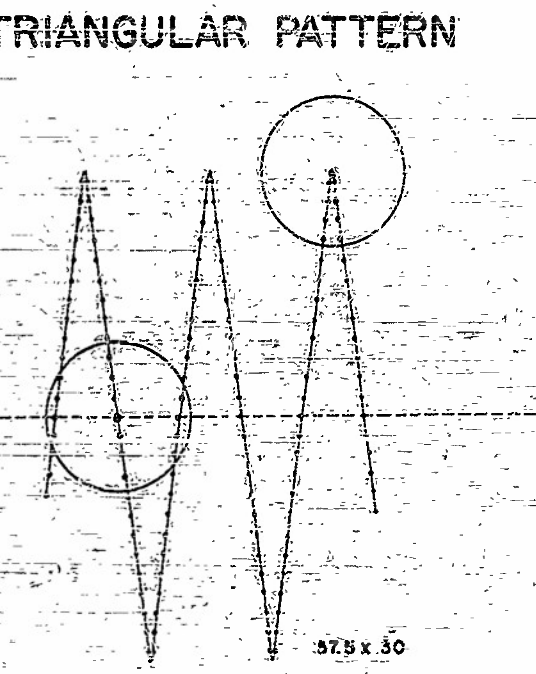

Figure 7 - Triangular wave pattern showing distribution of pulses

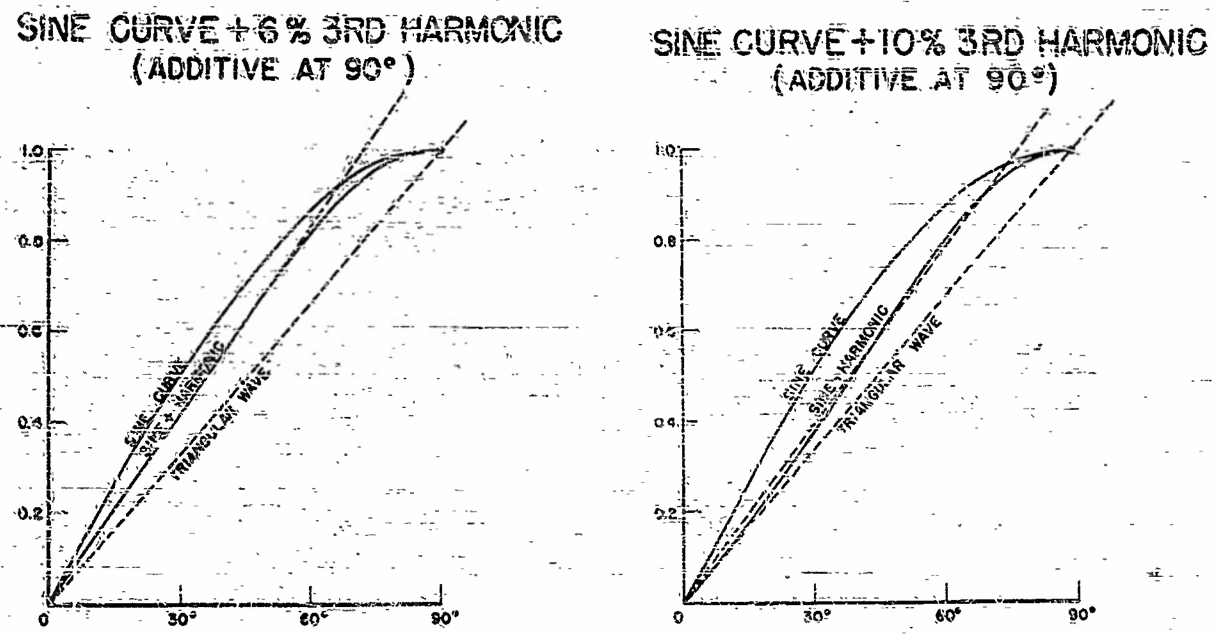

Figure 8 - Approximations to triangular wave

Figure 9 is a comparison between sine scan and sine plus 10 percent 3rd harmonic scan. The number of hits and echoes on a target located on the axis of the triangular scan during the time the beam is traveling one beamwidth is 7. Since the distribution of pulses is now nearly linear over most of the cycle, this same condition of 7 echoes also applies over most of the cycle. At the crest of the cycle, the number of hits and echoes on a target is only 10. These figures of 7 and 10 echoes for triangular scan may be compared with the figures of 5 and 13 echoes for sine scan.

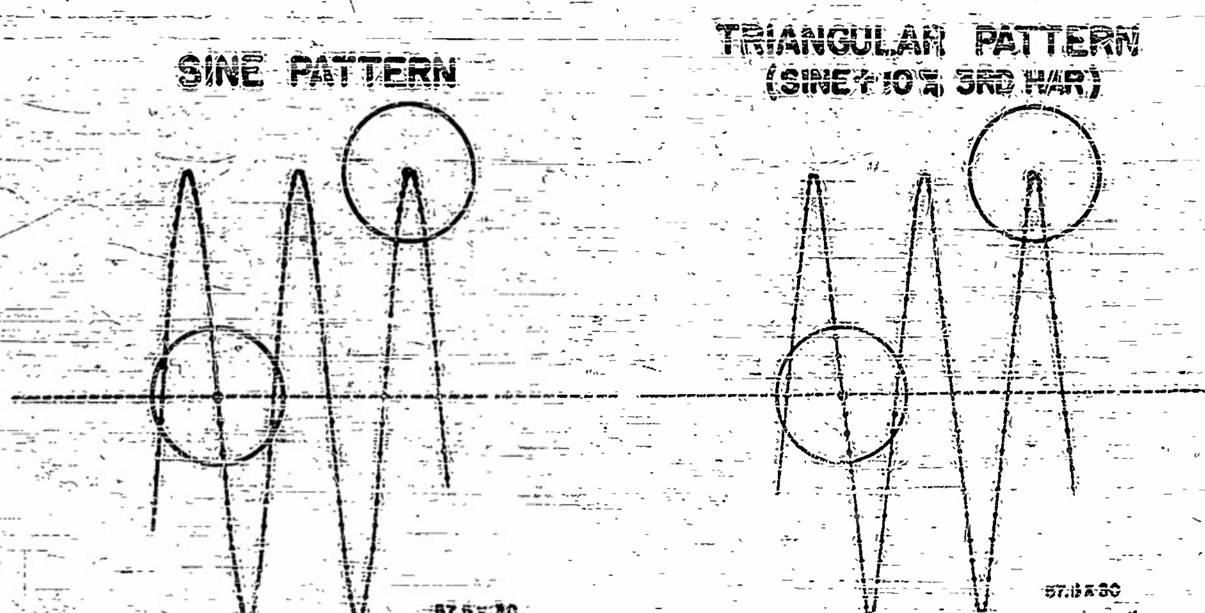

Figure 9 - Comparison of sine and triangular scan patterns

For long range service, a relatively low PRF is required; and regardless of what kind of scan is used, the scan frequency must be adjusted to yield at least one echo during the time the beam is traveling one beamwidth at any part of the cycle. Figure 10 is a sine scan pattern in which the scan frequency is too high, and large areas are not covered.

Figure 11 is a 3rd harmonic triangular scan pattern plotted under conditions identical with those in Figure 10; that is, the same PRF, the same range, and the same scan amplitude and frequency are used. Note that the triangular scan gives complete coverage with the exception of several negligibly small holes.

The mechanization of 3rd harmonic triangular scan appears to be quite practical even though the accelerations are approximately 2 to 1 higher than for sine scan.

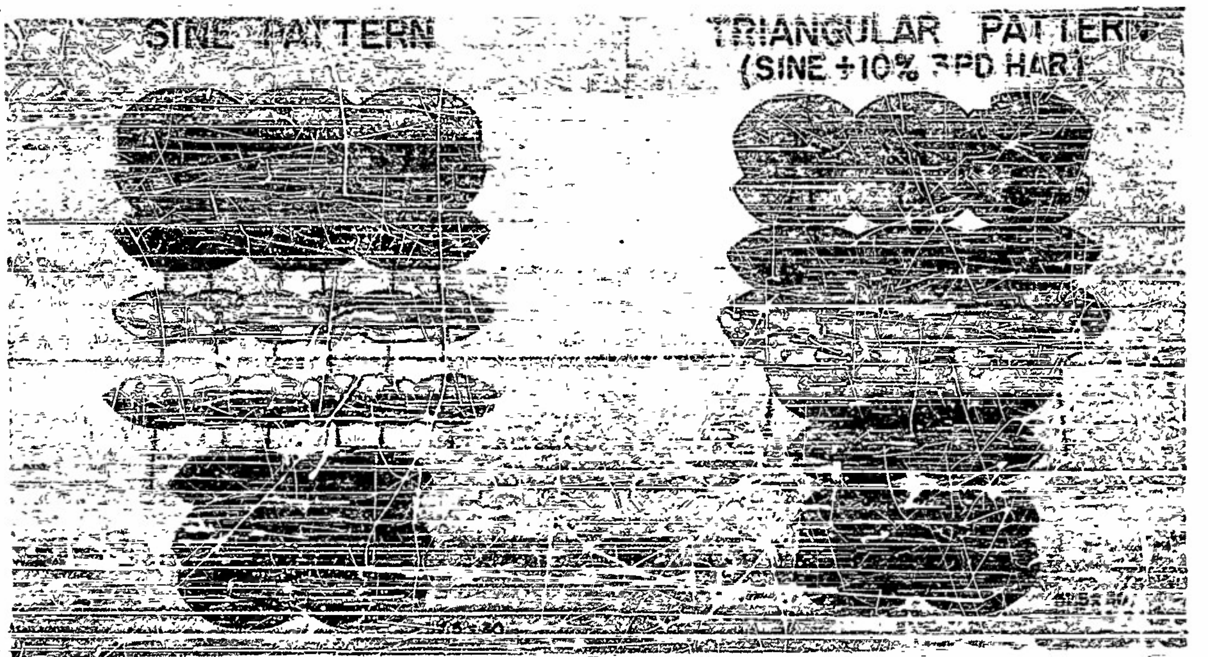

Figure 10 - Sine scan pattern - scan frequency too high

Figure 11 - Triangular scan pattern

DISCUSSION

Van Atta: (Hughes) The coverage diagrams presented by Mr. Counter are more black and white than is actually the case. The beam is not square ended. What might look like a hole is really 4 db rather than the 3 db given by the edges. This will have quite a smoothing effect on the patterns shown here.

Counter: (No Amer.) Yes, that is true.

ROUND TABLE DISCUSSIONS

SUMMARY OF CONFERENCE ON LOW-LEVEL COVERAGE*

Dr. G. A. Miller (Chairman)
National Research Council of Canada

Dr. G. A. Miller, conference chairman, suggested the following list of topics as being of possible interest to the group:

1. Counter-mortar problems
2. Carrier-controlled approach
3. Low-flying aircraft
   (a) Detection
   (b) Operation from low-flying aircraft
   (c) Light AA
4. Missile guidance
5. Battlefield surveillance
6. Detection of submarines

Mr. H. D. Sheitelman (BuShips) observed that most of the topics suggested could be classified as low-angle problems over land or water.

A show of hands revealed that the third item was of greatest interest to the group; and at Dr. Miller's invitation, Dr. R. C. Spencer (AFCRC) opened the discussion with some comments on the detection of low-flying aircraft. He indicated that, at least in certain quarters, the trend of current thinking is toward the conclusion that such detection will best be effected by more radars spaced closer together; hence simpler and cheaper radars will be required.

The next speaker, Mr. H. D. Sheitelman (BuShips), discussed carrier-controlled approach, in which it is desirable to monitor the height of an aircraft in almost level flight as it approaches a carrier from a distance of six miles or less.

Mr. A. W. Harbaugh (University of Texas) discussed the Brooks antenna system and also a quadruple-antenna interferometer system worked out by the Defense Research Laboratory.

Dr. Wilkes (Applied Physics Laboratory, Johns Hopkins University) spoke on power modulation and its possible use in missile guidance. Mr. A. A. Varela (NRL) contributed some remarks to this discussion.

Mr. W. C. Brown (National Research Council) listed the requirements of the Army for light AA work, including the surveillance of high-speed aircraft operating at altitudes of 50 to 500 feet.

Dr. Miller (National Research Council of Canada) expressed interest in the possibility of using tropospheric ducts near the surface of the ocean to improve the detection of

*Prepared by M. B. Sledd, Georgia Institute of Technology submarines. Dr. Wilkes and Mr. Varela discussed the use of low frequencies and special polarizations for this purpose.

ATTENDANCE
Conference on Low-Angle Coverage

NAME	ORGANIZATION
Brown, W. C.	National Research Council
Budenbom, H. T.	BTL
Crain, C. M.	University of Texas
Dantzig, H. P.	Bendix
Gerwin, H. L.	NRL
Harbaugh, A. W.	University of Texas
Harden, C. M.	Bendix
Horton, M. C.	Goodyear Aircraft
Hodgson, W. C.	NRL
Jones, S. S. D.	RRDE, England
Kilgallen, A.	BuOrd
Maciese, Arthur	British Joint Services Mission
Miller, G. A.	National Research Council of Canada
Rush, Stanley Capt.	Griffiss Air Force Base
Sensiper, S.	Hughes Aircraft
Sheitelman, H. D.	BuShips
Shapiro, Lawrence	Stavid Engineering
Sledd, M. B.	Georgia Tech
Spencer, R. C.	AFCRC
Varela, A. A.	NRL
Wallingford, L. E.	BuOrd
Whiting, W. E.	NRL
Wilkes, Gilbert	APL
Wilkinson, W. C.	RCA

SUMMARY OF CONFERENCE ON TWO-DIMENSIONAL SCANNING*

Captain S. Rush (Chairman)
Griffiss Air Force Base

The principal problem considered was a Ground Controlled Approach precision scan antenna. The system now in use is the CPN-4, which utilizes two fan beams in the manner illustrated in Figure 1. The azimuth sweep fan beam is about 2° x 1.2°, and the elevation sweep fan beam is about 3° x 0.6°. Each beam can be positioned manually so that the crossover region will occur at any desired position in the 7° x 20° scan area. The major difficulty experienced with this system is that accurate resolution is obtained only in the small 2° x 3° crossover region; thus, the larger portion of the desired 7° x 20° scan area is not covered.

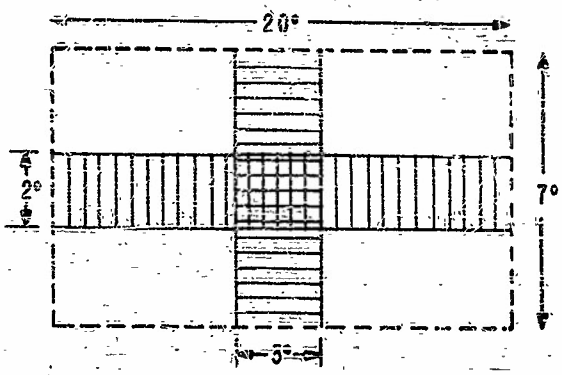

Figure 1 - Scan coverage of present CPN-4

The system now needed must be capable of providing accurate resolution information over the entire scan area in order that multiple plane landings may be adequately handled. Specifications for the new system were proposed by Captain Rush as follows: The 20° in azimuth by 7° in elevation scan area is to be swept in a "TV" type scan with a pencil beam of 3/4° in azimuth by 1/2° in elevation. The operating frequency is to be at X-band, the pulse repetition rate 9000 pps, the frame repetition rate 2 to 4 frames per second, and the range 10 miles. Each frame would contain about 27 beamwidths in azimuth and 14 beamwidths in elevation, or 378 elements. Pulses per target or pulses per element would therefore be

$$\frac{9000}{378} \times \frac{1}{4} \approx 6.$$

The r-f power required is estimated at less than 100 kw.

The first proposal to be discussed was the "TV" organ-pipe scanner described by Gabriel in the paper entitled "Ring Scanners with Applications." (Refer to Figure 10 in that paper.) The system consists of two Ring Scanners feeding a multiple-layer organ-pipe structure which, in turn, feeds an artificial dielectric delay lens. It incorporates a low-dead-time switch arrangement proposed by Hiatt. The chief points of interest brought out in this discussion were:

* Prepared by W. F. Gabriel, NRL

1. Probability that the system would be quite heavy and bulky, since lens dimensions must be about 10 ft x 15 ft and the organ-pipe structure about 4 ft in width. It was conceded that such would probably be the case with any system satisfying the above specifications.

2. Possibility that the organ-pipe structure might not be able to supply proper illumination taper for the lens, since feed horn size is restricted. Modification of organ-pipe structure was suggested to meet this objection. Also, the lens might be loaded with absorbing material near the edges to change the effective illumination taper.

3. Possibility that aperture coupling effects in organ-pipe structure might be quite harmful to lens illumination. There was no definite information available on this point. This must be determined experimentally.

4. Possibility that the Ring Scanner required would have excessively large radius, perhaps several feet. This objection resulted from a misunderstanding of the construction and operation of the Ring Scanner. The radius can be quite small, on the order of 8 to 12 inches, as will be shown later.

5. The fast-acting switch could be of the mechanical, rotating chopper-disc type, if electronic switches utilizing ferrites or gas-tubes are not available.

6. The question of MTI addition was raised. This might require compensation for the linear line-length change which occurs in the Ring Scanner, but it appeared to be feasible.

The second proposal suggested for consideration was made by Hiatt. His scheme involved two turnstile switches feeding in turn eight feed horns which illuminated a lens. The feed horns would rotate on a circle of about 5-ft radius and would be located at different levels to produce a television scan. The proposal was not applicable in this instance because it could feed a maximum of only 8 horns, and 14 are required for the 7-degree elevation scan with 1/2-degree beamwidth; consequently, it was not discussed in any detail.

The third proposal suggested for consideration was the adaptation of simultaneous lobing techniques. However, it was pointed out that the relatively broad beams to be utilized in this type of system would result in a high noise level due to ground return from the large ground area covered by the lower lobing beams. It was felt that a pencil beam was absolutely necessary because of the problem of ground return; therefore, simultaneous lobing was not discussed further.

The question was raised as to why it was proposed to have a 7-degree scan in elevation when in practice it is found that a 4-degree scan is adequate for landing all present types of aircraft. No adequate explanation could be found for the 7-degree figure other than the additional safety factor involved. Since every degree of reduction in scan angle helps out in terms of size and weight, it was recommended that a 5-degree elevation scan angle be adopted in place of the 7-degree angle.

ATTENDANCE

Conference on Two-Dimensional Scanning

NAME	ORGANIZATION
Berkowitz, B.	Sperry
Dantzig, H. P.	Bendix Radio
Gabriel, W. F.	NRL
Gerwin, H. L.	NRL
Harden, C. M.	Bendix Radio
Hiatt, R. E.	AFCRC
Holt, F. S.	AFCRC
Kelleher, K. S.	NRL
Lampl, S.	BuShips
Peeler, G. D. M.	NRL
Rotman, W.	AFCRC
Rush, S. Capt.	Griffiss Air Force Base
Sensiper, S.	Hughes Aircraft
Sheitelman, H. D.	BuShips

DETAILS OF TV ORGAN-PIPE SCANNER FOR GCA SYSTEM

W. F. Gabriel
Naval Research Laboratory

As a result of the Two-Dimensional Scanning Conference, some of the more relevant details of the "TV" organ-pipe scanner required for the proposed GCA system have been considered and are presented herein for the scrutiny of those who are interested in this specific problem.

Let us begin by restating the scanning specifications which are to be met: It is desired to scan a sector which is 5° in elevation by 20° in azimuth by means of a pencil beam of beamwidths 1/2° in elevation by 3/4° in azimuth. A "television"-type scan is to be employed in which the frame repetition rate is 4 per second and the pulse repetition rate is 9000 per second. The number of hits per target would therefore be:

$$\frac{9000}{20 \times \frac{4}{3} \times 5 \times 2} \times \frac{1}{4} \cong 8.5 \quad .$$

The frequency of operation is to be at X-band, and the transmitter power required is 100 kilowatts or less.

For the purpose of making sample calculations, let the operating frequency be fixed at 9375 Mc. Lens dimensions may then be calculated from the specified beamwidths:

$$\text{Lens vertical} = \frac{70\lambda}{\text{B.W.}} = \frac{70 \times 1.26}{(1/2)} = 176 \text{ inches}$$

$$\text{Lens horizontal} = \frac{70\lambda}{\text{B.W.}} = \frac{70 \times 1.26}{(3/4)} = 118 \text{ inches}$$

The focal length of the lens is quite arbitrary from the standpoint of the organ-pipe feed system in this proposal because of the unique type of organ-pipe construction contemplated. Therefore, it may ultimately be chosen on the basis of its effect upon the lens performance, the complexity of the lens construction, and the overall size, weight, and cost of the system. For the moment, however, we are interested only in making sample calculations, and for this purpose a focal length of 141 inches shall be used. This results in the following f/D ratios for the lens:

$$\text{Vertical f/D} = \frac{141}{176} = .8$$

$$\text{Horizontal f/D} = \frac{141}{118} = 1.2$$

Knowing the focal length and the dimensions of the lens, one can determine the lens illumination angles. In addition, since the scan angles have been specified, the over-all dimensions of the stacked organ-pipe feed aperture may be found. These quantities are illustrated in Figure 1. It will be noted that the aperture line of the organ-pipe structure in the horizontal plane is shown as an arc of a circle whose radius is the focal length. This was done partly to simplify organ-pipe line-length adjustments and partly to conform to the best focus arc, although the latter factor will depend upon the type of lens used and may require that a different aperture line be used for best focus.

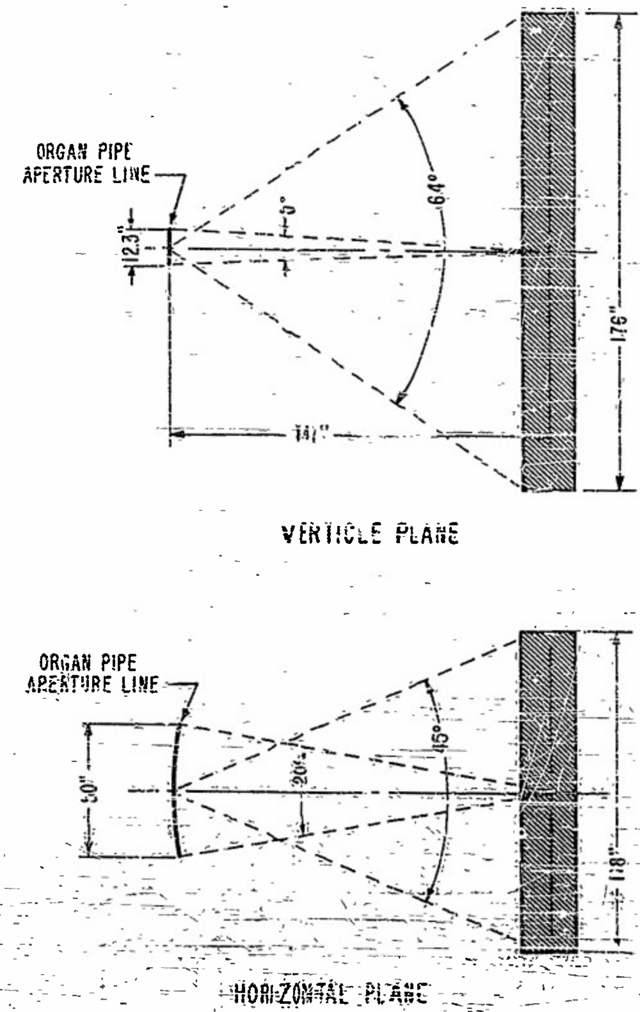

Figure 1 - Geometrical relationships of system

The proposal for the organ-pipe structure is illustrated in Figures 2 and 3. It is to consist of ten organ-pipe levels separated by a distance of 1.23 inches; that is, since a shift from one level to the next must produce a beam shift of $1/2^0$, then the level separation is:

$$\text{focal length} \times \tan 1/2^0 =$$

$$141 \times .00873 = 1.23 \text{ inches}$$

The ten levels are indicated in Figure 2 (front view) partly by dashed lines and partly in detail. It will be noted in the detail portion of the drawing that the levels are "interwoven" at the aperture. This type of construction was chosen because it permits the individual waveguide channels in each level to be flared out to the proper dimension for obtaining the required lens illumination angle in the vertical plane for any given focal length. For the chosen focal length of 141 inches, we saw in Figure 1 that the required lens illumination angle was 64^0 in the vertical plane, which would require that the waveguide channels be flared out to a dimension of about 2.1 inches for a 10-db illumination taper. In order to obtain the required illumination angle in the horizontal plane, one can vary the number of channels energized and also the separation between channels. For the 45-degree angle shown in Figure 1, the correct illumination taper would be obtained by energizing about three channels at a time with a spacing of about one inch between channel center lines. This is indicated in Figure 2 (front view), where three channels have been blacked in in the seventh level. One obvious consequence of the proposed construction to be noted here is that the energized channels in a given level do not lie side by side as in the usual organ pipe but, instead, are separated by one channel width. This places a restriction on the maximum allowable channel width because of the fact that the radiation pattern usually becomes unsatisfactory if the centers of the energized channels are separated by more than about one wavelength. Thus, the width of each channel must be kept less than about half a wavelength. In the present instance, a channel width of 1/2 inch was considered satisfactory, and, since the aperture line extends for 50 inches, this results in 50 channels per level plus two extra at each end for scan continu... Each level, then, has a total of 54 waveguide channels.

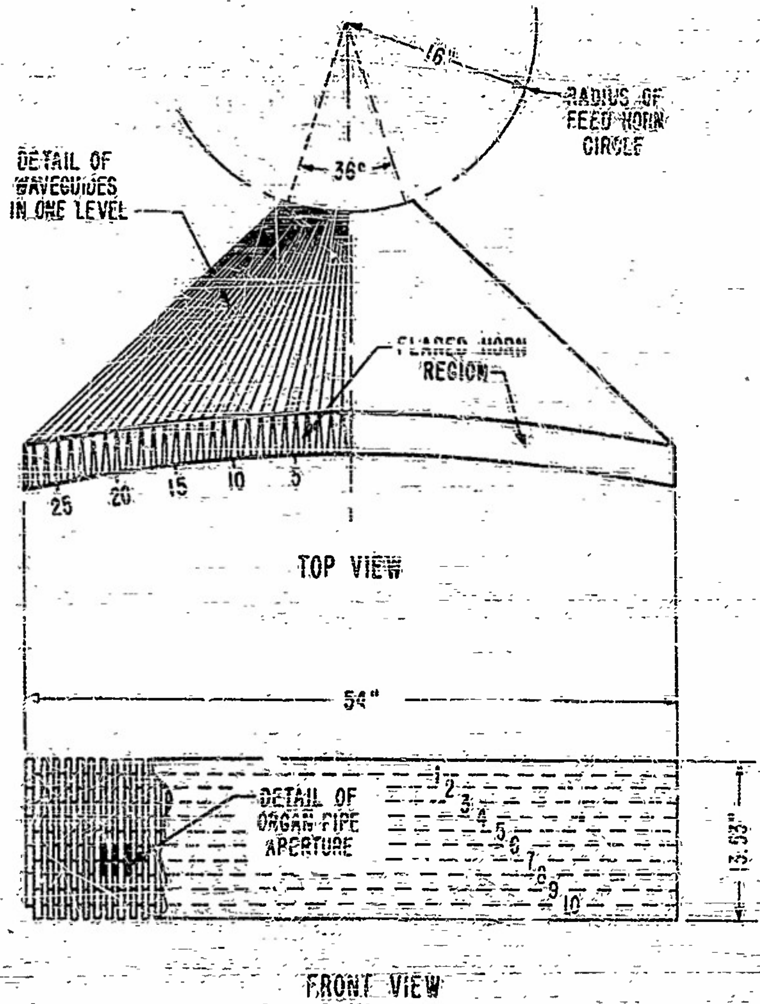

Figure 2 - Detail of organ-pipe structure

In order to bring the 54 channels back to a feed circle of reasonable radius, it is necessary to taper the channel widths to a smaller value. In the present instance, a feed-circle channel width of 0.2 inches was chosen for convenience; and this resulted in a feed-circle radius of about 16 inches; that is:

$$\text{radius} = \frac{\text{no. levels x feed arc}}{2\pi} = \frac{10 \times (50 \times .2)}{2\pi} = 15.9 \text{ inches}$$

The top view in Figure 2 illustrates how the waveguide channels may be tapered and brought back to the feed circle.

Figure 3 illustrates a small portion of a type of "layer" construction which would make the organ-pipe assembly quite simple. Each layer would contain all of the bottom halves for the 54 channels in one level, and all of the top halves for the 54 channels in the following

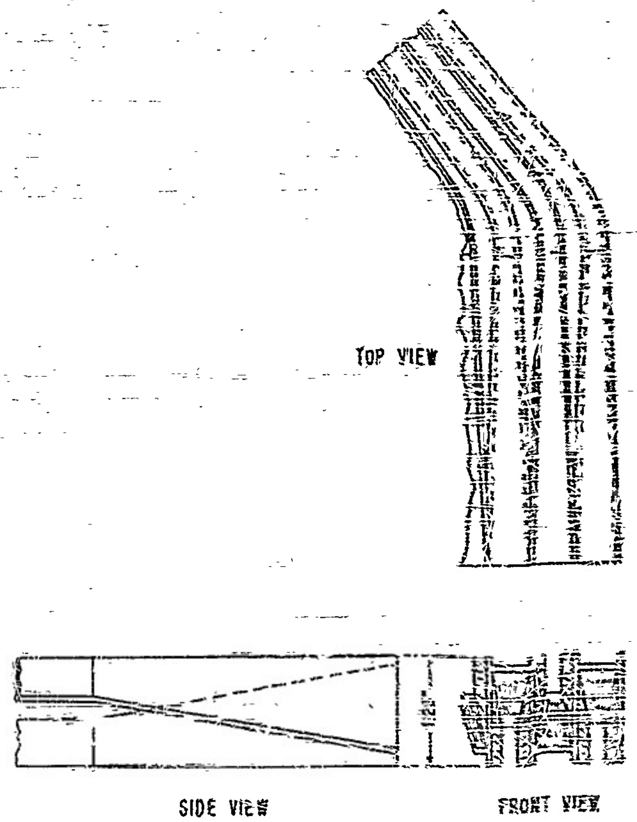

Figure 3 - Detail of "layer" construction for organ pipe

level. It should be possible to accurately die cast it in a one-piece unit from a light-weight alloy metal, and it would then require very little, if any, machining. The finished organ pipe would then be formed simply by placing these layers one on top of the other, with alternate layers "upside down" with respect to the others. Eleven layers would be required to form the proposed ten organ-pipe levels. The break in the metal between layers occurs in the center of the broad sides of the waveguide channels and, therefore, would not disturb the propagation of energy. It should be obvious that one of the major advantages of this type of construction is that it would enable quantity production of high-quality finished organ pipes. Another advantage is that it permits an easy solution to the problem of equalizing the electrical lengths of the various waveguide channels without adding more weight. This can be accomplished here by tapering the H-plane dimension of the waveguide channels to a larger or smaller value in order to get the desired phase delay or advance respectively; that is, the central channels would be tapered to a wider dimension to introduce desired amounts of phase delay, and the outer channels would be tapered to a narrower dimension to introduce desired amounts of phase advance.

The Ring Scanner feed system required to feed the ten organ-pipe levels is indicated schematically in Figure 4. Both Ring scanners are to be machined back-to-back on a single wheel, thus simplifying construction and alignment. Their proposed mean radius is 9.5 inches, but, if desired, it could be made even smaller than this because the fast-acting switch arrangement allows the radius of the Ring Scanners to be set at any value for which the switching dead time angle is less than 36°. This means that the minimum radius permitted in this instance is about 3 inches. For the sake of clarity, only the top Ring Scanner and its associated plumbing is shown in detail. It feeds organ pipe levels Nos. 1, 3, 5, 7, and 9. The location of the output feed horns fed by the bottom Ring Scanner is indicated in the top view of Figure 4 by the dashed horns numbered 2, 4, 6, 8, and 10. The number associated with each horn corresponds to the organ-pipe level which it feeds. Also indicated in the top view is the 36-degree active feed angle.

On the basis of the angle subtended by the foregoing organ-pipe structure, it appears feasible to feed simultaneously as many as five organ-pipe structures, and thus five entire lens systems, with the single Ring Scanner feed system outlined above. It would require the addition of the necessary extra inputs and feed arcs around the Ring Scanner, of course. Each system could operate independently, with its own transmitter and receiver indicators if desired.

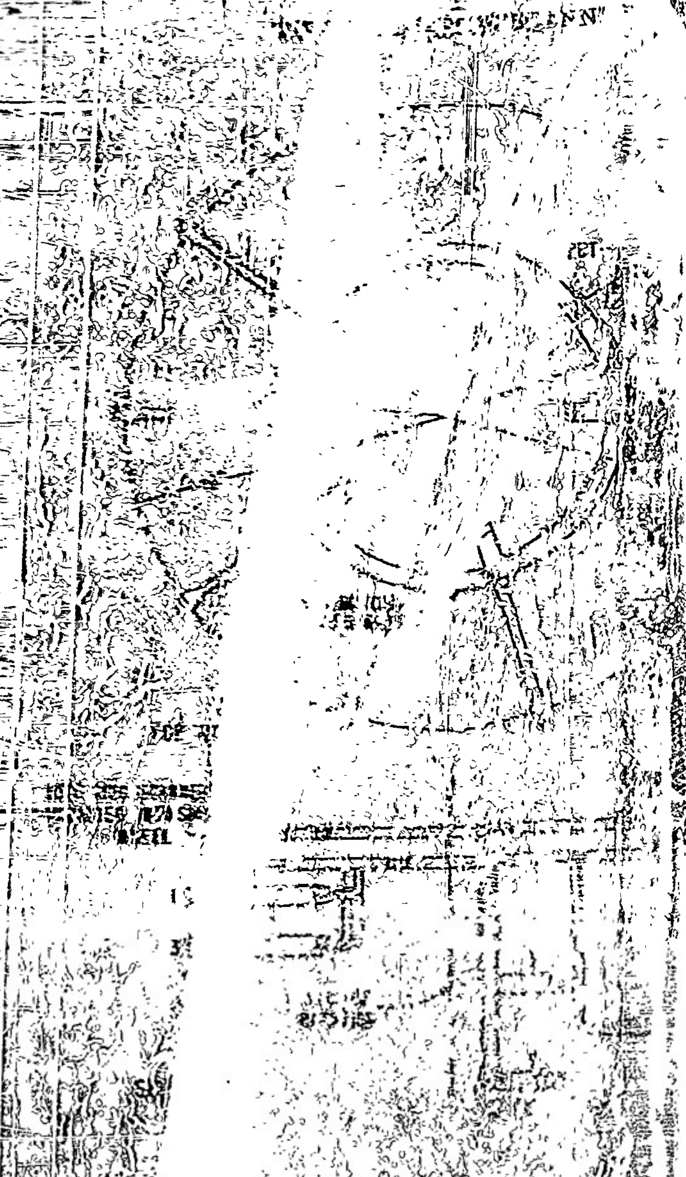

[illegible] 4 - Detail of [illegible]

In conclusion, [illegible] be pointed out that [illegible] a specific solution [illegible] upon present knowledge [illegible] factors may, of course, [illegible] quire some changes [illegible] a more satisfactory [illegible]

Acknowledgment [illegible] given to Kenneth S. Kelleher for [illegible] ating the above pr[illegible]